R2D2: a xenon TPC for neutrinoless double beta decay search

A.Meregaglia, F.Piquemal (LP2i Bordeaux - CNRS/IN2P3)
On Behalf of R2D2

LLR - 10/02/2025

Introduction: physics case

- The observation of **neutrinoless double beta decay ($\beta\beta0\nu$)** is fundamental to determine the nature of neutrino.

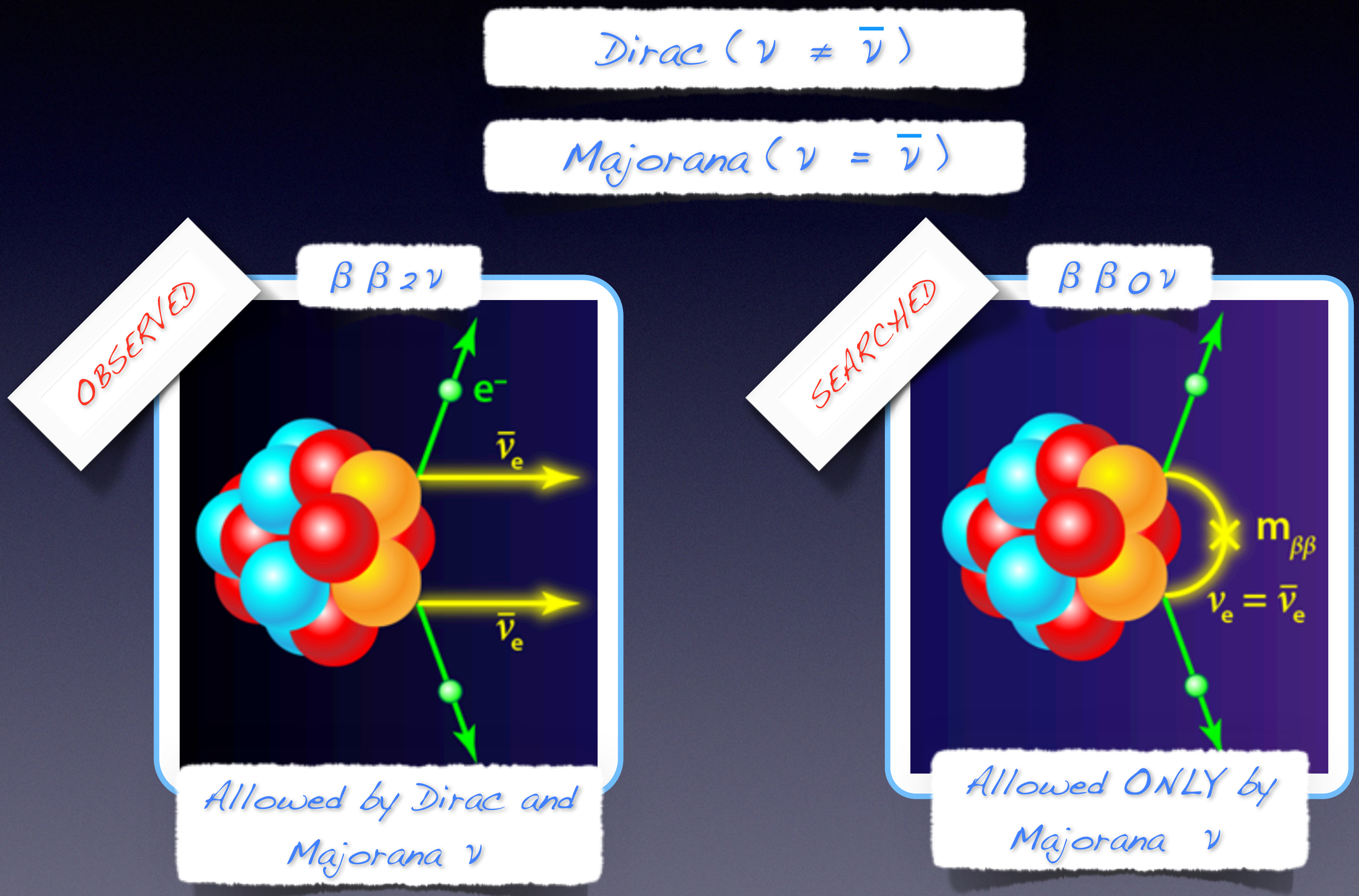

- The observation of $\beta\beta0\nu$ decay would have **implications in patricle physics** (generation of neutrino masses) and **cosmology** (leptogenesis model).

Introduction: physics case

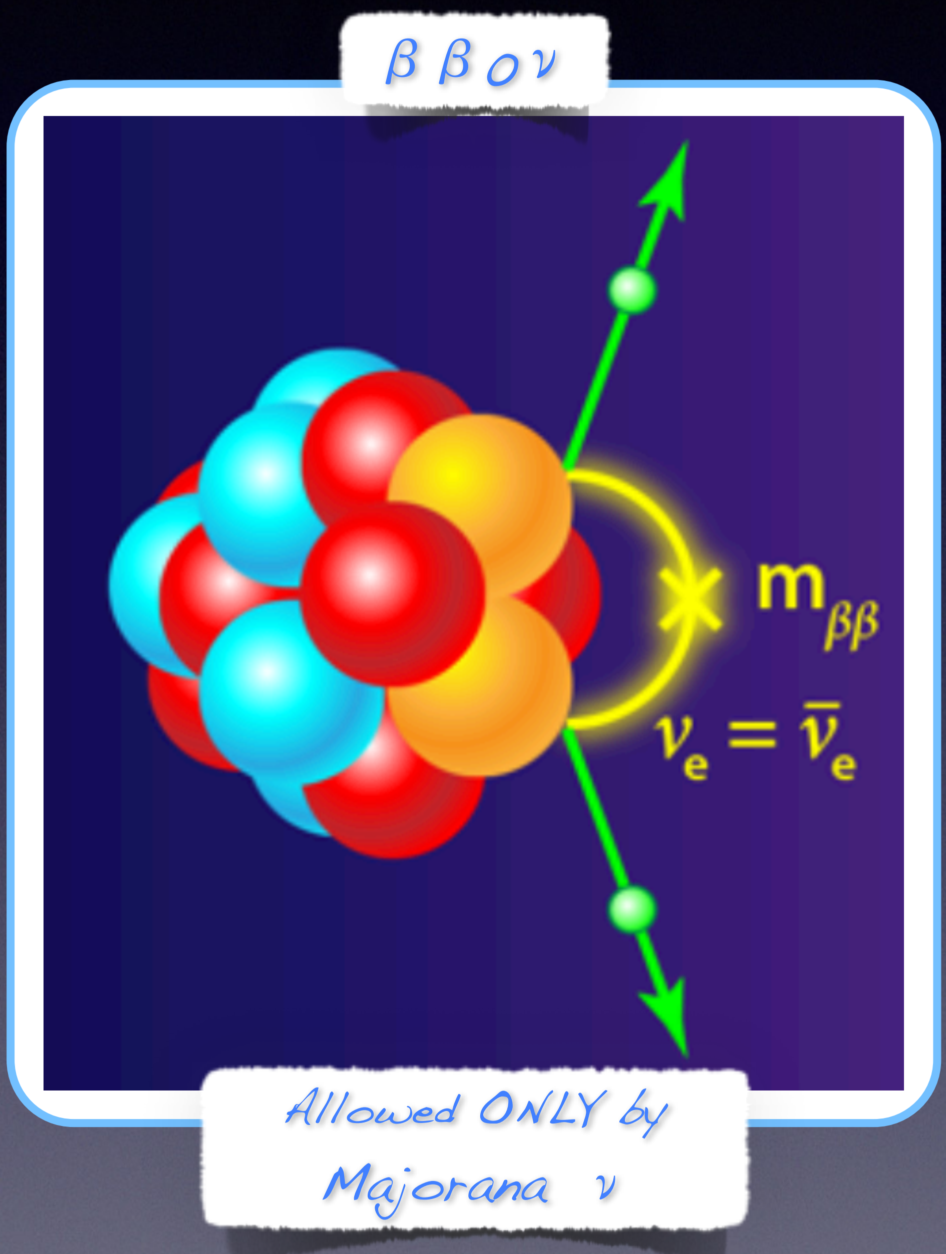

Introduction: physics case

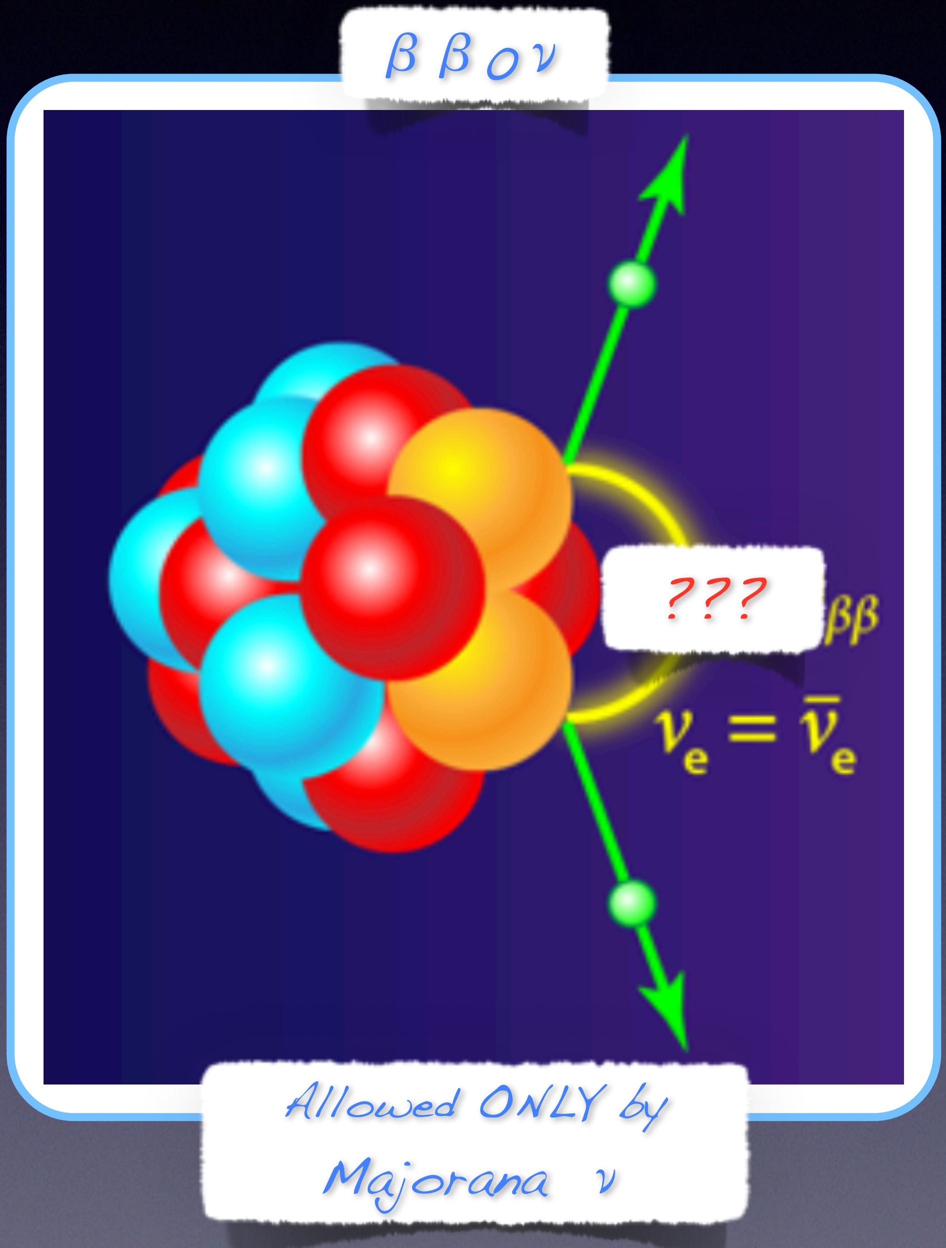

Introduction: physics case

ββ0ν

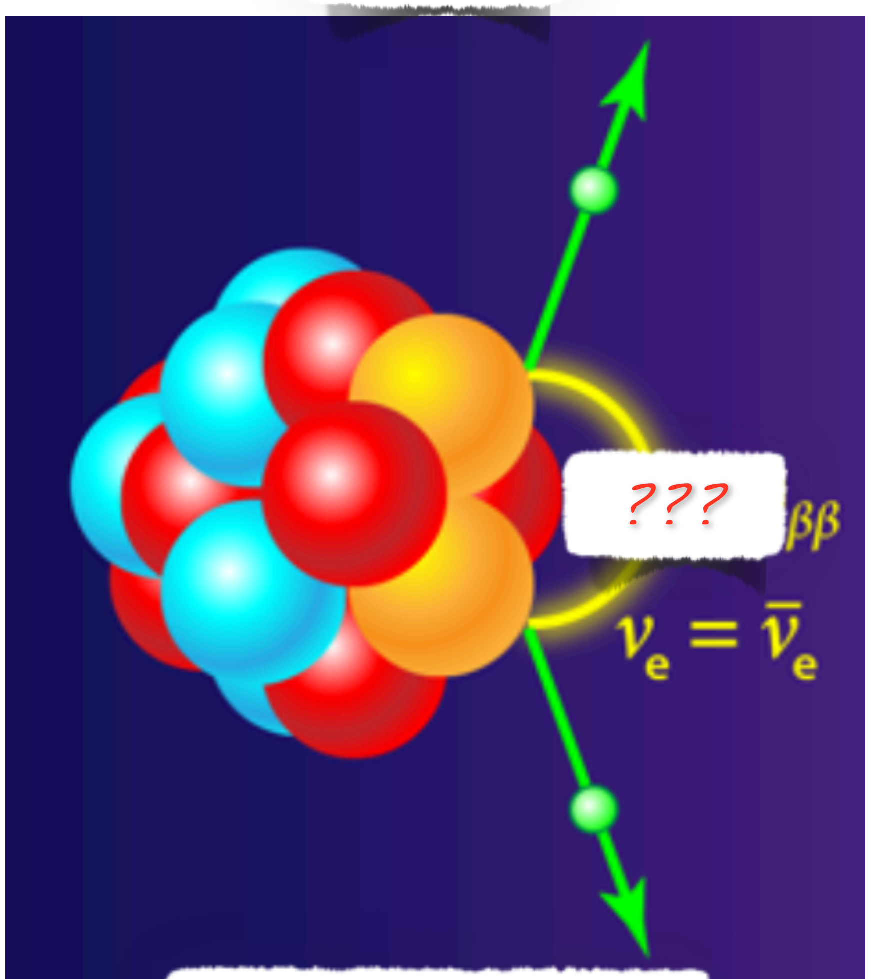

Allowed ONLY by Majorana ν

Light neutrino exchange →

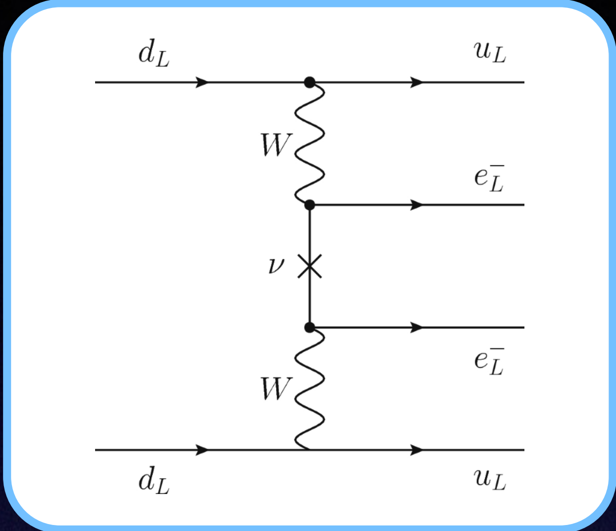

Heavy neutrino exchange →

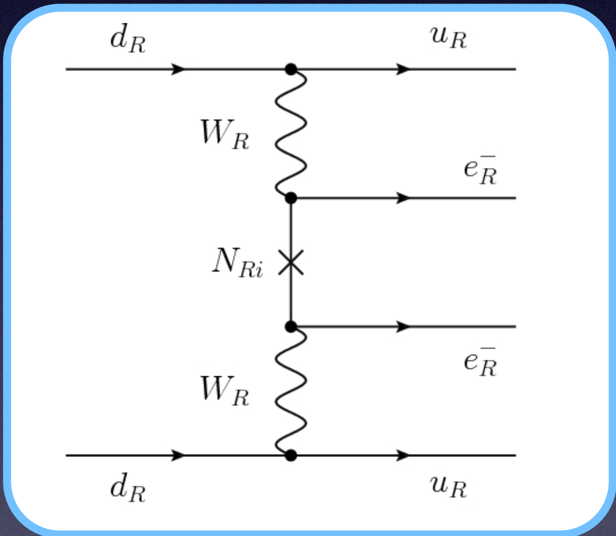

Majoron emission →

... and other BSM processes ...

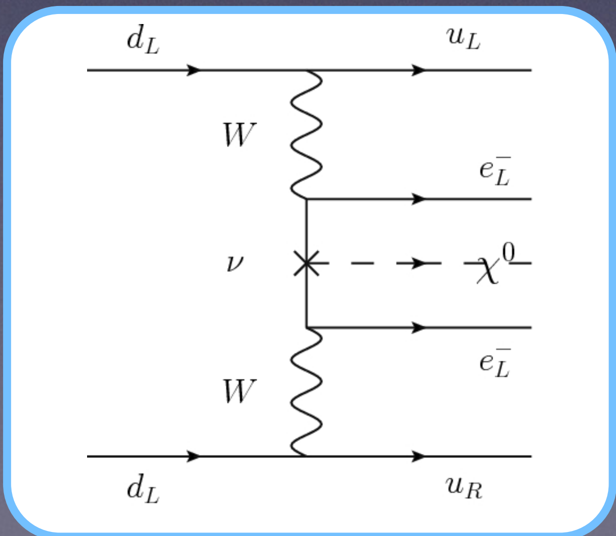

Introduction: physics case

ββ0ν

Allowed …

Majora…

Light neutrino exchange

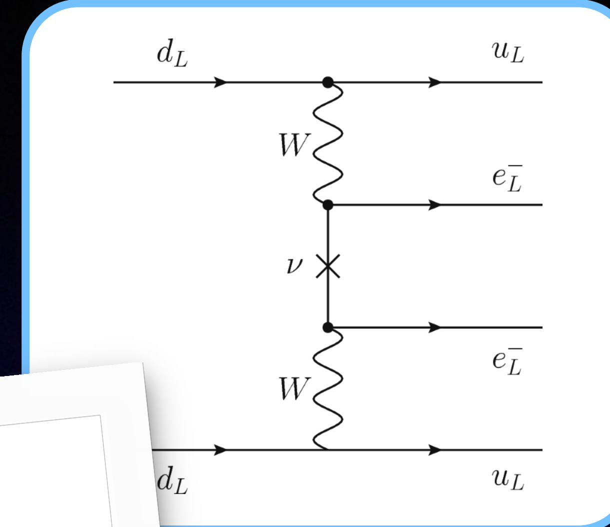

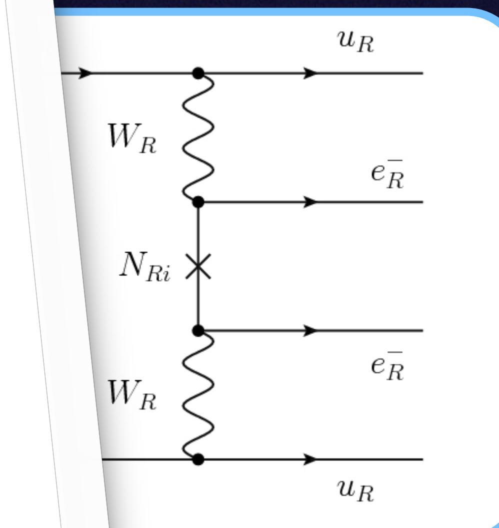

Depending on the mechanism driving the decay, the observation could be a door to:

- Neutrino mass hierarchy
- Absolute neutrino mass
- Right-handed current interaction
- CP violation in leptonic sector
- Search for supersymmetric particles

Majoron emission

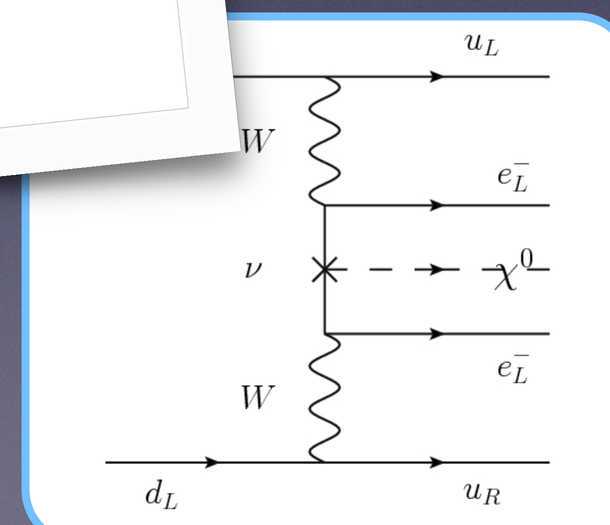

… and other BSM processes …

Experimental observables

- The **signature** of the decay is given by the **sum of the kinetic energy of the two emitted electrons**.

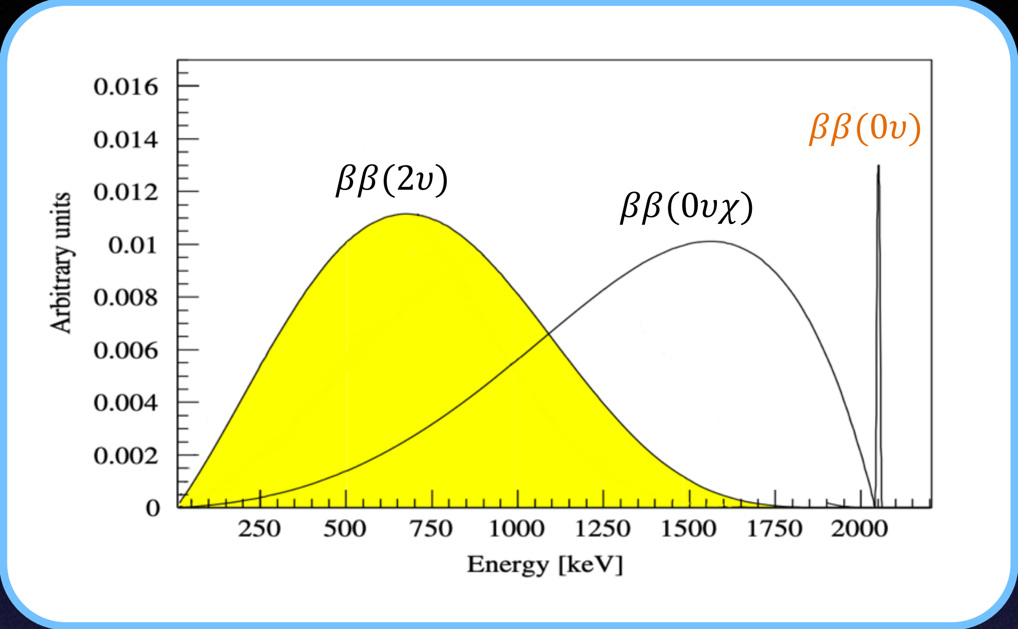

Experimental observables

- The **signature** of the decay is given by the **sum of the kinetic energy of the two emitted electrons**.

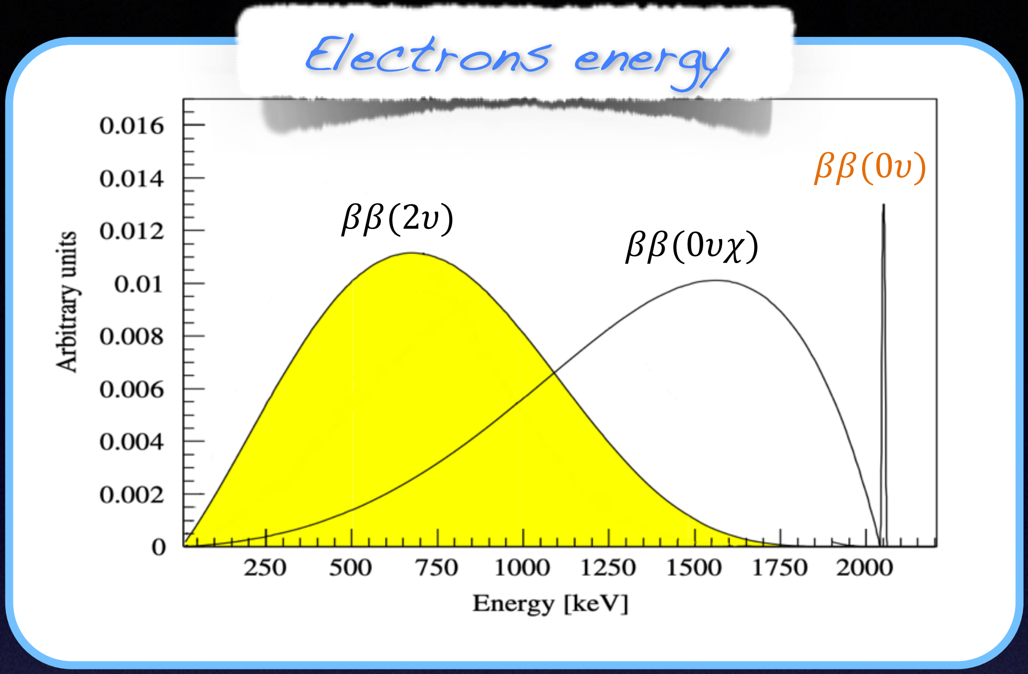

Experimental observables

- The **signature** of the decay is given by the **sum of the kinetic energy of the two emitted electrons**.
- The measurement of other **kinematical variables** could cast light on the driving mechanism.

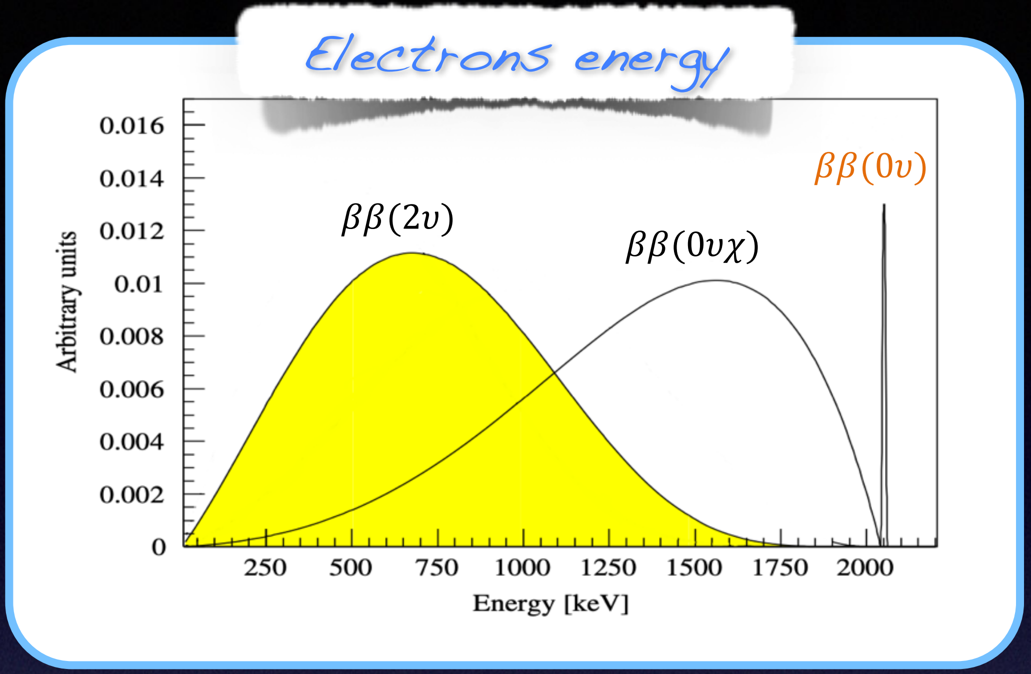

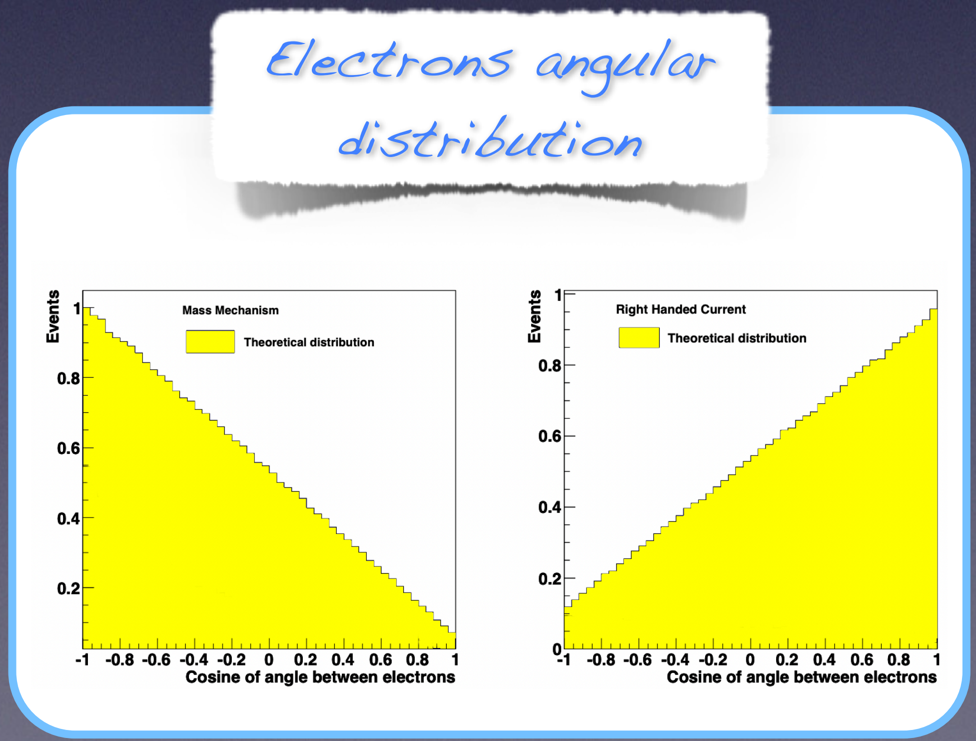

Experimental observables

- The **signature** of the decay is given by the **sum of the kinetic energy of the two emitted electrons**.
- The measurement of other **kinematical variables** could cast light on the driving mechanism.
- Furthermore the **identification of excited states** and **daugther nucleus** could forster the detection.

Electrons energy

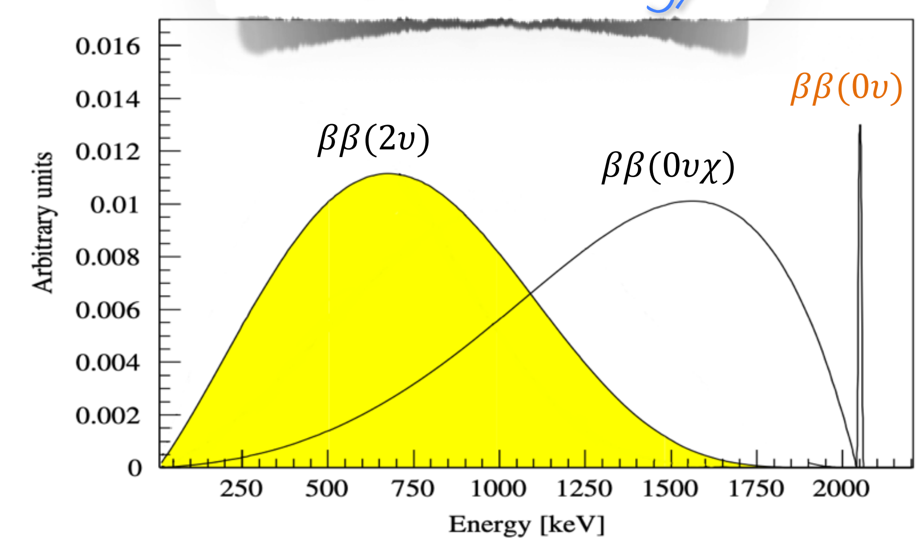

Electrons angular distribution

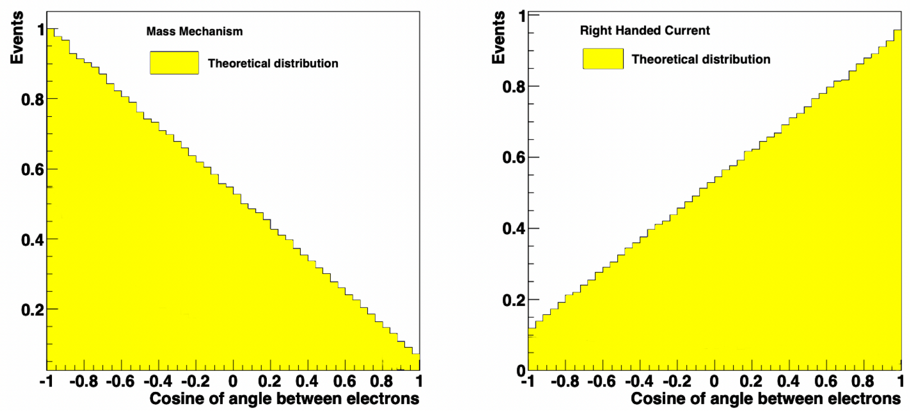

Decay to excited states

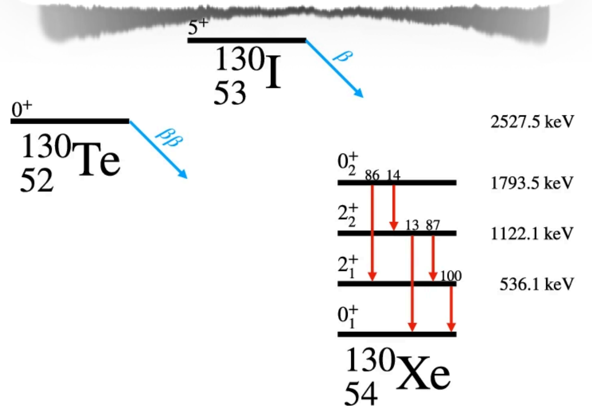

(A,Z)→(A,Z+2) + 2 e⁻ + γ's

1 or 2 additional γ-rays

Daughter identification

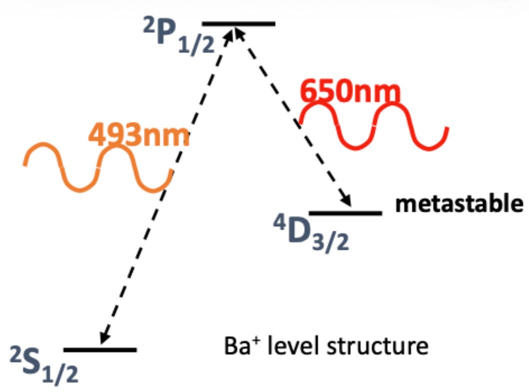

$$^{136}_{54}Xe \rightarrow ^{136}_{56}Ba^{++} + 2e^- + 2\bar{\nu}_e$$

Isotopes

- The isotopes concerned by ββ decay must have a **single β decay forbidden** (by energy conservation) or strongly suppressed (due to large angular momentum change).

About 35 possible ββ emitters and only 10 experimentally observed with typical half-life of 10^{18} - 10^{21} years

isotope	Q-value [MeV]	natural abundance [%]
^{48}Ca	4.27	0.187
^{150}Nd	3.37	5.6
^{96}Zr	3.35	2.8
^{100}Mo	3.03	9.8
^{82}Se	3.00	8.7
^{116}Cd	2.81	7.5
^{130}Te	2.53	34.1
^{136}Xe	2.46	8.86
^{124}Sn	2.29	5.8
^{76}Ge	2.04	7.73

Isotopes

- The isotopes concerned by ββ decay must have a **single β decay forbidden** (by energy conservation) or strongly suppressed (due to large angular momentum change).

isotope	Q-value [MeV]	natural abundance [%]
^{48}Ca	4.27	0.187
^{150}Nd	3.37	5.6
^{96}Zr	3.35	2.8
^{100}Mo	3.03	9.8
^{82}Se	3.00	8.7
^{116}Cd	2.81	7.5
^{130}Te	2.53	34.1
^{136}Xe	2.46	8.86
^{124}Sn	2.29	5.8
^{76}Ge	2.04	7.73

About 35 possible ββ emitters and only 10 experimentally observed with typical half-life of $10^{18} - 10^{21}$ years

Current limit for neutrinoless double beta decay of $10^{25} - 10^{26}$ years

Phase space factor

Nuclear matrix element

$$\frac{1}{T^{0\nu}_{1/2}} = G^{0\nu}|M^{0\nu}|^2 < m_{\beta\beta} >^2$$

Effective Majorana mass

Isotopes

- The isotopes concerned by ββ decay must have a **single β decay forbidden** (by energy conservation) or strongly suppressed (due to large angular momentum change).

isotope	Q-value [MeV]	natural abundance [%]
^{48}Ca	4.27	0.187
^{150}Nd	3.37	5.6
^{96}Zr	3.35	2.8
^{100}Mo	3.03	9.8
^{82}Se	3.00	8.7
^{116}Cd	2.81	7.5
^{130}Te	2.53	34.1
^{136}Xe	2.46	8.86
^{124}Sn	2.29	5.8
^{76}Ge	2.04	7.73

About 35 possible ββ emitters and only 10 experimentally observed with typical half-life of 10^{18} – 10^{21} years

Current limit for neutrinoless double beta decay of 10^{25} – 10^{26} years

Phase space factor — Nuclear matrix element

$$\frac{1}{T_{1/2}^{0\nu}} = G^{0\nu}|M^{0\nu}|^2 <$$

Isotope-dependent

Effective Majorana mass

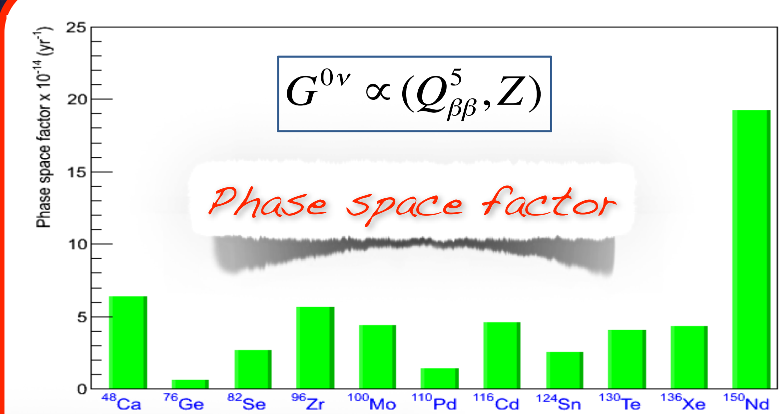

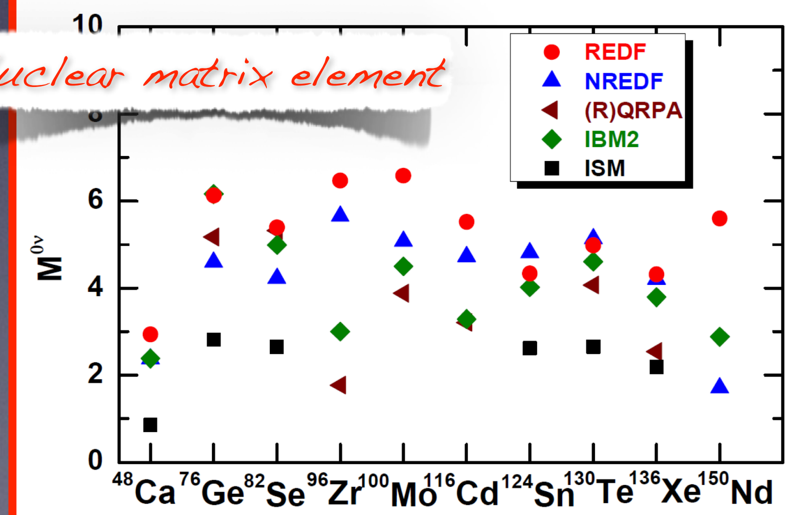

Isotopes

- The isotopes concerned by ββ decay must have a **single β decay forbidden** (by energy conservation) or strongly suppressed (due to large angular momentum change).

isotope	Q-value [MeV]	natural abundance [%]
^{48}Ca	4.27	0.187
^{150}Nd	3.37	5.6
^{96}Zr	3.35	2.8
^{100}Mo	3.03	9.8
^{82}Se	3.0	

Important discrepancies between models

About 35 possible ββ emitters and only 10 experimentally observed with typical half-life of $10^{18} - 10^{21}$ years

Current limit for neutrinoless double beta decay of $10^{25} - 10^{26}$ years

Phase space factor — *Nuclear matrix element*

$$\frac{1}{T^{0\nu}_{1/2}} = G^{0\nu}|M^{0\nu}|^2 <$$

Isotope-dependent

Effective Majorana mass

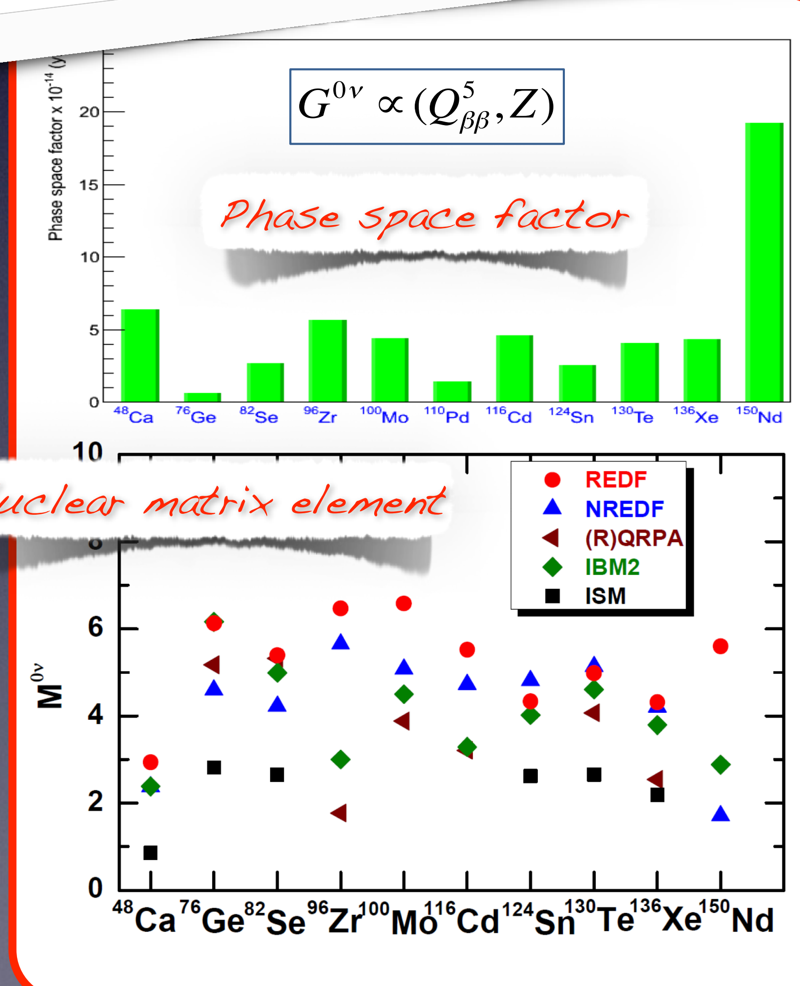

Background

- The main source of background is **natural radioactivity**.

- Other background sources are:
  - Muons (depending of underground laboratory).
  - γ from (n,γ) reactions or μ bremstrahlung.
  - Muon spallation products.
  - α from materials bulk or surface contaminations for calorimeters.
  - $\beta\beta2\nu$ (if modest energy resolution).

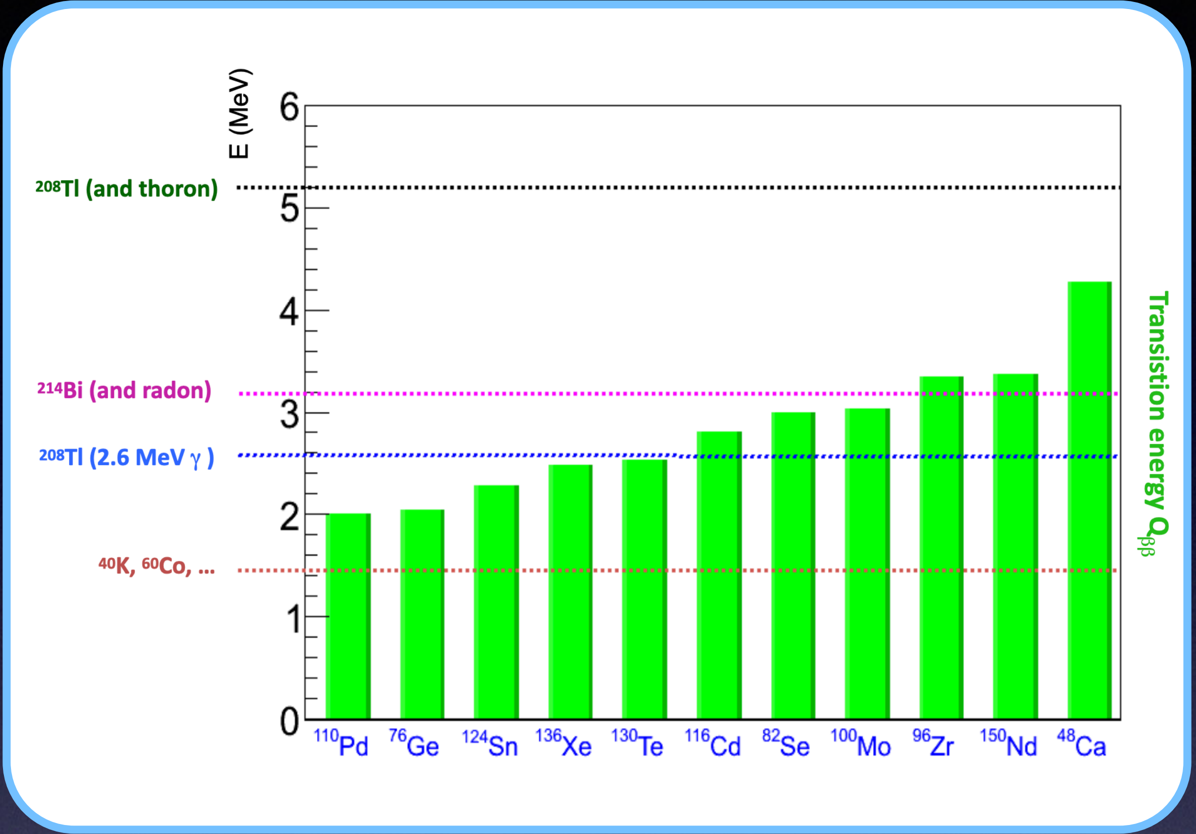

Background

- The main source of background is **natural radioactivity**.
- Other background sources are:
  - Muons (depending of underground laboratory).
  - γ from (n,γ) reactions or μ bremstrahlung.
  - Muon spallation products.
  - α from materials bulk or surface contaminations for calorimeters.
  - $\beta\beta2\nu$ (if modest energy resolution).

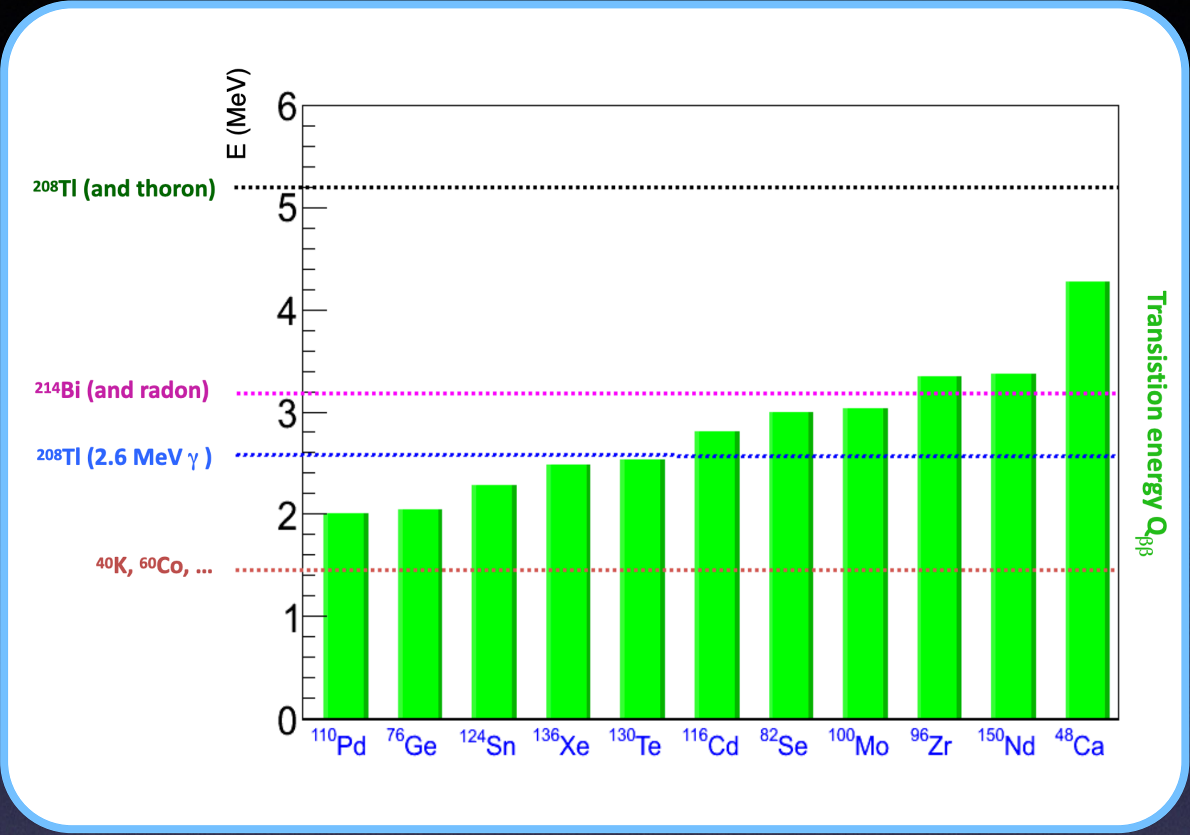

Different strategies to elimanate the background →

Isotope with high $Q_{\beta\beta}$
Material screening
Excellent energy resolution
Identification of electrons
Active veto
...

Experiment sensitivity

- The experimental sensitivity can be computed in terms of a limit of the half life.

$$T_{1/2}^{0\nu} > \ln(2)\varepsilon \frac{N_A m}{M} \frac{t}{S_{up}}$$

Signal efficiency

Isotope active mass

Exposure in years

Signal upper limit

Isotope molar mass

Experiment sensitivity

- The experimental sensitivity can be computed in terms of a limit of the half life.

Signal efficiency

Isotope active mass

$$T_{1/2}^{0\nu} > \ln(2)\varepsilon \frac{N_A m}{M} \frac{t}{S_{up}}$$

Exposure in years

Signal upper limit

Isotope molar mass

- The **signal upper limit depends** on the chosen confidence level and **on the experimental background**:

Experiment sensitivity

- The experimental sensitivity can be computed in terms of a limit of the half life.

Signal efficiency

Isotope active mass

$$T^{0\nu}_{1/2} > \ln(2)\varepsilon\frac{N_A m}{M}\frac{t}{S_{up}}$$

Exposure in years

Signal upper limit

Isotope molar mass

- The **signal upper limit depends** on the chosen confidence level and **on the experimental background**:

Zero backgound → Signal limit = constant → Half-life limit linear with exposure

Experiment sensitivity

- The experimental sensitivity can be computed in terms of a limit of the half life.

$$T^{0\nu}_{1/2} > \ln(2)\varepsilon \frac{N_A m}{M} \frac{t}{S_{up}}$$

Signal efficiency

Isotope active mass

Exposure in years

Signal upper limit

Isotope molar mass

- The **signal upper limit depends** on the chosen confidence level and **on the experimental background**:

Zero backgound → Signal limit = constant → Half-life limit linear with exposure

Non-zero backgound → Background increases with exposure and therefore Signal limit increase as well → Half-life limit dependence as square root of exposure (if Gaussian description of background holds)

Experiment sensitivity

- The experimental sensitivity can be computed in terms of a limit of the half life.

$$T_{1/2}^{0\nu} > \ln(2)\varepsilon \frac{N_A m}{M} \frac{t}{S_{up}}$$

Signal efficiency

Isotope active mass

Exposure in years

Signal upper limit

Isotope molar mass

- The **signal upper limit depends** on the chosen confidence level and **on the experimental background**:

Zero backgound → Half-life limit linear with exposure

Non-zero backgound → … signal limit increase as well → Half-life limit dependence as square root of exposure (if Gaussian description of background holds)

Clear importance of background free experiment

Experiment sensitivity

Zero backgound → Signal limit = constant → Half-life limit linear with exposure

Non-zero backgound → Background increases with exposure and therefore Signal limit increase as well → Half-life limit dependence as square root of exposure (if Gaussian description of background holds)

Experiment sensitivity

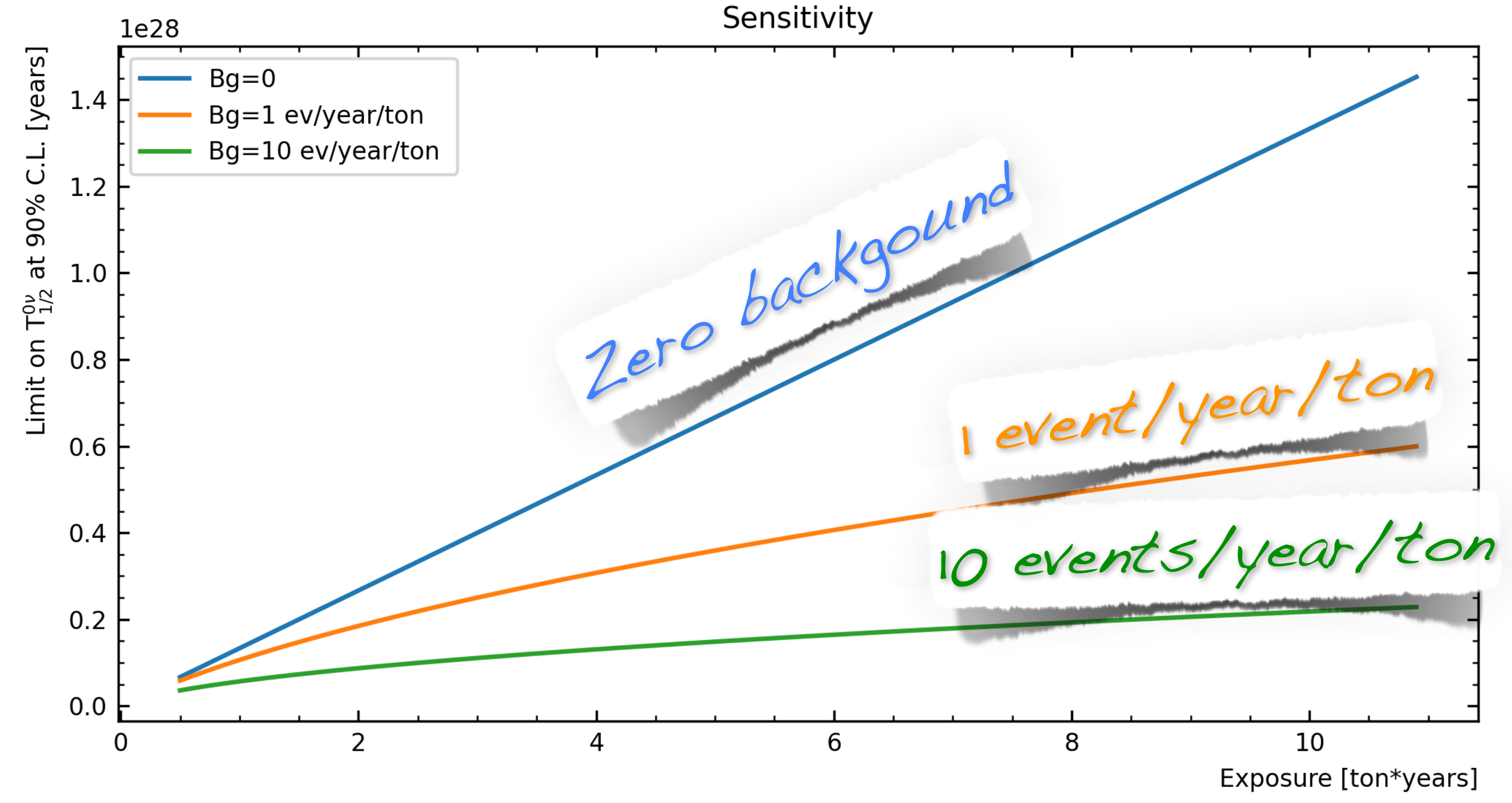

Zero backgound → Signal limit = constant → Half-life limit linear with exposure

Non-zero backgound → Background increases with exposure and therefore Signal limit increase as well → Half-life limit dependence as square root of exposure (if Gaussian description of background holds)

Status of the art

Status of the art

LEGEND

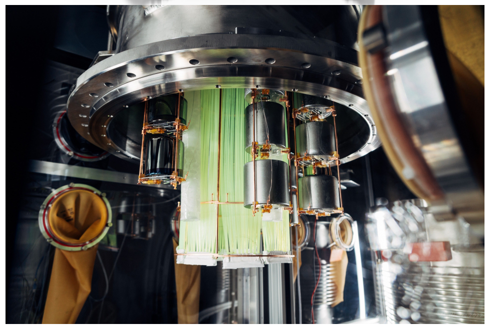

200 kg – 1000 kg of ^{76}Ge diodes
$\Delta E/E$ = 0.1 % (FWHM) at $Q_{\beta\beta}$

CUPID-Mo

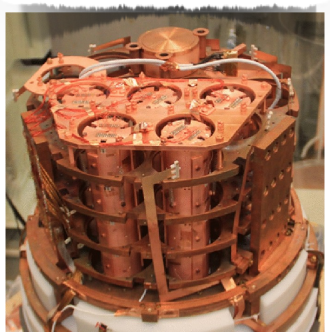

4 kg – 1000 kg of ^{100}Mo bolometers diodes
$\Delta E/E$ = 0.2 % (FWHM) at $Q_{\beta\beta}$

Status of the art

LEGEND

200 kg – 1000 kg of ^{76}Ge diodes
$\Delta E/E$ = 0.1 % (FWHM) at $Q_{\beta\beta}$

CUPID-Mo

4 kg – 1000 kg of ^{100}Mo bolometers diodes
$\Delta E/E$ = 0.2 % (FWHM) at $Q_{\beta\beta}$

Excellent energy resolution

Status of the art

Excellent energy resolution

LEGEND

200 kg – 1000 kg of ^{76}Ge diodes
$\Delta E/E$ = 0.1 % (FWHM) at $Q_{\beta\beta}$

CUPID-Mo

4 kg – 1000 kg of ^{100}Mo bolometers diodes
$\Delta E/E$ = 0.2 % (FWHM) at $Q_{\beta\beta}$

KamLAND-ZEN

800 kg of 136Xe dissolved in liquid scintillator
$\Delta E/E$ = 10 % (FWHM) at $Q_{\beta\beta}$

EXO-200

200 kg – n tons of liquid xenon
$\Delta E/E$ = 3 % (FWHM) at $Q_{\beta\beta}$

Status of the art

LEGEND

200 **kg** – 1000 kg of ^{76}Ge diodes
$\Delta E/E = 0.1$ % (FWHM) at $Q_{\beta\beta}$

CUPID-Mo

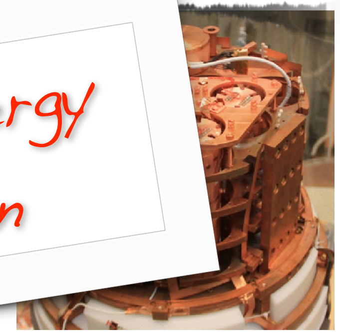

4 kg – 1000 kg of ^{100}Mo
bolometers diodes
$\Delta E/E = 0.2$ % (FWHM) at $Q_{\beta\beta}$

Excellent energy resolution

KamLAND-ZEN

800 kg of 136Xe dissolved
in liquid scintillator
$\Delta E/E = 10$ % (FWHM) at $Q_{\beta\beta}$

EXO-200

200 kg – n tons of liquid xenon
$\Delta E/E = 3$ % (FWHM) at $Q_{\beta\beta}$

Large masses

Status of the art

Excellent energy resolution

LEGEND

200 kg – 1000 kg of ^{76}Ge diodes
$\Delta E/E$ = 0.1 % (FWHM) at $Q_{\beta\beta}$

CUPID-Mo

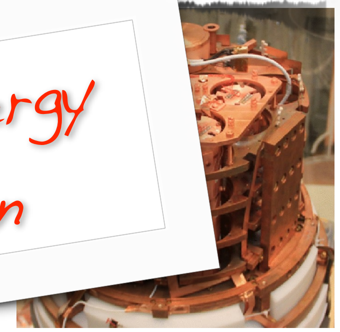

4 kg – 1000 kg of ^{100}Mo bolometers diodes
$\Delta E/E$ = 0.2 % (FWHM) at $Q_{\beta\beta}$

SuperNEMO

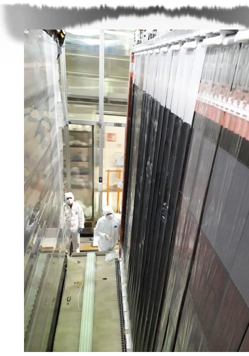

Tracko-calo **7 kg**– 100 kg ^{82}Se foil
$\Delta E/E$ = 5% (FWHM) at $Q_{\beta\beta}$

Large masses

KamLAND-ZEN

800 kg of 136Xe dissolved in liquid scintillator
$\Delta E/E$ = 10 % (FWHM) at $Q_{\beta\beta}$

EXO-200

200 kg – n tons of liquid xenon
$\Delta E/E$ = 3 % (FWHM) at $Q_{\beta\beta}$

NEXT-White

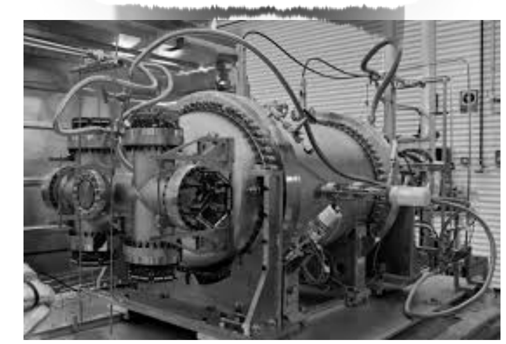

TPC **5 kg** – ntons 10 bars Xe TPC
$\Delta E/E$ = 1% (FWHM) at $Q_{\beta\beta}$

Status of the art

LEGEND

200 kg – 1000 kg of ^{76}Ge diodes
$\Delta E/E$ = 0.1 % (FWHM) at $Q_{\beta\beta}$

CUPID-Mo

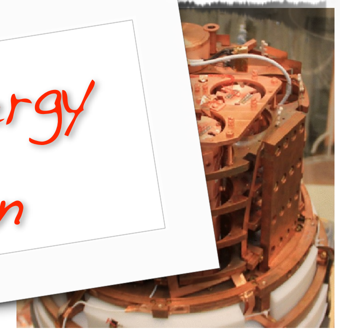

4 kg – 1000 kg of ^{100}Mo bolometers diodes
$\Delta E/E$ = 0.2 % (FWHM) at $Q_{\beta\beta}$

Excellent energy resolution

SuperNEMO

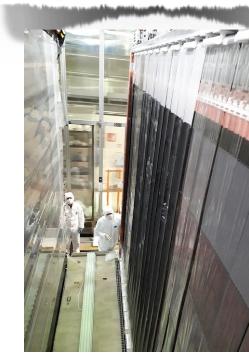

Tracko-calo **7** – 100 kg ^{82}Se foil
$\Delta E/E$ = 5% (F M) at Q

Tracking

KamLAND-ZEN

800 kg of 136Xe dissolved in liquid scintillator
$\Delta E/E$ = 10 % (FWHM) at $Q_{\beta\beta}$

EXO-200

200 kg – n tons of liquid xenon
$\Delta E/E$ = 3 % (FWHM) at $Q_{\beta\beta}$

Large masses

NEXT-White

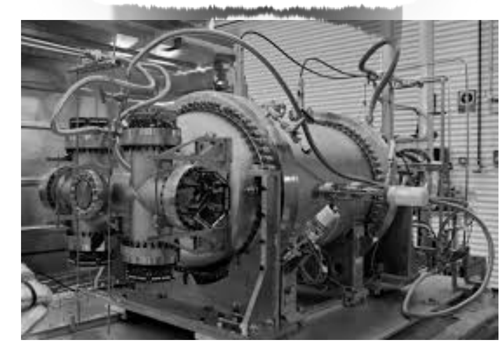

TPC **5 kg** – ntons 10 bars Xe TPC
$\Delta E/E$ = 1% (FWHM) at $Q_{\beta\beta}$

Status of the art

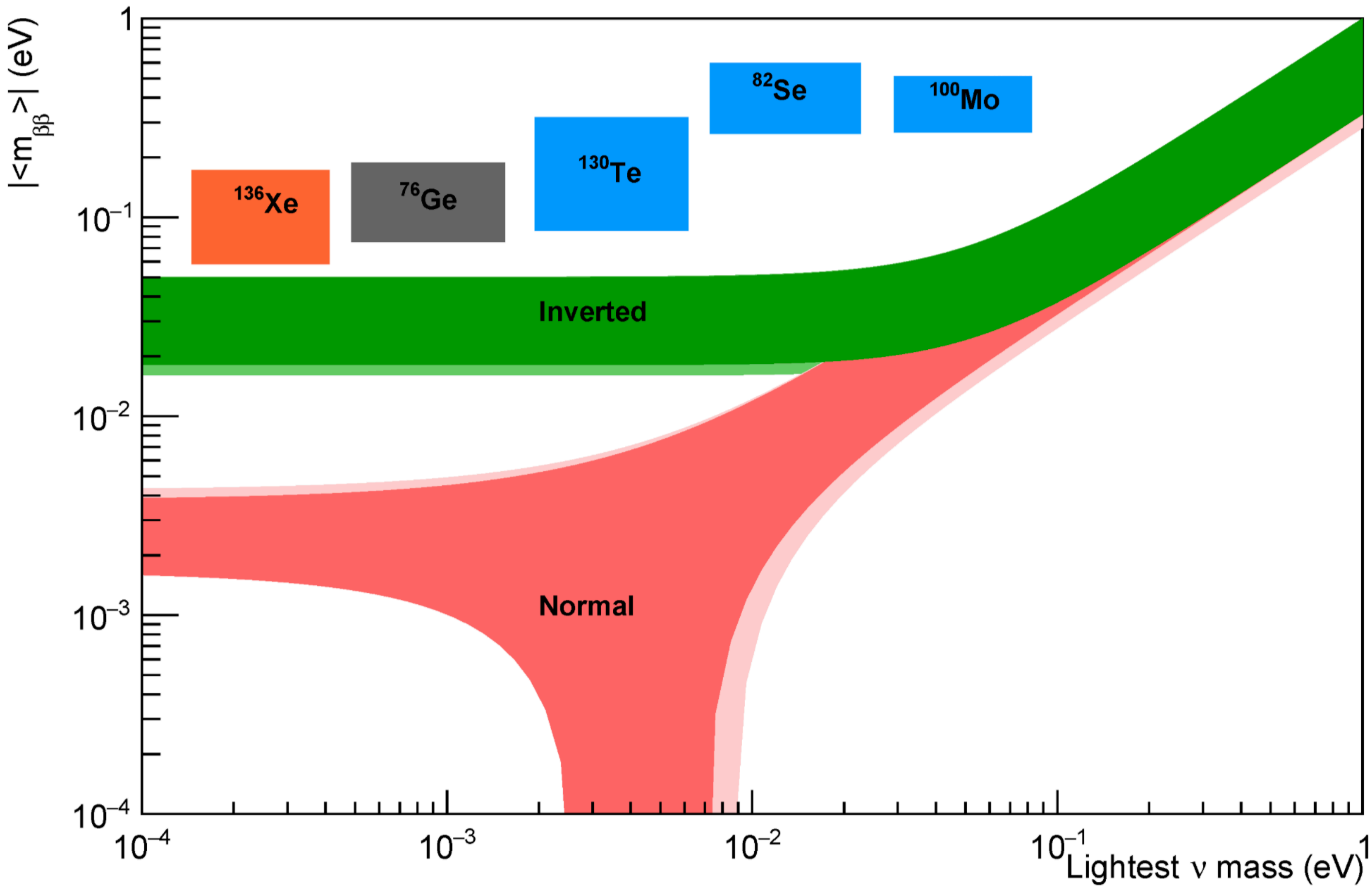

Status of the art

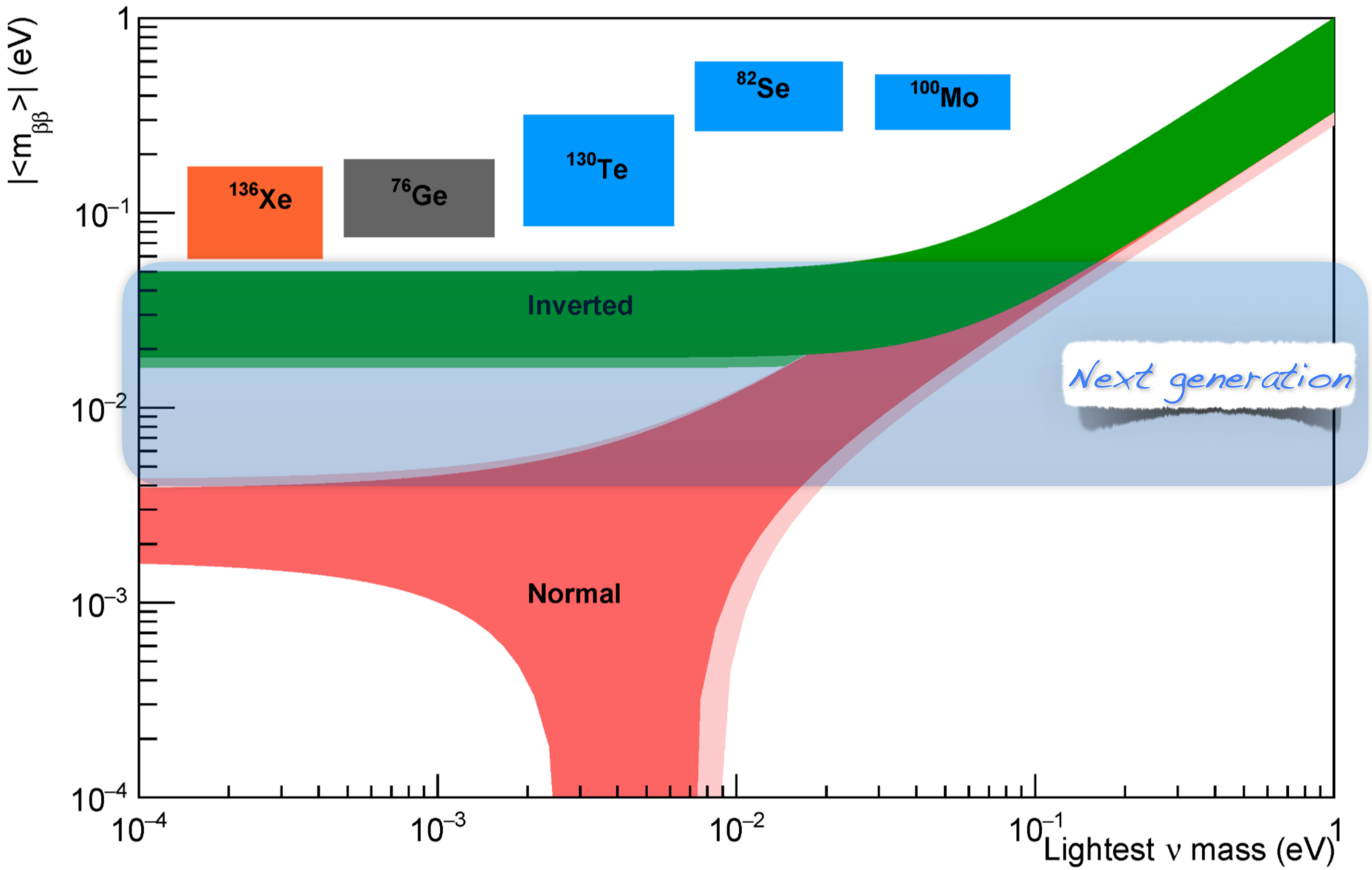

Birth of R2D2

- The three **main requirements** to search for $0\nu\beta\beta$ decay are:

Birth of R2D2

- The three **main requirements** to search for $0\nu\beta\beta$ decay are:

Excellent energy resolution

Birth of R2D2

- The three **main requirements** to search for $0\nu\beta\beta$ decay are:

Excellent energy resolution

Low background

Birth of R2D2

- The three **main requirements** to search for $0\nu\beta\beta$ decay are:

Excellent energy resolution

Low background

Large masses of isotopes

Birth of R2D2

- The three **main requirements** to search for 0νββ decay are:

Excellent energy resolution

Low background

Large masses of isotopes

→ Can we meet all the requirements at the same time?

Birth of R2D2

- The three **main requirements** to search for 0νββ decay are:

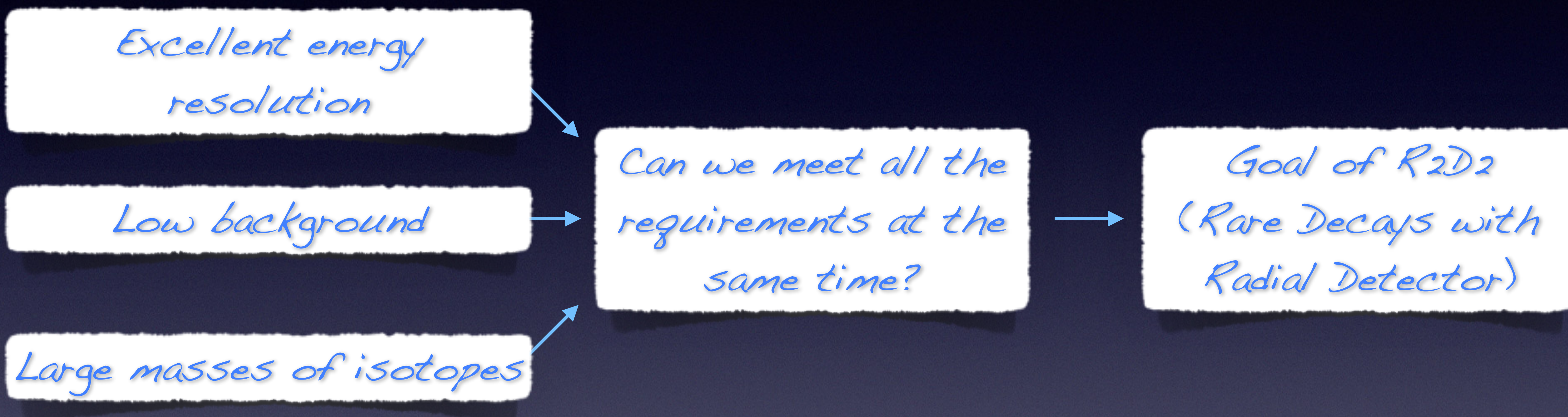

Birth of R2D2

- The three **main requirements** to search for $0\nu\beta\beta$ decay are:

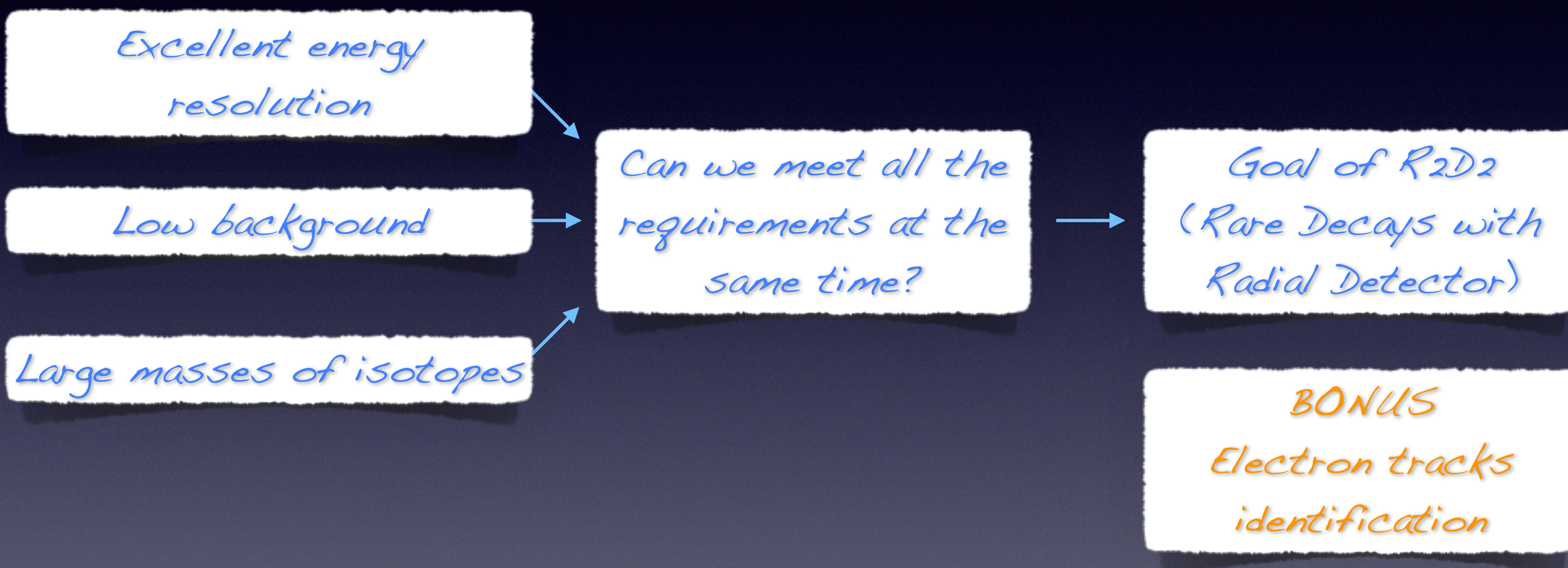

Birth of R2D2

- The three **main requirements** to search for 0νββ decay are:

Excellent energy resolution

Low background

Large masses of isotopes

Can we meet all the requirements at the same time?

Goal of R2D2 (Rare Decays with Radial Detector)

BONUS
Electron tracks identification

- R2D2 is an **R&D program started in 2017** aiming at the development of a **zero background ton scale detector** to search for the neutrinoless double beta decay.

How?

Using a radial high pressure xenon TPC

Two geometrical options

- **Two options** were considered in the R&D: a **spherical** Xenon gas TPC (**STPC**) as used today in the NEWS-G collaboration for the search of dark matter by Giomataris et al., and a **cylindrical** TPC (**CTPC**).
- The working principle is the same.

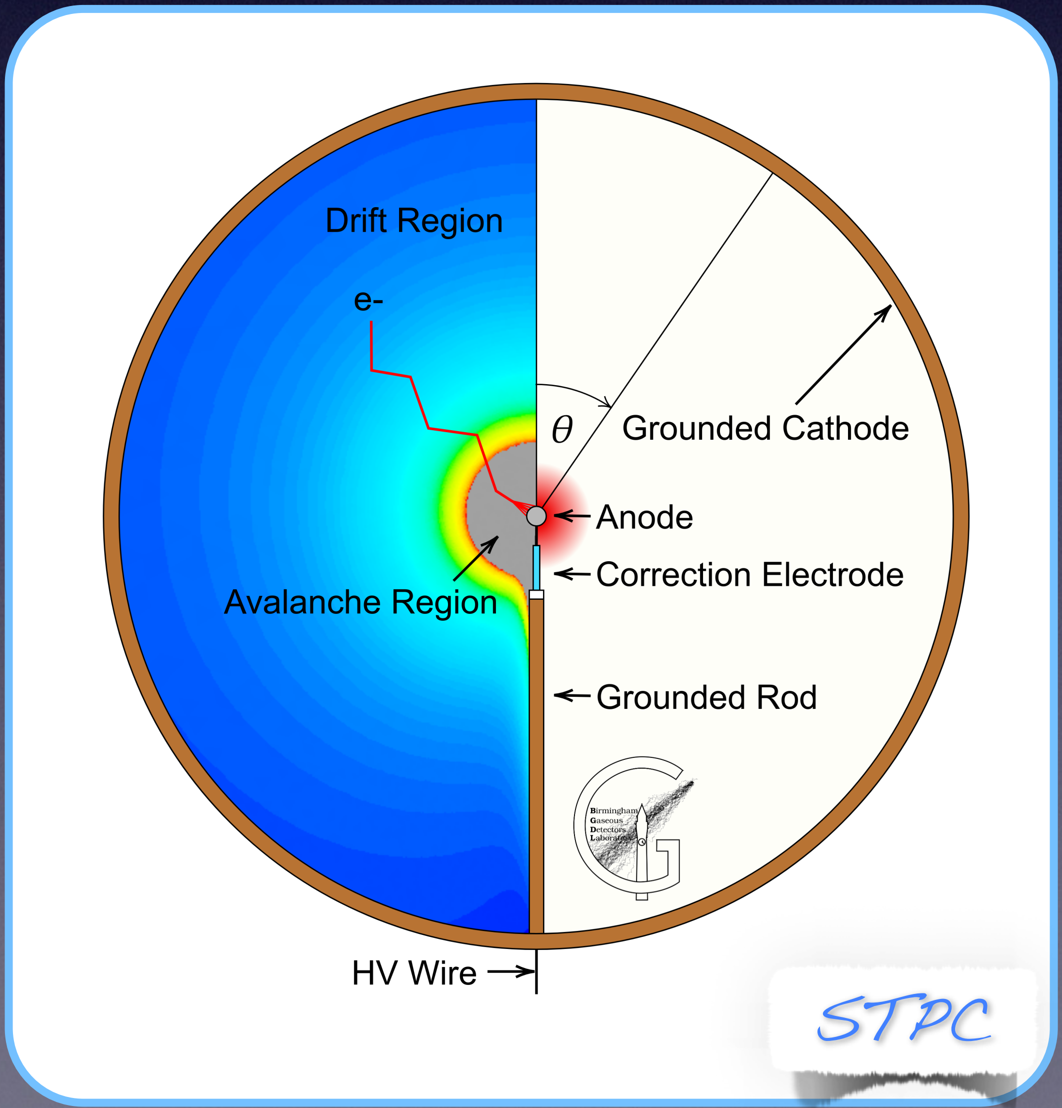

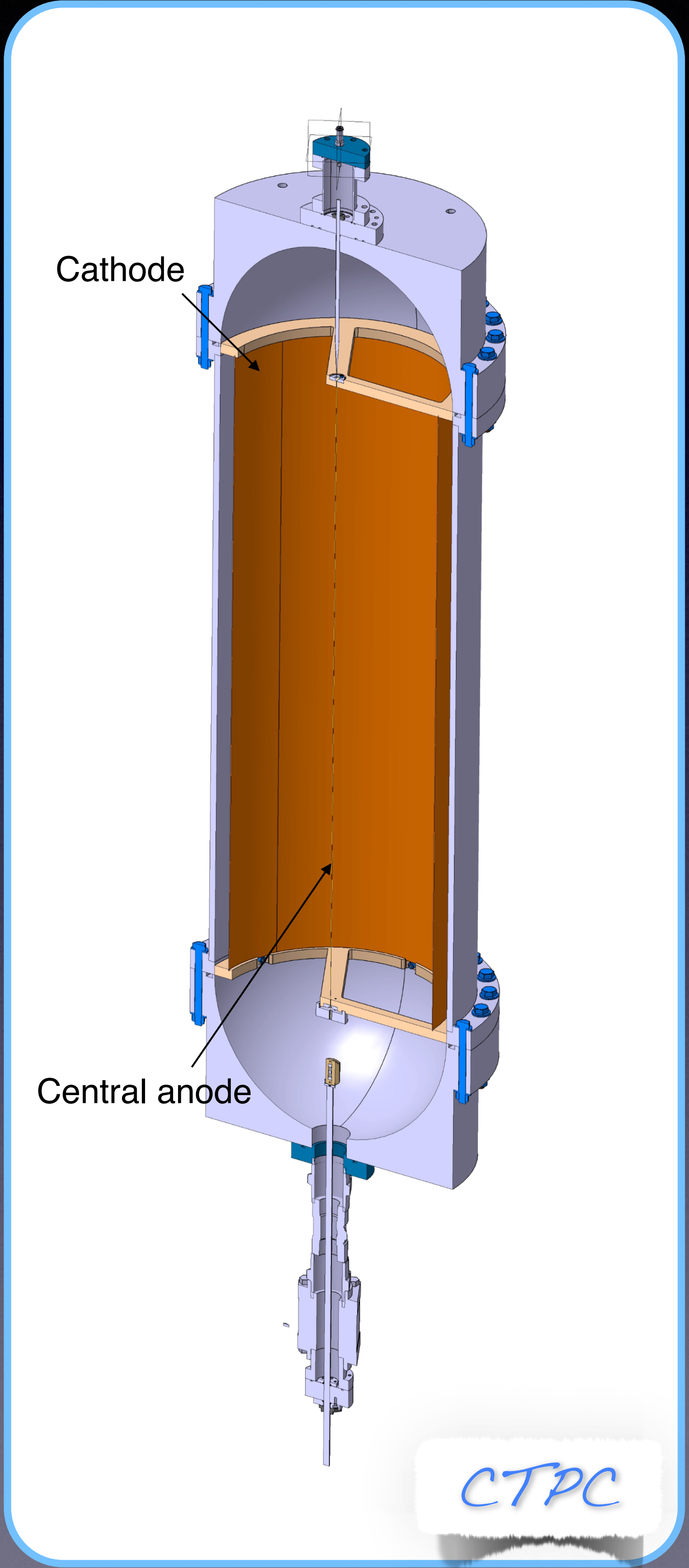

Two geometrical options

- **Two options** were considered in the R&D: a **spherical** Xenon gas TPC (**STPC**) as used today in the NEWS-G collaboration for the search of dark matter by Giomataris et al., and a **cylindrical** TPC (**CTPC**).
- The working principle is the same.
- Both geometries have in principle the needed detector features.

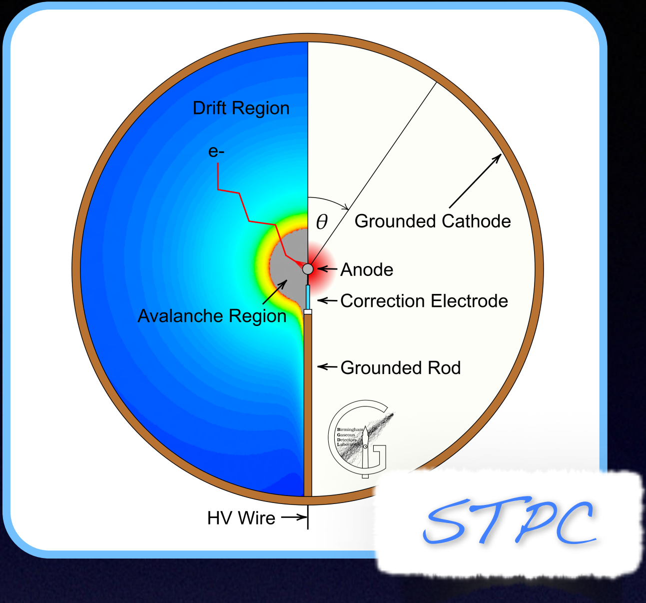

Detector features

- Excellent energy resolution (goal of 1% FWHM at ^{136}Xe $Q_{\beta\beta}$).
- Extremely low background due to the very low material budget.
- Scalability to large isotope masses.
- Simplicity of the detector readout with only one readout channel.

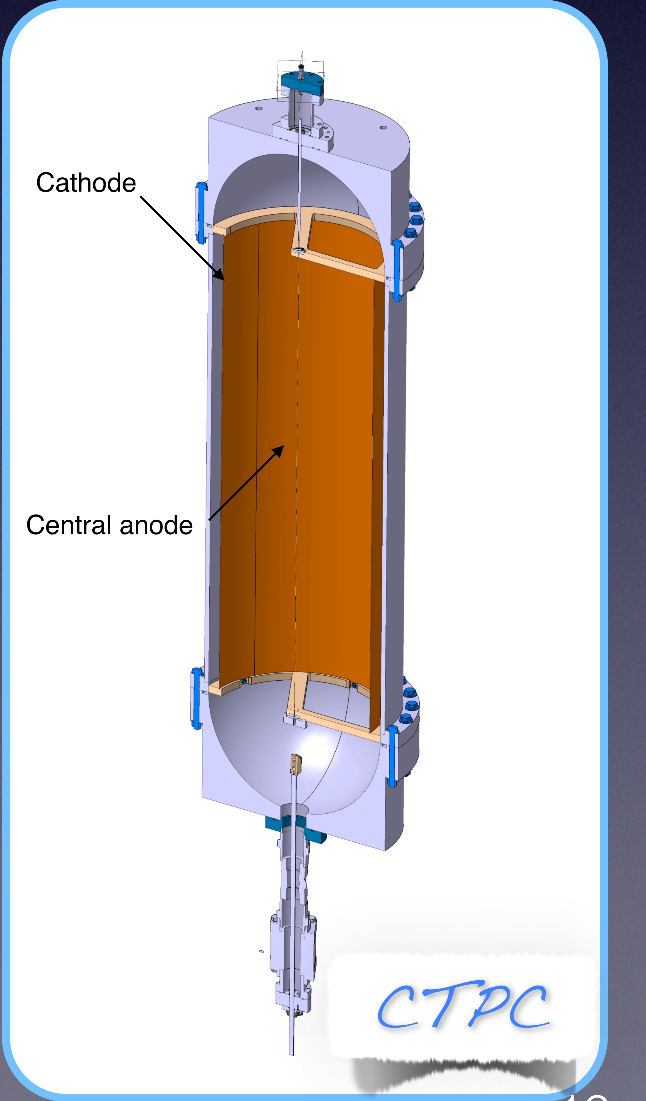

Two geometrical options

- **Two options** were considered in the R&D: a **spherical** Xenon gas TPC (**STPC**) as used today in the NEWS-G collaboration for the search of dark matter by Giomataris et al., and a **cylindrical** TPC (**CTPC**).
- The working principle is the same.
- Both geometries have in principle the needed detector features.

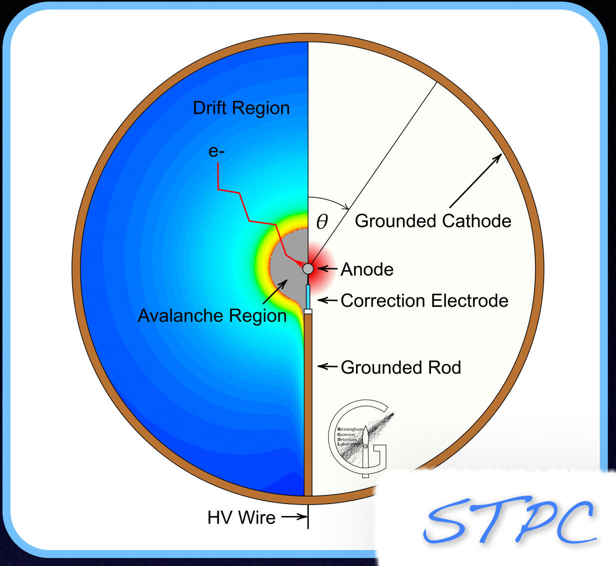

Detector features

- Excellent energy resolution (goal of 1% FWHM at ^{136}Xe $Q_{\beta\beta}$).
  Main goal of the R2D2 R&D NOW VALIDATED
- Extremely low background due to the very low material budget.
  Ongoing R&D with innovative materials (see later)
- Scalability to large isotope masses.
- Simplicity of the detector readout with only one readout channel.
  True by conception

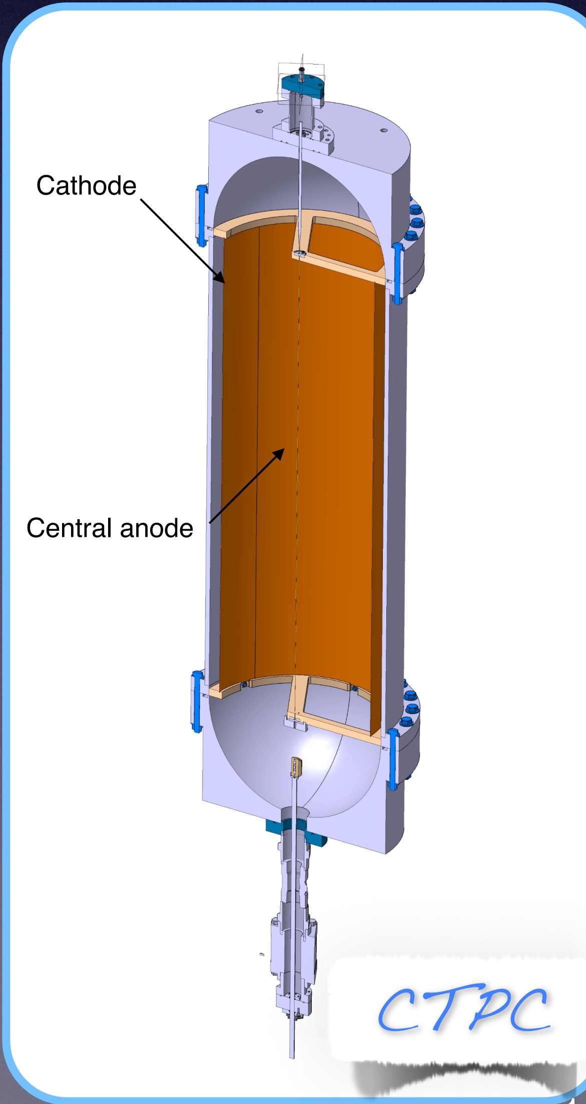

Two geometrical options

	STPC	CTPC
Field Uniformity	Issues around the supporting rod	Homogeneous around the anodic wire
Field Strength	Weak at cathode ($1/R^2$)	Stronger at cathode ($1/R$)
Xenon volume	Optimal Volume/Surface	Volume/Surface not maximised
Noise	HV dependent (positive HV on anode)	HV independent (negative HV on cathode and grounded anodic wire)

Two geometrical options

Considering the advantages, CTPC is the baseline option for R2D2

	STPC	CTPC
Field Uniformity	Issues around the supporting rod	Homogeneous around the anodic wire
Field Strength	Weak at cathode ($1/R^2$)	Stronger at cathode ($1/R$)
Xenon volume	Optimal Volume/Surface	Volume/Surface not maximised
Noise	HV dependent (positive HV on anode)	HV independent (negative HV on cathode and grounded anodic wire)

Two operation modes

- The CTPC can be operated in two modes: **ionisation** (i.e. no gain) or **proportional** (i.e. avalanche near the anode with a resulting gain).
- To understand the two modes of operation and appreciate the different pro and cons it has to be reminded that the signal observed is a current induced according to the **Shockley-Ramo theorem**.

Induced current — Weighted electric field

$$I(r) = e \times v_e(r) \times E_w(r)$$

Electron charge — Drift radial velocity

- The electric field in a CTPC can be described as:

Electric field — Weighted electric field

$$E(r) = V_0 \times E_w(r) = V_0 \times \frac{1}{r} \times \frac{1}{log(r_{cathode}/r_{anode})}$$

Potential difference between anode and cathode — Cathode and anode radii

Two operation modes

ionisation

IONISATION

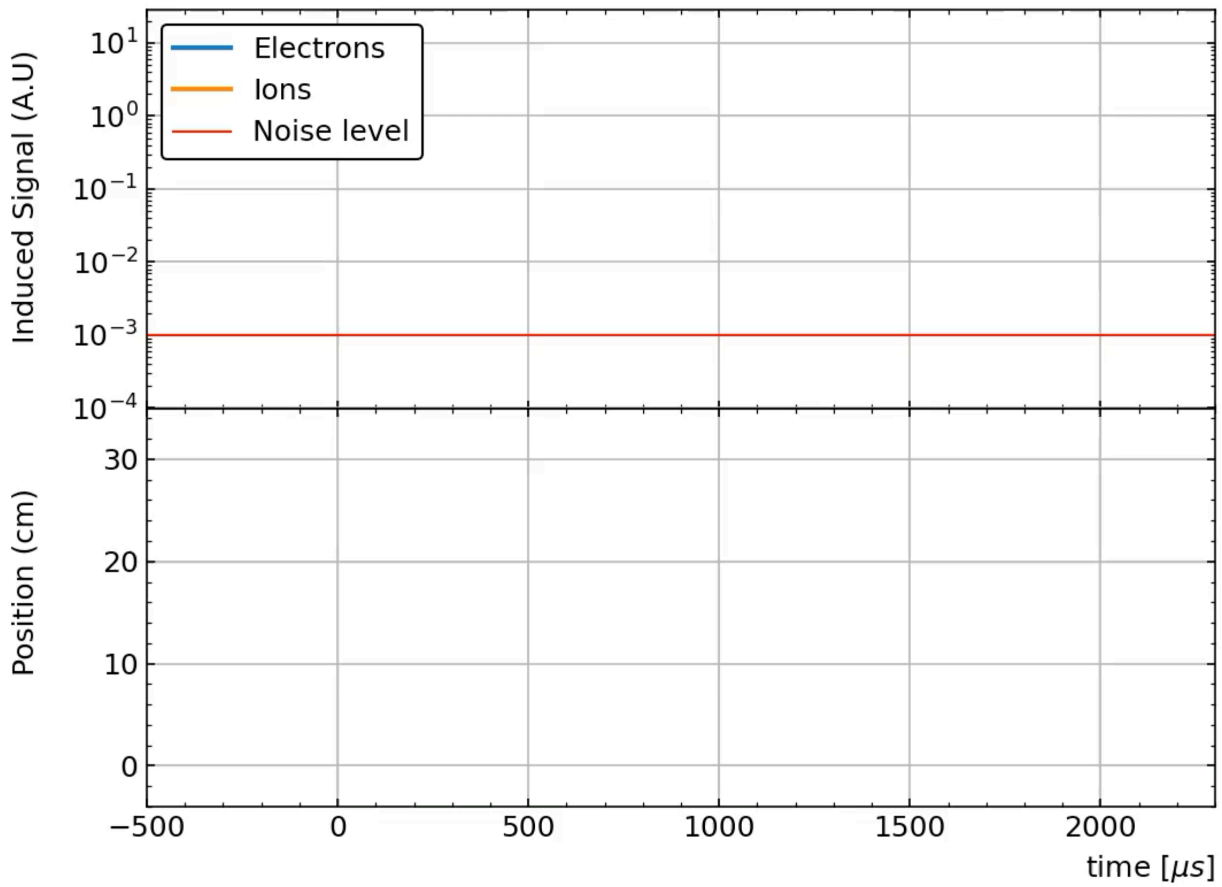

Anode

Two operation modes

ionisation

IONISATION

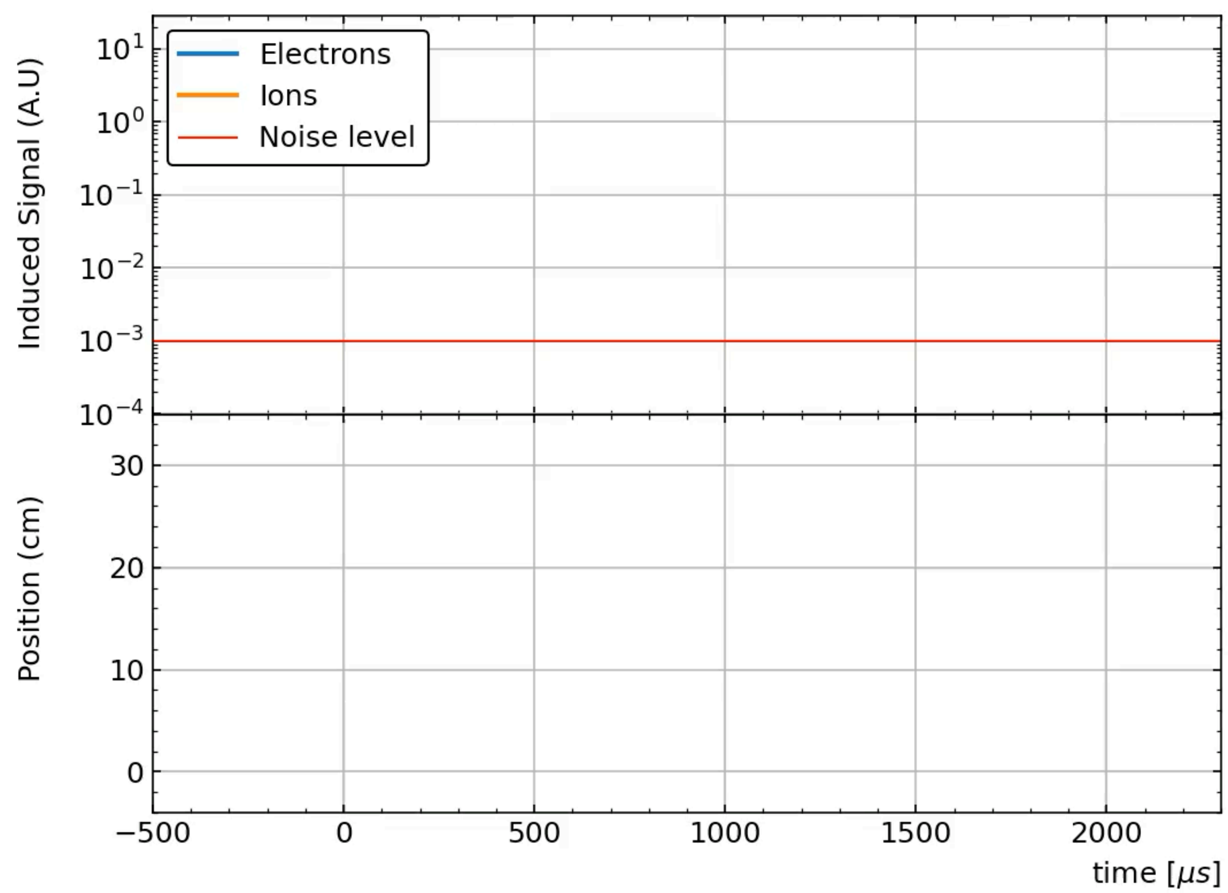

Anode

Two operation modes

ionisation

IONISATION

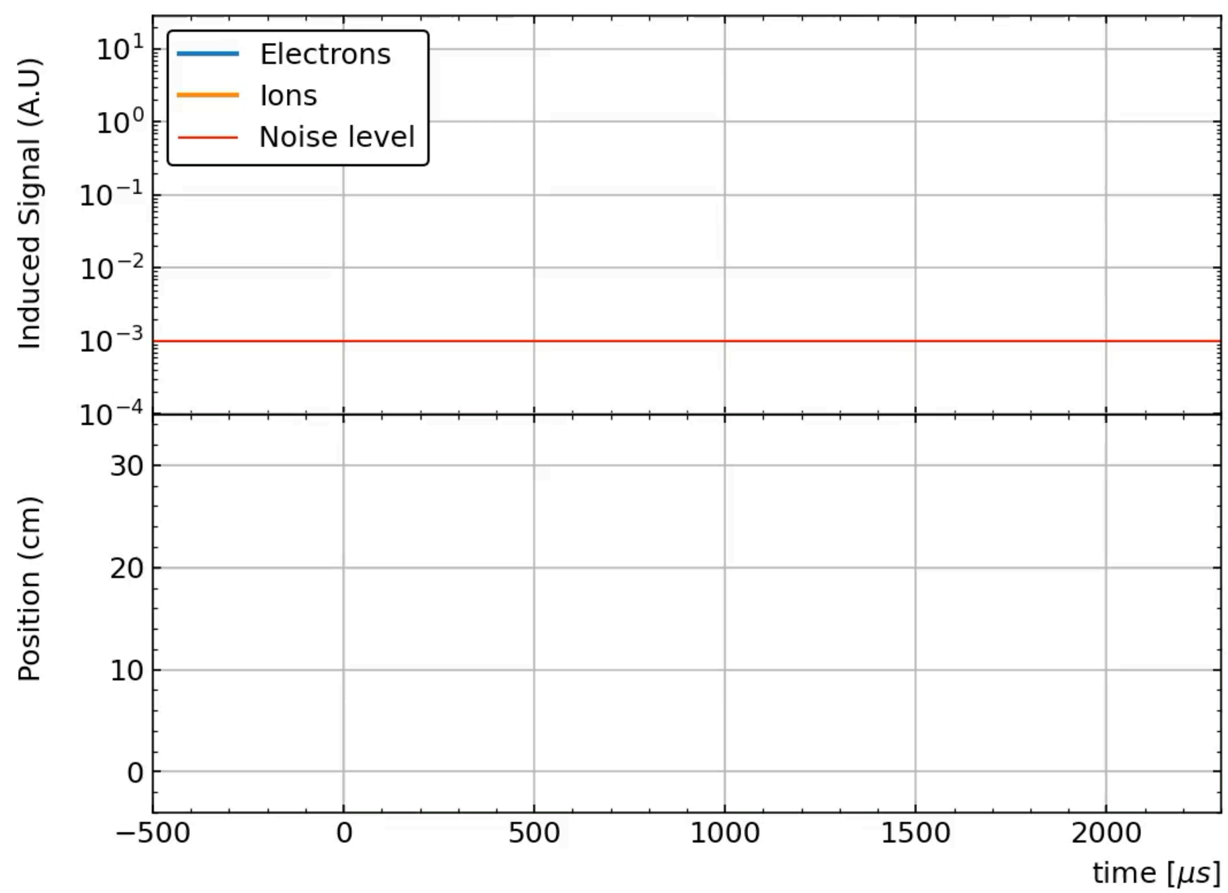

Anode

Two operation modes

ionisation

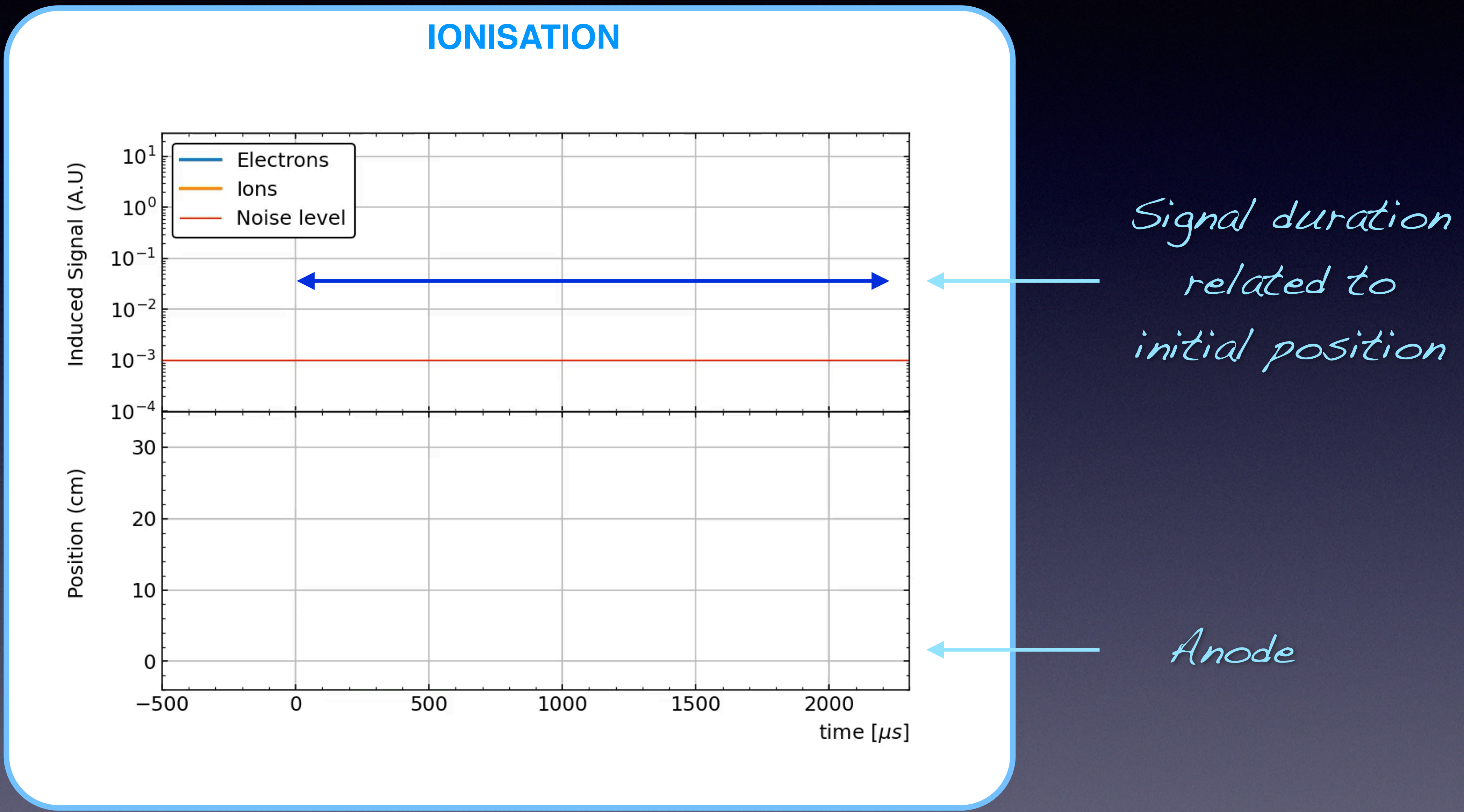

- The signal is due by the **drift of the electrons** wherease the signal due to ions is typically below throshod due to the low mobility.
- The signal with is **directly related to the radial position of the energy deposit**.

Two operation modes

proportional

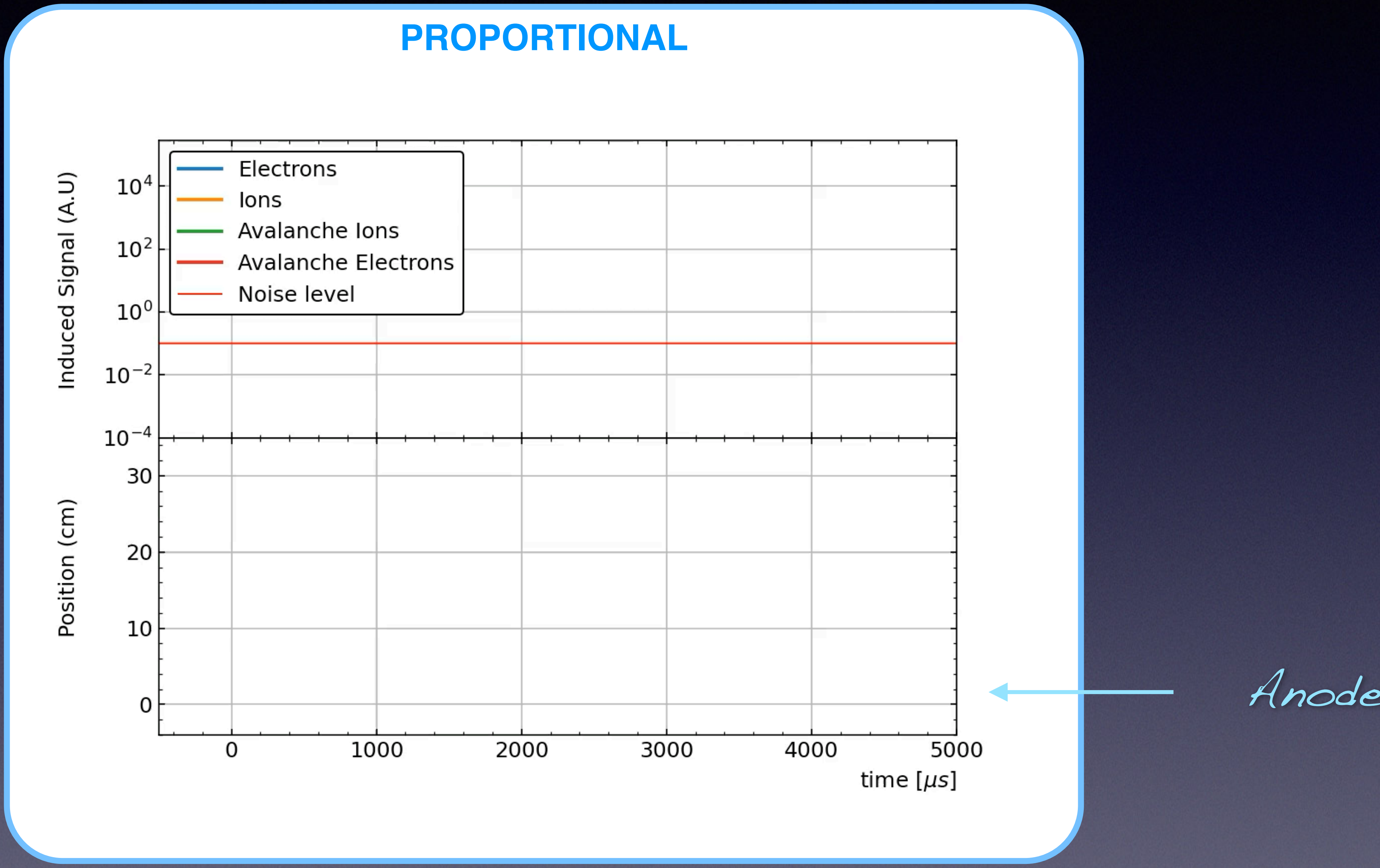

Two operation modes

proportional

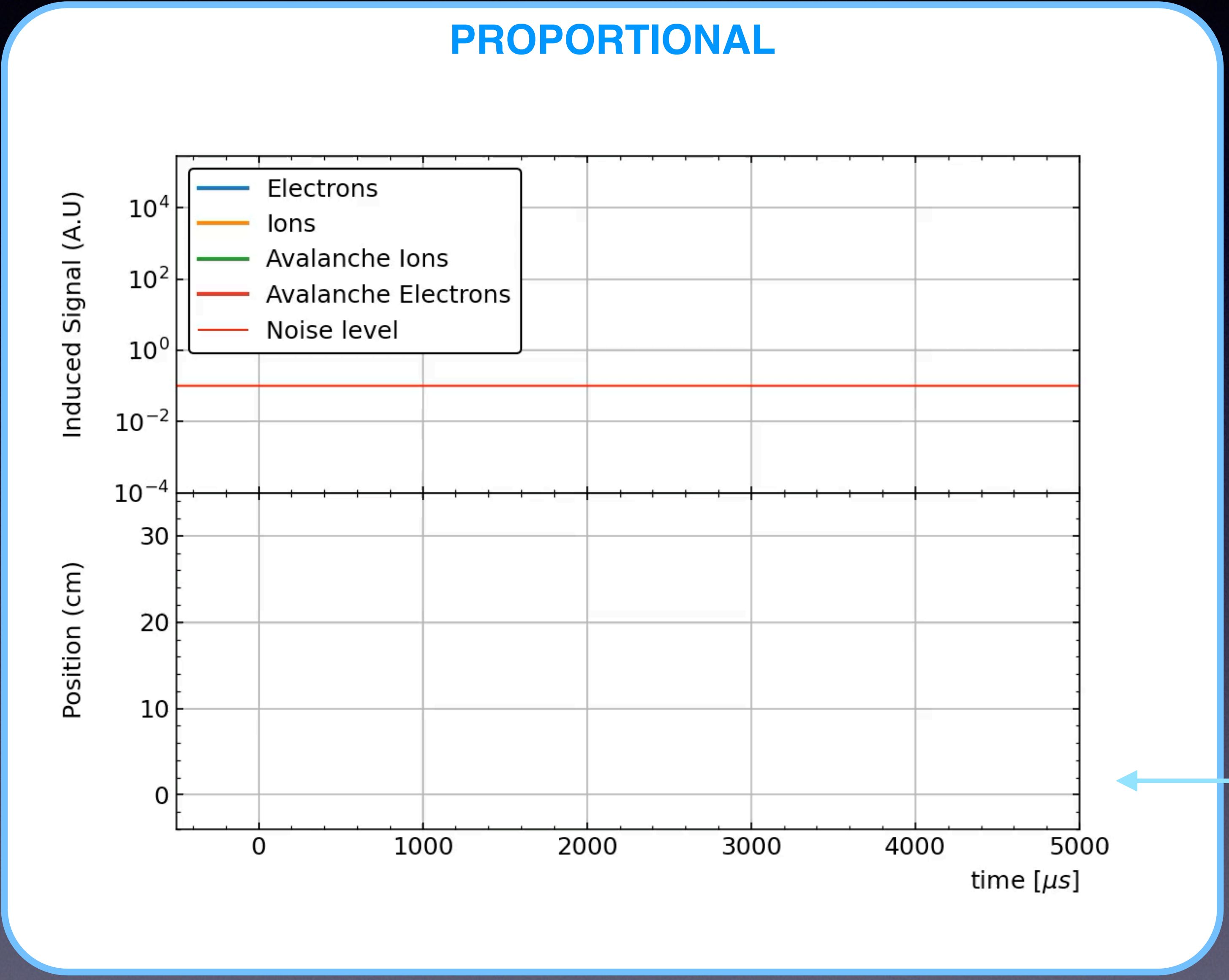

Anode

Two operation modes

proportional

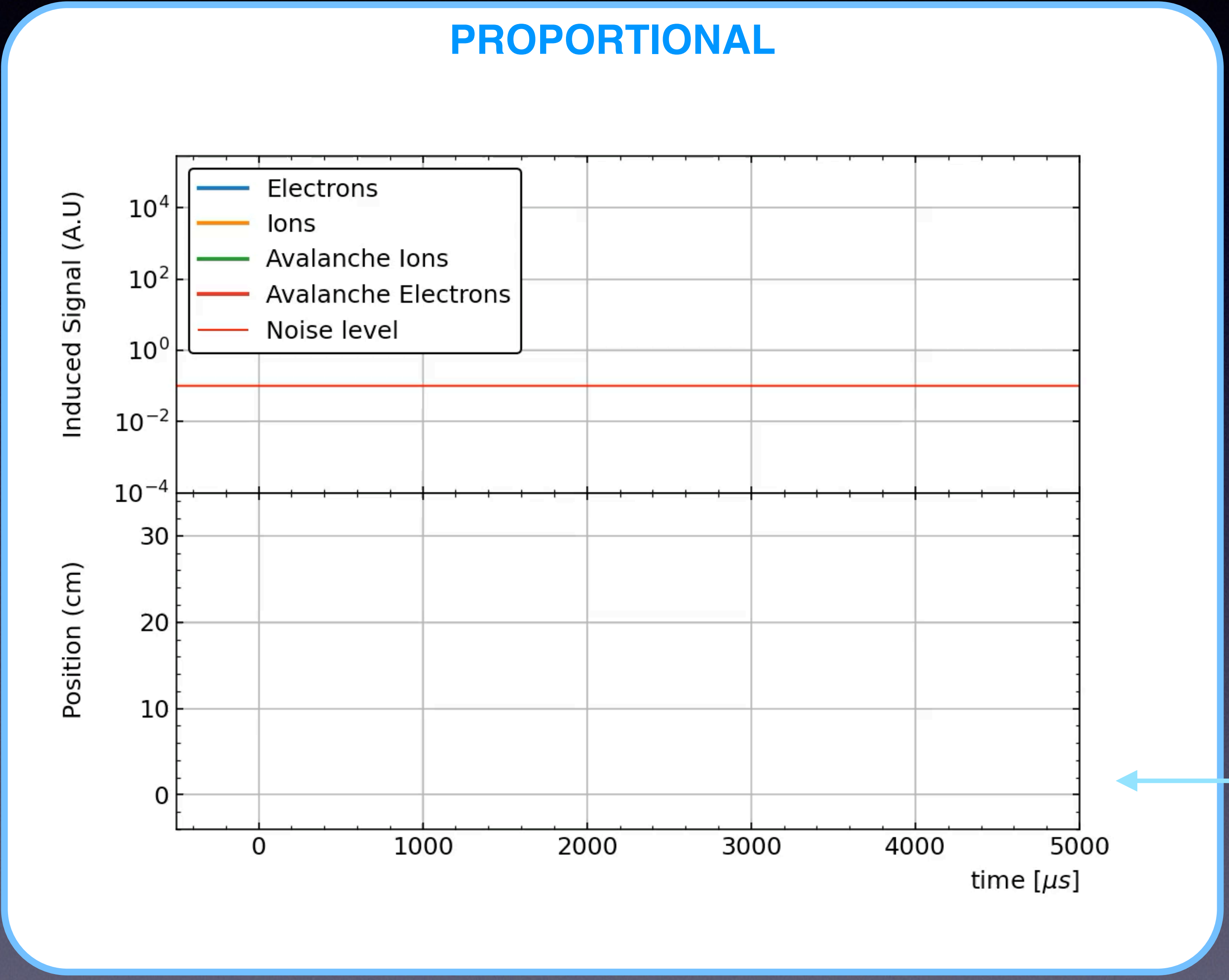

Anode

Two operation modes

proportional

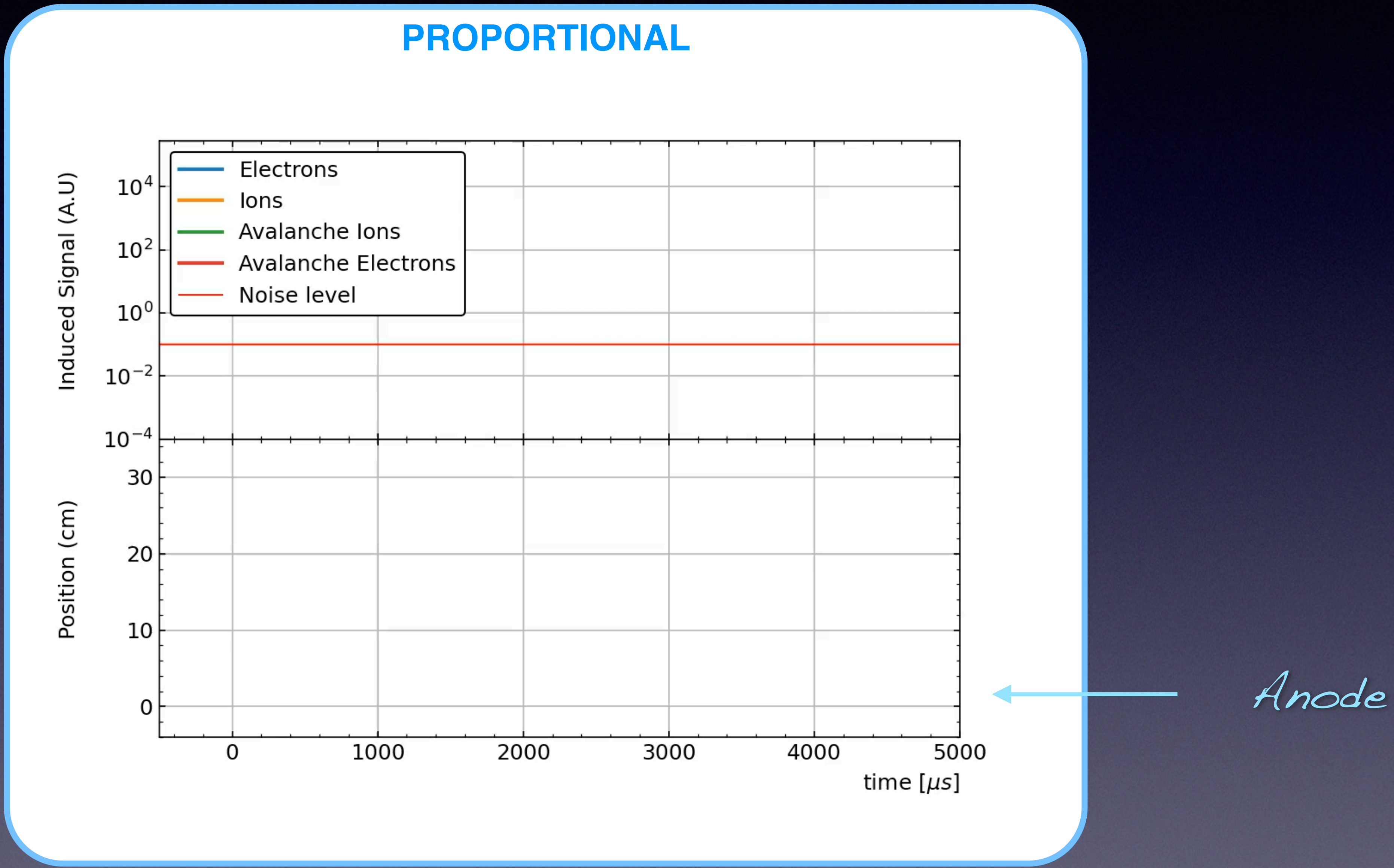

- The signal is due by the **drift of the ions** produced in the avalanche.
- The signal with is **only weakly related to the radial position of the energy deposit** (through the arrival time of the primaries i.e. through the risetime).

Two operation modes

Two operation modes

Detector operated in ionisation mode

Two operation modes

Detector operated in ionisation mode

Best possible energy resolution avoiding any stochastic fluctuation due to the avalanche process

Two operation modes

Detector operated in ionisation mode

Best possible energy resolution avoiding any stochastic fluctuation due to the avalanche process

No impact of wire inhomogeneities (different gain in proportional mode)

Two operation modes

Detector operated in ionisation mode

Best possible energy resolution avoiding any stochastic fluctuation due to the avalanche process

No impact of wire inhomogeneities (different gain in proportional mode)

Smaller impact of electronegative impurities (signal given by electrons with much higher mobility than ions)

Two operation modes

Detector operated in ionisation mode

Best possible energy resolution avoiding any stochastic fluctuation due to the avalanche process

No impact of wire inhomogeneities (different gain in proportional mode)

Smaller impact of electronegative impurities (signal given by electrons with much higher mobility than ions)

Less demanding HV (possible use of thick wires)

History and milestones

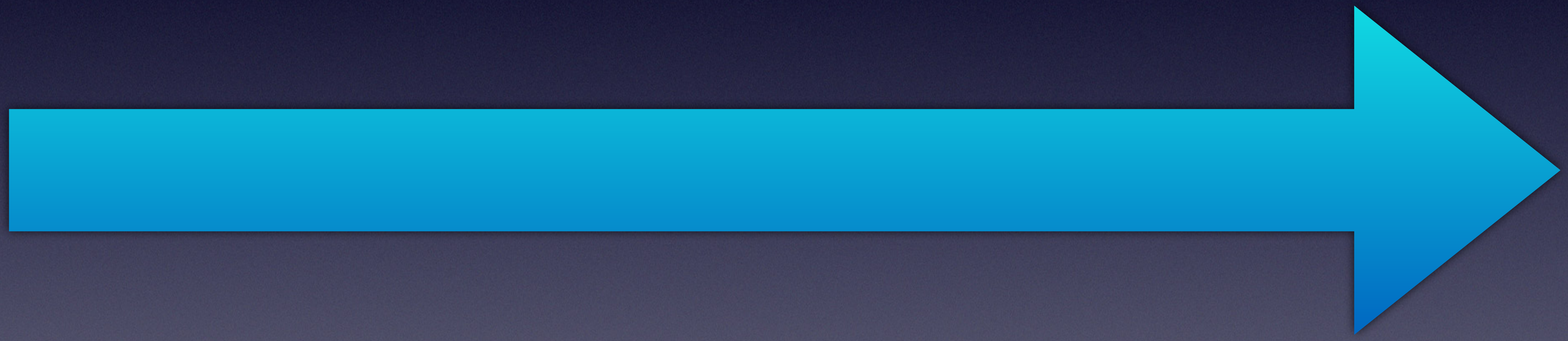

History and milestones

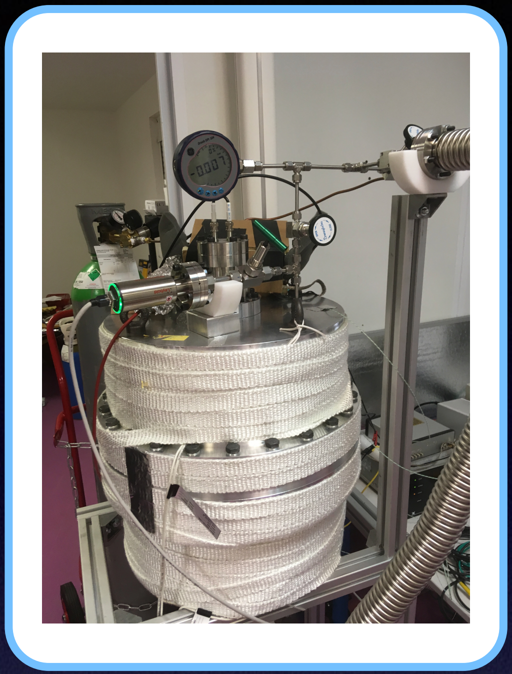

First STPC (no high pressure)

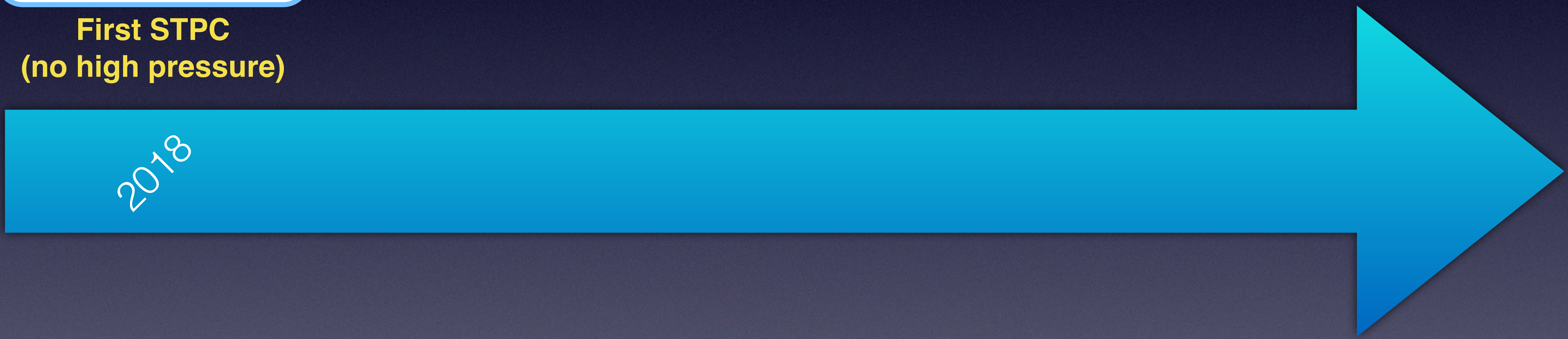

History and milestones

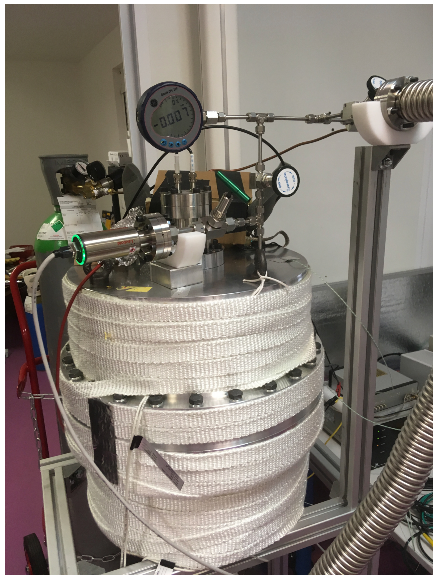

First STPC (no high pressure)

2018

About 3-4 cm tracks

About 15-20 cm tracks

1.1 bar - 2000V

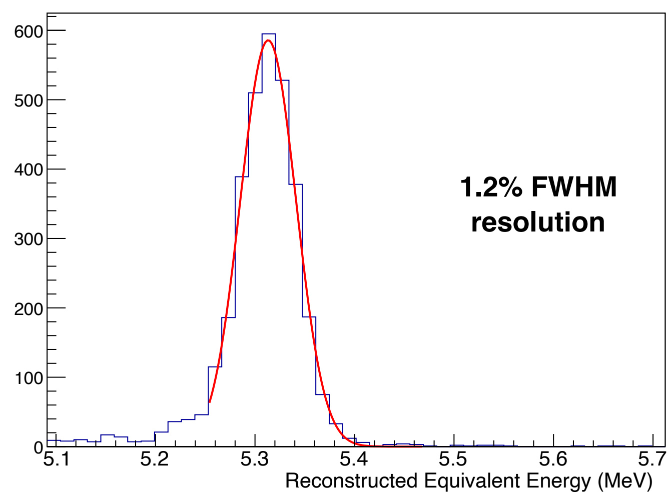

200 mbar - 720 V

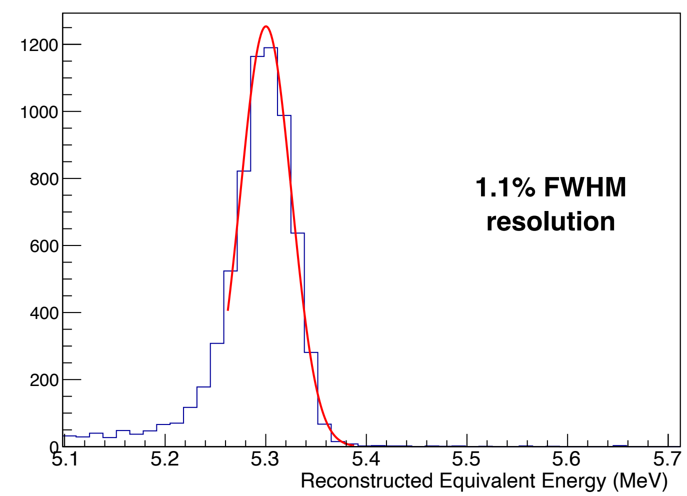

JINST 16 (2021) 03, P03012

Same resolution for short and long tracks (Ar)

History and milestones

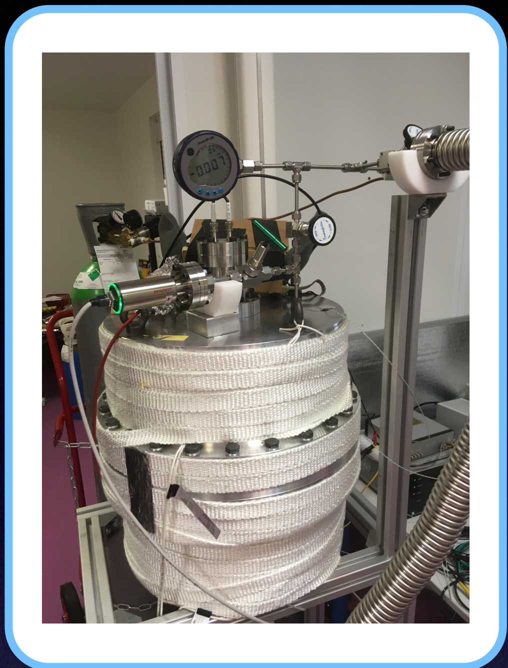

First STPC (no high pressure)

2018

Same resolution for short and long tracks (Ar)

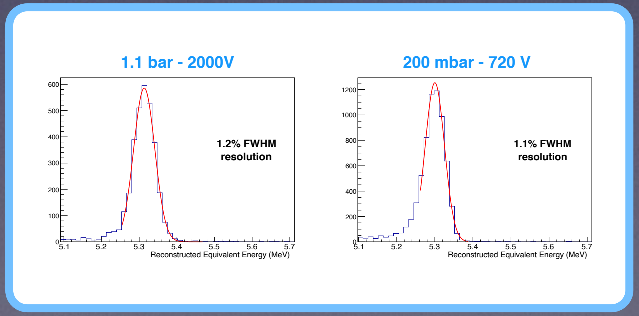

JINST 16 (2021) 03, P03012

History and milestones

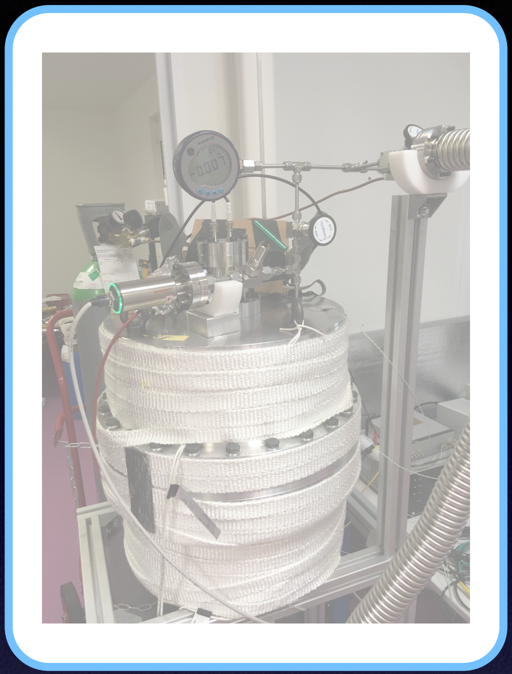

Second STPC
(certified to 40 bar)

2018

2021

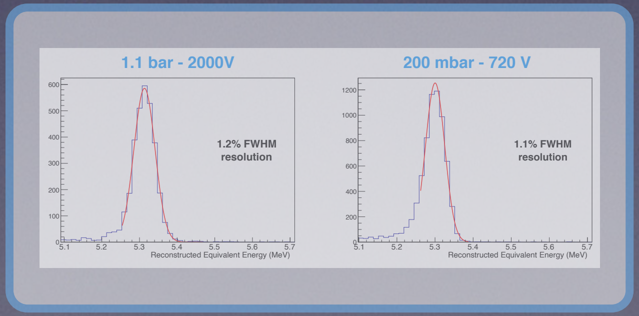

History and milestones

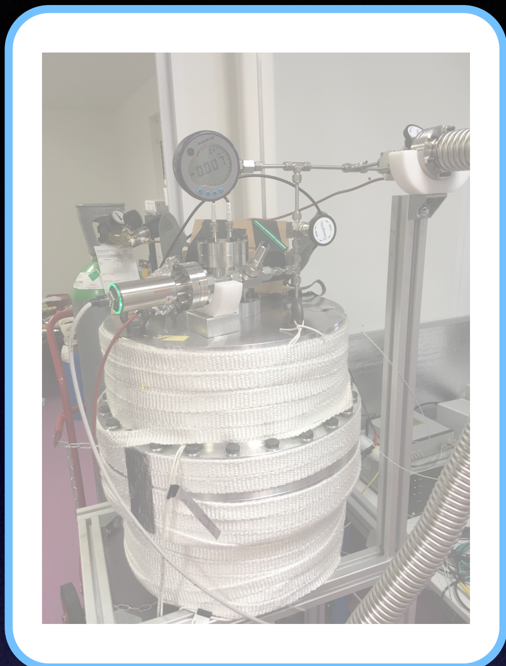

Second STPC (certified to 40 bar)

2018

2021

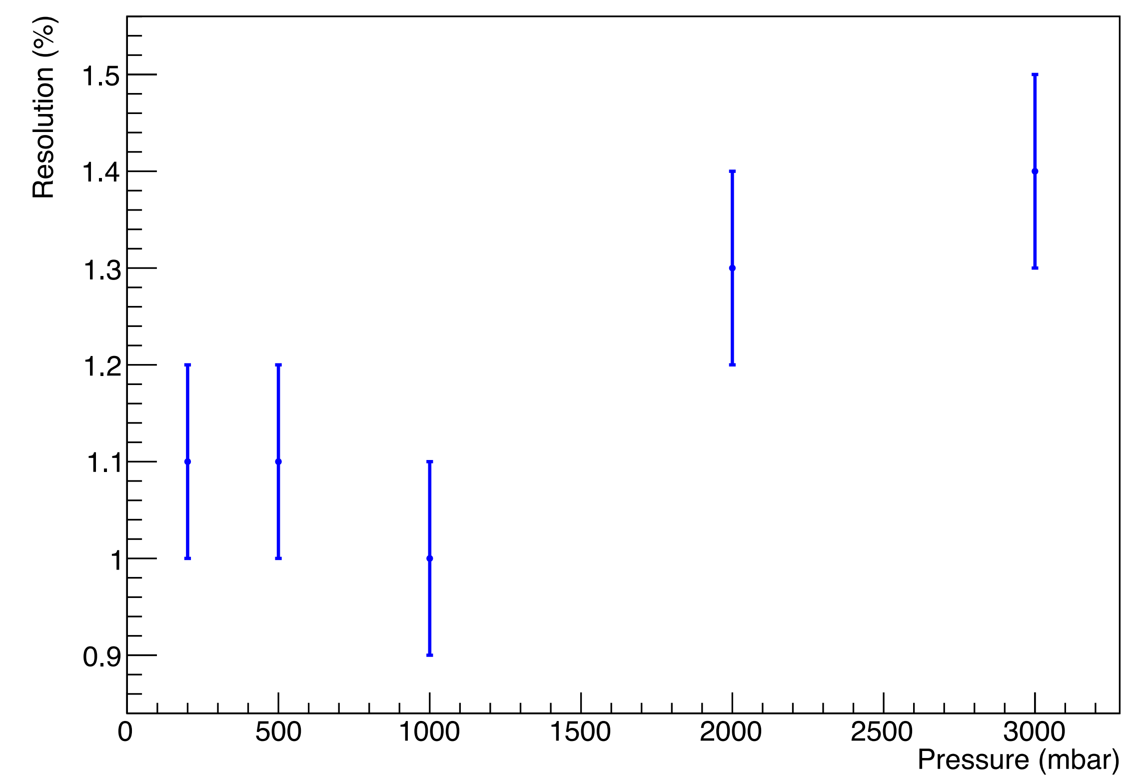

JINST 18(2023) 10, T10001

Stable resolution up to 3 bar Ar (limited by HV at 3900V)

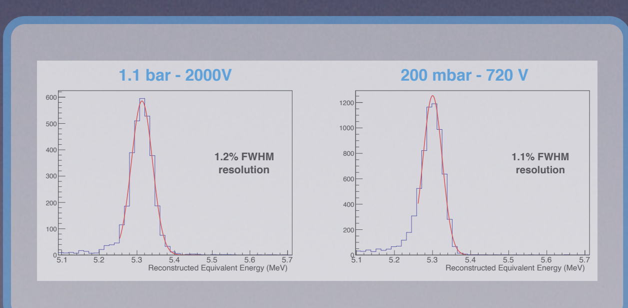

History and milestones

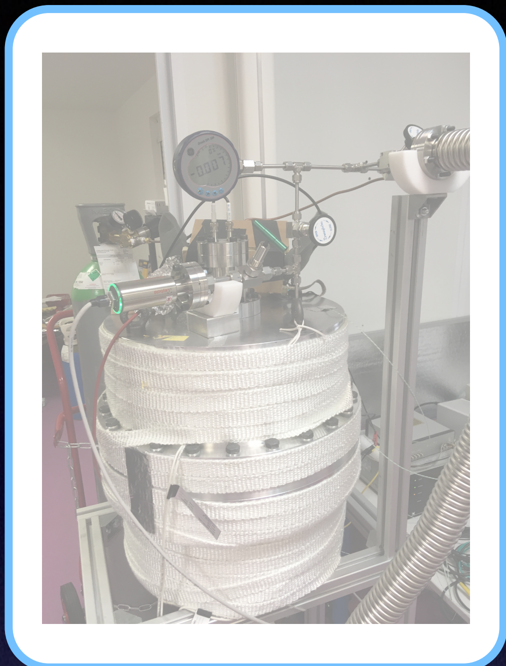

Second STPC (certified to 40 bar)

2018

2021

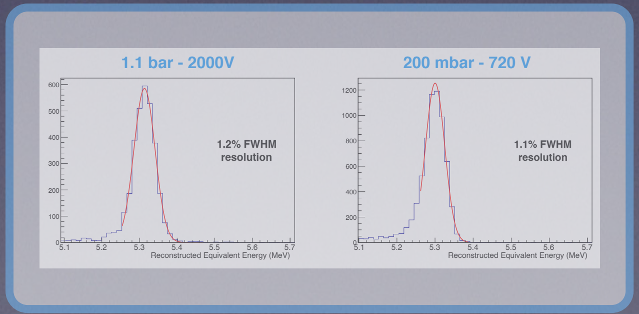

Stable resolution up to 3 bar Ar (limited by HV)

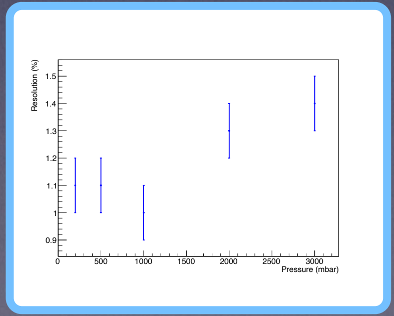

JINST 18(2023) 10, T10001

History and milestones

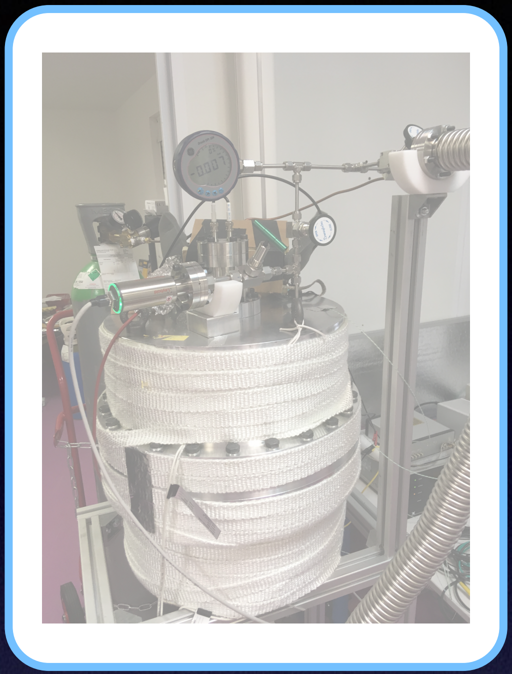

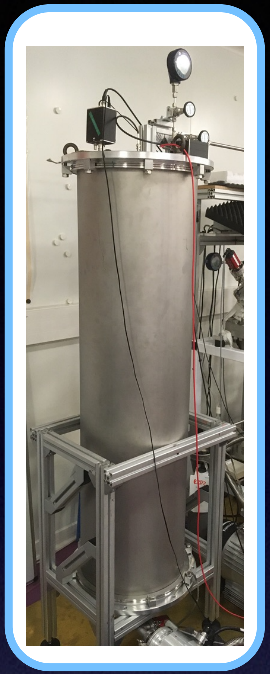

First CTPC (no high pressure)

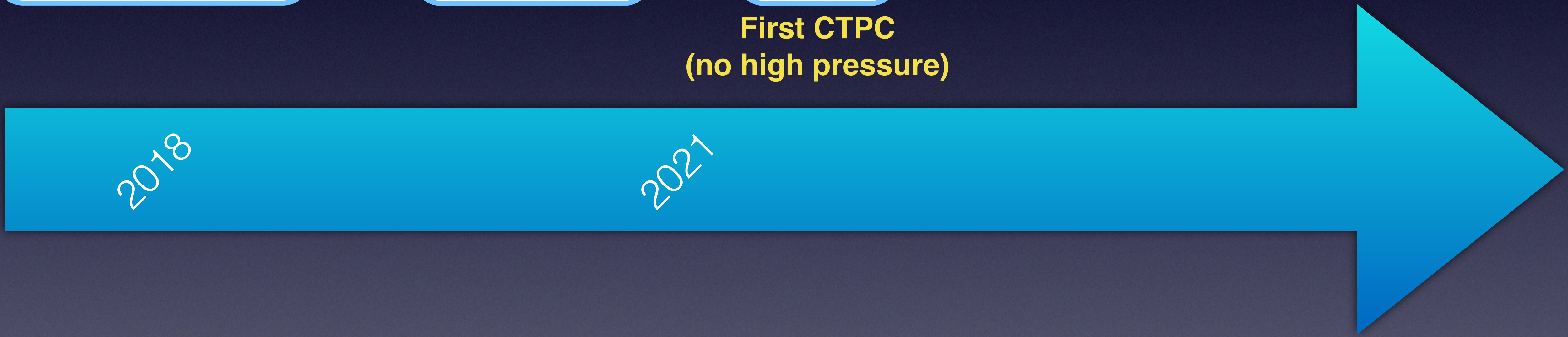

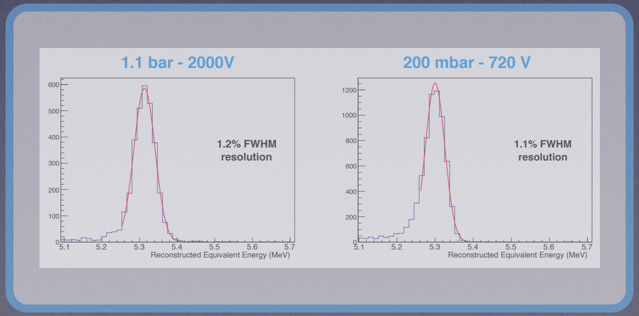

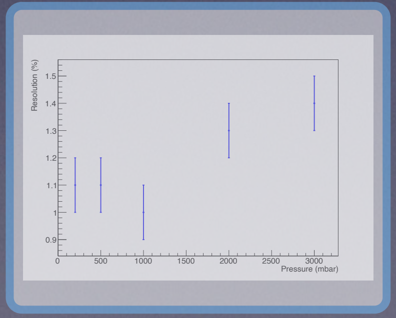

History and milestones

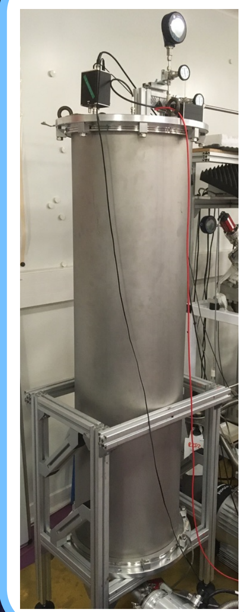

First CTPC
(no high pressure)

021

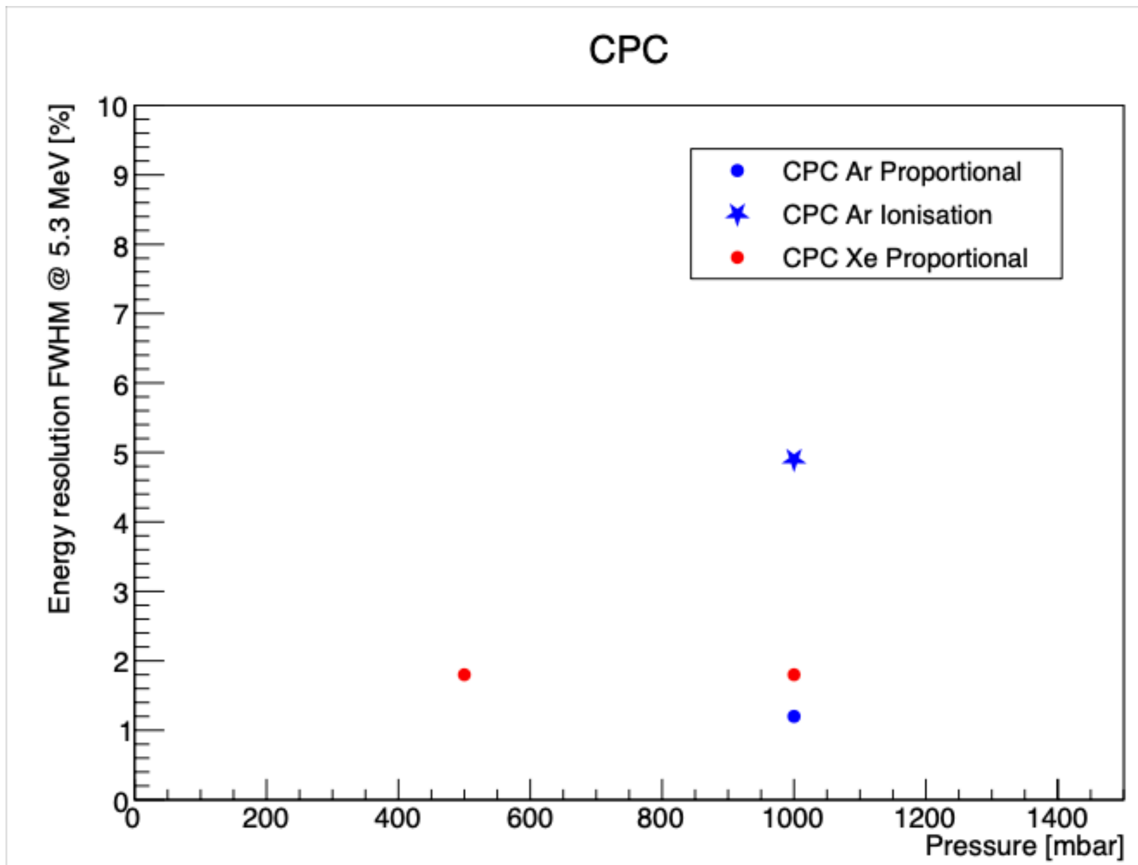

JINST 18(2023) 10, T10001

Similar resolution in Ar and Xe

History and milestones

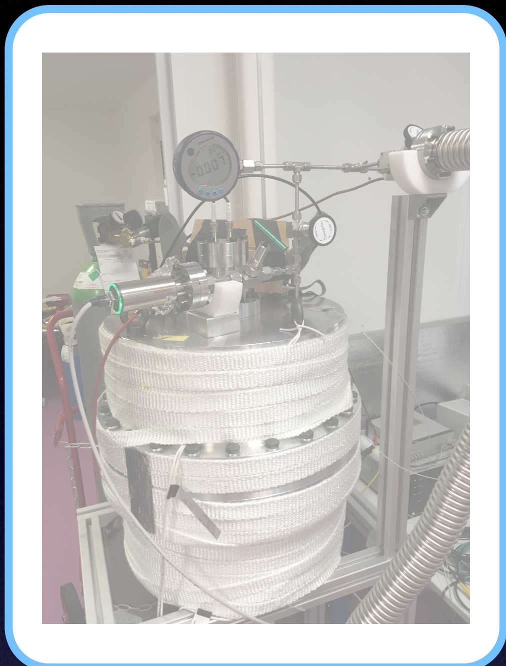

First CTPC
(no high pressure)

2018

2021

Similar resolution
in Ar and Xe

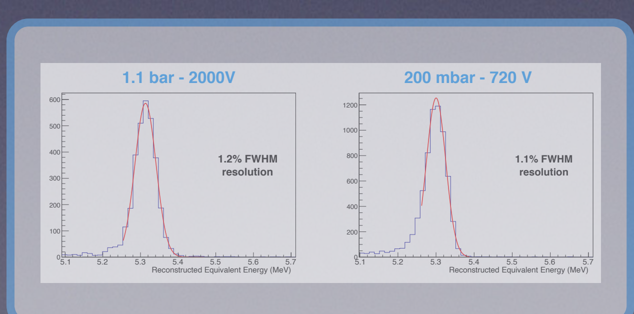

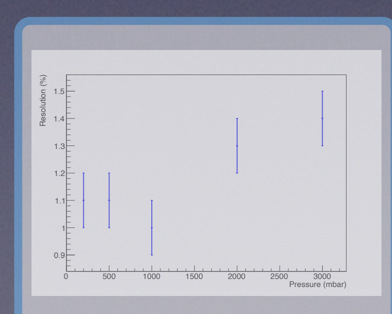

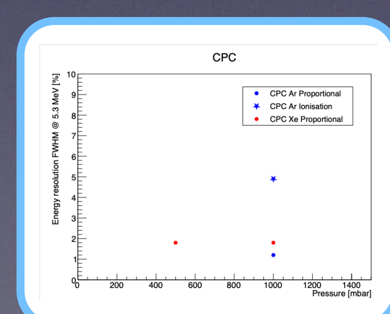

JINST 18(2023) 10, T10001

History and milestones

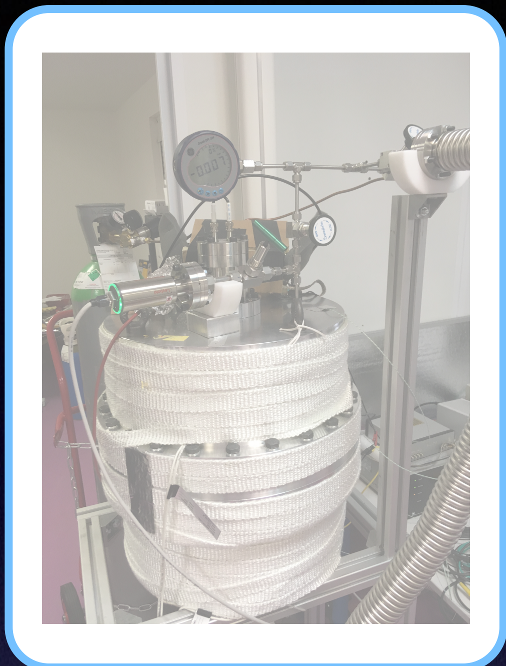

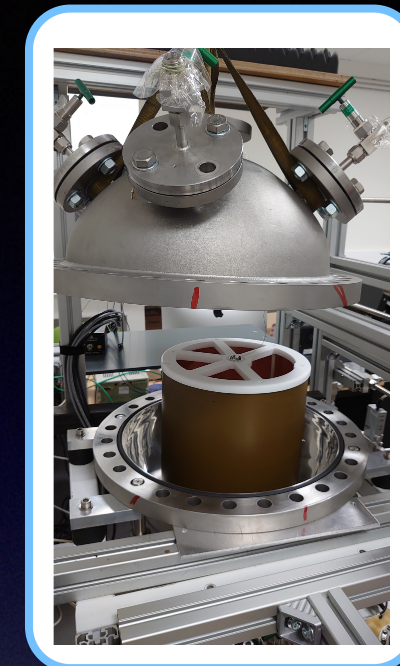

Second CTPC (certified to 40 bar)

2018

2021

2023

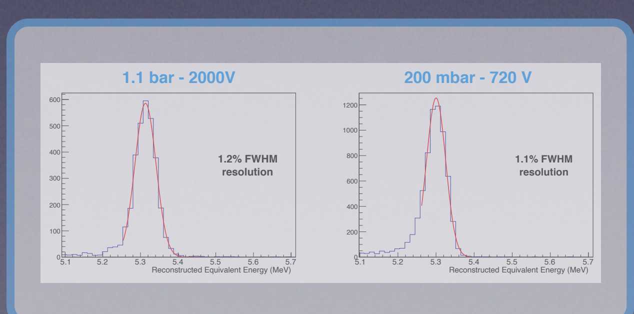

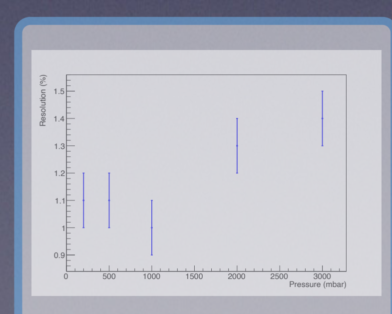

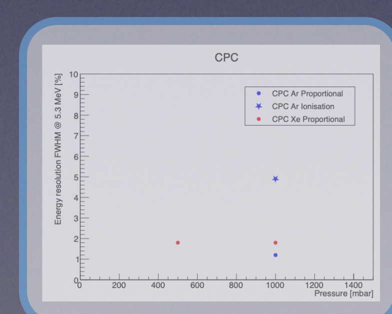

History and milestones

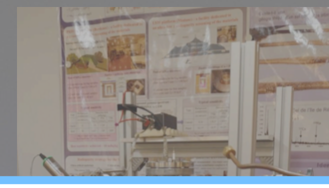

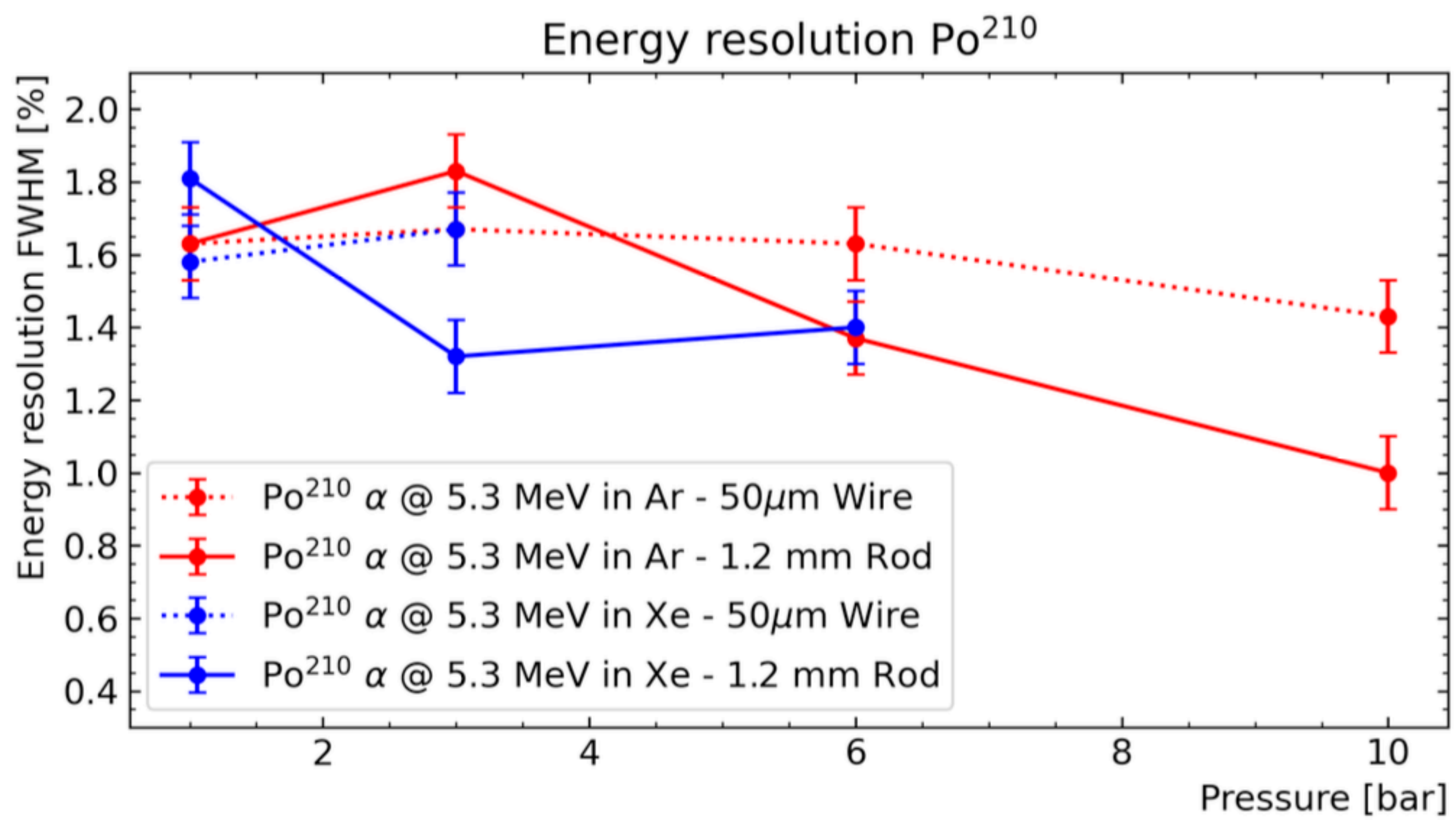

Eur.Phys.J.C 84 (2024) 5, 512

Good resolution in Ar/Xe up to 10/6 bar
(limited by the purification system)

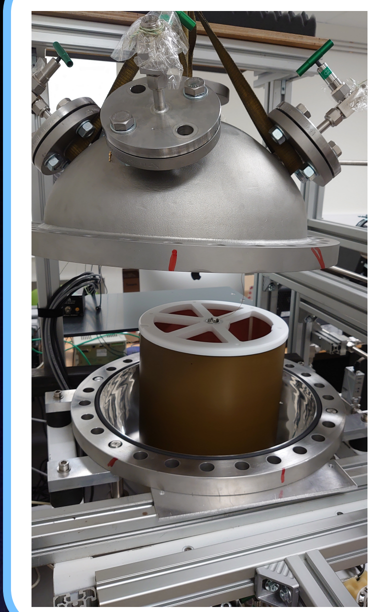

Second CTPC
(certified to 40 bar)

2023

More on these results and on this prototype in the following slides

CTPC 2.0 - prototype design

- The second CPC prototype built in 2023 has a height of 27 cm and a radius of 11 cm. The CTPC is inserted in the previous STPC vessel to take measurements up to 40 bar.
- Measurements of material outgassing were made for the choice of cathode and supporting structure and we finally chose Teflon as supporting structure and a cathode made of 200 μm thick Aluminum.

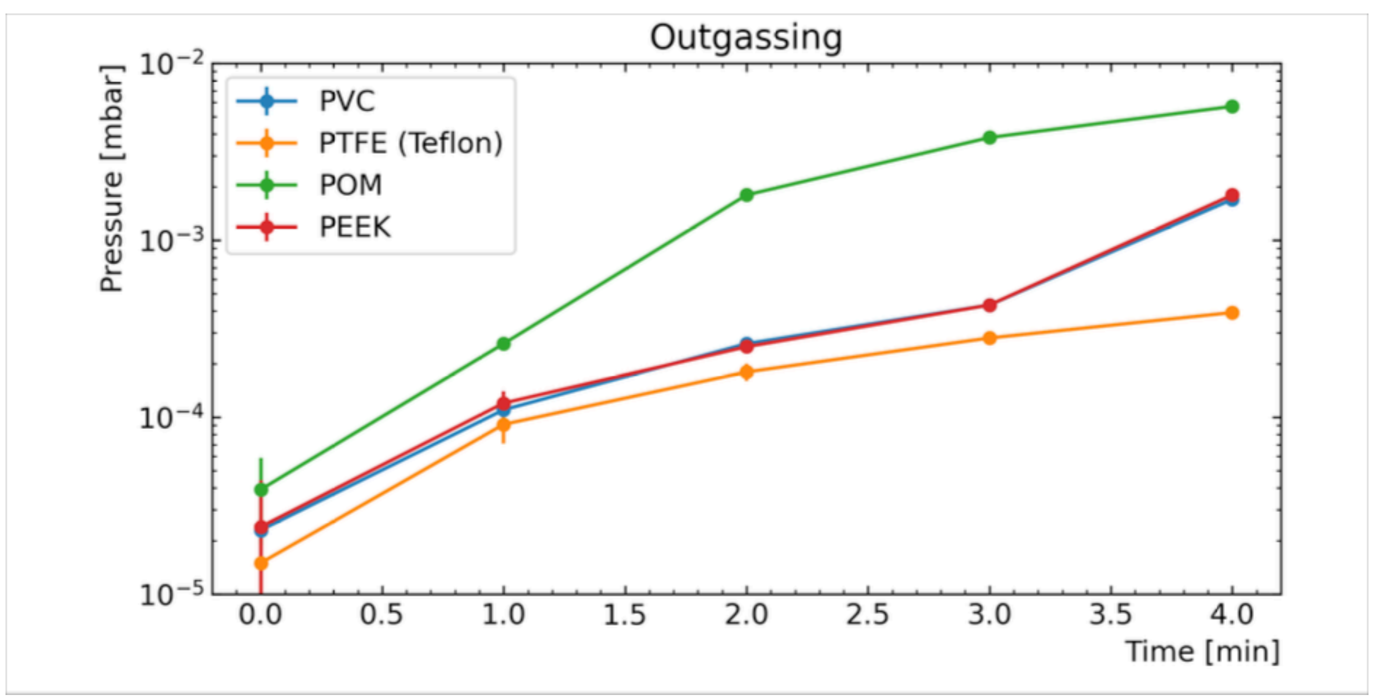

CTPC 2.0 - prototype design

- The second CPC prototype built in 2023 has a height of 27 cm and a radius of 11 cm. The CTPC is inserted in the previous STPC vessel to take measurements up to 40 bar.
- Measurements of material outgassing were made for the choice of cathode and supporting structure and we finally chose Teflon as supporting structure and a cathode made of 200 µm thick Aluminum.

Plastic polymers considered for supporting structure

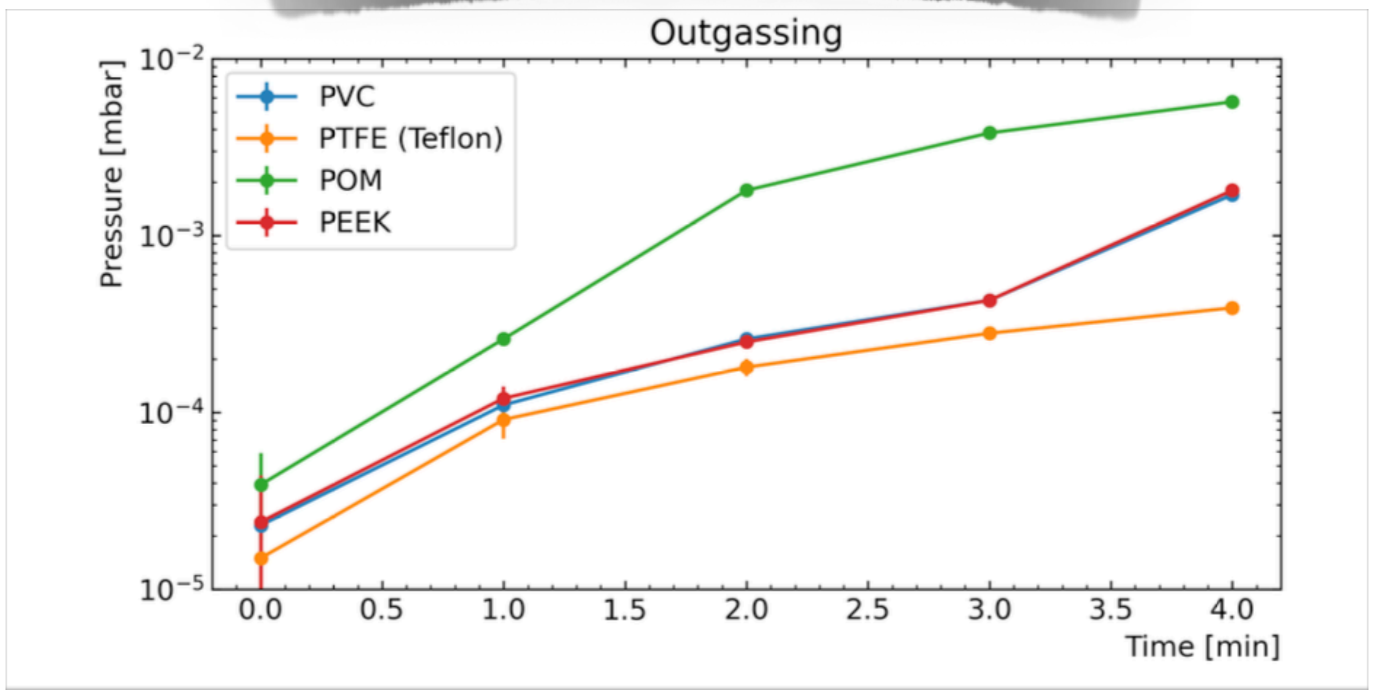

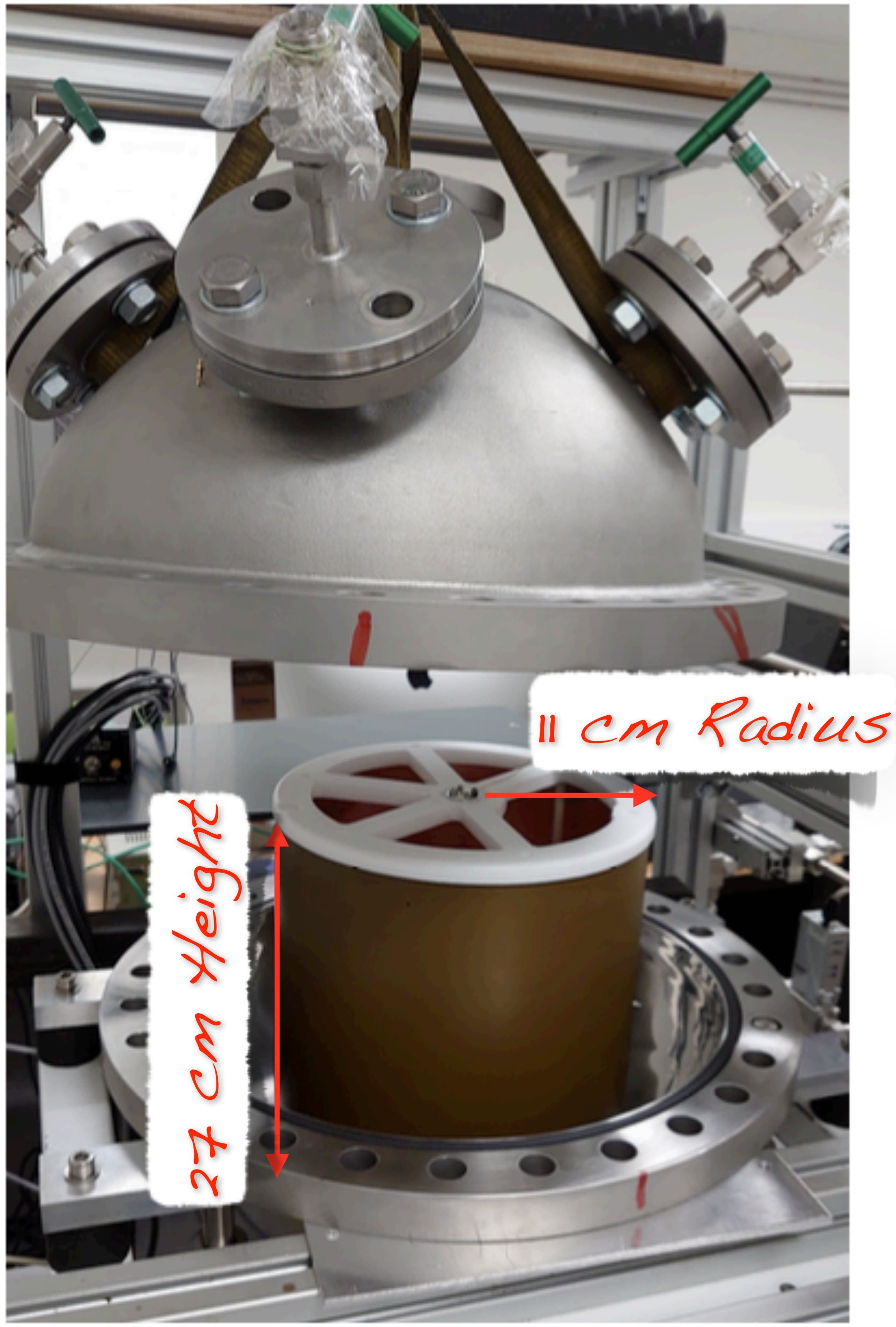

CTPC 2.0 - prototype design

- The HV was applied to the cathode up to values of 5 kV.

- Different anodes were tested from wires of 50 μm diameter, to rods of 1.2 and 12 mm diameter.

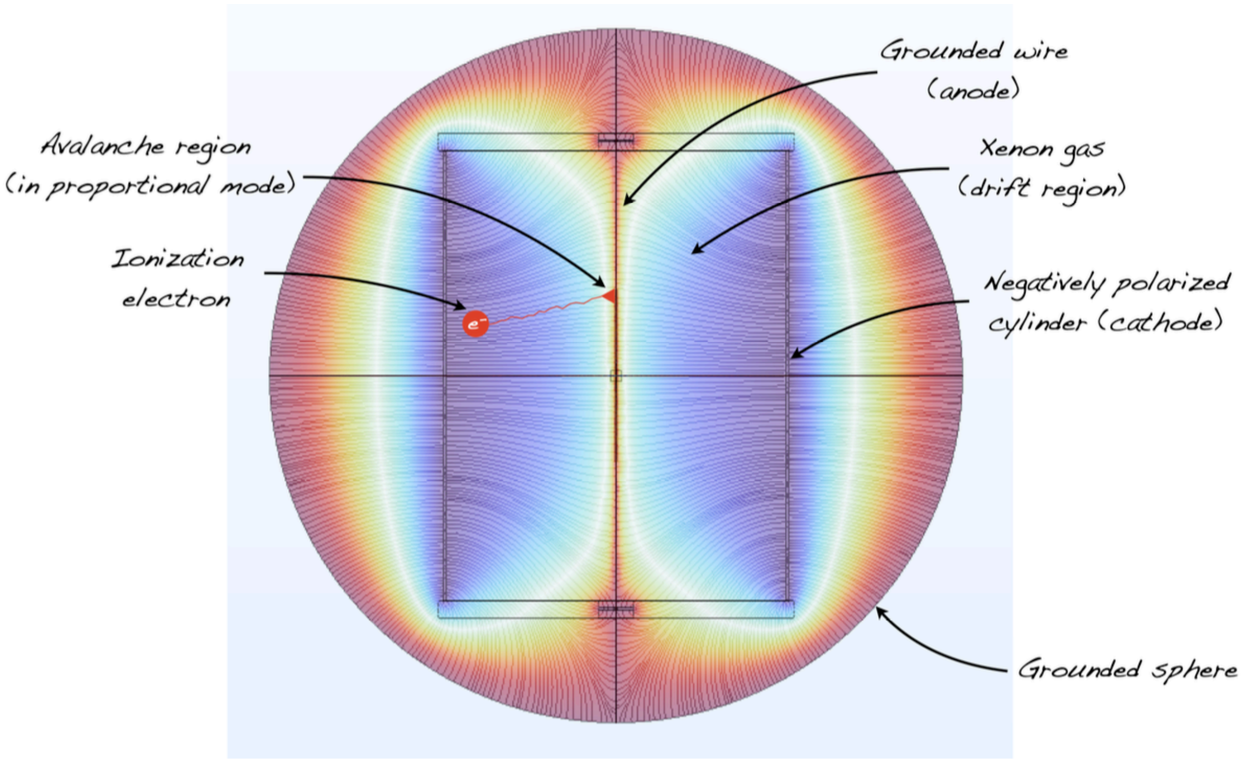

Different tested anodes

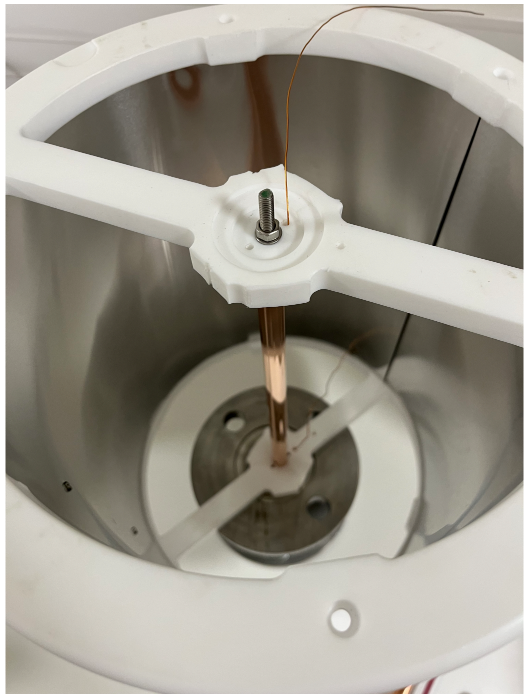

CTPC 2.0 - prototype design

- The HV was applied to the cathode up to values of 5 kV.
- Different anodes were tested from wires of 50 μm diameter, to rods of 1.2 and 12 mm diameter.

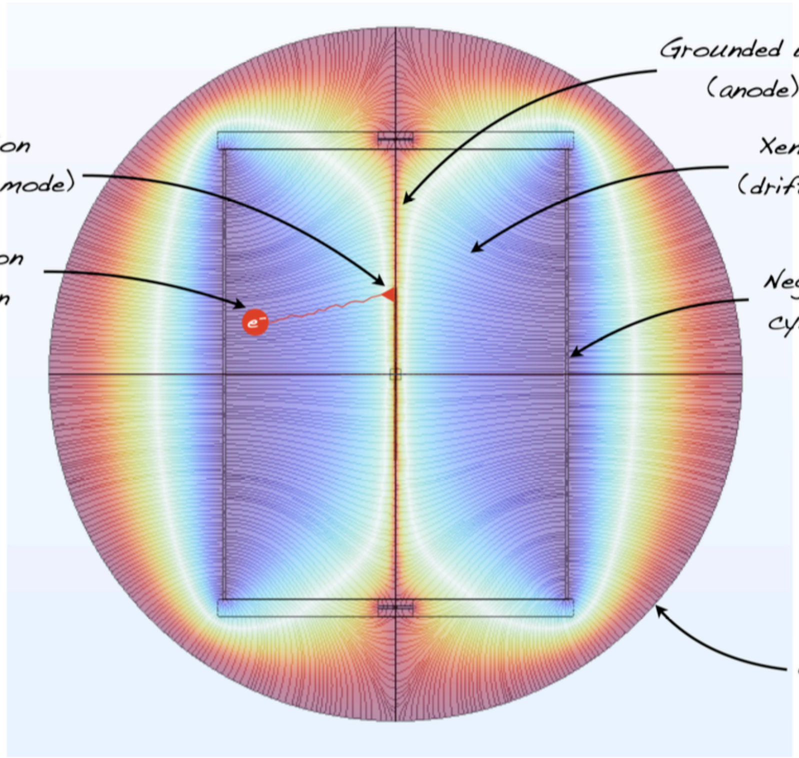

Different tested anodes

CTPC 2.0 - prototype design

- Two calibration sources were used:
  - ➡ A **^{210}Po α source of 5.3 MeV** deposited on a silver plate of 0.6 × 0.6 cm^2, and positioned on the outside of the cathode behind a hole of 1 mm radius.
  - ➡ Diffuse **^{222}Rn in the gas emitting α of 5.5 MeV** in all the volume.
- The daughters of the Rn decay chain can also be used used (although they are typically positively charged and they drift more and more towards the cathode)

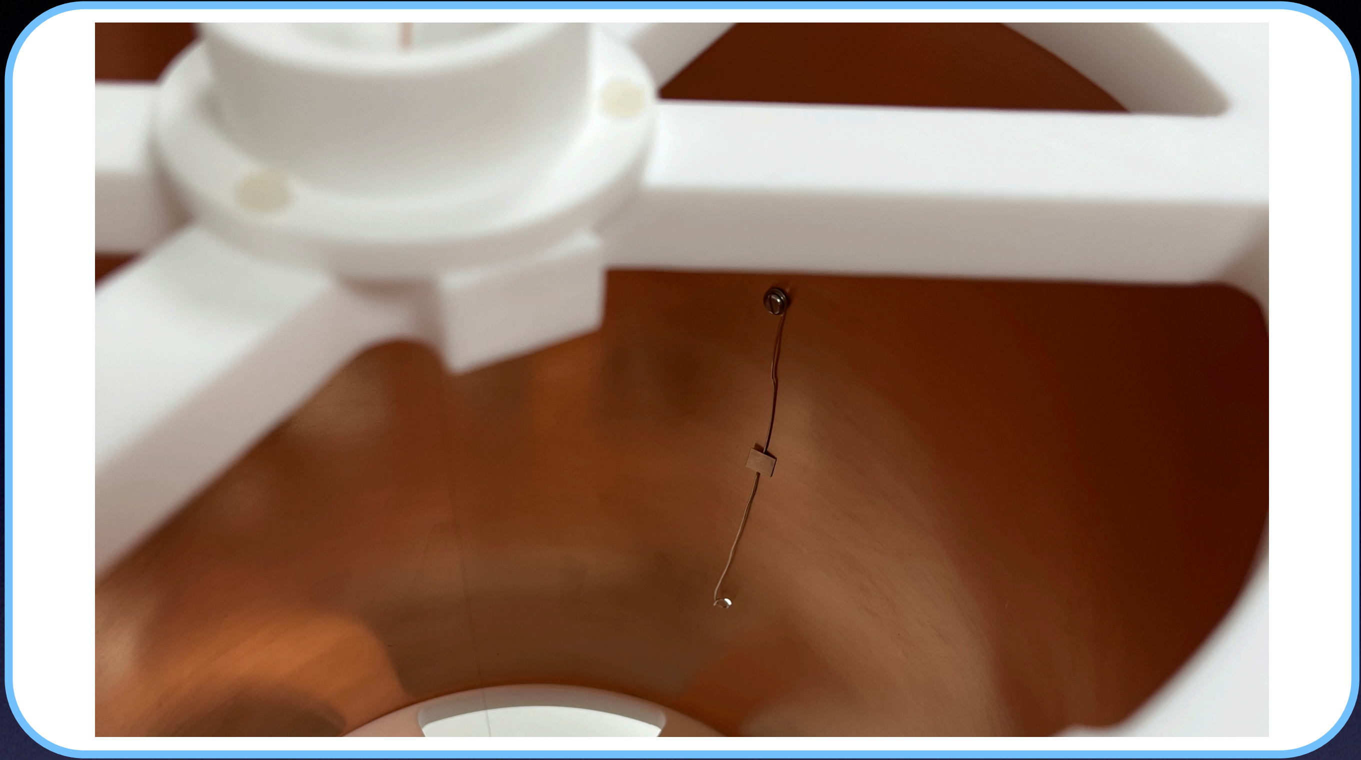

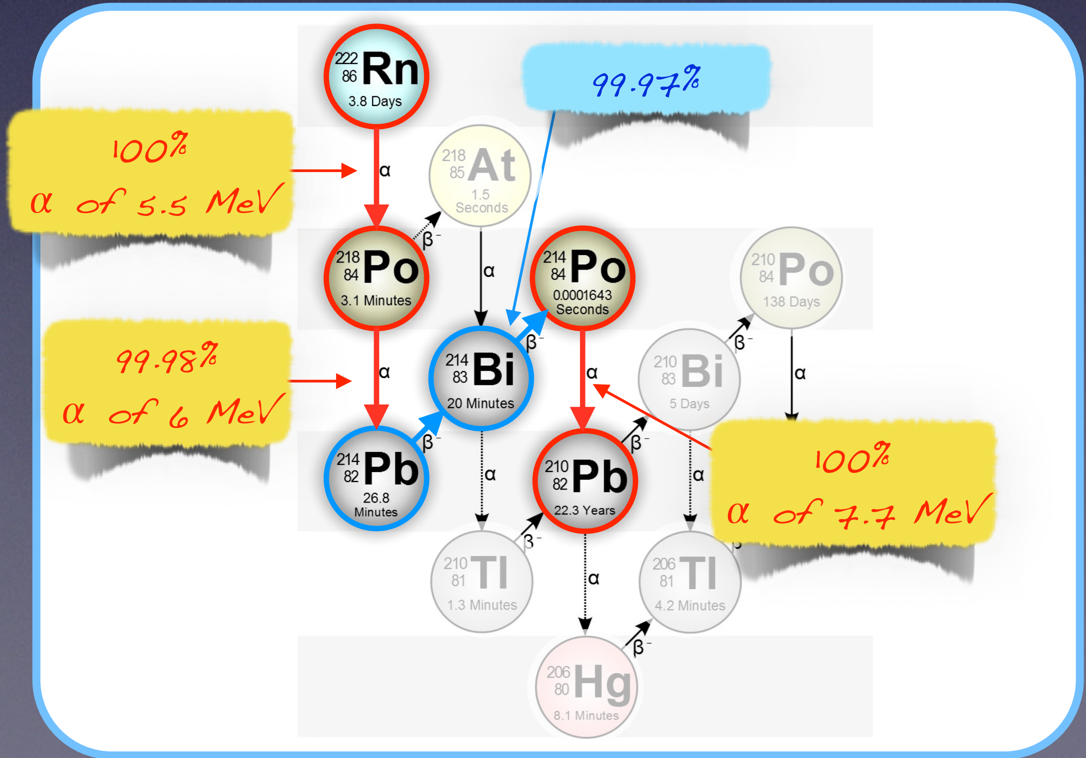

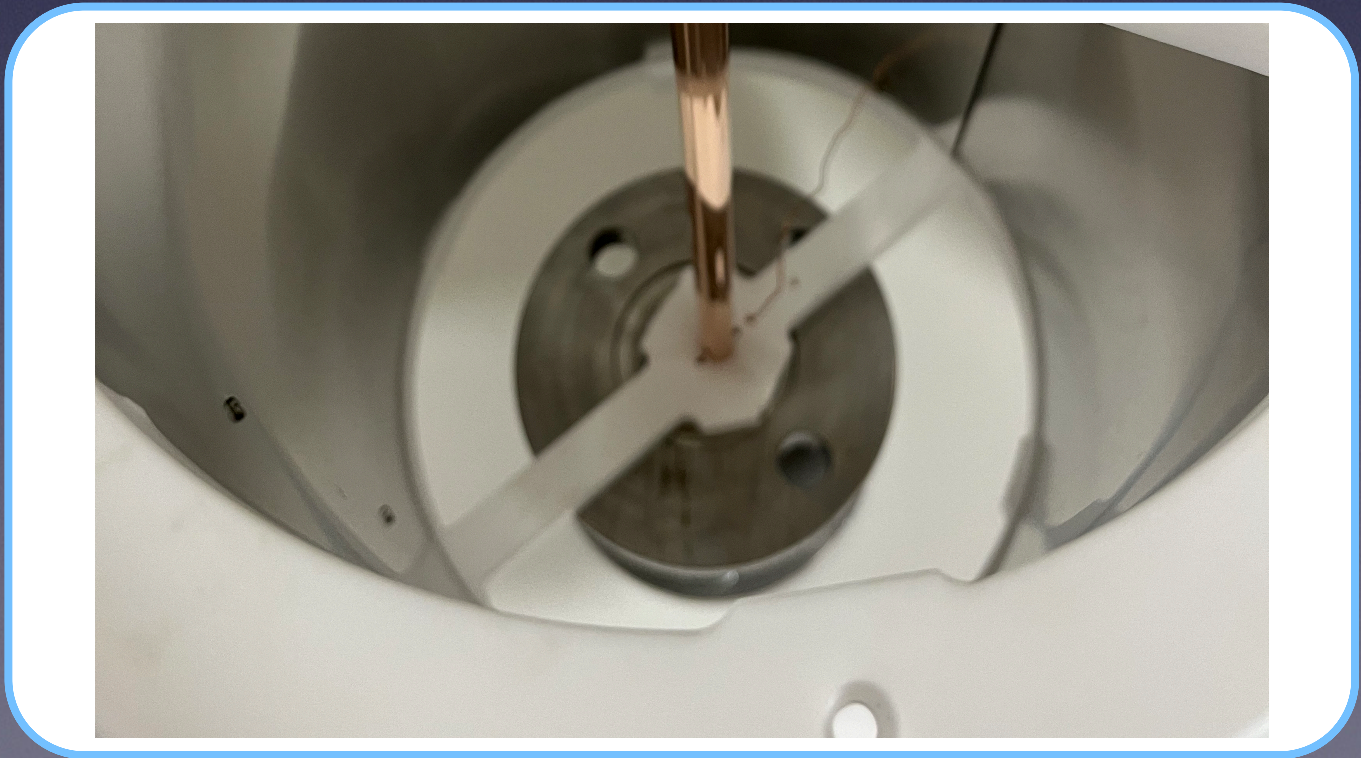

CTPC 2.0 - prototype design

- Two calibration sources were used:
  - ➡ A **^{210}Po α source of 5.3 MeV** deposited on a silver plate of 0.6 × 0.6 cm^2, and positioned on the outside of the cathode behind a hole of 1 mm radius.
  - ➡ Diffuse **^{222}Rn in the gas emitting α of 5.5 MeV** in all the volume.
- The daughters of the Rn decay chain can also be used used (although they are typically positively charged and they drift more and more towards the cathode)

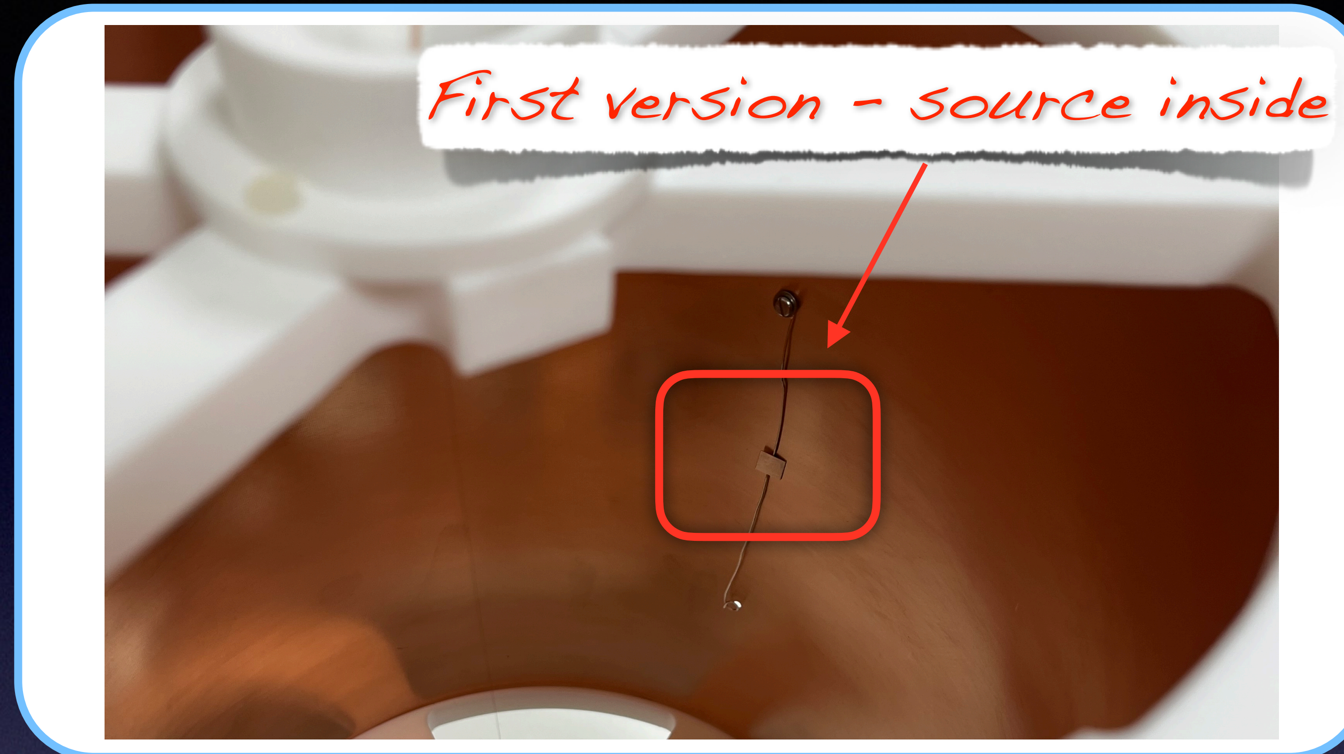

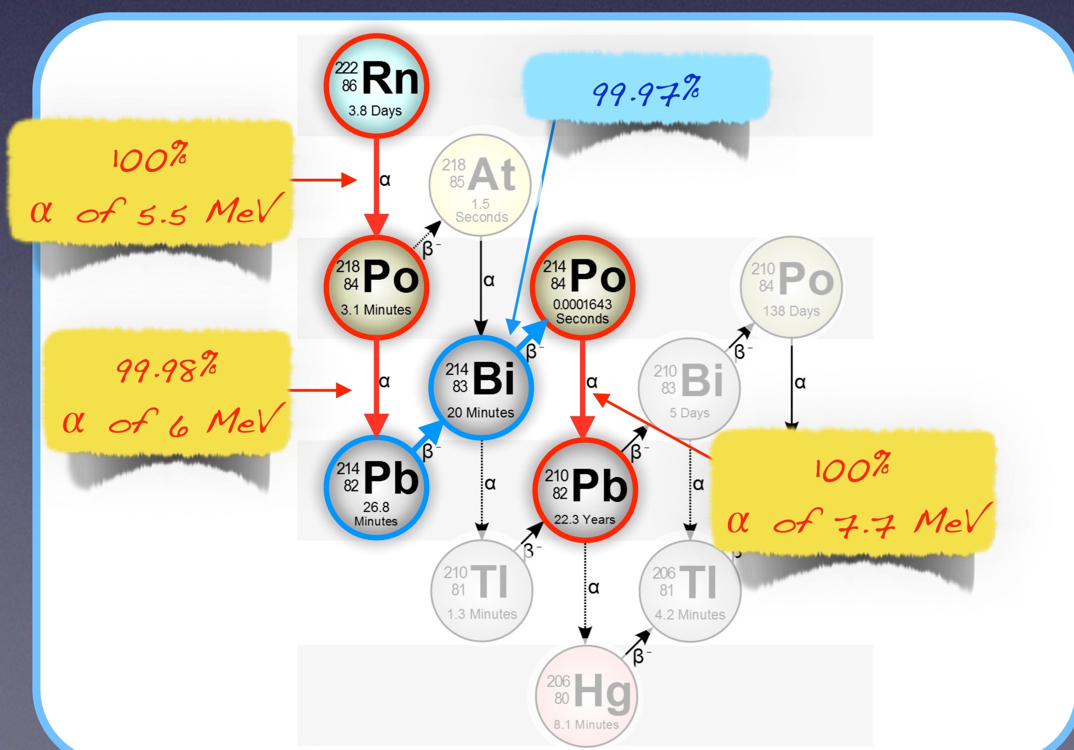

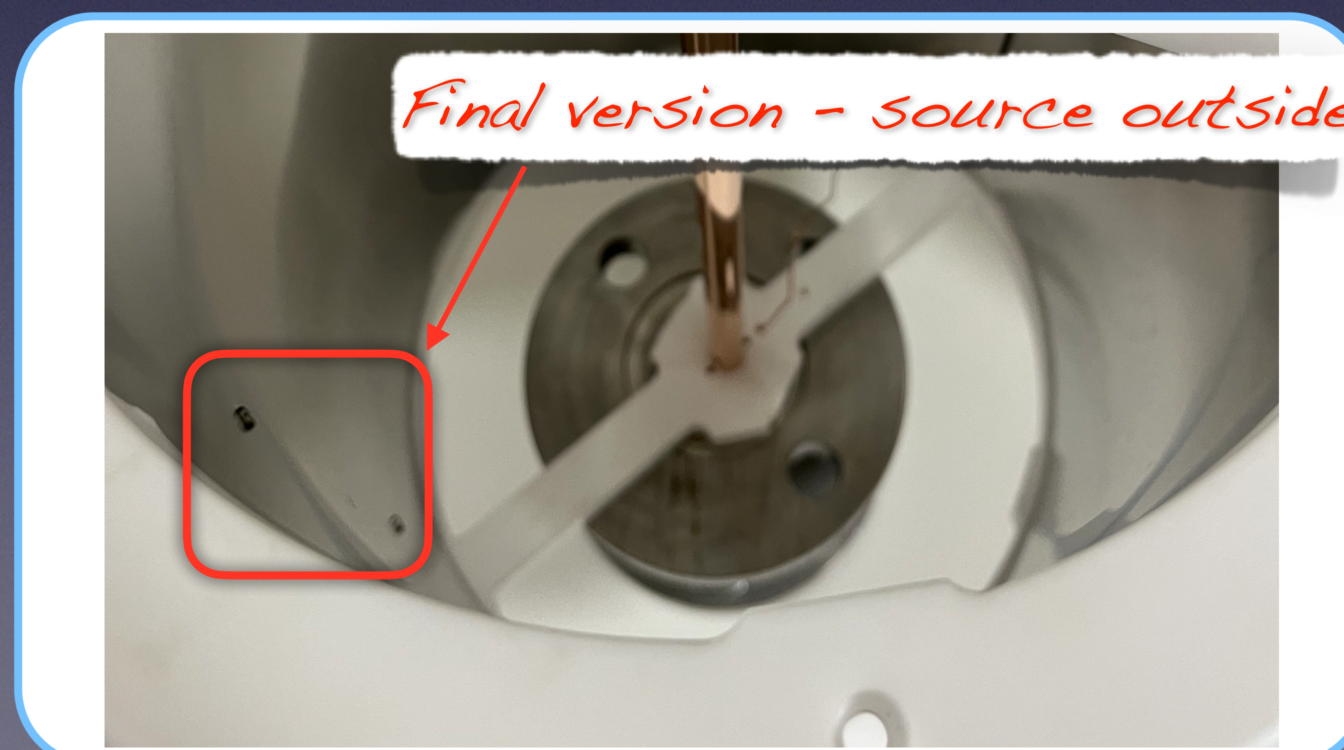

Gas purity

- Gas purity is a key issue for the operation of the CTPC.
- A system based on **cold and hot getter** was set up granting purities up to few ppb in terms of electronegative impurities such as Oxygen.

Gas purity

- Gas purity is a key issue for the operation of the CTPC.
- A system based on **cold and hot getter** was set up granting purities up to few ppb in terms of electronegative impurities such as Oxygen.

Gas purity

- Gas purity is a key issue for the operation of the CTPC.
- A system based on **cold and hot getter** was set up granting purities up to few ppb in terms of electronegative impurities such as Oxygen.
- However, the **purification system limits the operation of the detector at 10 bar**.

Gas purity

- Gas purity is a key issue for the operation of the CTPC.
- A system based on **cold and hot getter** was set up granting purities up to few ppb in terms of electronegative impurities such as Oxygen.
- However, the **purificatio**... **peration of th**...

Upgrade based on spark discharge ongoing

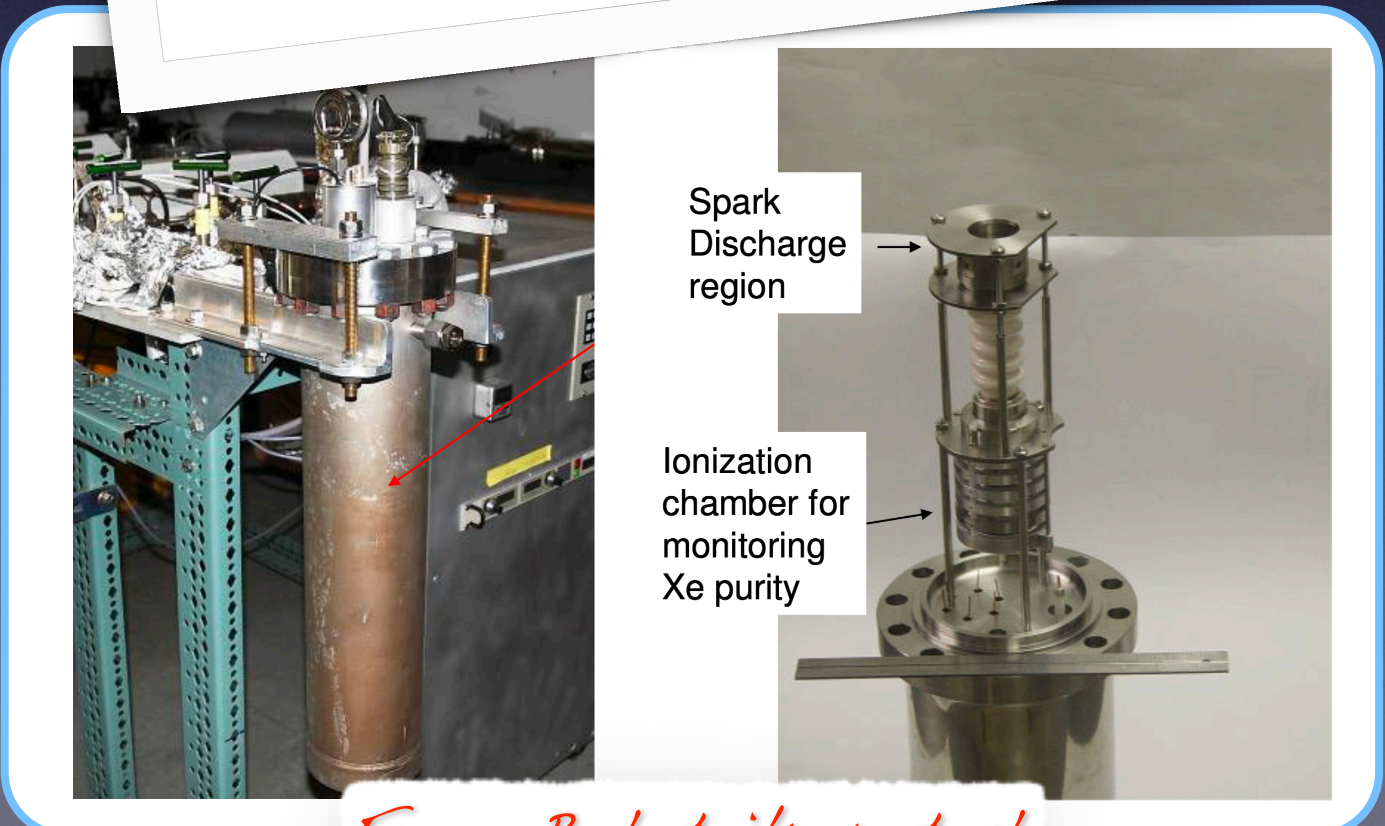

From Bolotnikov et al.

Gas purity

- The gas is **constantly recirculated** through the getter to grant a constant purity.

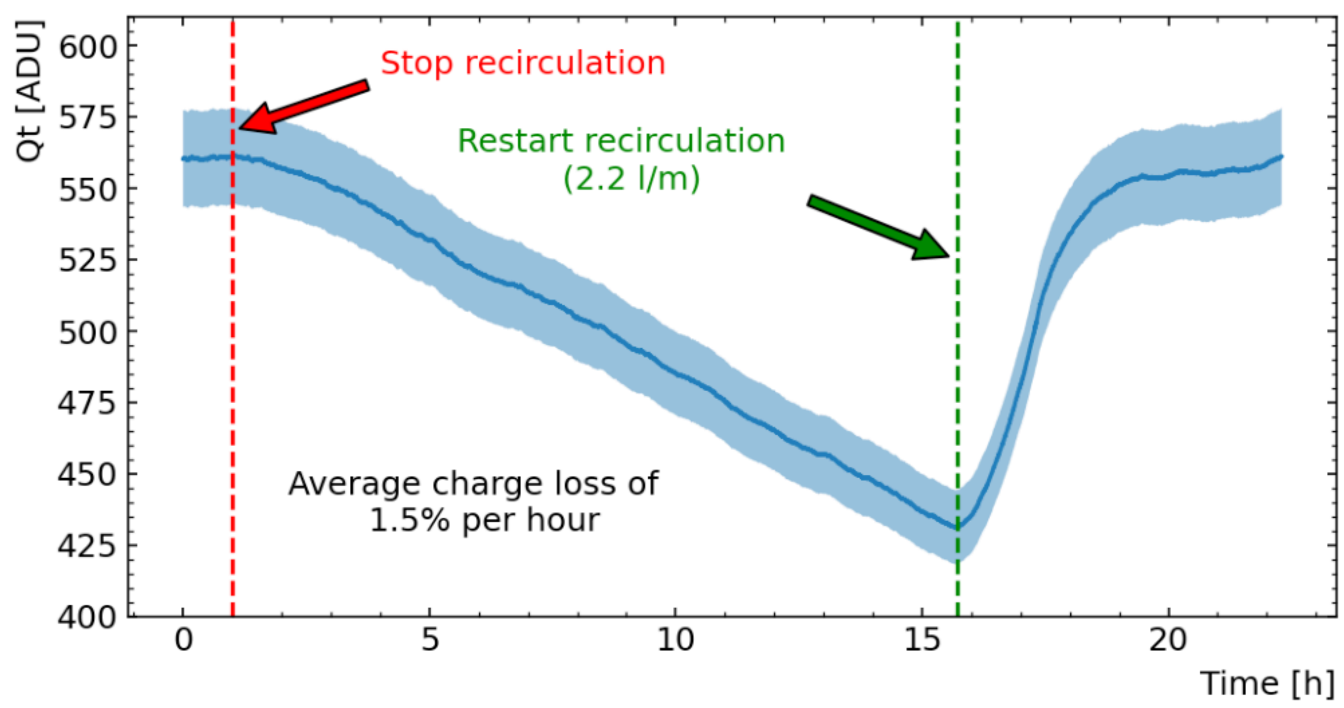

Gas purity

- The gas is **constantly recirculated** through the getter to grant a constant purity.

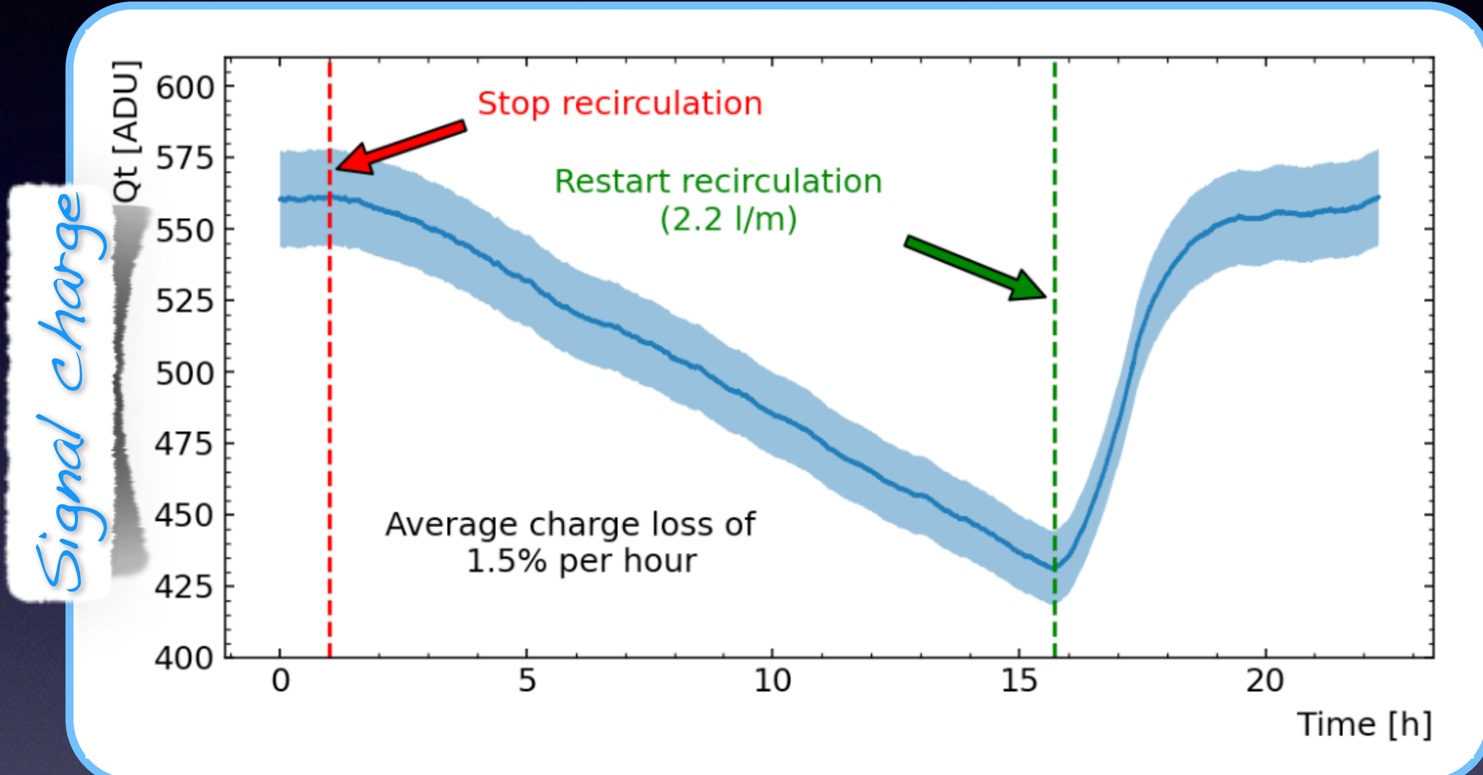

Gas purity

- The gas is **constantly recirculated** through the getter to grant a constant purity.

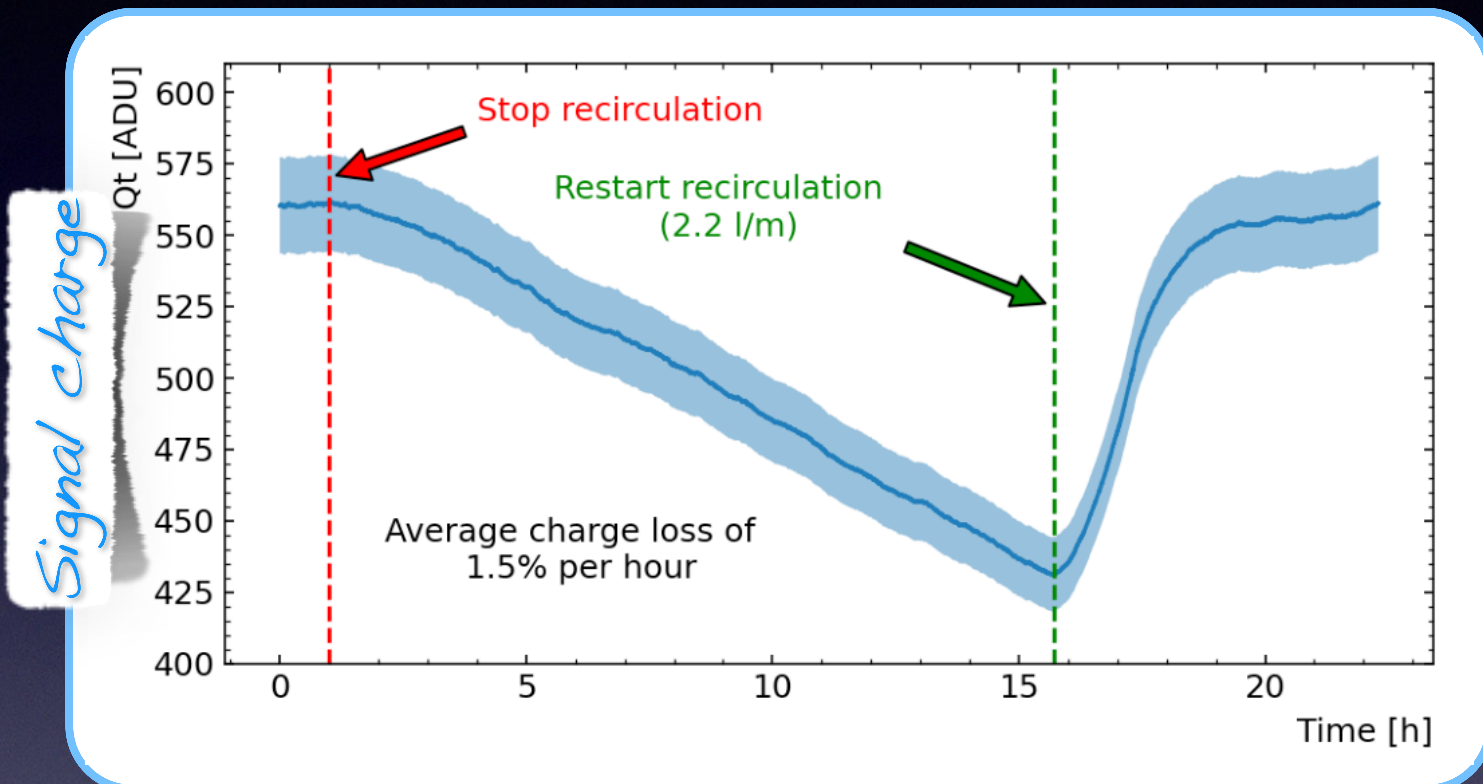

- However the **pump produces vibrational noise** and it is source of **outgassing**.

Gas purity

- The gas is **constantly recirculated** through the getter to grant a constant purity.

Signal charge

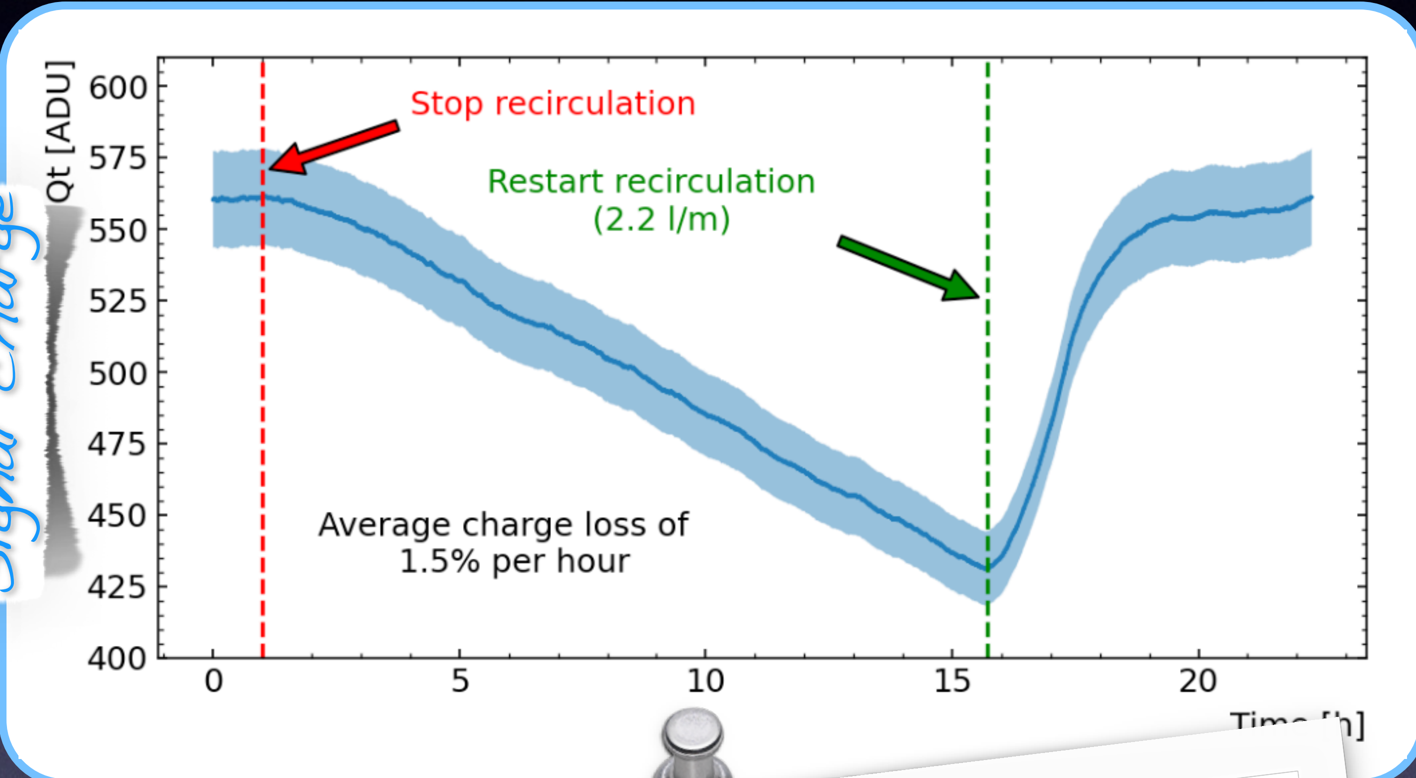

Possible solution with magnetically driven piston pump and better mechanical insulation under study

- ... nd it i...

Recirculation pump chamber

Gas purity

- The electron lifetime was computed fitting with an exponential curve the signal amplitude as a function of the drift time.
- Practically the HV was changed assuming to know the drift time (based on Garfield simulation) since it was not possible to move the source radially without affecting the electric field.

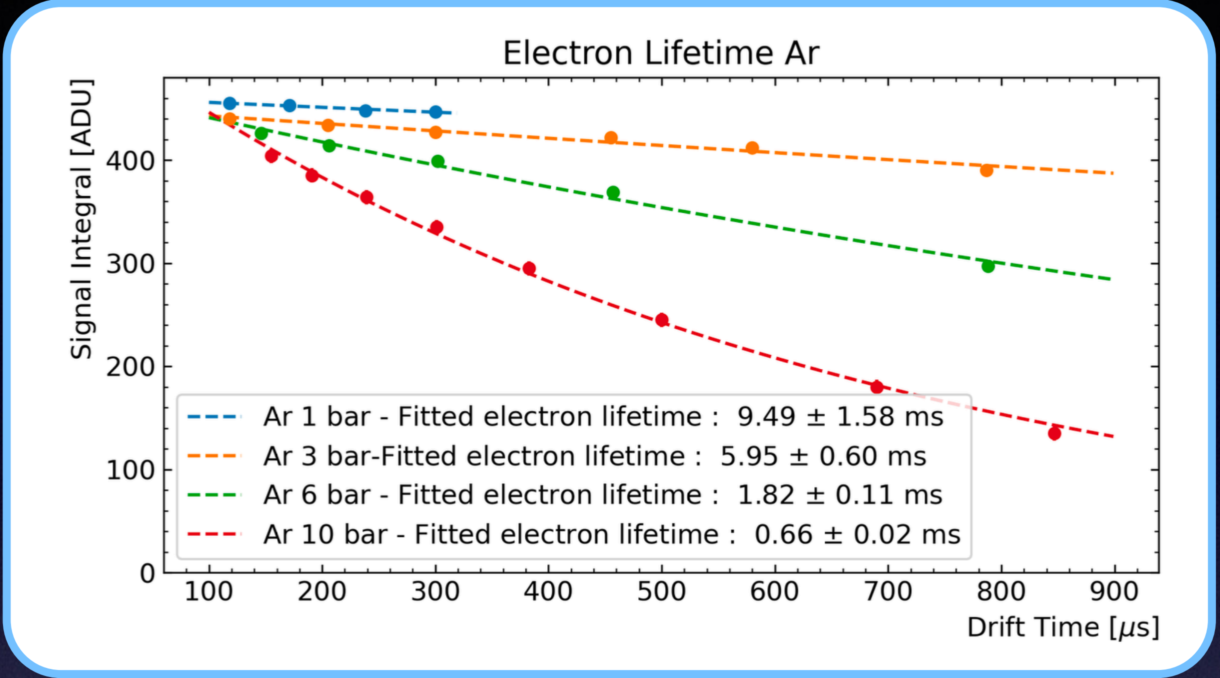

- The achieved purity in tems of electron lifetime is **good enough for the prototype** but **far from the values obtained in liquid argon and xenon at the level of 20 ms and 10 ms**, respectively.

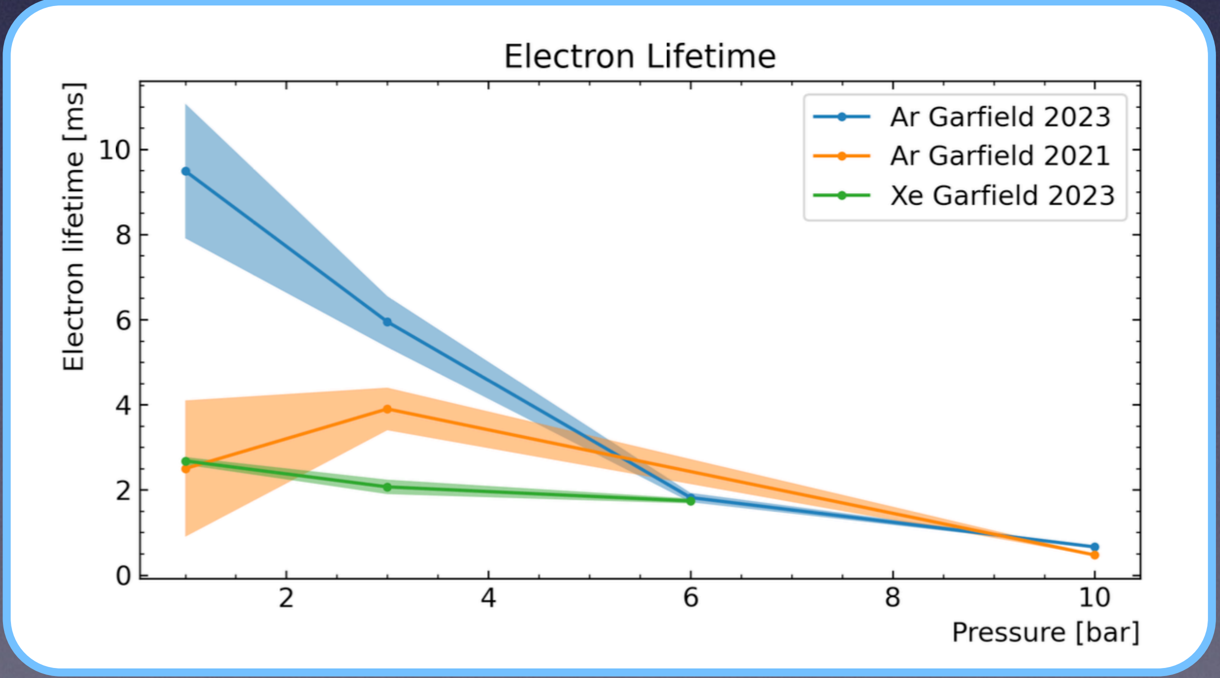

Gas purity

- The electron lifetime was computed fitting with an exponential curve the signal amplitude as a function of the drift time.
- Practically the l

Conservative results which will improve with a better gas purification at the level already achieved by running experiments

- T ... electron lif ... **enough for the prototype** but **far from the values obtained in liquid argon and xenon at the level of 20 ms and 10 ms**, respectively.

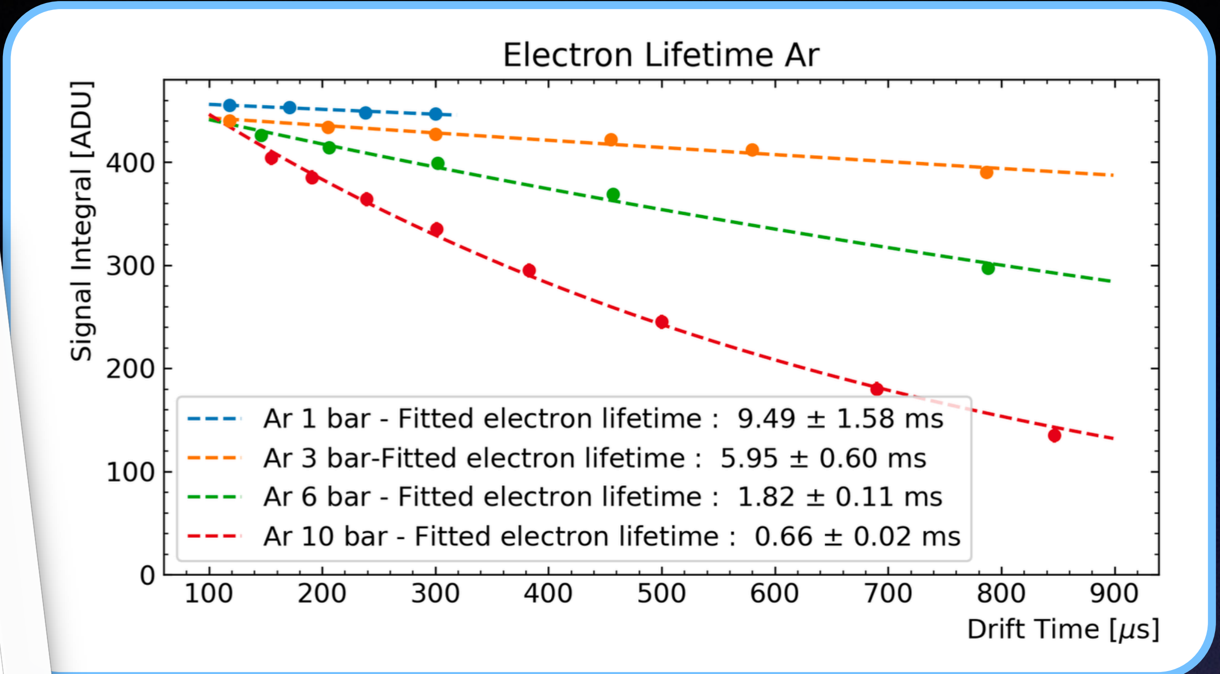

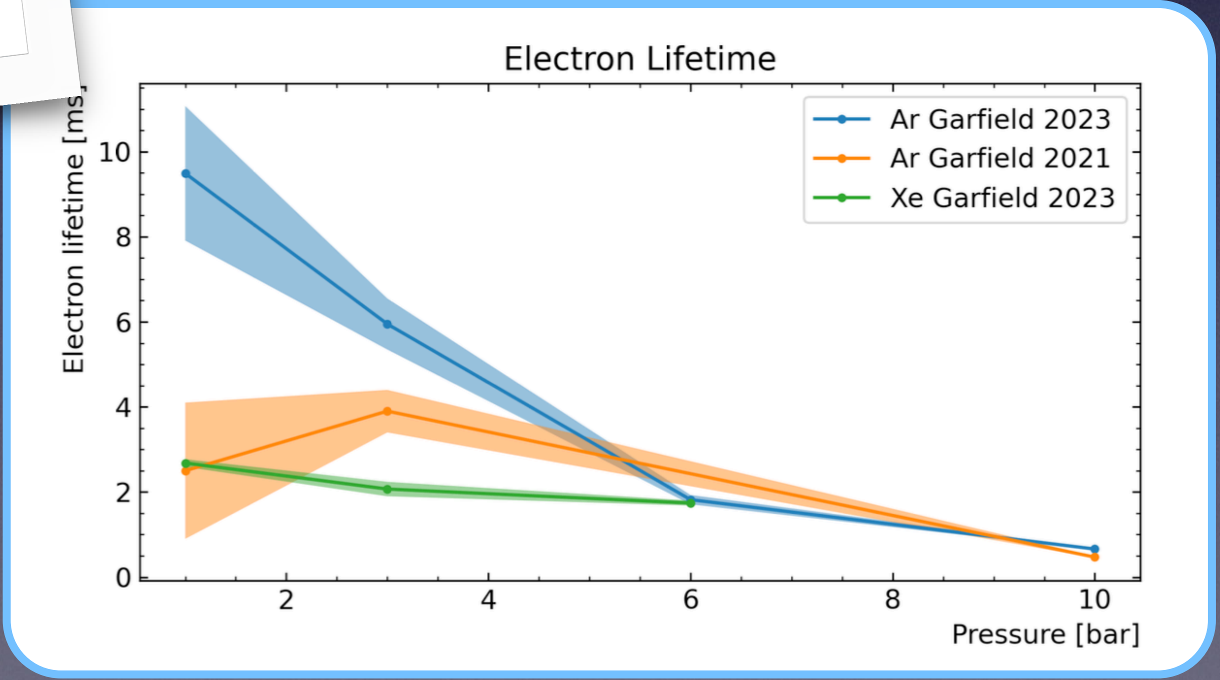

Temperature corrections

- Variations of the temperature also affect the signal integral.
- The **temperature variations impact the measurements in two ways**:
  - ➡ Gas temperature variations implying **pressure variations**.
  - ➡ Variations of the **electronics chain response**.
- To obtain a resolution at the percent level, the **temperature has to be stable within 1 degree at the most**, or corrections have to be applied.

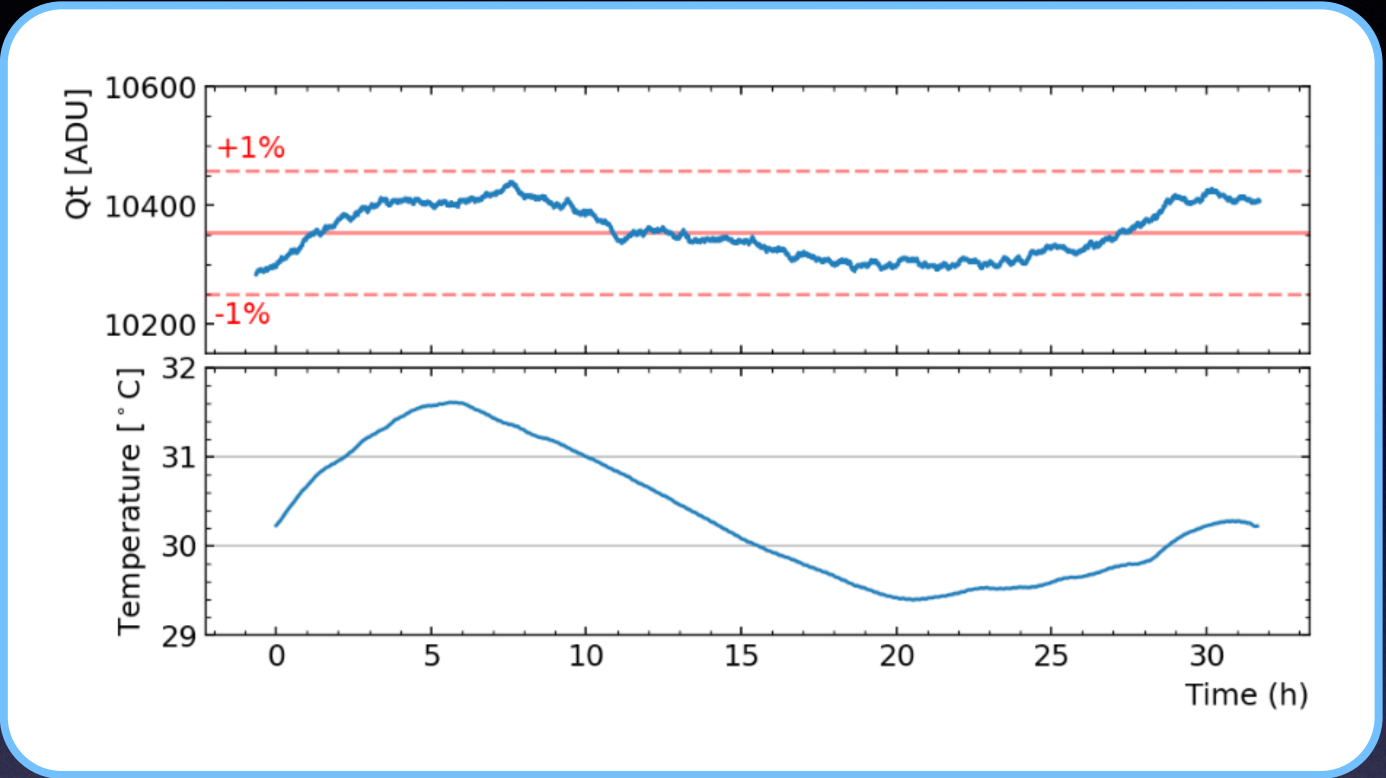

Temperature corrections

- Variations of the temperature also affect the signal integral.
- The **temperature variations impact the measurements in two ways**:
  - ➡ Gas temperature variations implying **pressure variations**.
  - ➡ Variations of the **electronics chain response**.
- To obtain a resolution at the percent level, the **temperature has to be stable within 1 degree at the most**, or corrections have to be applied.

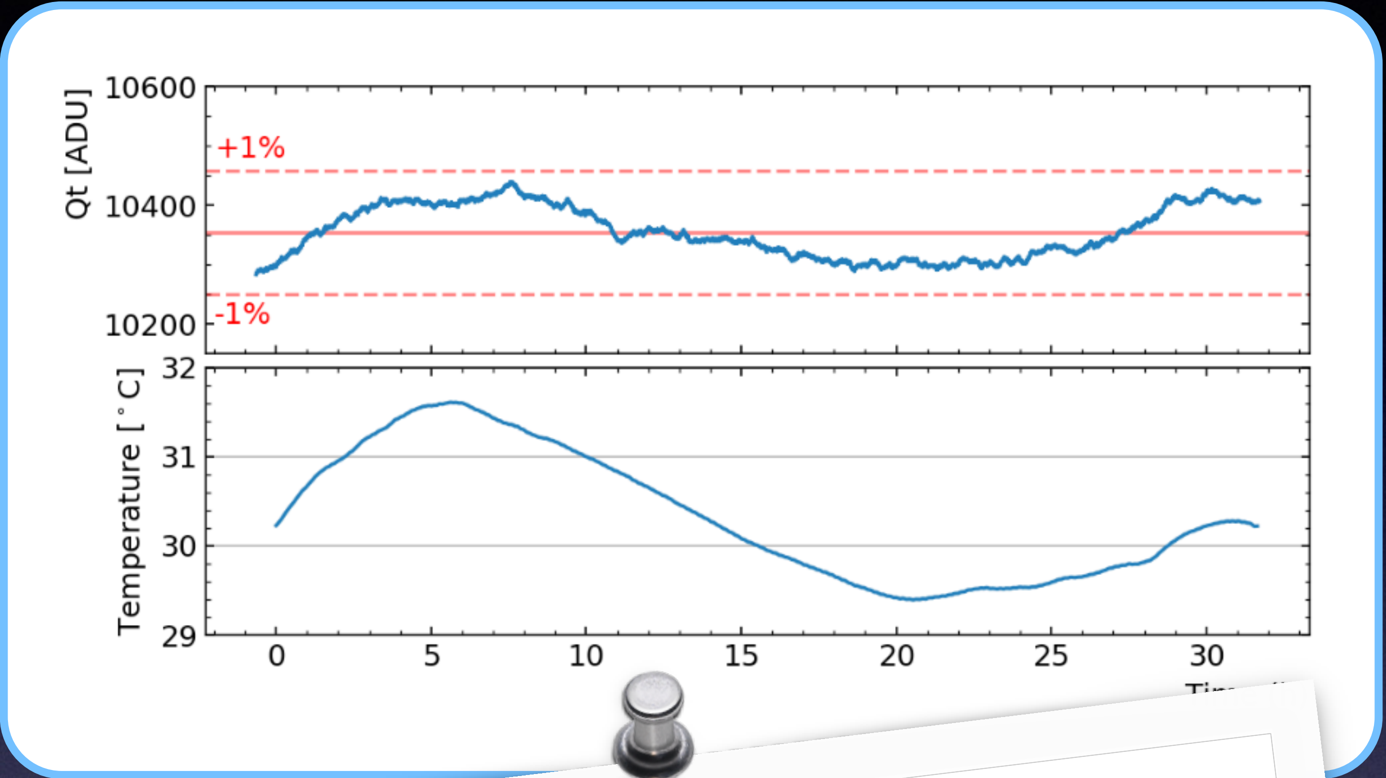

The temperature is monitored constantly and corrections are applied to long runs lasting more than 1 hour (i.e. for run using Radon source).

DAQ chain

DAQ chain

Anodic signal

Signal induced on the anode

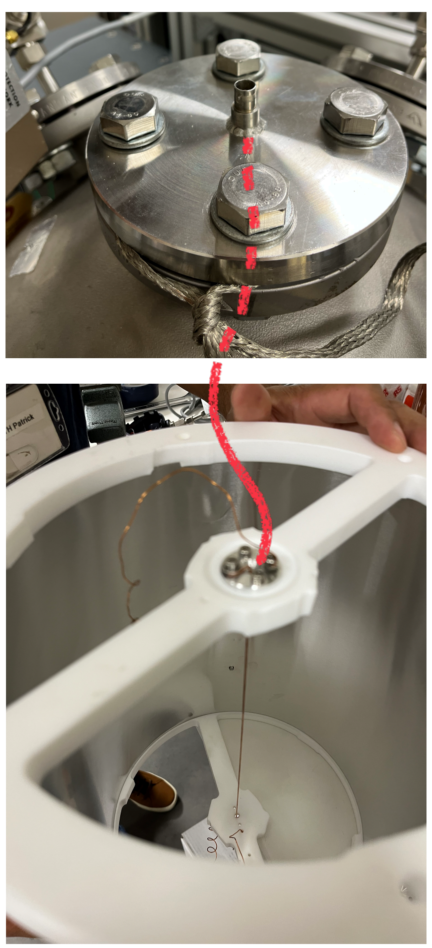

DAQ chain

Anodic signal → Preamplifier → →

Signal induced on the anode

ORTEC charge preamplifier

DAQ chain

Anodic signal → Preamplifier → Digitization →

Signal induced on the anode

ORTEC charge preamplifier

CALI card developed for Edelweiss

DAQ chain

Anodic signal → Preamplifier → Digitization → Data processing and analysis

Signal induced on the anode

ORTEC charge preamplifier

CALI card developed for Edelweiss

SAMBA program developed for CALI card

DAQ chain

Anodic signal → Preamplifier → Digitization → Data processing
sis

am
LI card

Several improvements ongoing:

- Resistive anode with readout at both sides
- Current amplifier based on ASICS technology
- More flexible DAQ development
- Embedded AI on FPGA for signal selection ongoing

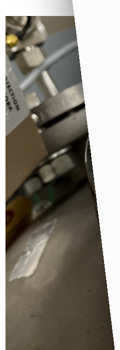

Noise

- A lot of work was done to reduce as much as possible the noise on the readout signal, which had two origins: **mechanical and electronic**.
- Vibrations can be seen on the waveform exhibiting low frequency.
- Perturbations of the electric network (many experiments ongoing on the same ground in the room) are seen with some specifics peaks in the Fourrier transform of the waveform.
- The most dangerous noise is the one which changes the baseline between its evaluation (first 1.5 ms) and its subtraction (following 1.5 ms) i.e a frequency around 350 Hz.

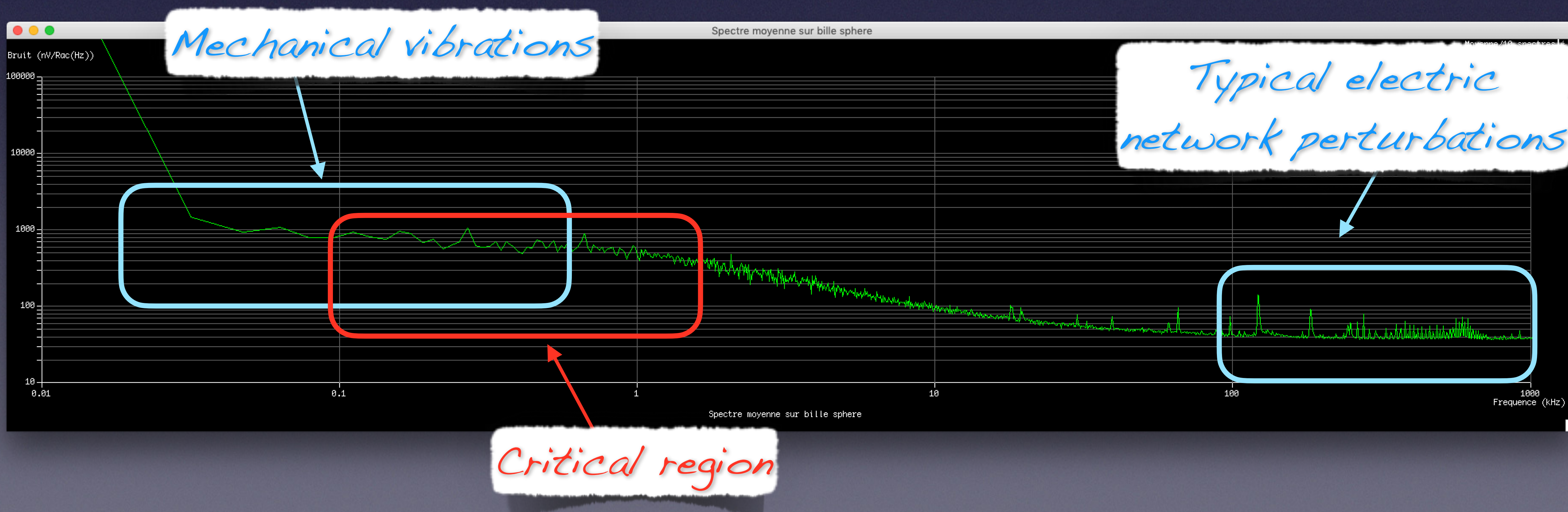

Noise

- A lot of work was done to reduce as much as possible the noise on the readout signal, which had two origins: **mechanical and electronic**.
- Vibrations can be seen on the waveform exhibiting low frequency
- Perturbations of the electric netw … ame ground in the room) are se … veform.
- The most da … its evaluation (first 1.5 ms) and i …

It is important to isolate mechanically and electrically the detector. Ideally a dedicated mass, DAQ on battery and calm environment.

Signal

- The reconstructed waveforms are used to extract observables such as the total charge of the event, its duration and the width at half height.
- Each observable is associated to a specific feature of the original signal.

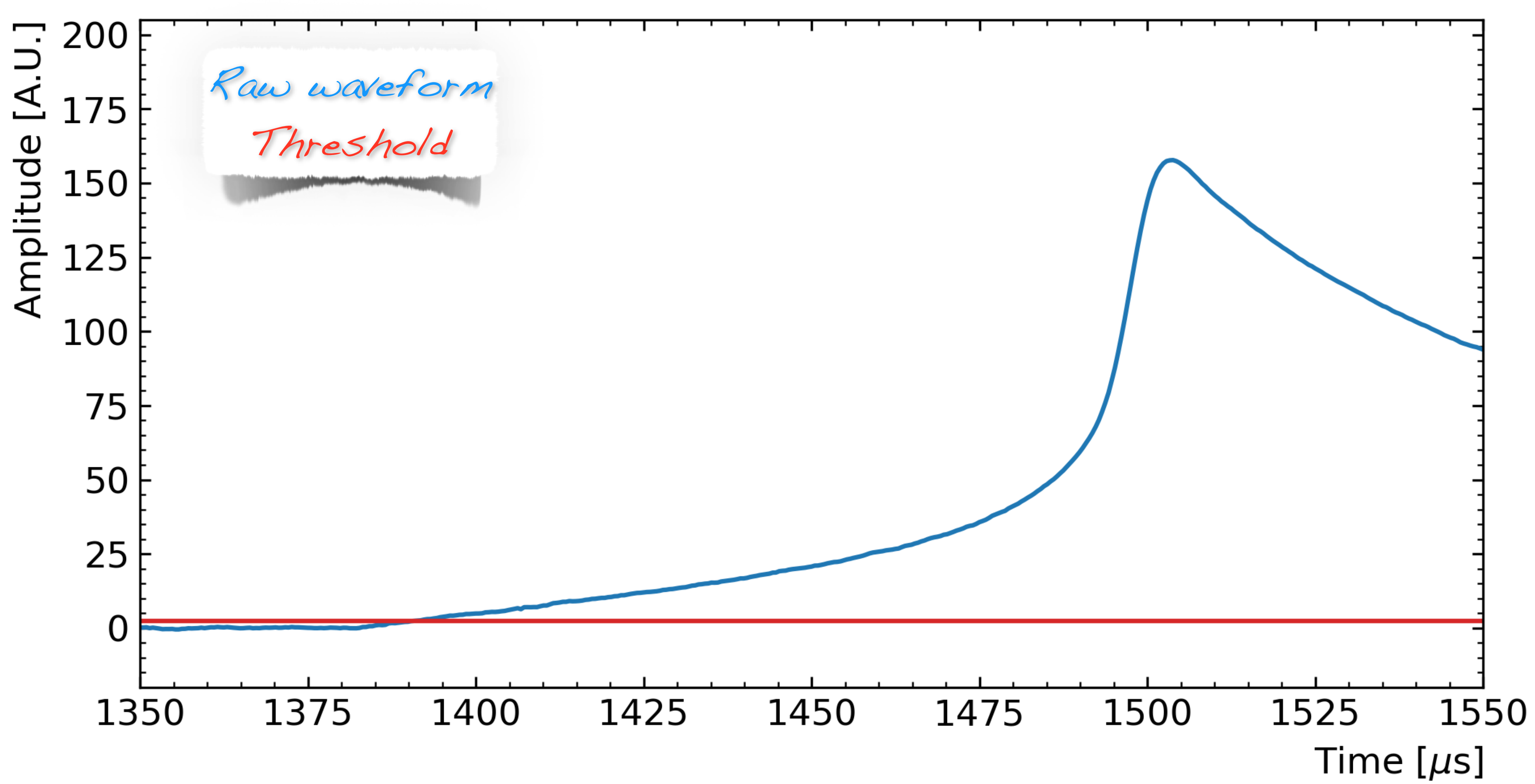

Signal

- The reconstructed waveforms are used to extract observables such as the total charge of the event, its duration and the width at half height.
- Each observable is associated to a specific feature of the original signal.

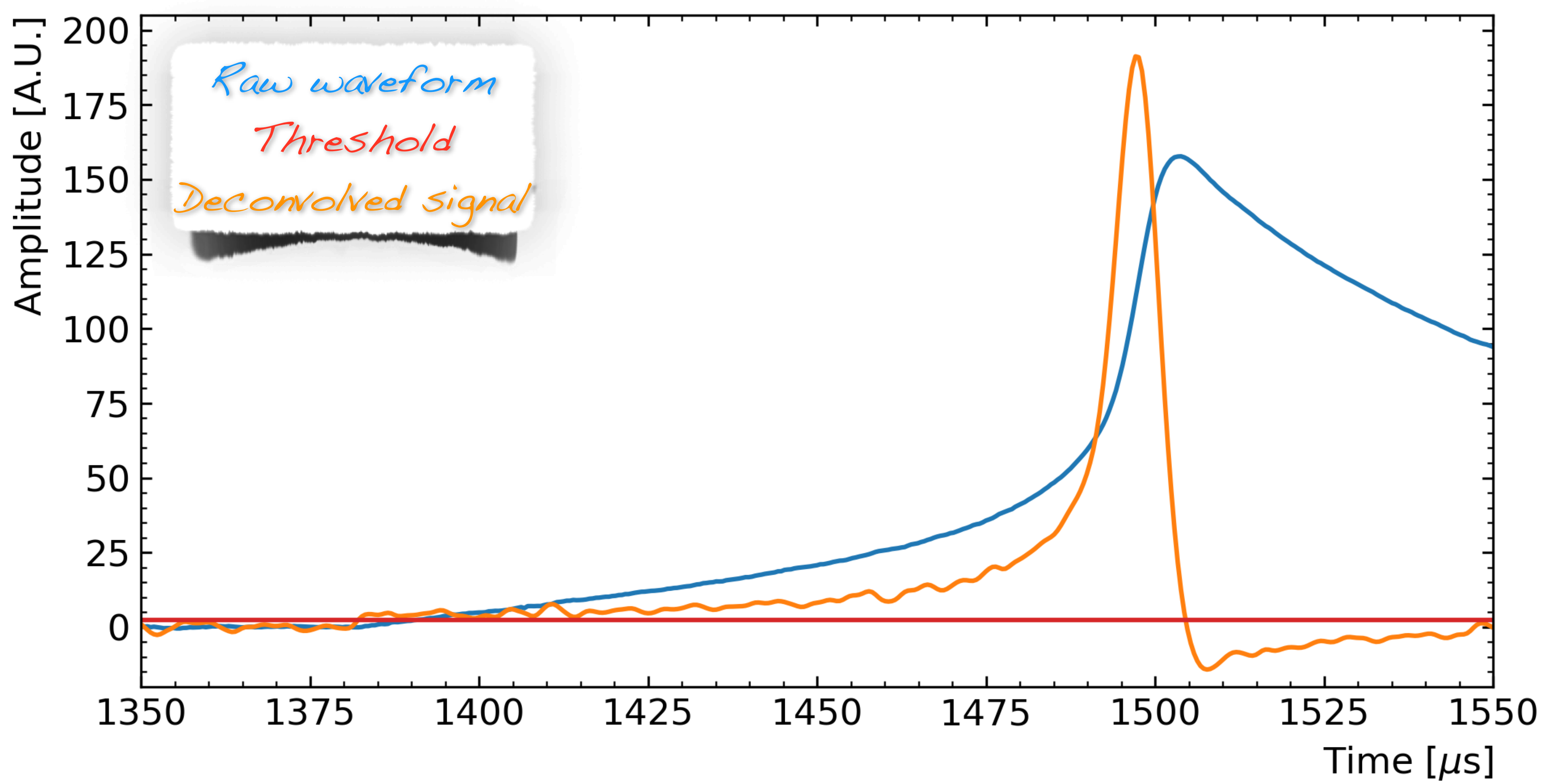

Signal

- The reconstructed waveforms are used to extract observables such as the total charge of the event, its duration and the width at half height.
- Each observable is associated to a specific feature of the original signal.

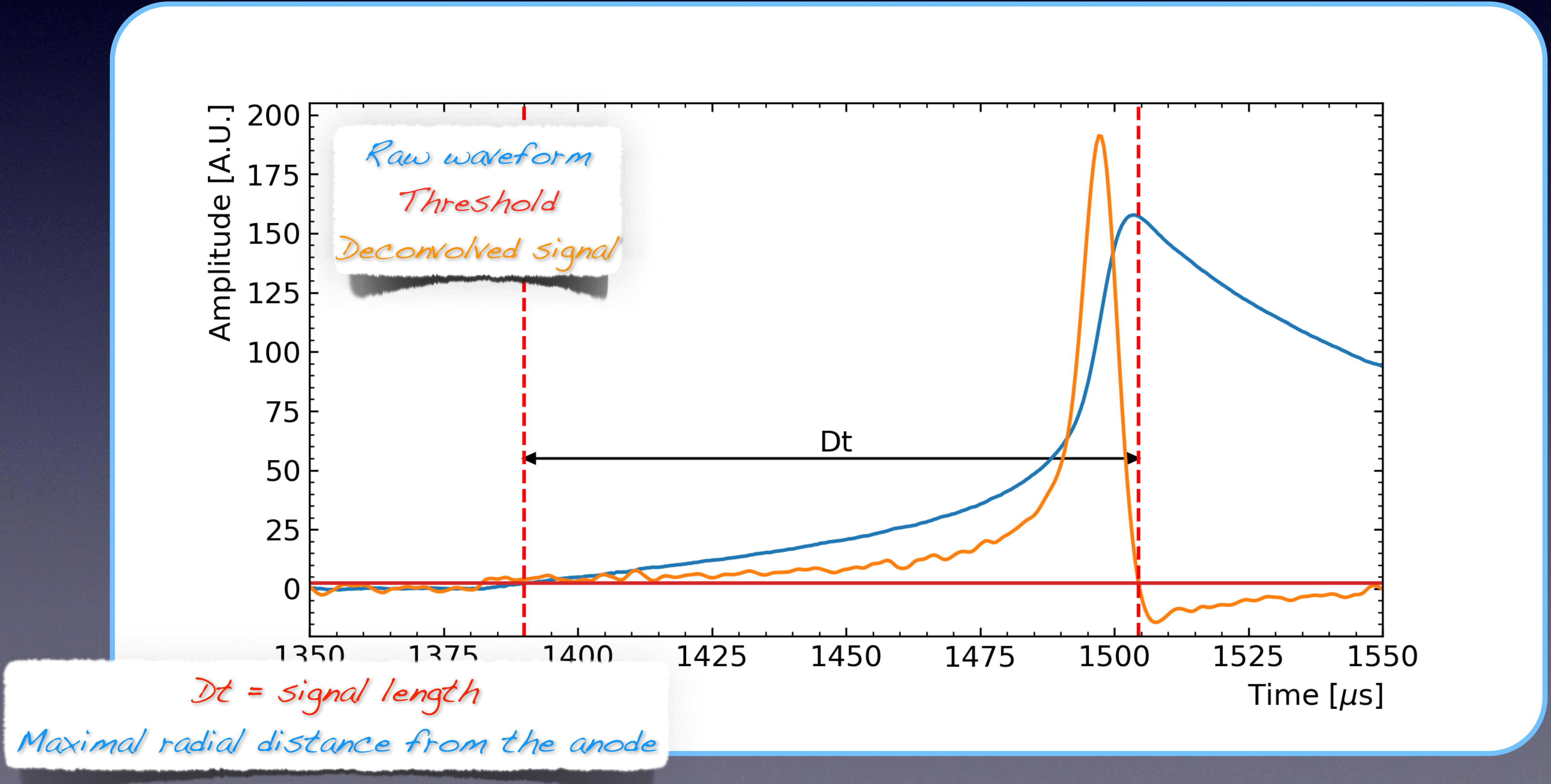

Signal

- The reconstructed waveforms are used to extract observables such as the total charge of the event, its duration and the width at half height.
- Each observable is associated to a specific feature of the original signal.

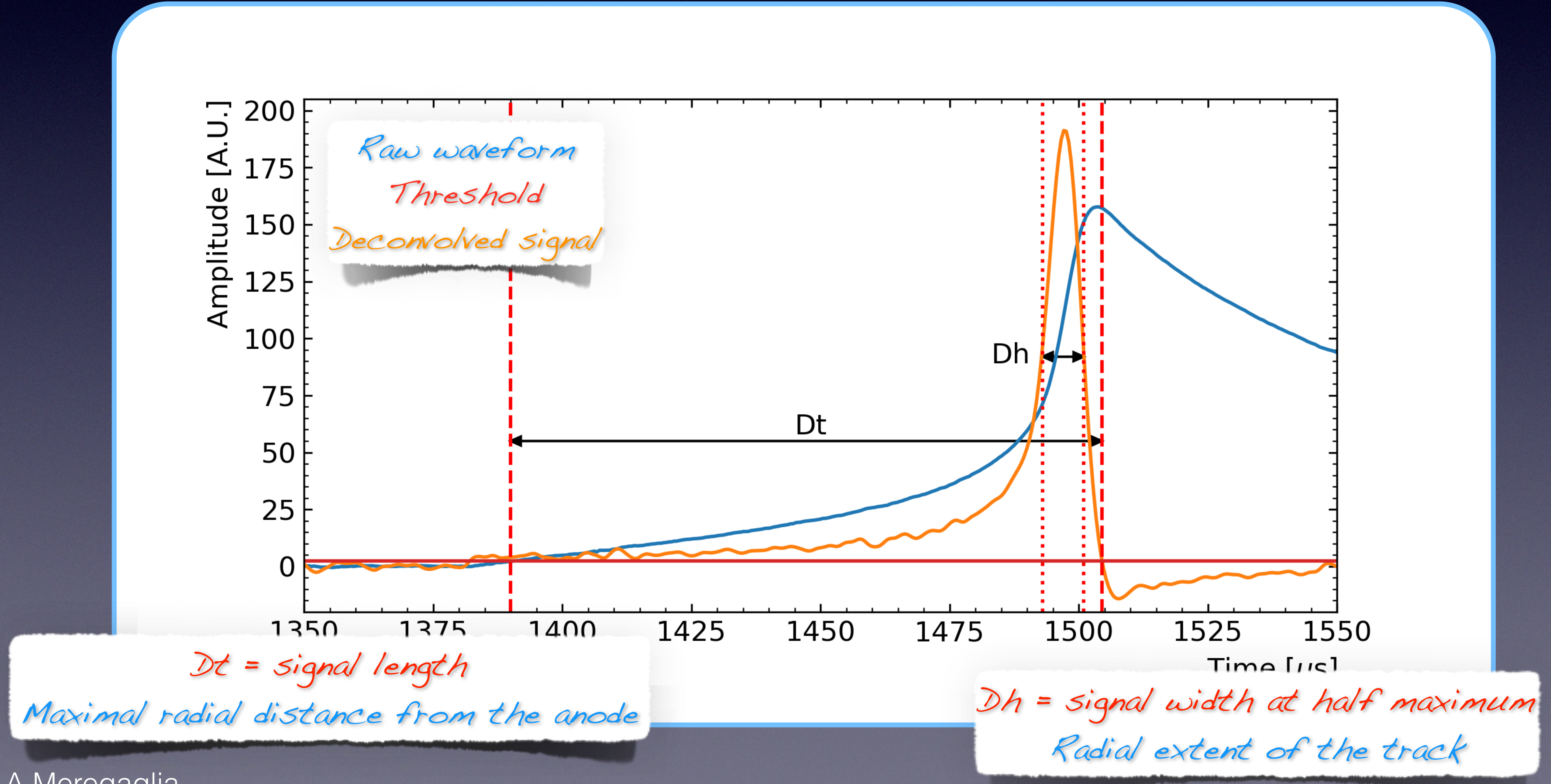

Signal

- The reconstructed waveforms are used to extract observables such as the total charge of the event, its duration and the width at half height.
- Each observable is associated to a specific feature of the original signal.

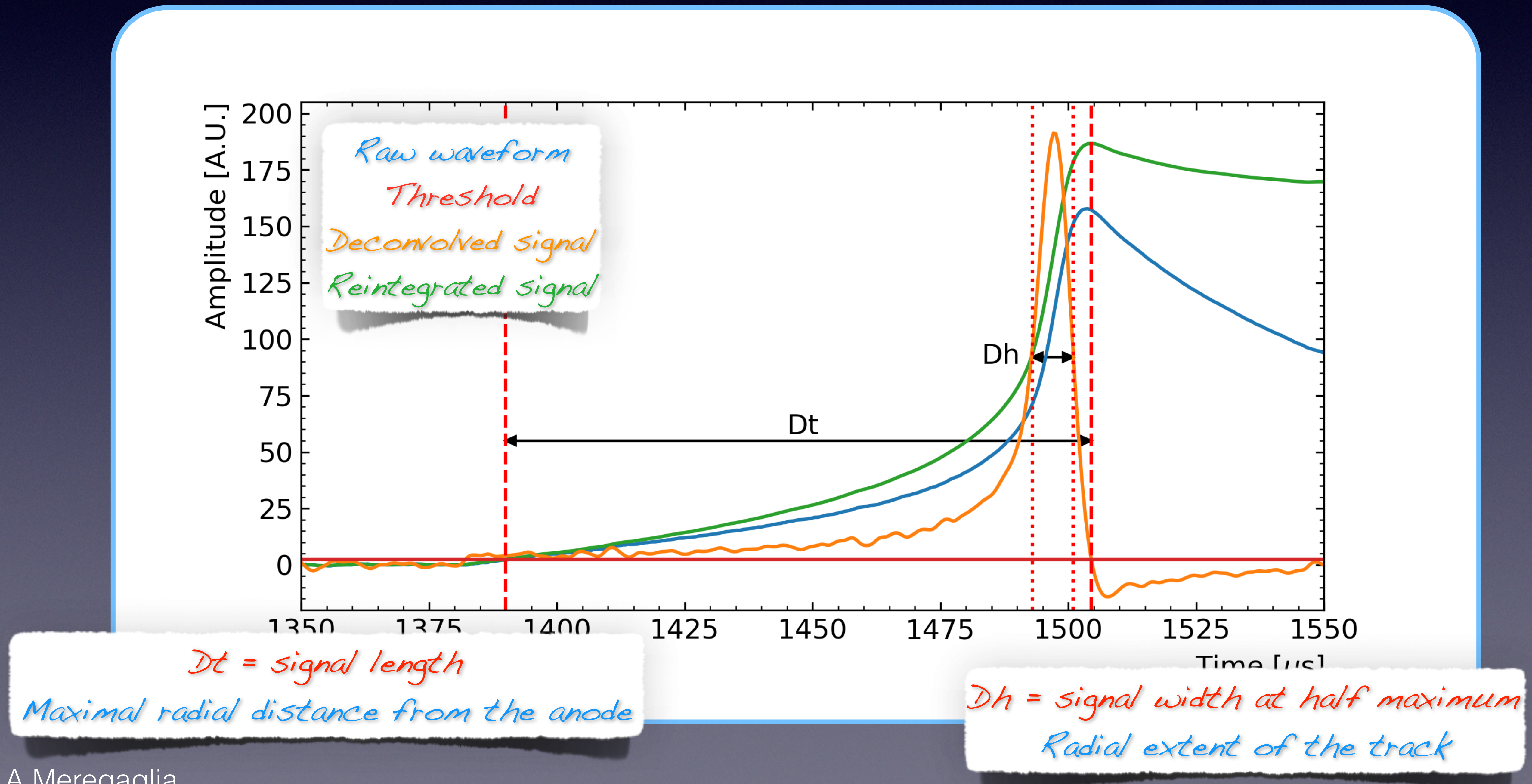

Signal

- The reconstructed waveforms are used to extract observables such as the total charge of the event, its duration and the width at half height.
- Each observable is associated to a specific feature of the original signal.

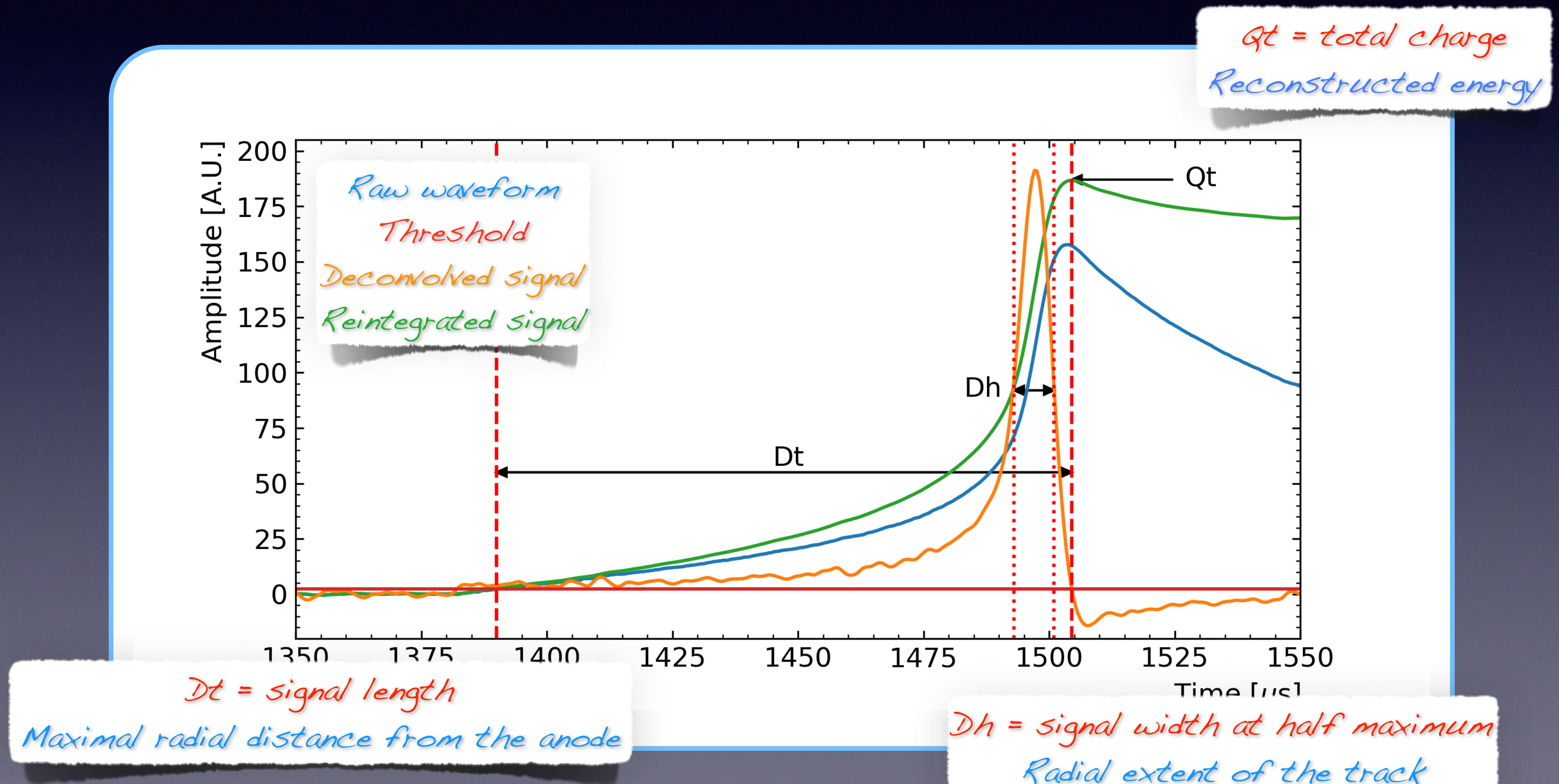

Signal

- A simulation based on the Shockley-Ramo theorem was developed and a very good agreement was found between the registered and the simulated waveforms.
- The simulation was used to confirm our understanding of the observables.

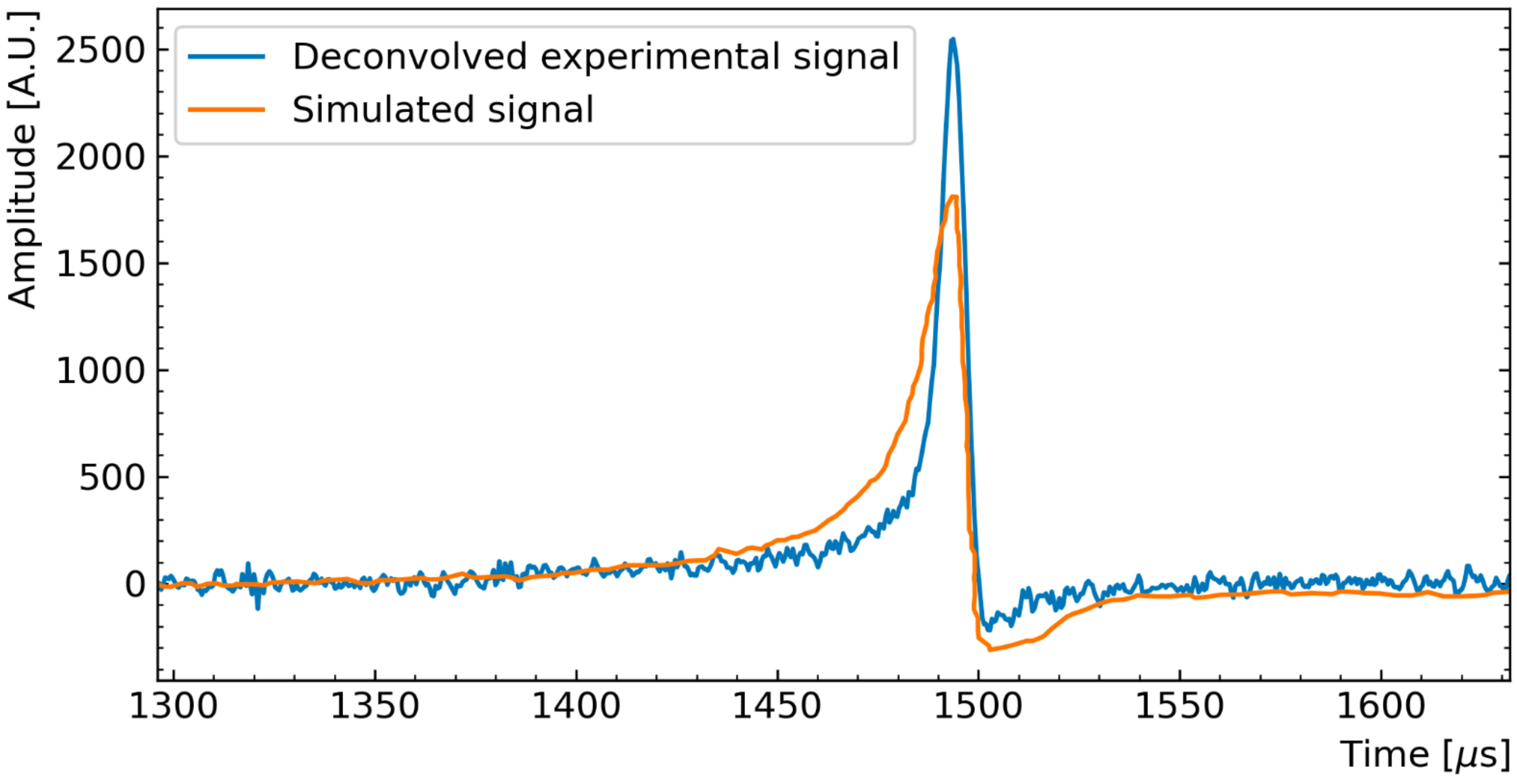

Further studies on the signal

- Based on real data and on GARFIELD simulation of the drift time, the **signal tratment** was further pushed to reconstruction energy deposits of the same event.
- In the signal study a resistive anode with readout at both side was assumed, allowing to reconstruct also the longitudinal position of the events.

DISLCLAIMER!

The signal treatment presented in the next few slides is not applied to data analyis published so far (new analysis and data taken with non-resistive anode and readout on one side only)

The new signal treatment will further improve the detector performances
with respect to published results presented in this talk

Further studies on the signal

- The signal studies were carried out assuming a CTPC filled with xenon at 40 bar with 1 cm radius anode, 50 cm radius cathode, 20kV HV.
- A **realistic noise** was assumed based on collected data with the prototype.

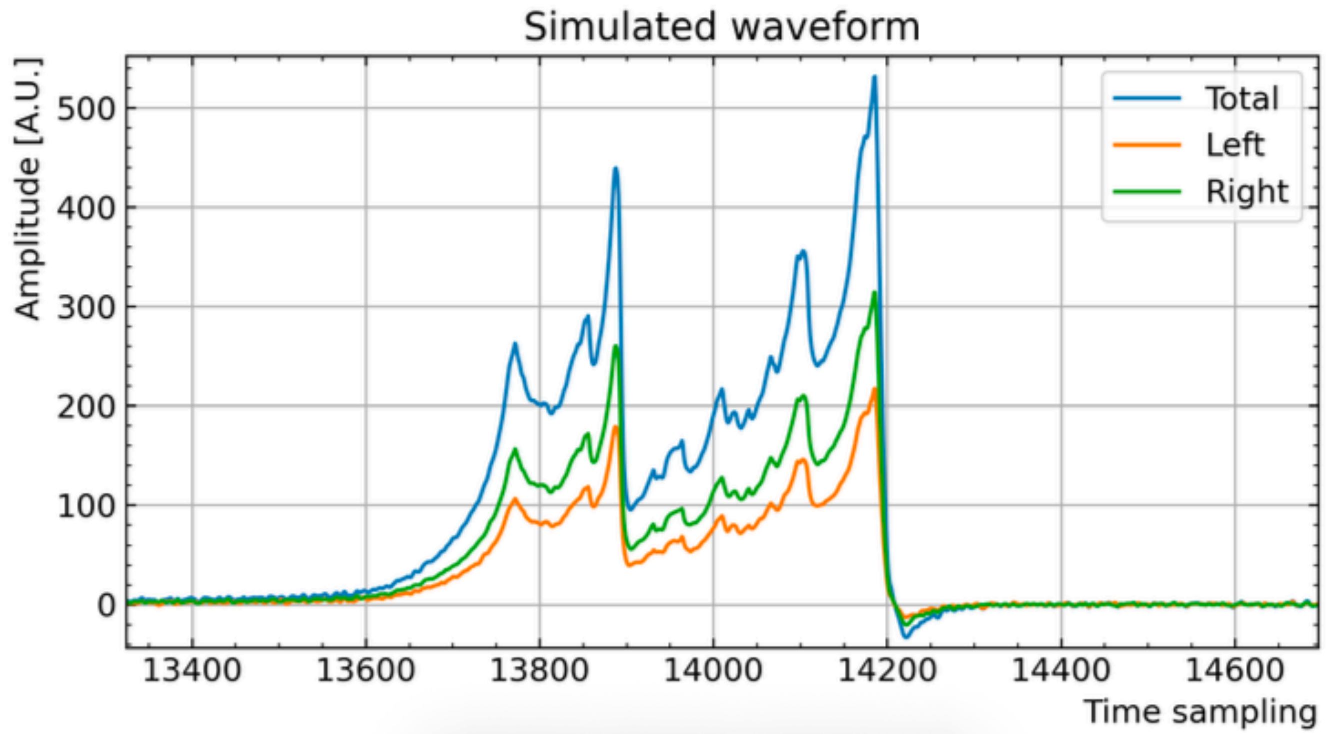

Step 1
signal simulation

ββ0ν signal simulated in GEANT4

The drift time for each energy deposit is computed with GARFIELD

Using the Shockley-Ramo theorem two partial waveforms are reconstructed for each energy deposit

Further studies on the signal

- The signal is treated to reconstruct the different energy deposits.
- The procedure is base on an iterative method and on the knowledge of the expected signal from a single electron.
- The template signal depends on the detector (geometry, HV, readout electronics…) and should be properly measured to apply the same procedure on real data (ongoing…!)

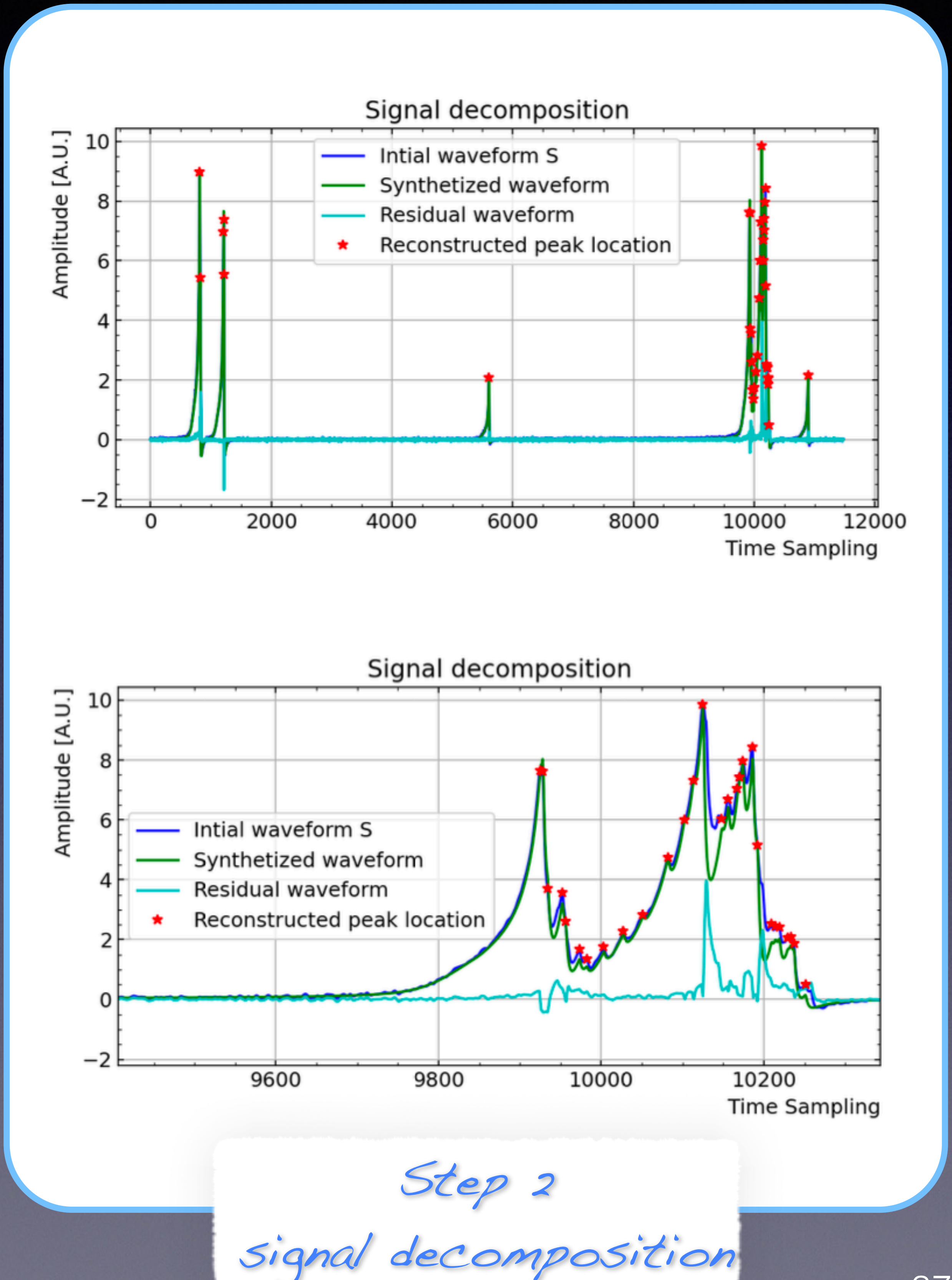

Further studies on the signal

- By analysing the different peaks, it is possible to reconstruct the radial position R via the drift time and the longitudinal position Z via the amplitude ratio of the partial waveforms.

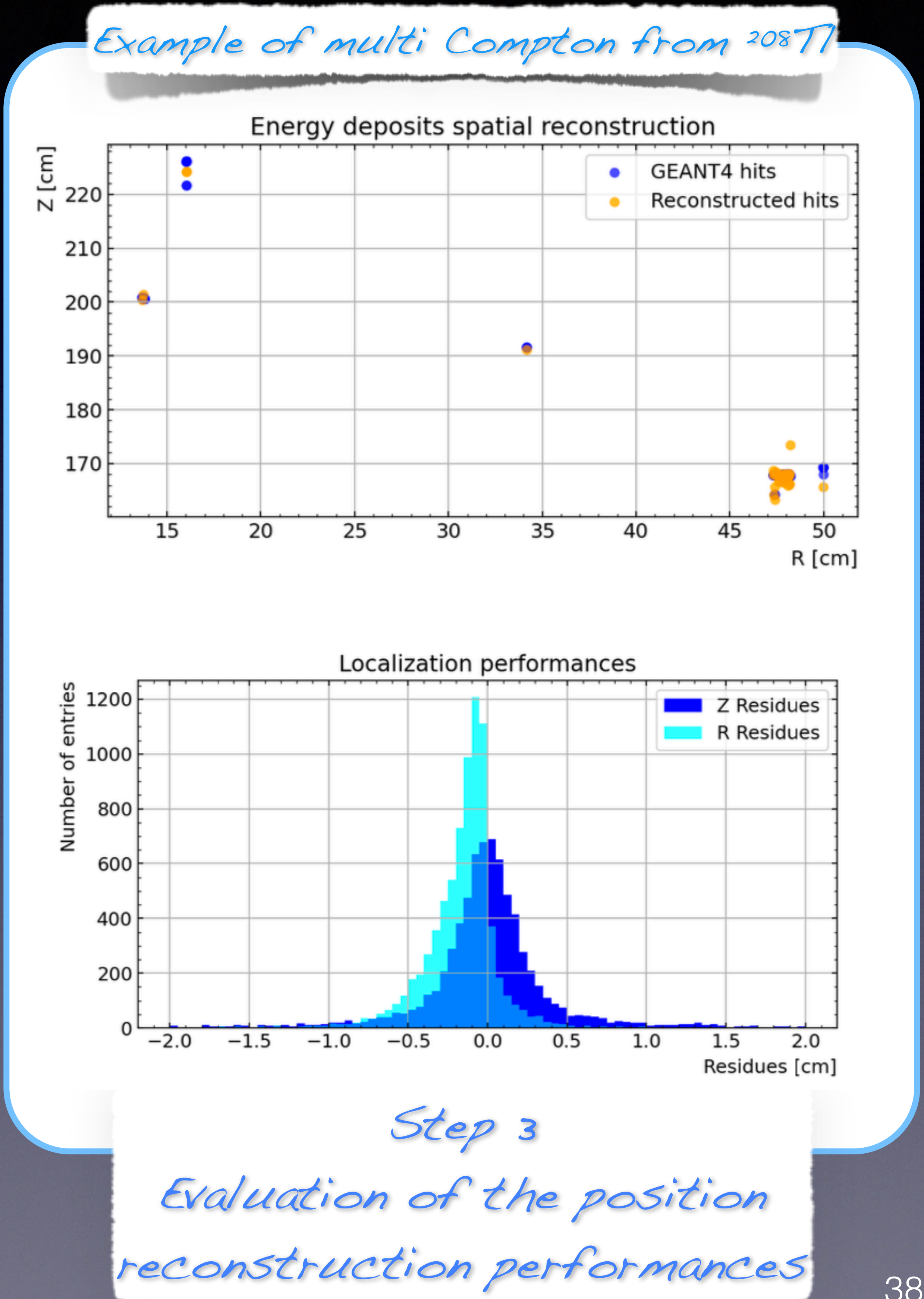

Further studies on the signal

- By analysing the different peaks, it is possible to reconstruct the radial position R via the drift time and the longitudinal position Z via the amplitude ratio of the partial waveforms.

A position reconstruction of the energy deposits with a precision better than 1 cm can be achieved!

Example of multi Compton from ^{208}Tl

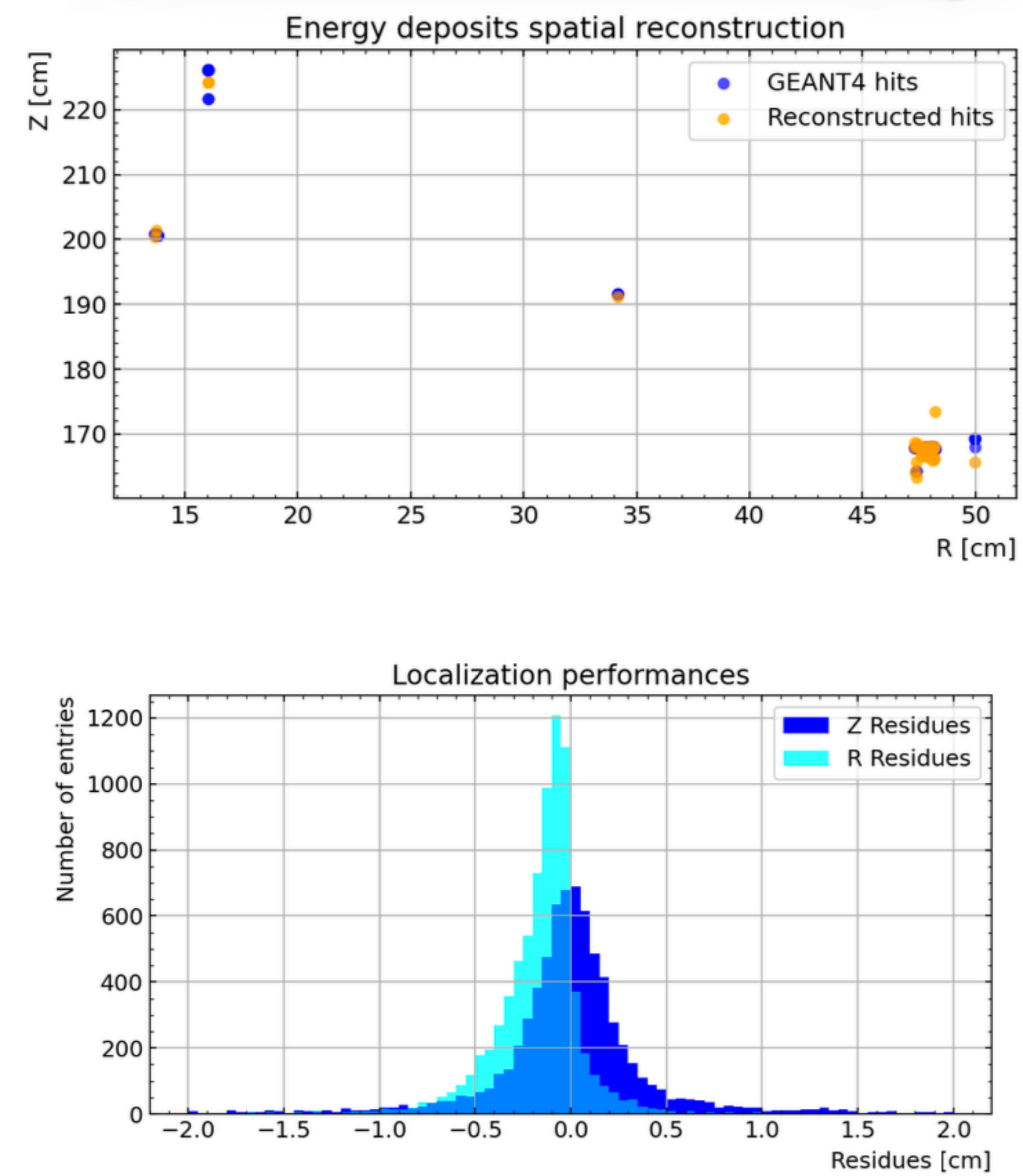

Step 3
Evaluation of the position reconstruction performances

Further studies on the signal

- Since the signal in ionization mode is made only by the electrons (ions under threshold), **the total charge depends on the radial position where the ionization electrons are created**.

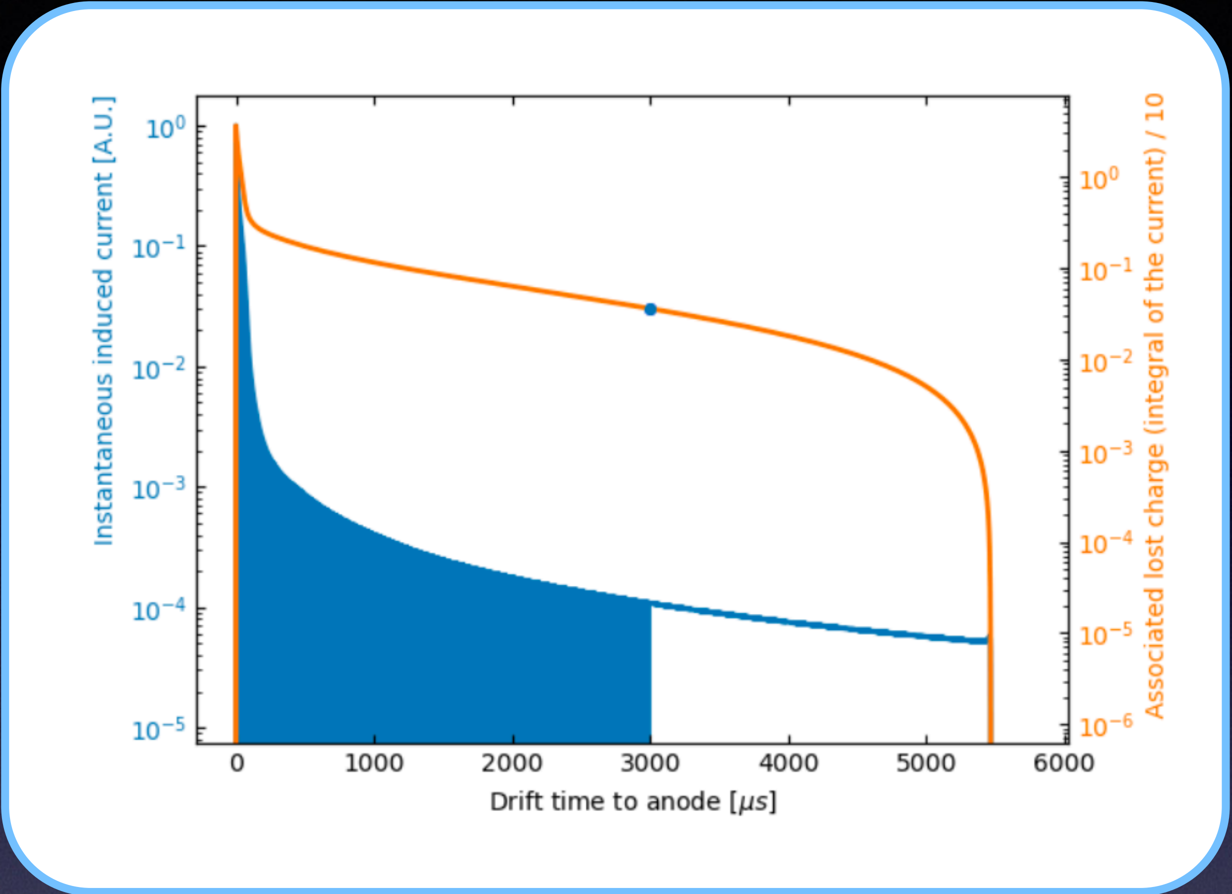

Further studies on the signal

- Since the signal in ionization mode is made only by the electrons (ions under threshold), **the total charge depends on the radial position where the ionization electrons are created**.
- This explain the typical **shape of the reconstructed charge versus the initial position**.

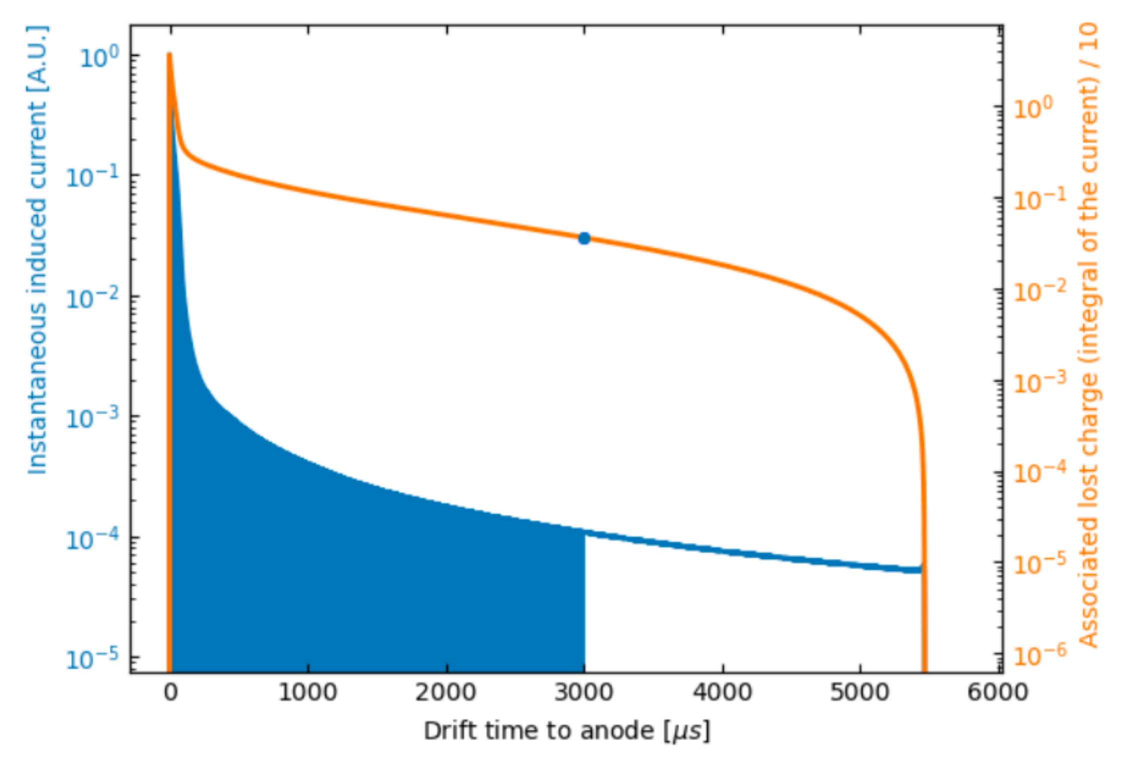

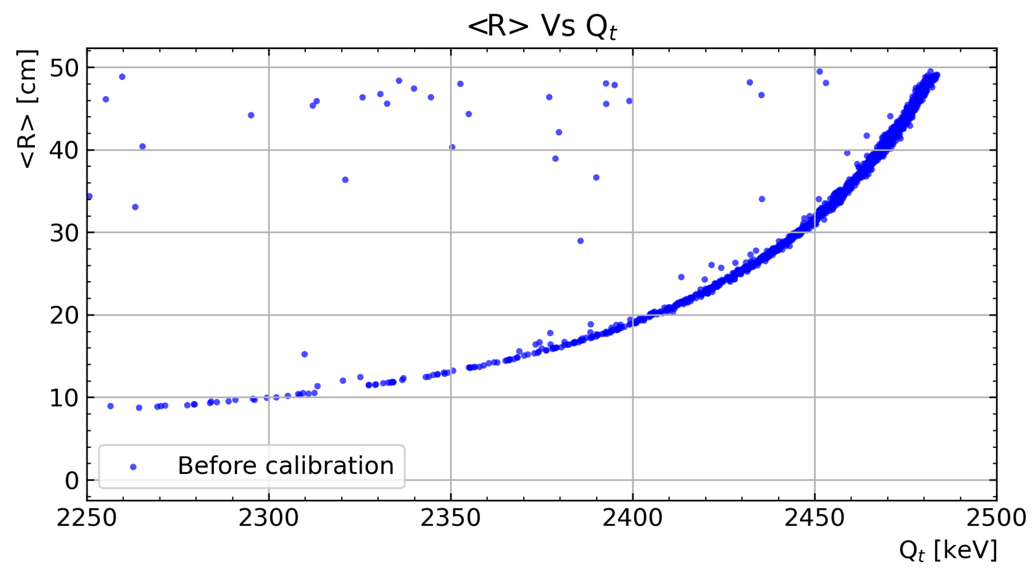

Further studies on the signal

- Since the signal in ionization mode is made only by the electrons (ions under threshold), **the total charge depends on the radial position where the ionization electrons are created**.
- This explain the typical **shape of the reconstructed charge versus the initial position**.

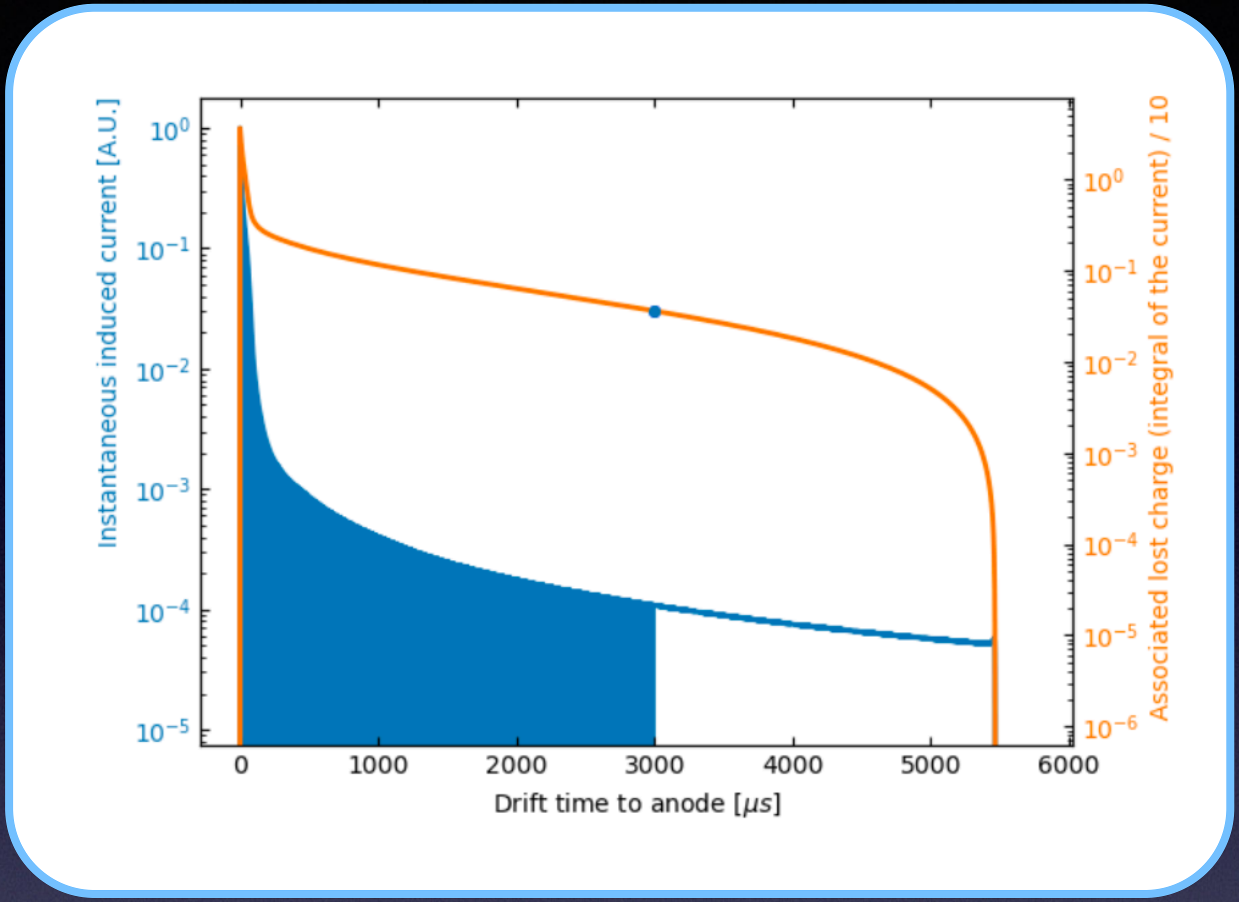

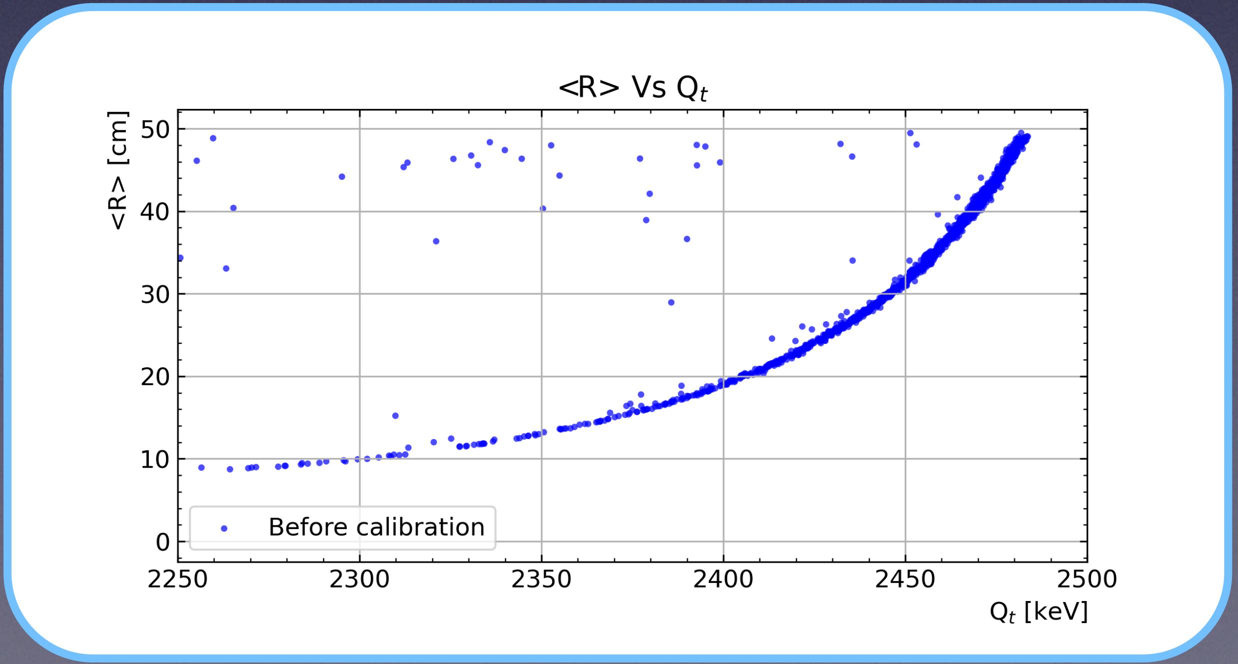

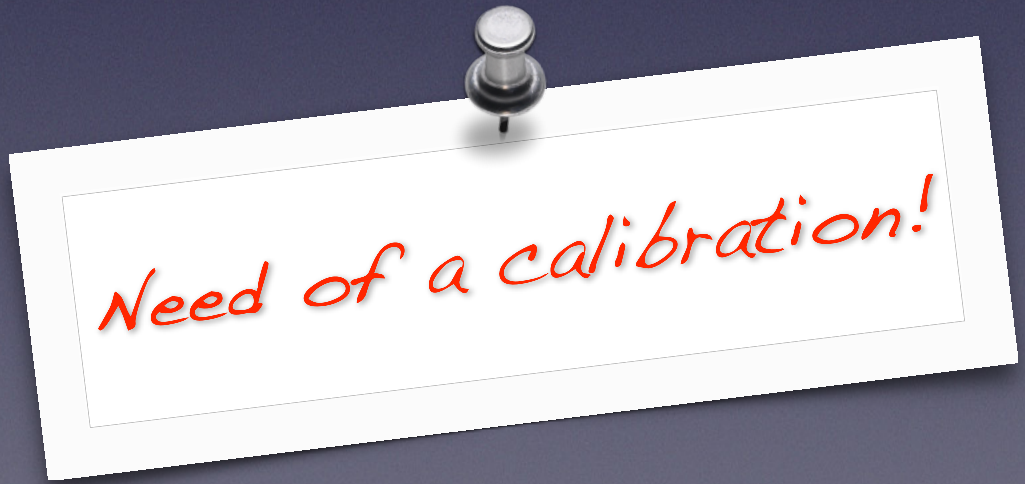

Further studies on the signal

- A calibration was performed and the reconstructed charge was corrected.

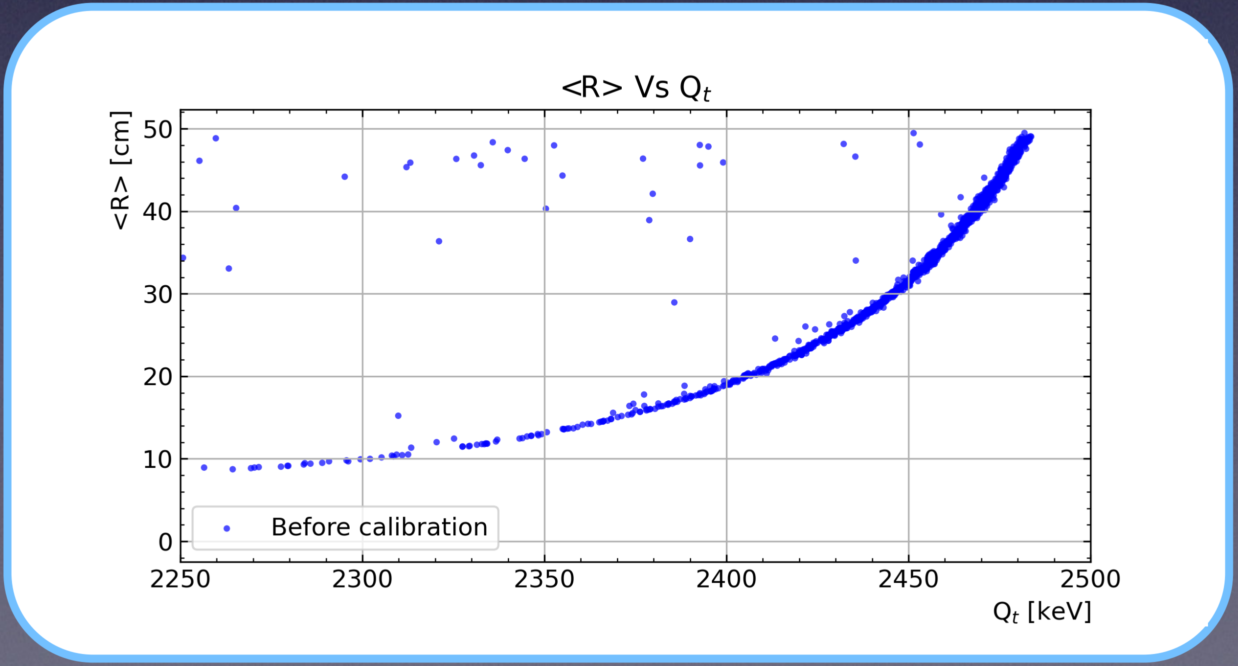

Further studies on the signal

- A calibration was performed and the reconstructed charge was corrected.

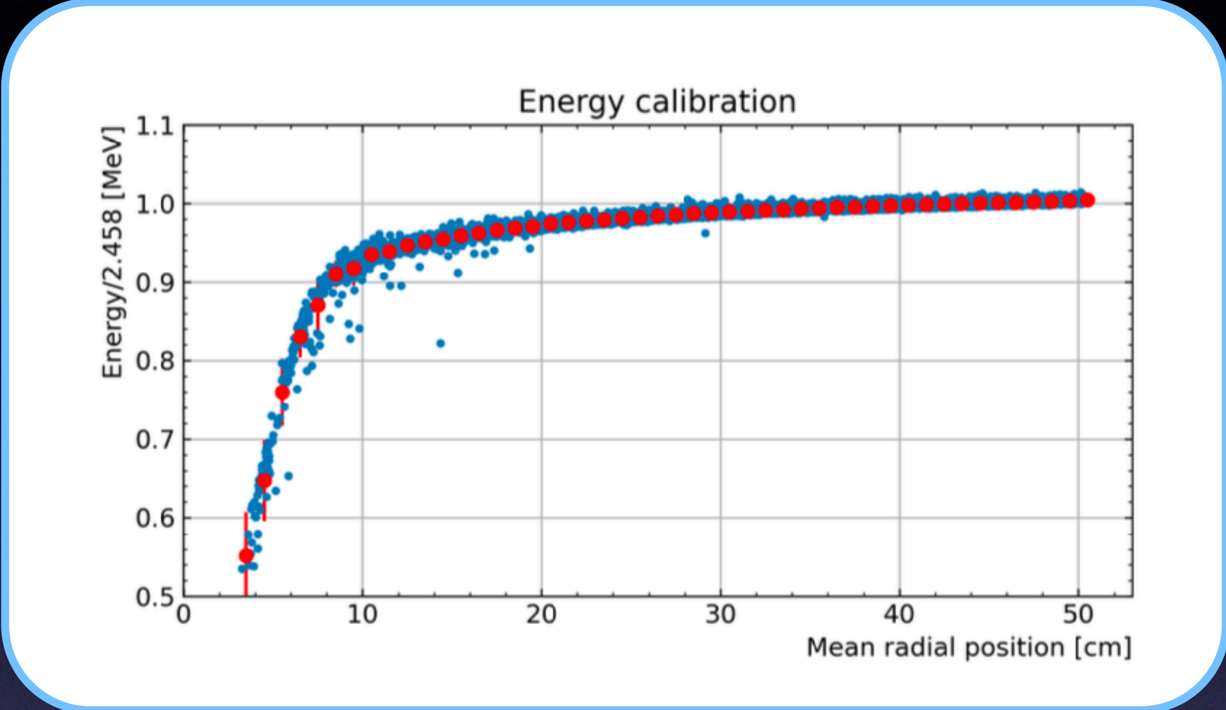

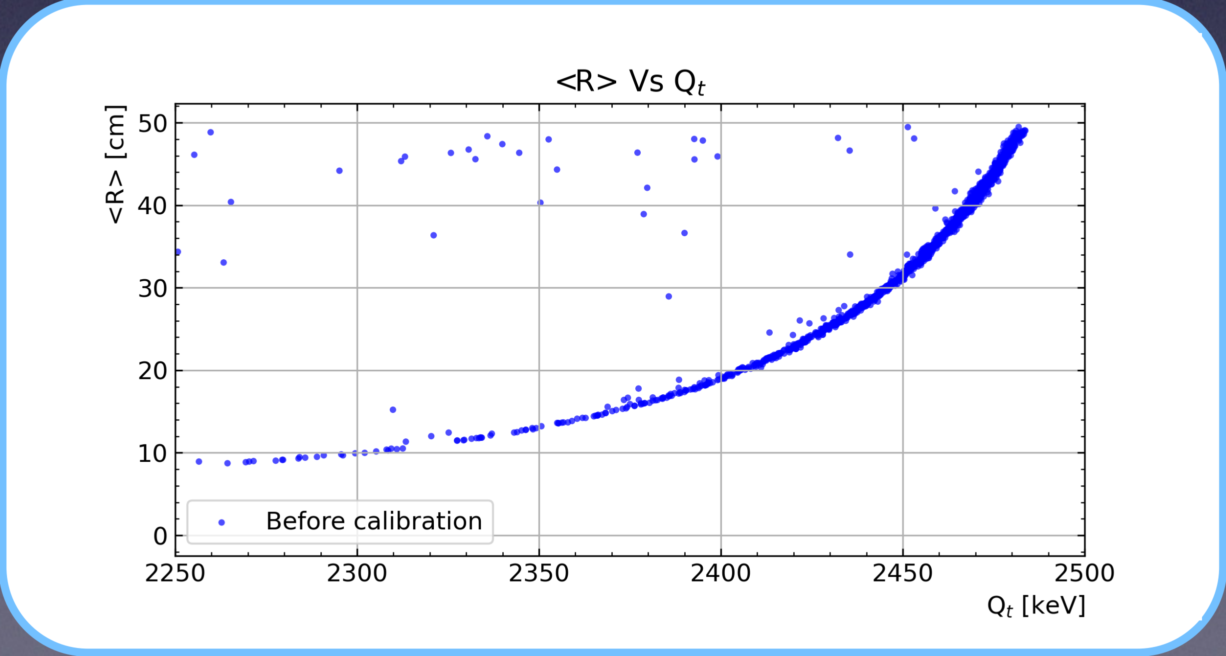

Further studies on the signal

- A calibration was performed and the reconstructed charge was corrected.

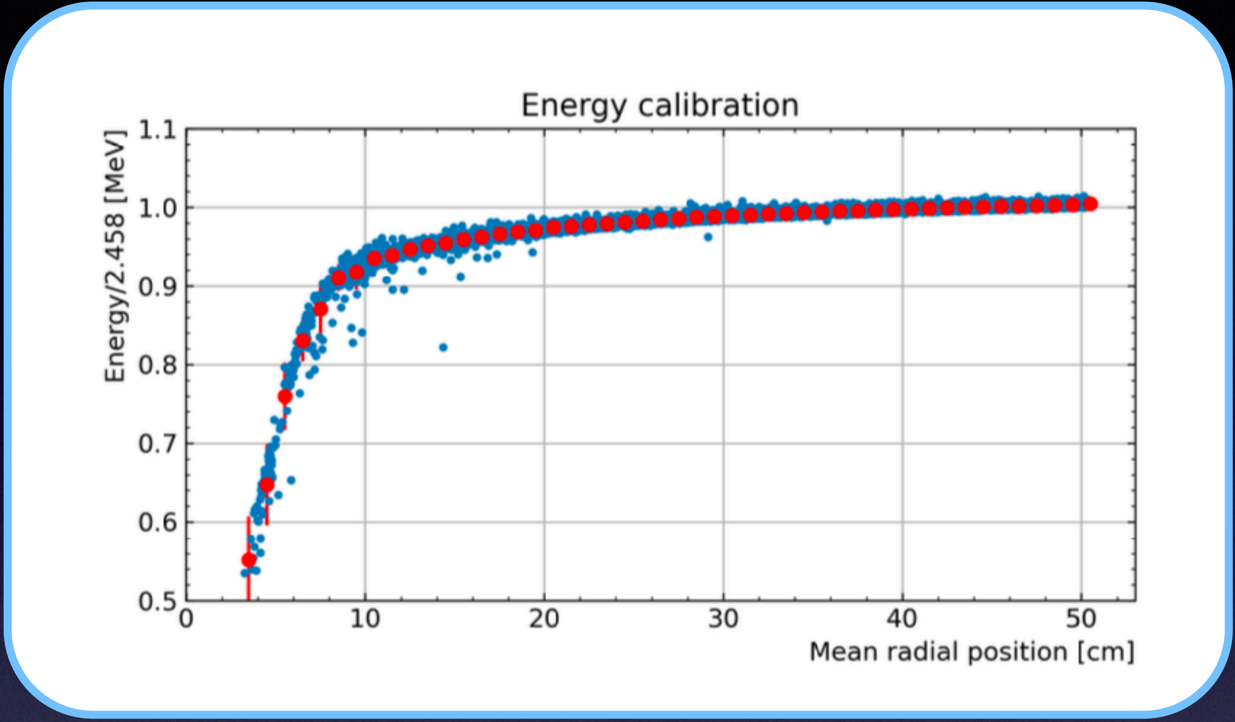

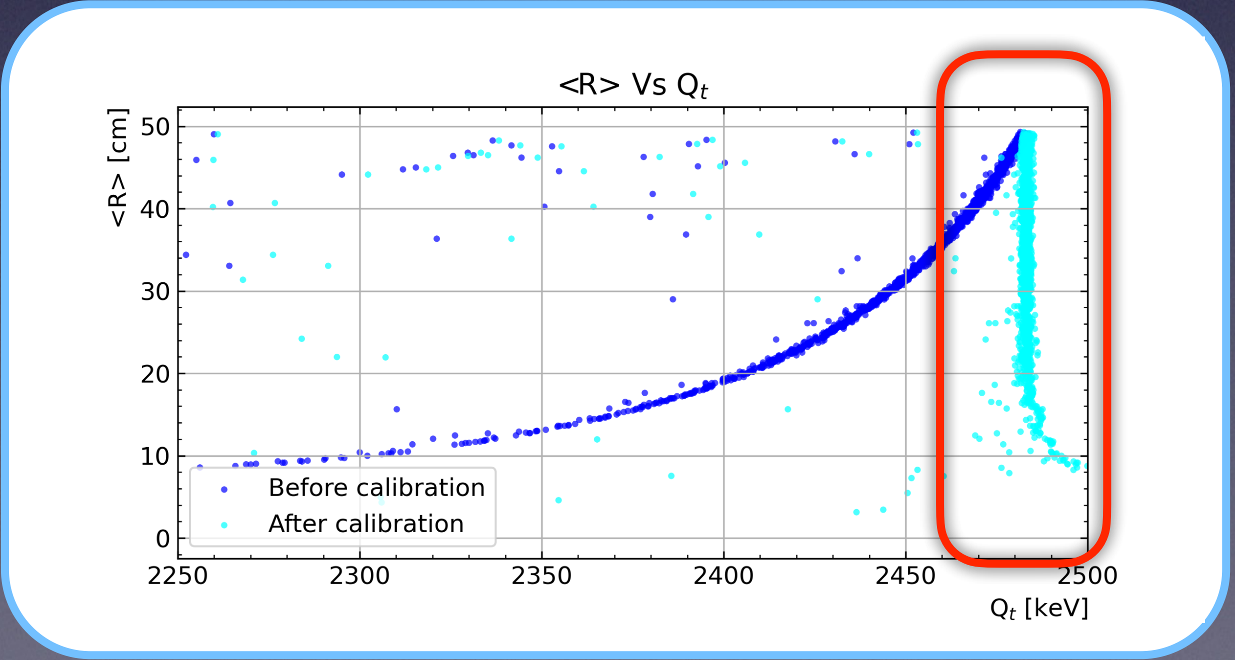

Further studies on the signal

- A calibration was performed and the reconstructed charge was corrected.
- A small calibration helps even for the charge computed in the synthetization process (sum of the found peaks) and overall we get 0.1% FWHM (limit of the method with no statistical fluctuations).

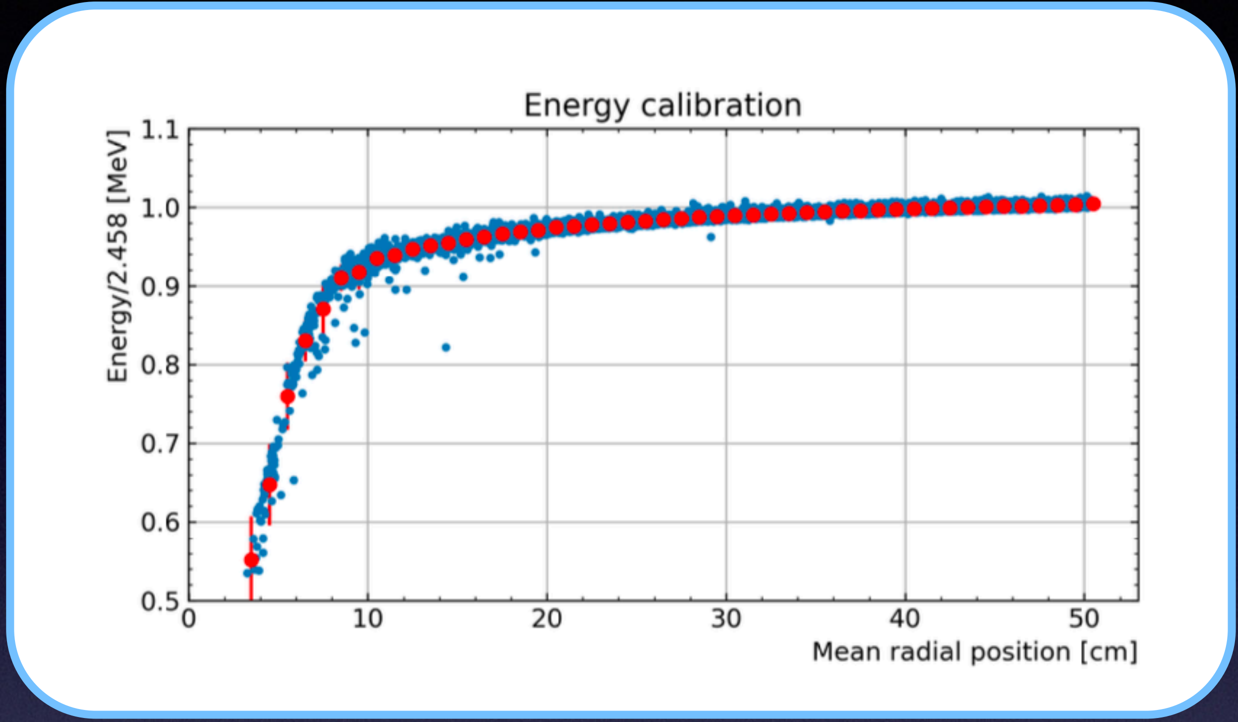

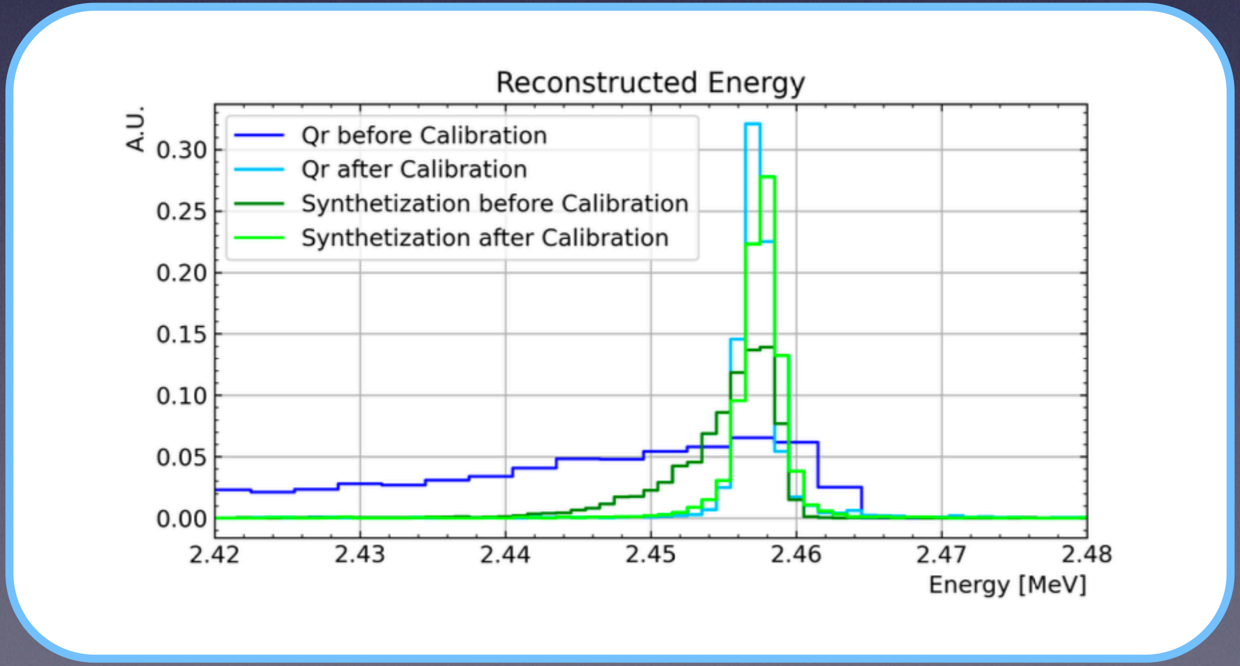

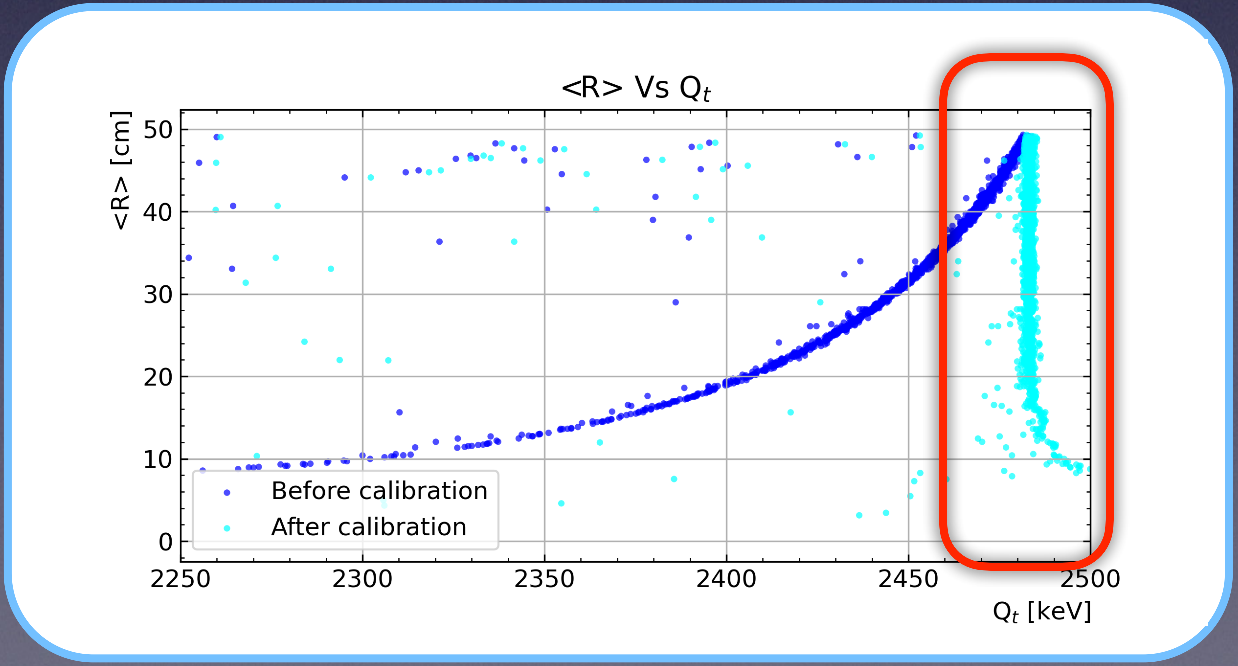

Further studies on the signal

- A calibration was performed and the reconstructed charge was corrected.
- A small ca computed of the foun FWHM (lim fluctuations)

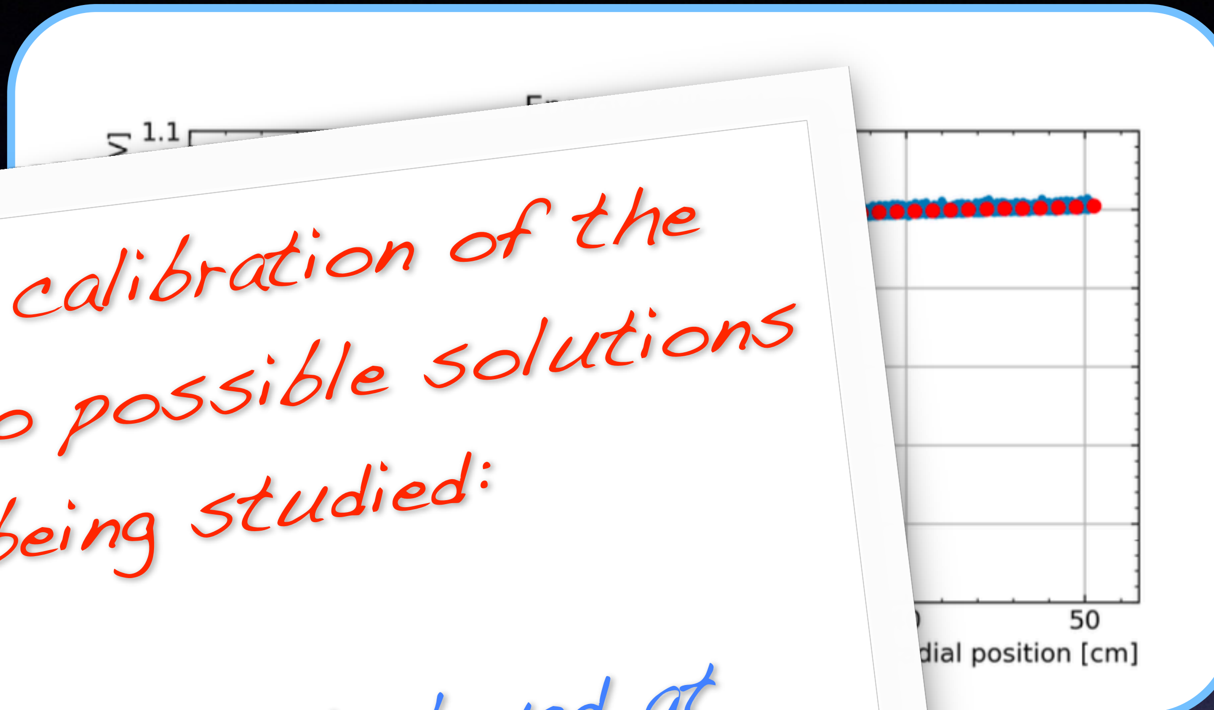

In real life an energy calibration of the detector is needed. Two possible solutions are currently being studied:

- Point-like alpha source deployed at specific radial positions (potential distortion of electric field).
- Diffuse radon dissolved in the gas.

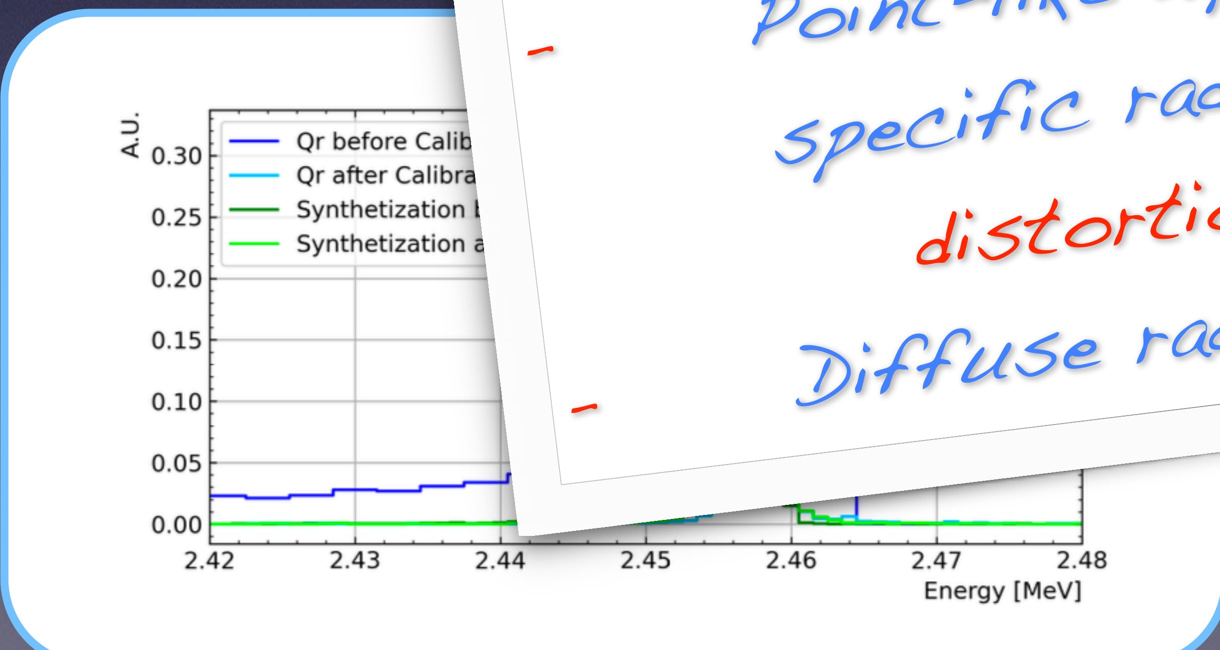

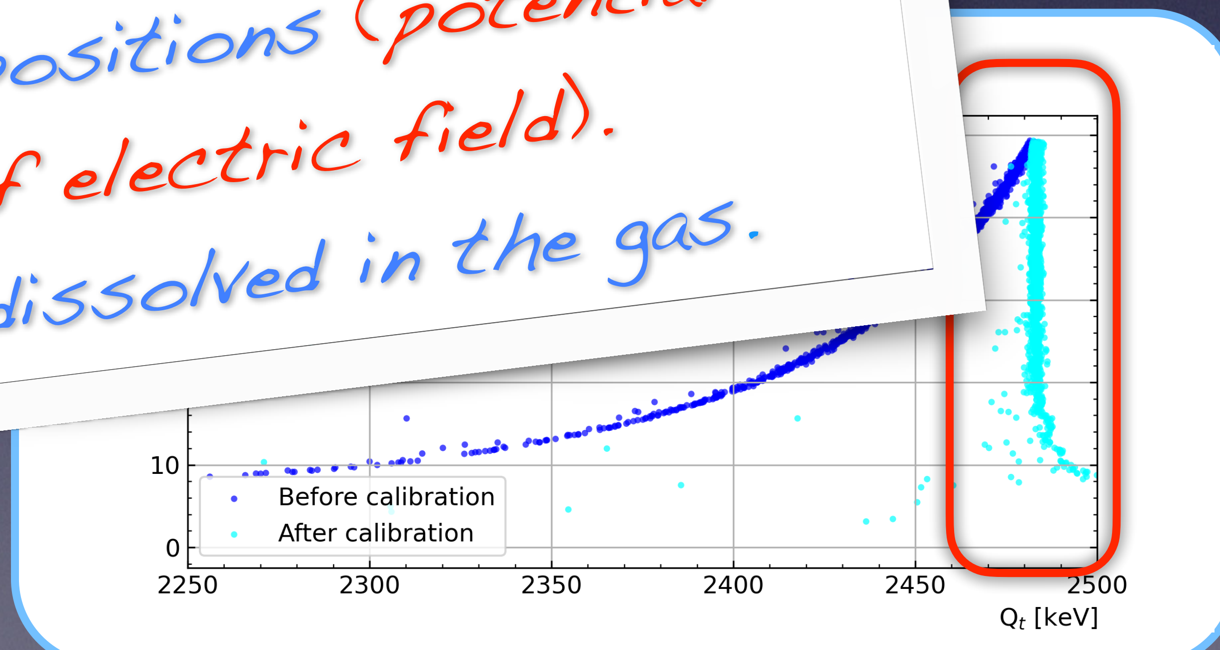

Data selection

- The observables were used to select the events, namely the Po or the Rn issued alphas.

Data for xenon at 3 bar, anode of 1.2 mm diameter, and -3000 V applied to the cathode

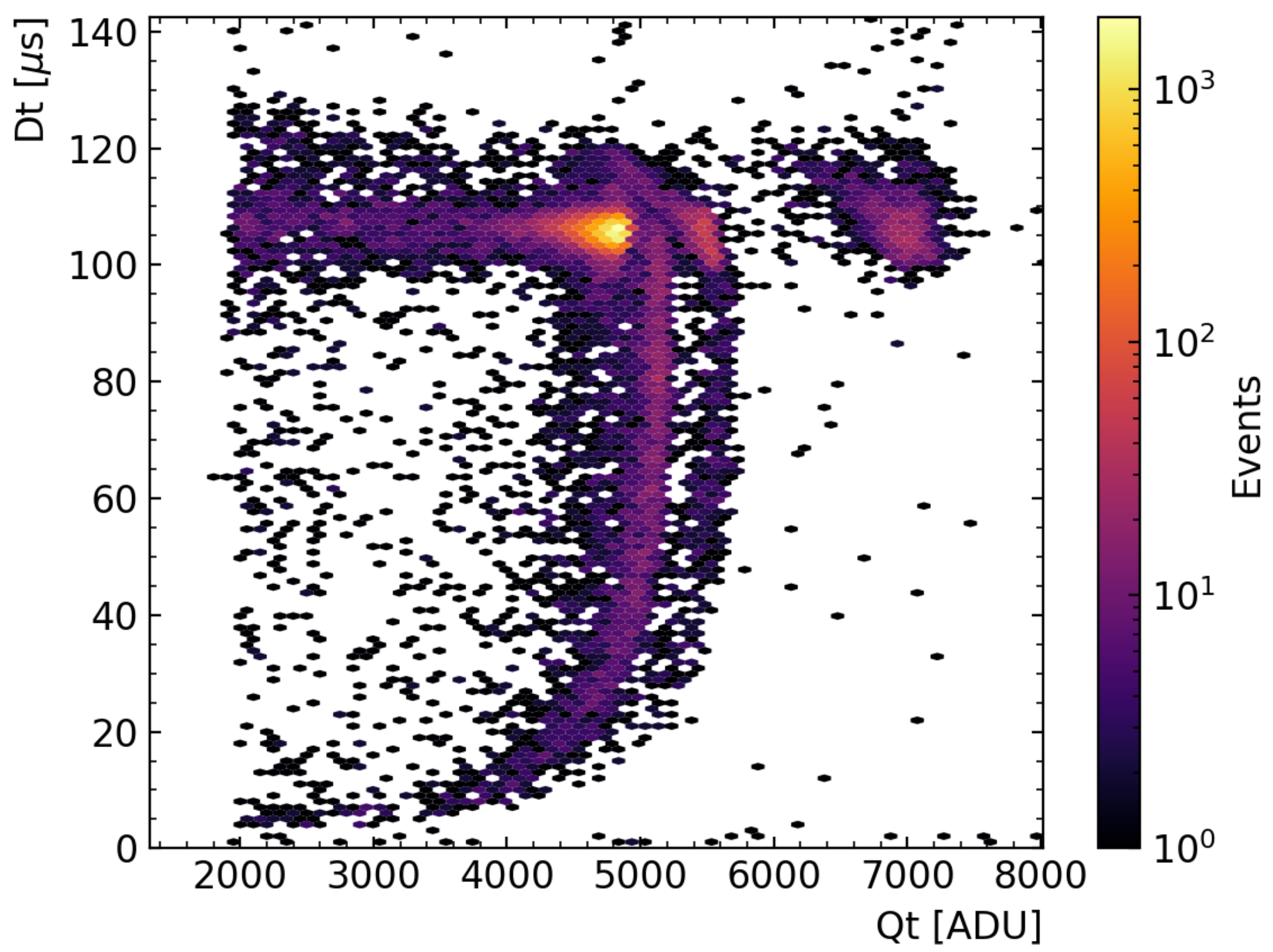

Data selection

- The observables were used to select the events, namely the Po or the Rn issued alphas.

Data for xenon at 3 bar, anode of 1.2 mm diameter, and -3000 V applied to the cathode

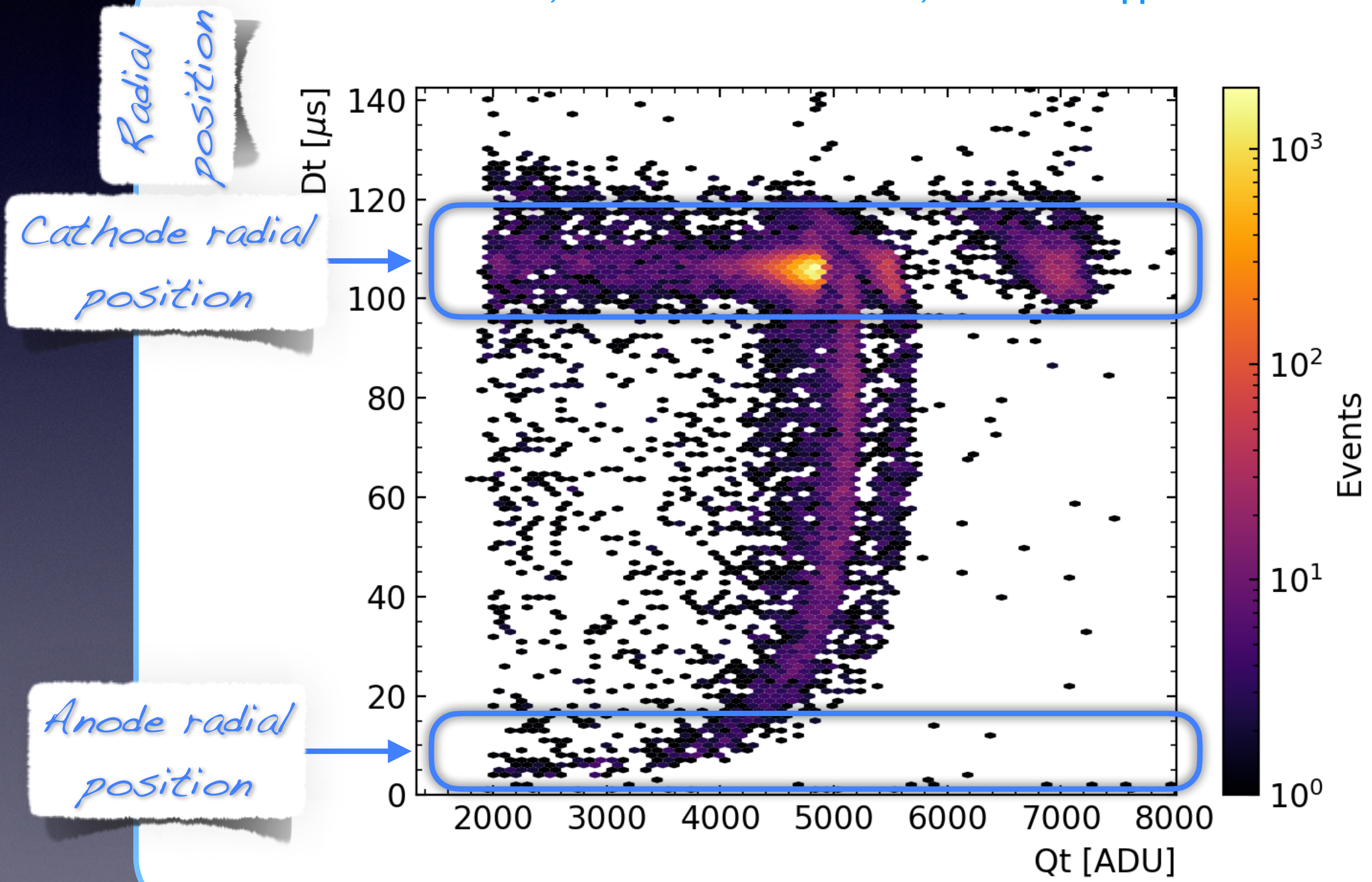

Data selection

- The observables were used to select the events, namely the Po or the Rn issued alphas.

Data for xenon at 3 bar, anode of 1.2 mm diameter, and -3000 V applied to the cathode

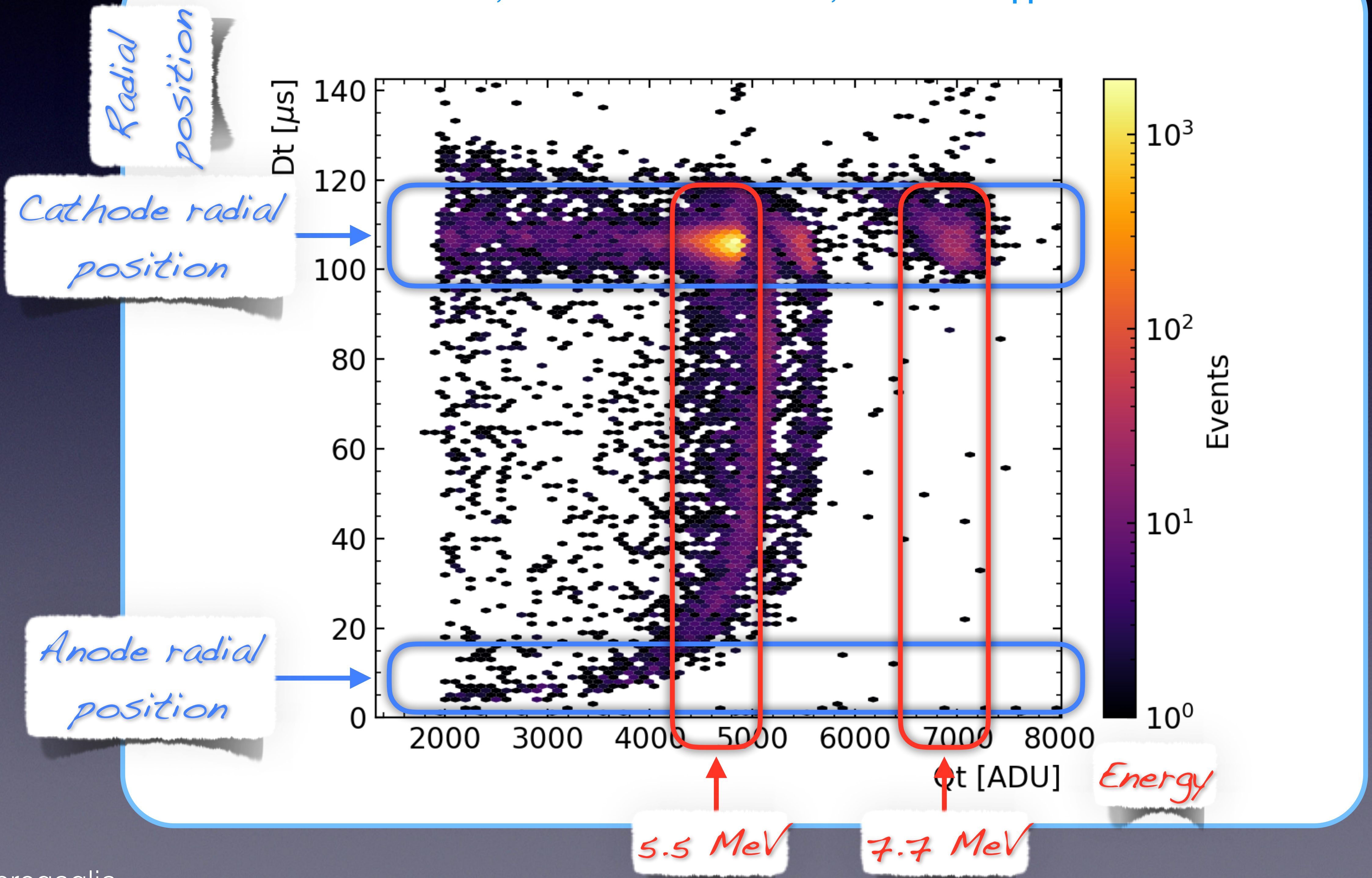

Data selection

- The observables were used to select the events, namely the Po or the Rn issued alphas.

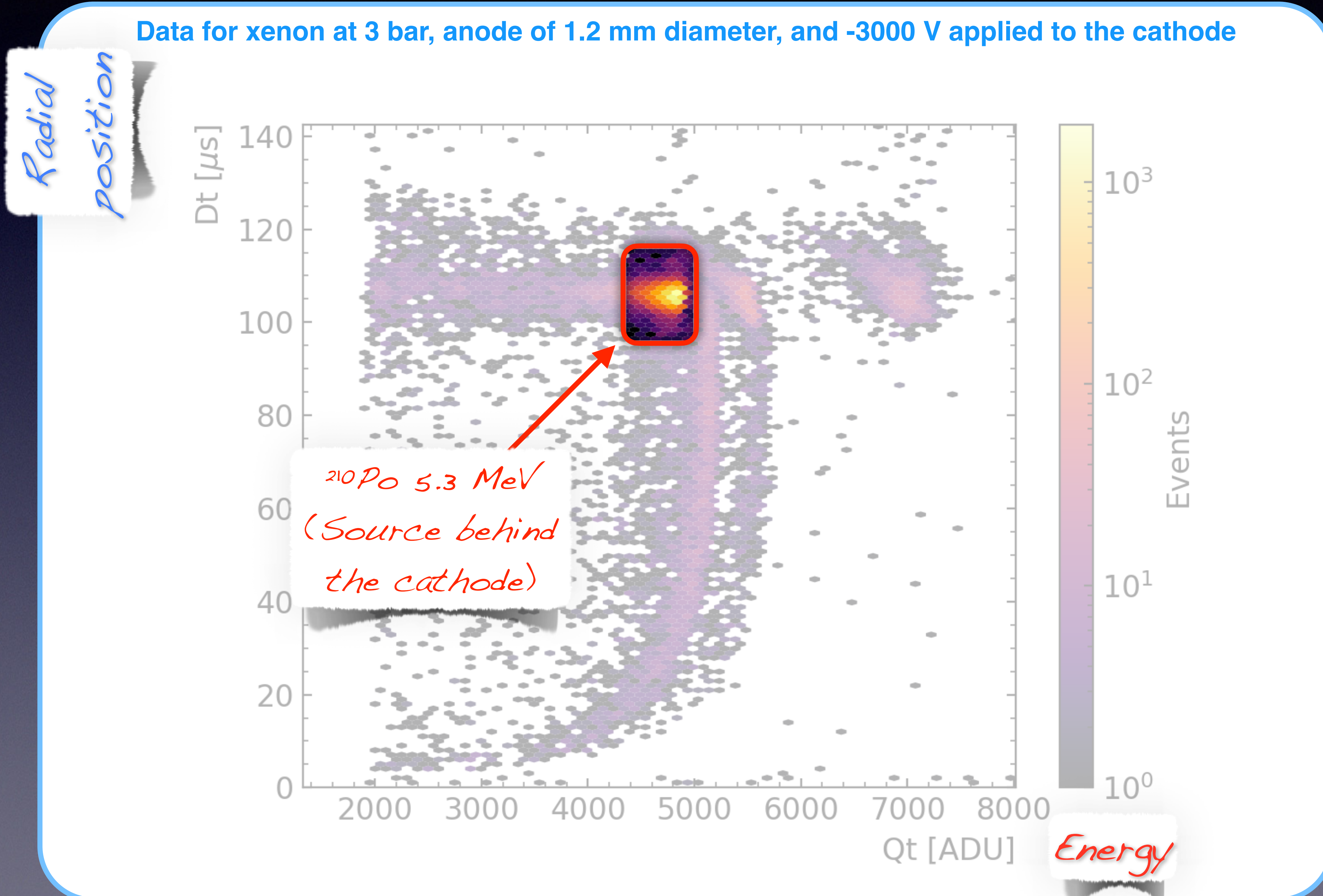

Data selection

- The observables were used to select the events, namely the Po or the Rn issued alphas.

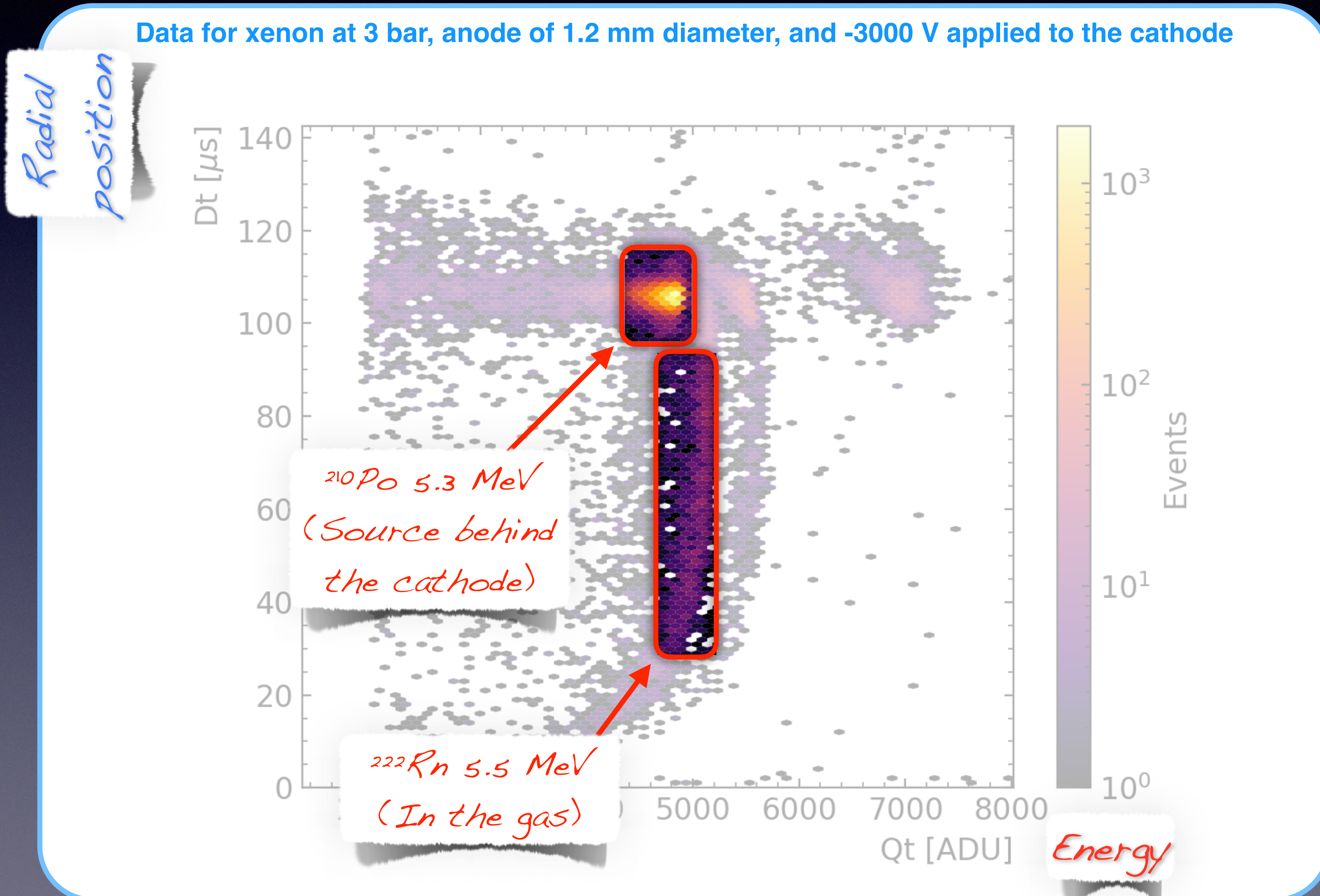

Data selection

- The observables were used to select the events, namely the Po or the Rn issued alphas.

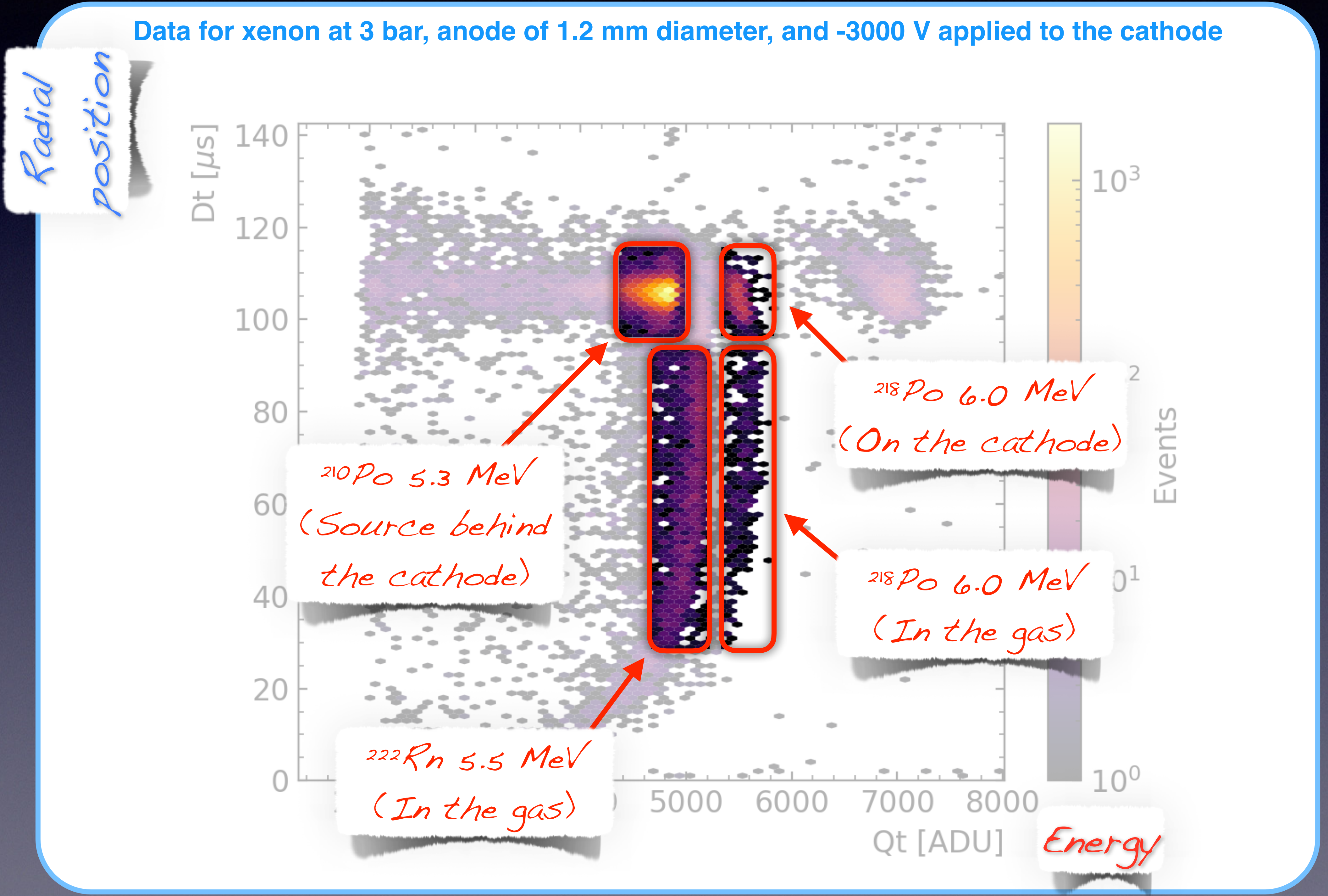

Data selection

- The observables were used to select the events, namely the Po or the Rn issued alphas.

Data for xenon at 3 bar, anode of 1.2 mm diameter, and -3000 V applied to the cathode

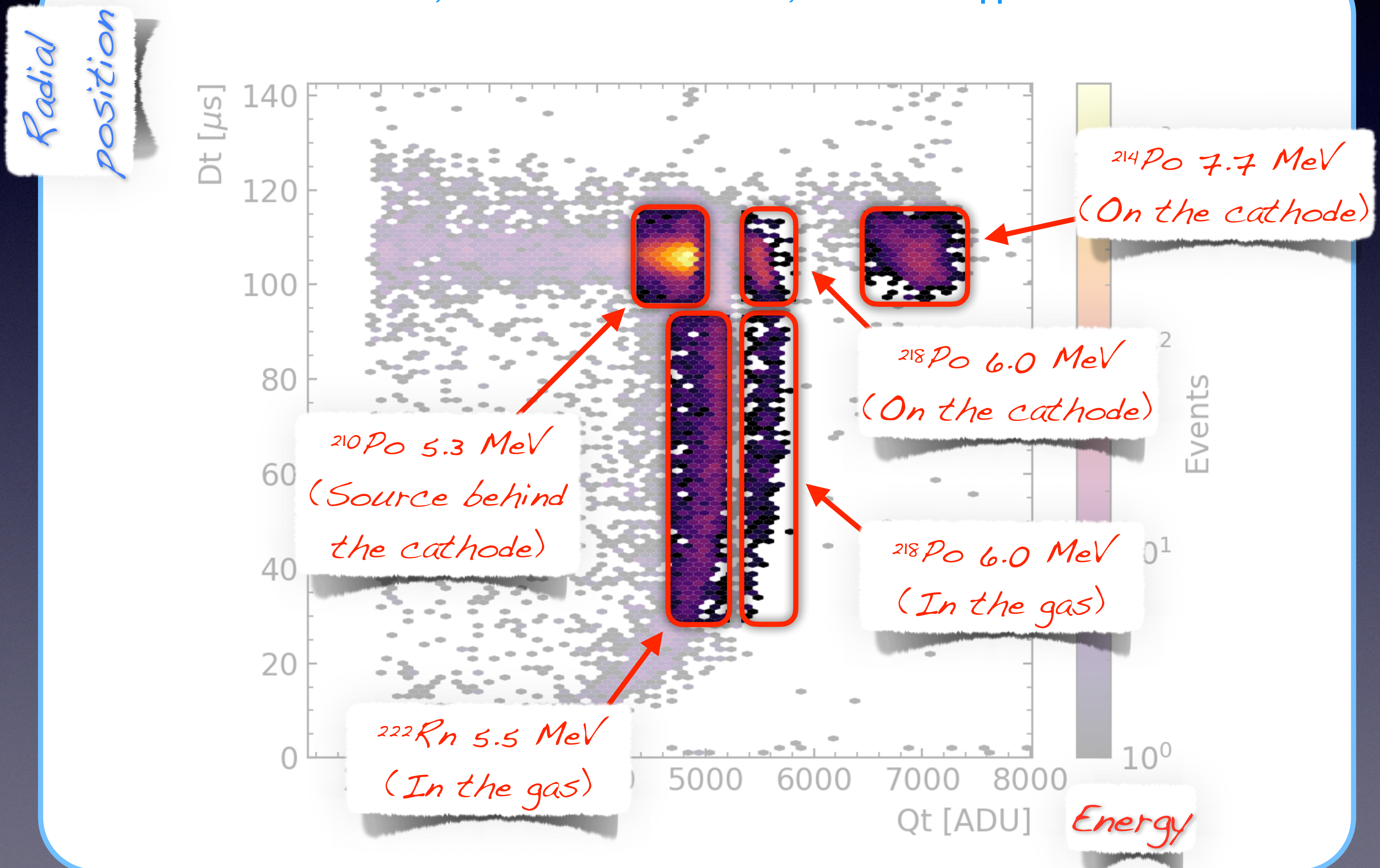

Data selection

- The observables were used to select the events, namely the Po or the Rn issued alphas.

Data for xenon at 3 bar, anode of 1.2 mm diameter, and -3000 V applied to the cathode

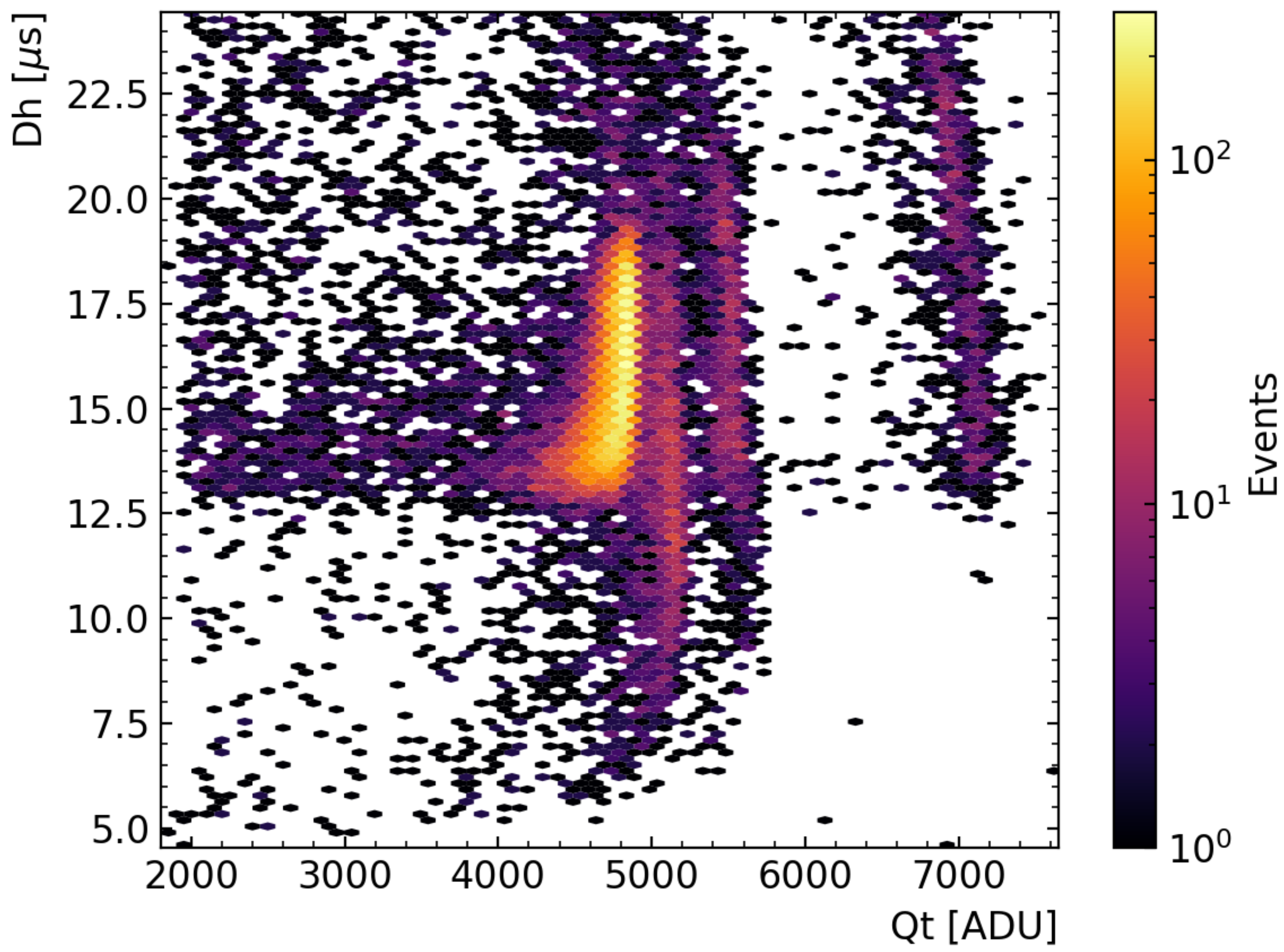

Data selection

- The observables were used to select the events, namely the Po or the Rn issued alphas.

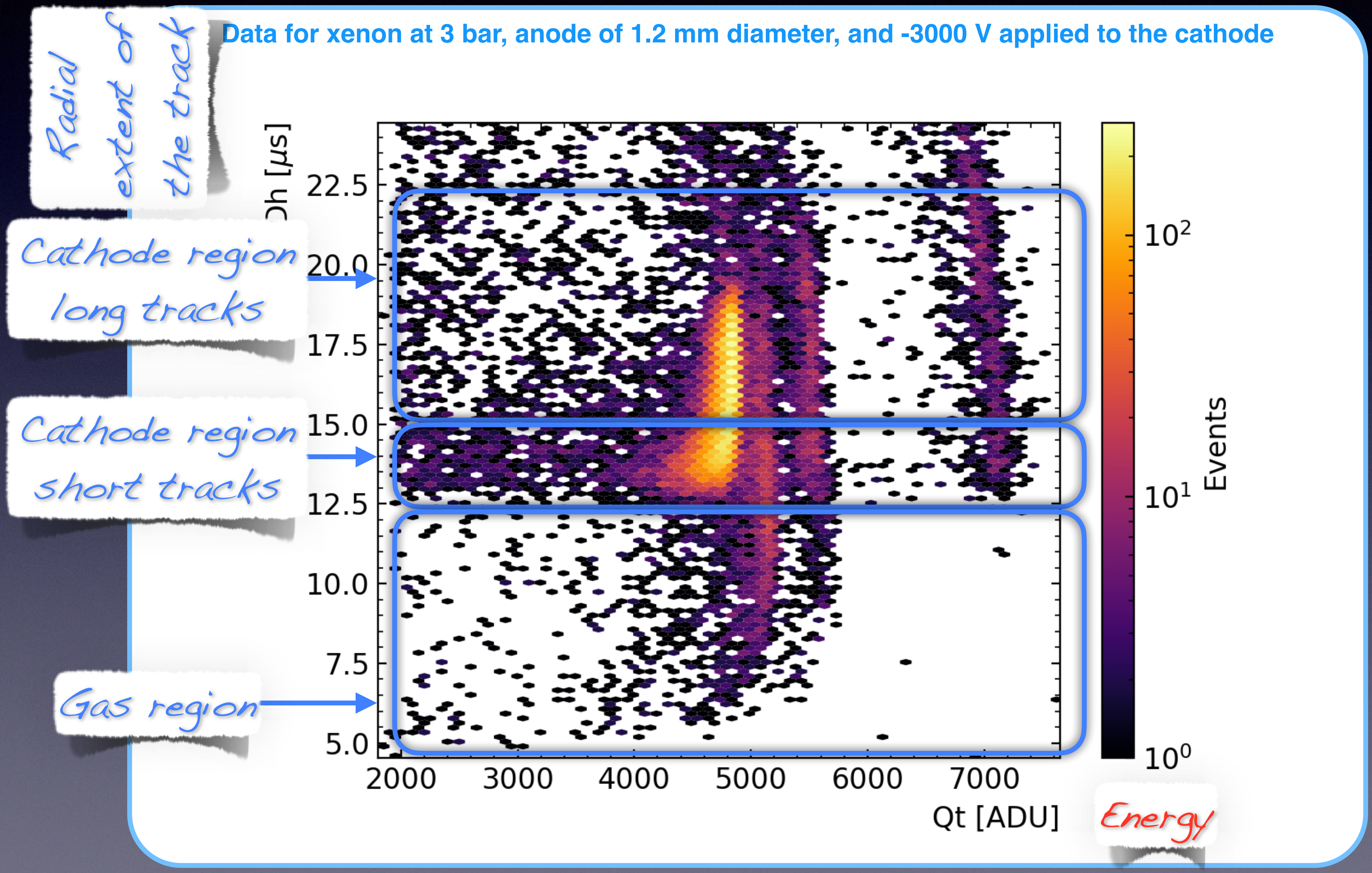

Data selection

- The observables were used to select the events, namely the Po or the Rn issued alphas.

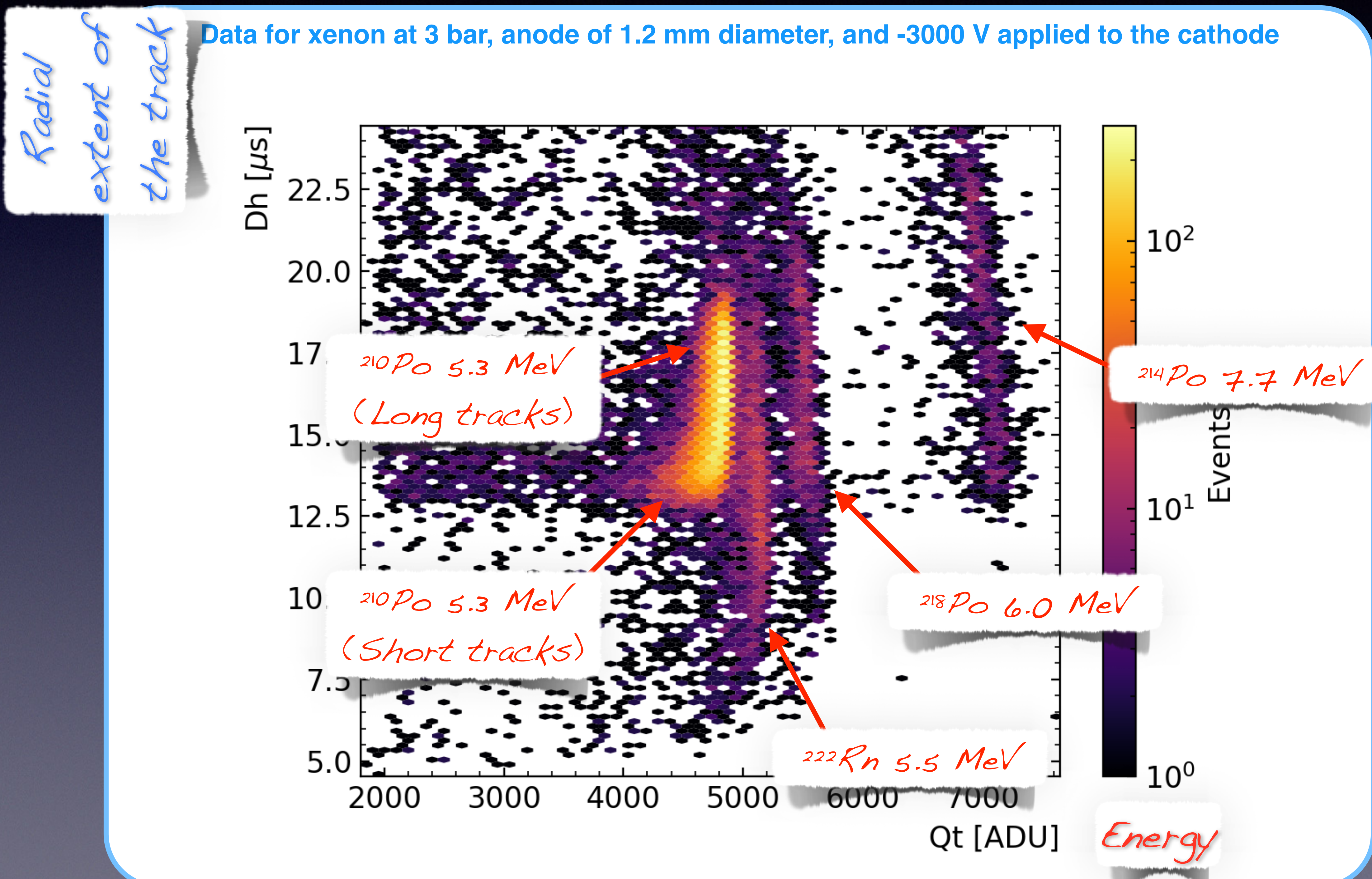

Data analysis

- The Qt of selected events (cuts on Dt and Dh) were fitted to establish the energy resolution.

Data for xenon at 3 bar, anode of 1.2 mm diameter, and -3000 V applied to the cathode

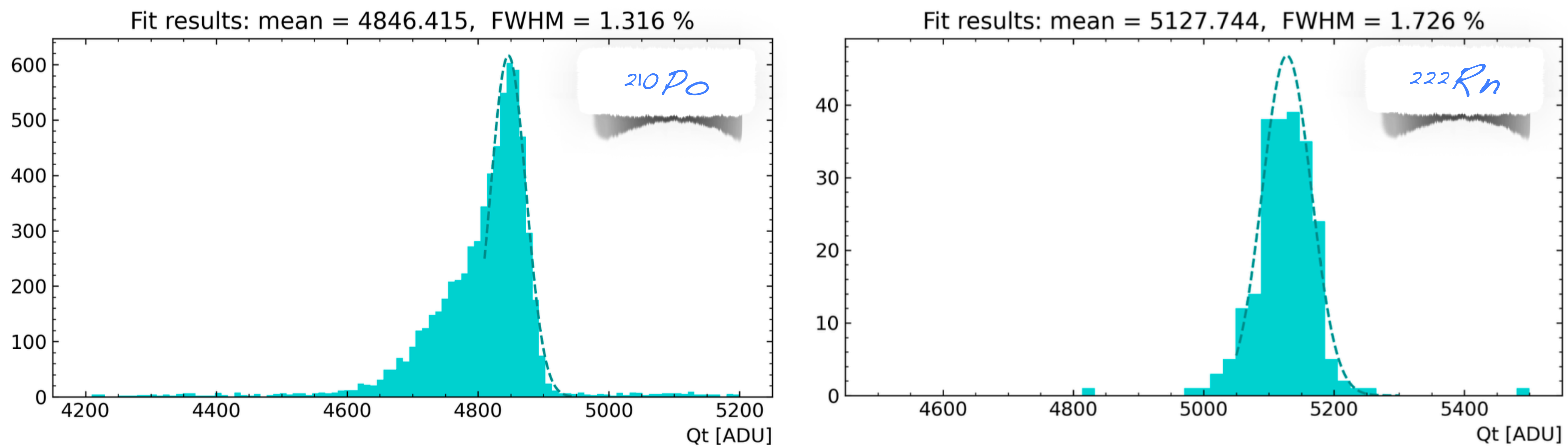

Data analysis

- The Qt of selected events (cuts on Dt and Dh) were fitted to establish the energy resolution.

Data for xenon at 3 bar, anode of 1.2 mm diameter, and -3000 V applied to the cathode

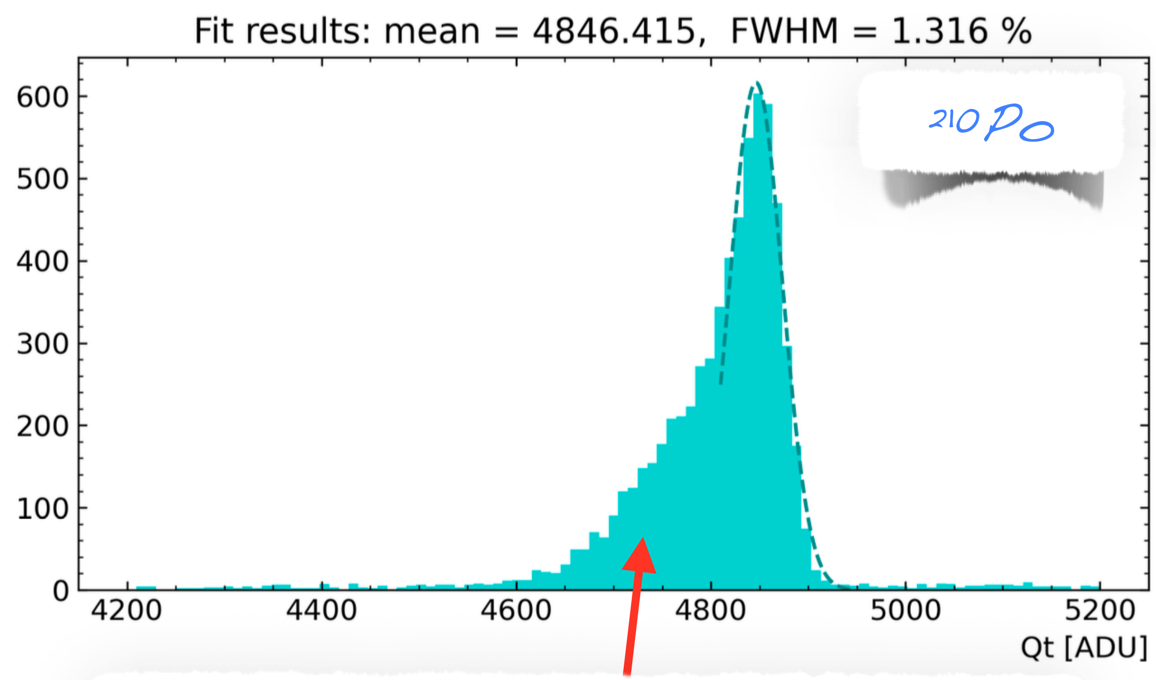

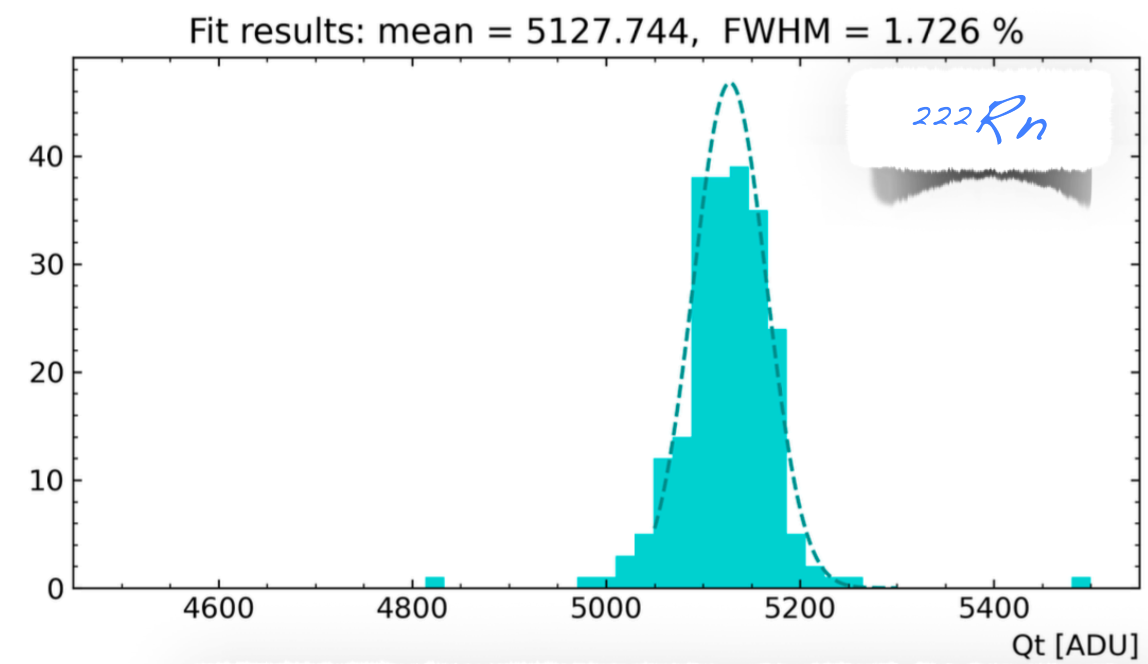

Tail due to alphas losing energy while passing in the hole in the cathode

Distribution more symmetric since no edge effects are present inside the xenon volume (however much lower statistics...)

Resolution results

- The same procedure was applied filling the detector with different gases (Ar and Xe) at various pressures and with different anode sizes.

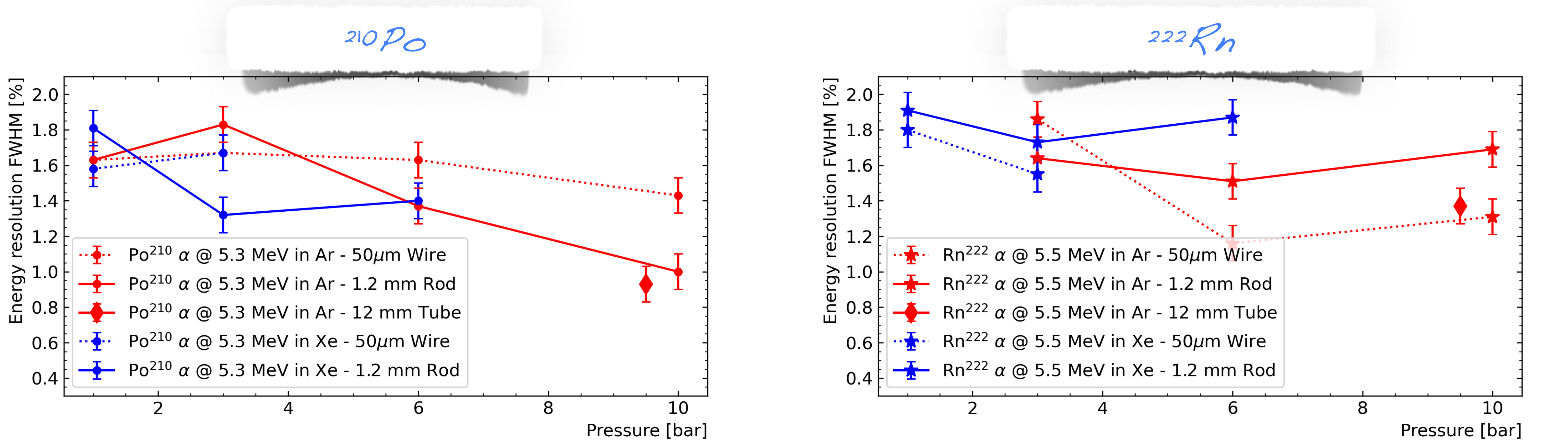

Resolution results

- The same procedure was applied filling the detector with different gases (Ar and Xe) at various pressures and with different anode sizes.

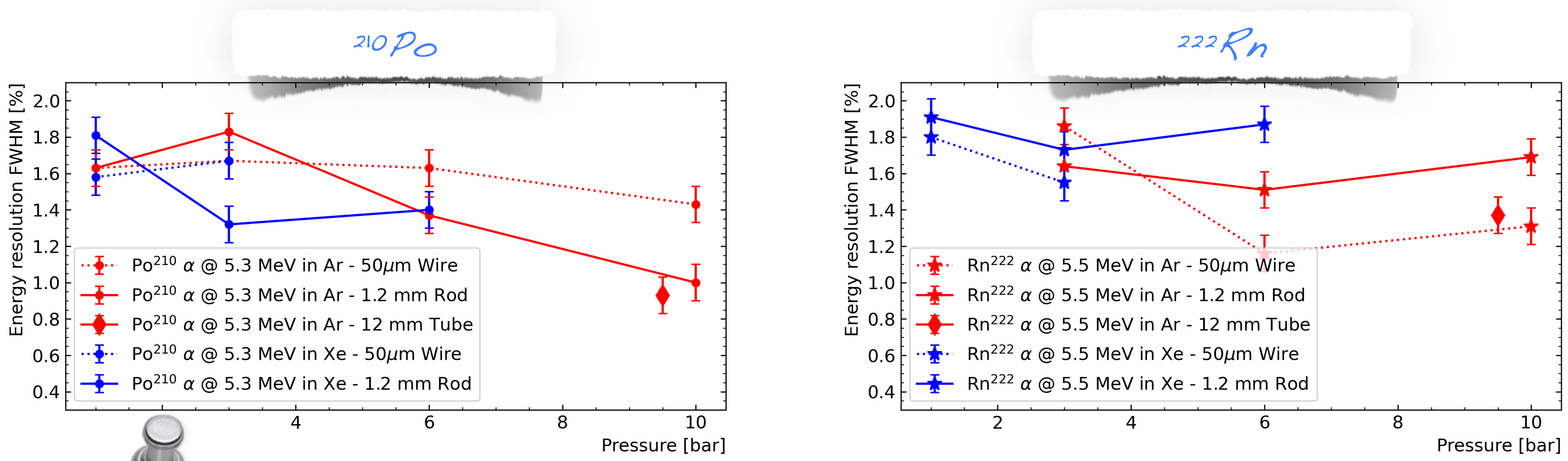

The resolution is mostly independent on the gas nature.

Resolution results

- The same procedure was applied filling the detector with different gases (Ar and Xe) at various pressures and with different anode sizes.

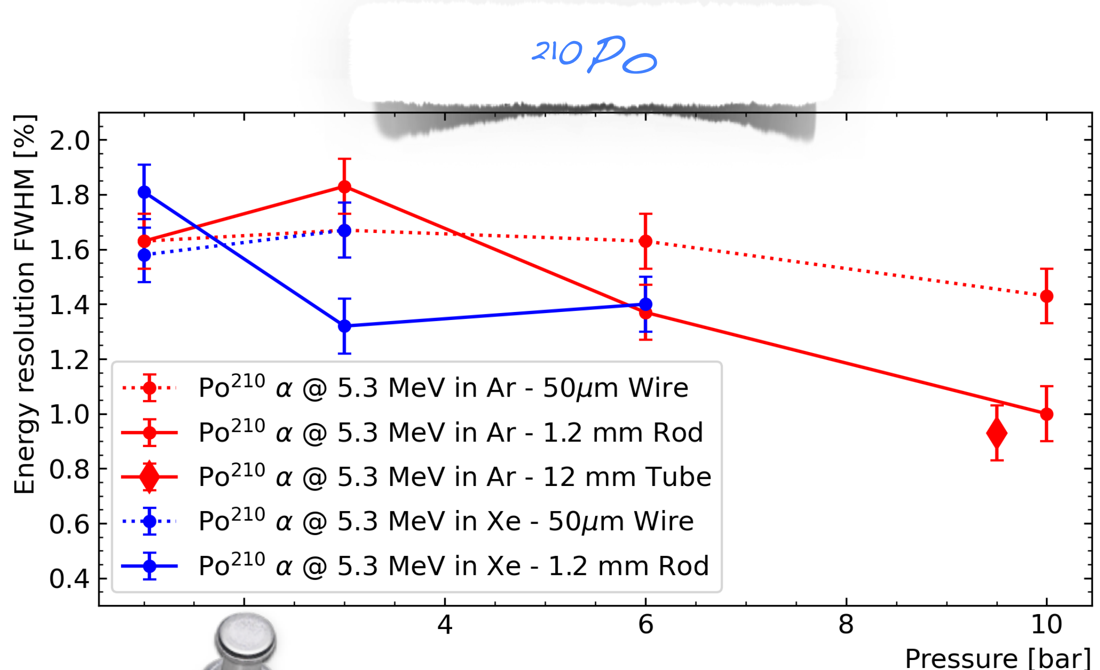

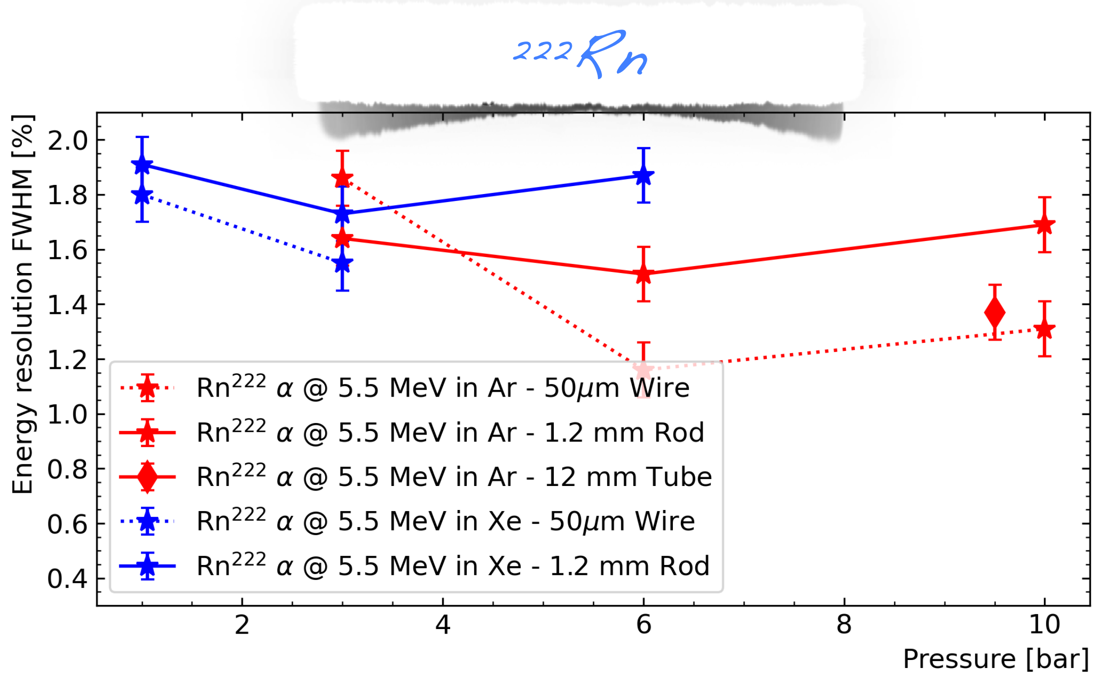

The resolution is mostly independent on the gas nature.

The resolution is mostly independent on the gas pressure.

Resolution results

- The same procedure was applied filling the detector with different gases (Ar and Xe) at various pressures and with different anode sizes.

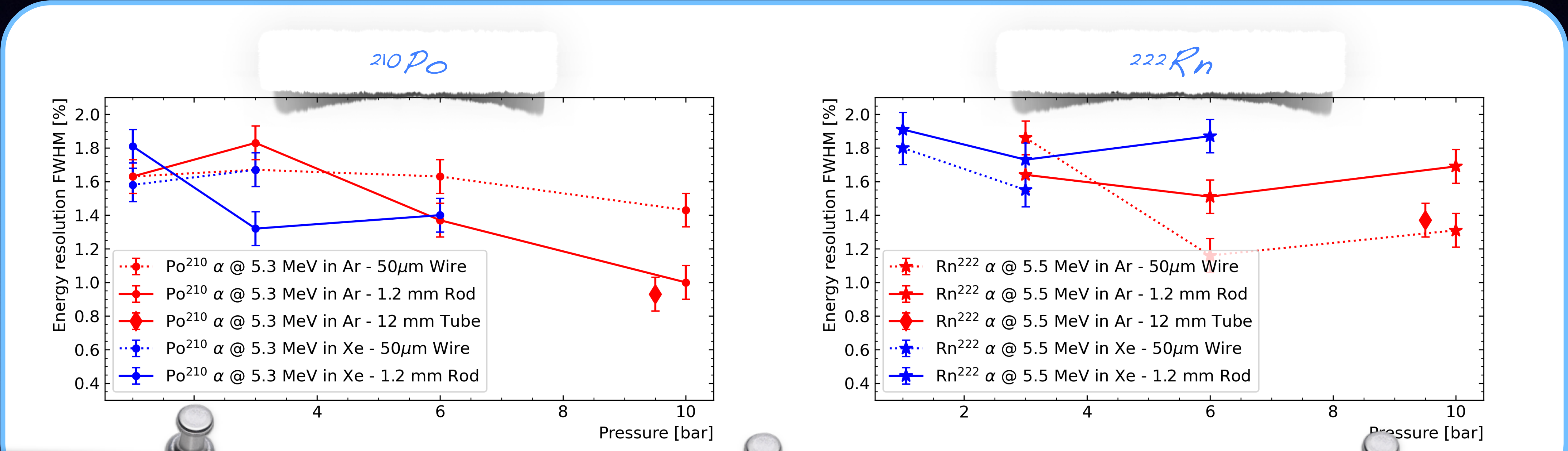

The resolution is mostly independent on the gas nature.

The resolution is mostly independent on the gas pressure.

The resolution is similar for diffuse and point-like sources.

From R&D to the experiment

- The **R&D allowed to validate the energy resolution** and to fully understand the detector response.
- Based on the achieve detector knowledge a **detailed study to compute the sensitivity** on **neutrinoless double beta decay** was carried out.

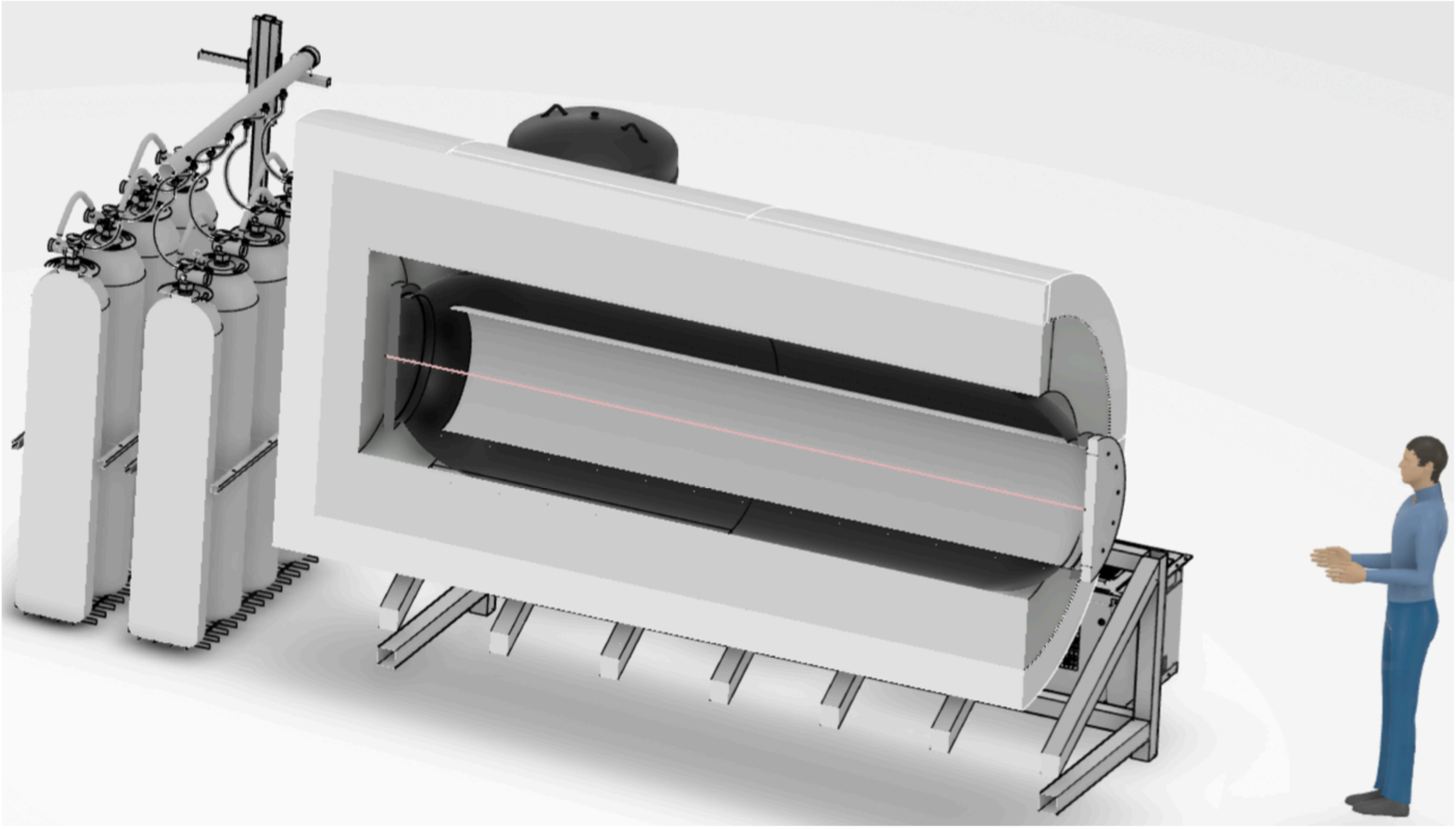

From R&D to the experiment

- The **R&D allowed to validate the energy resolution** and to fully understand the detector response.
- Based on the achieve detector knowledge a **detailed study to compute the sensitivity** on **neutrinoless double beta decay** was carried out.

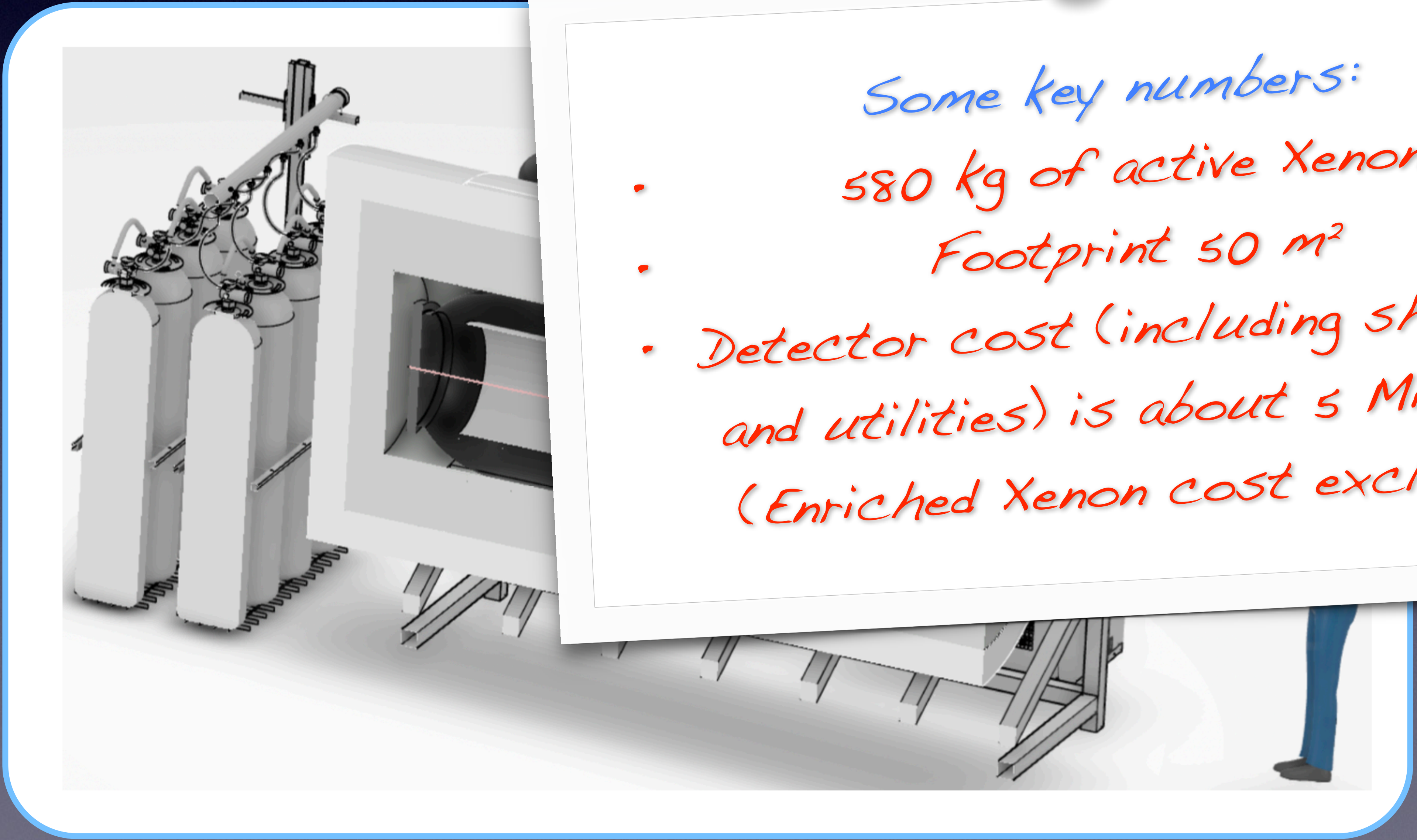

Some key numbers:

- 580 kg of active Xenon
- Footprint 50 m^2
- Detector cost (including shielding and utilities) is about 5 Millions (Enriched Xenon cost excluded)

The detector

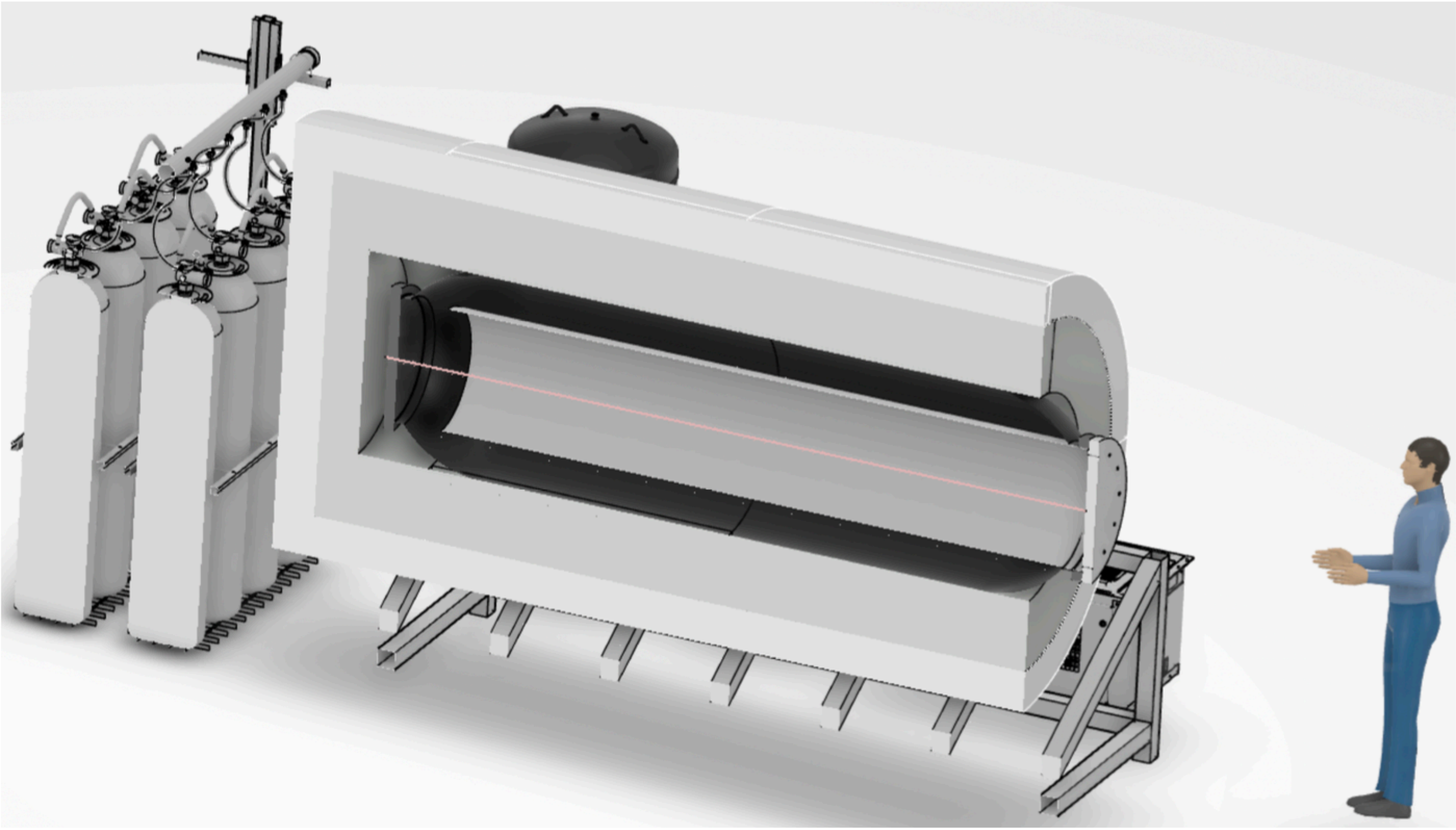

The detector

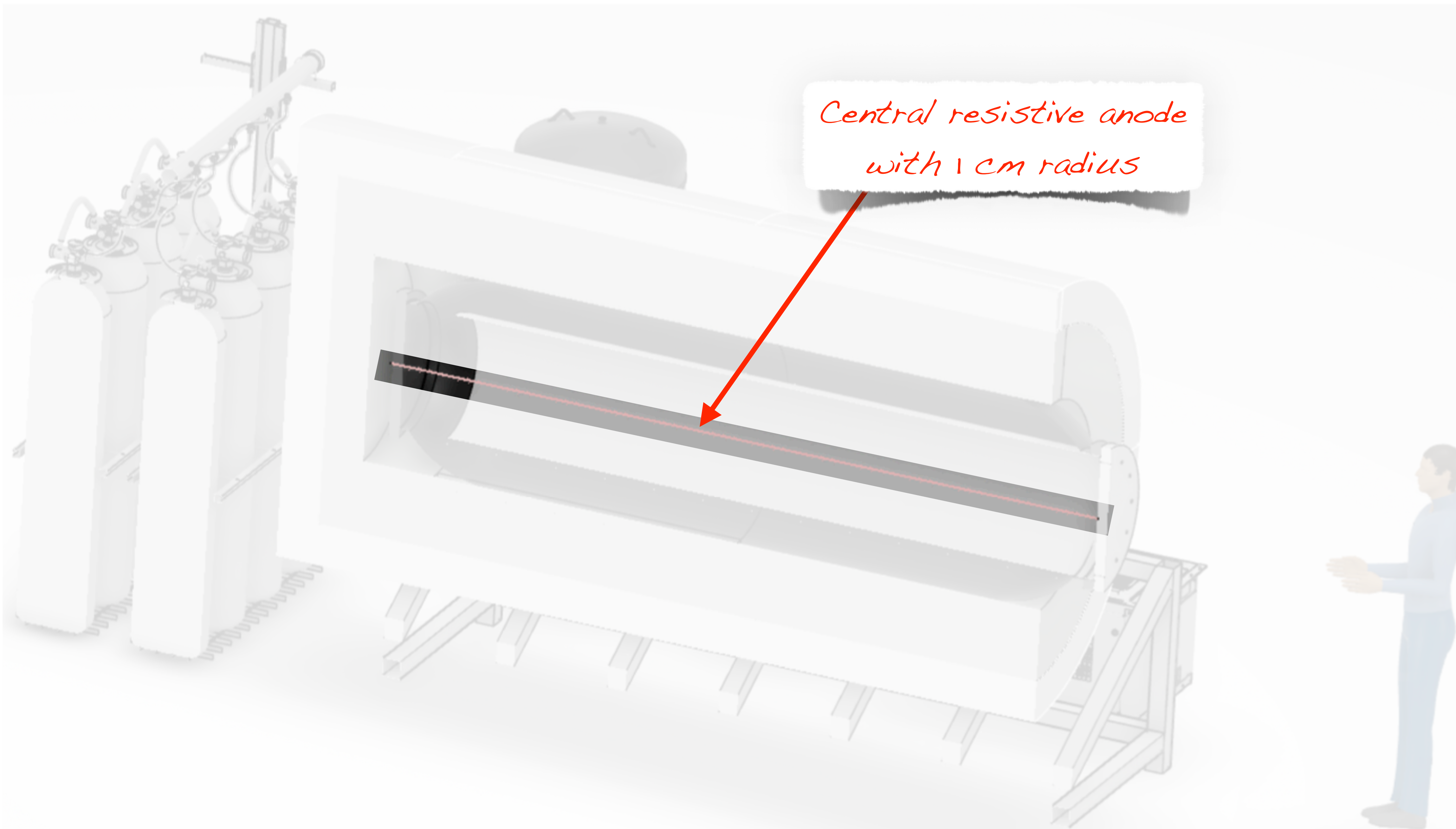

The detector

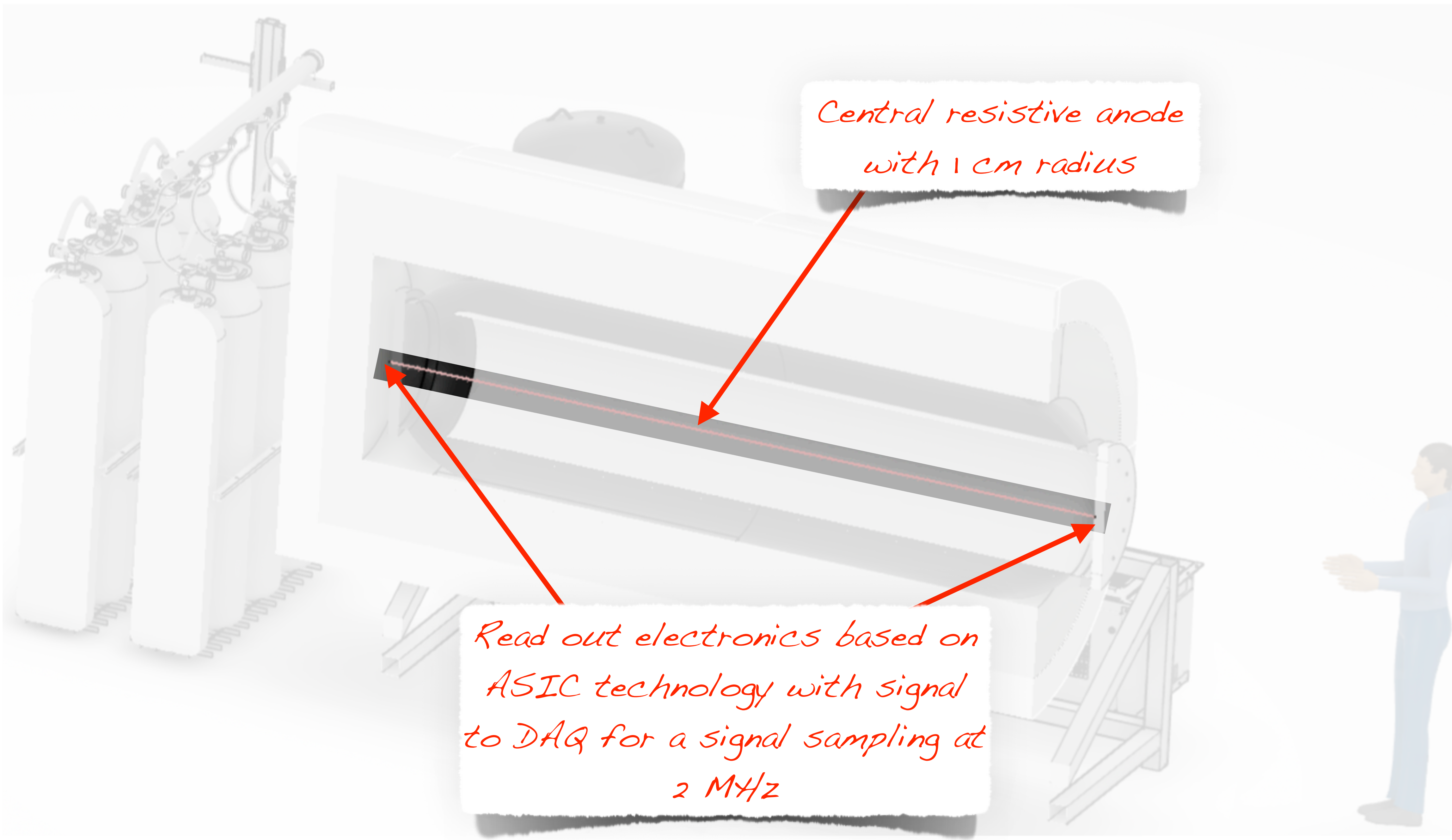

The detector

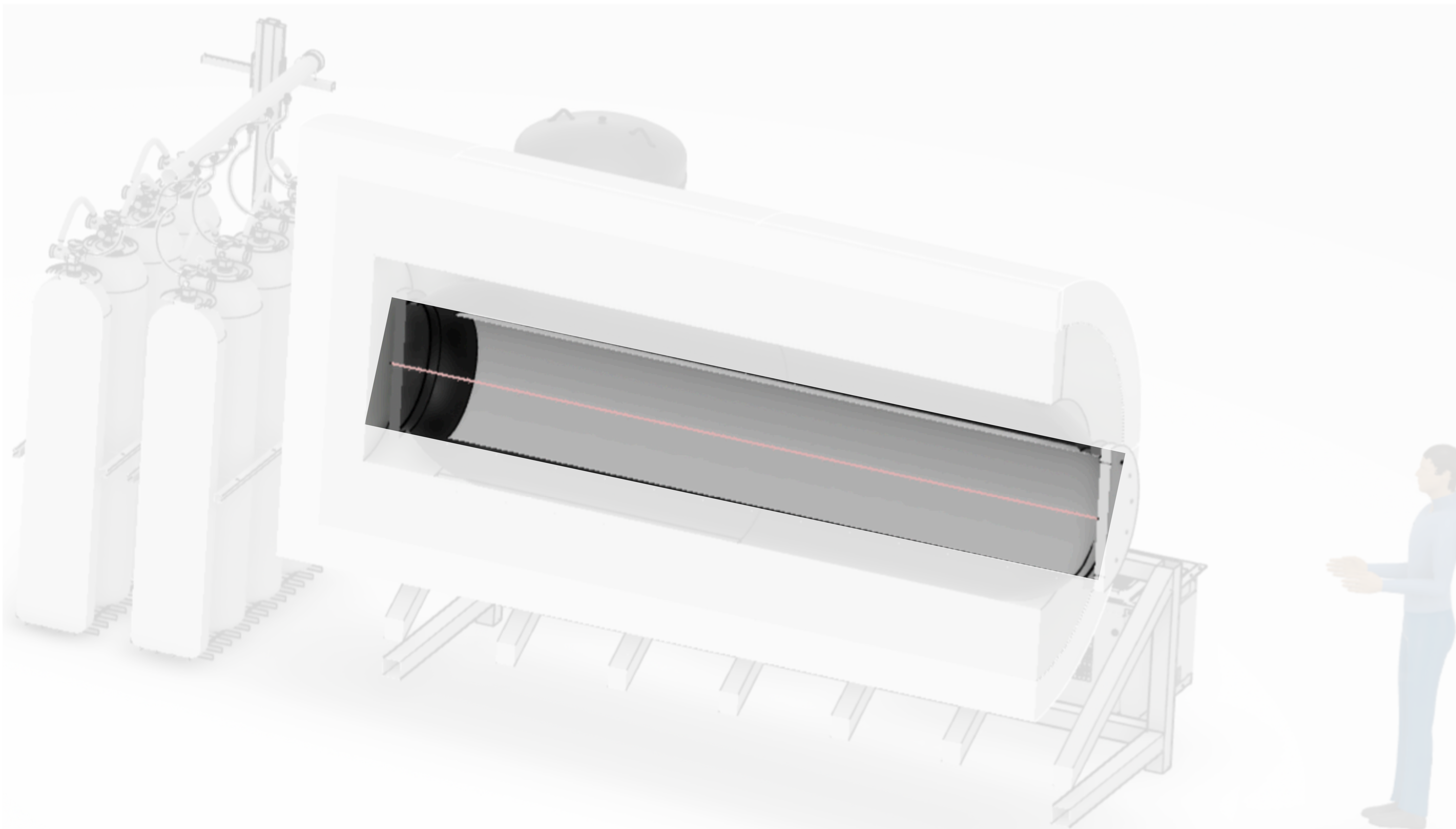

The detector

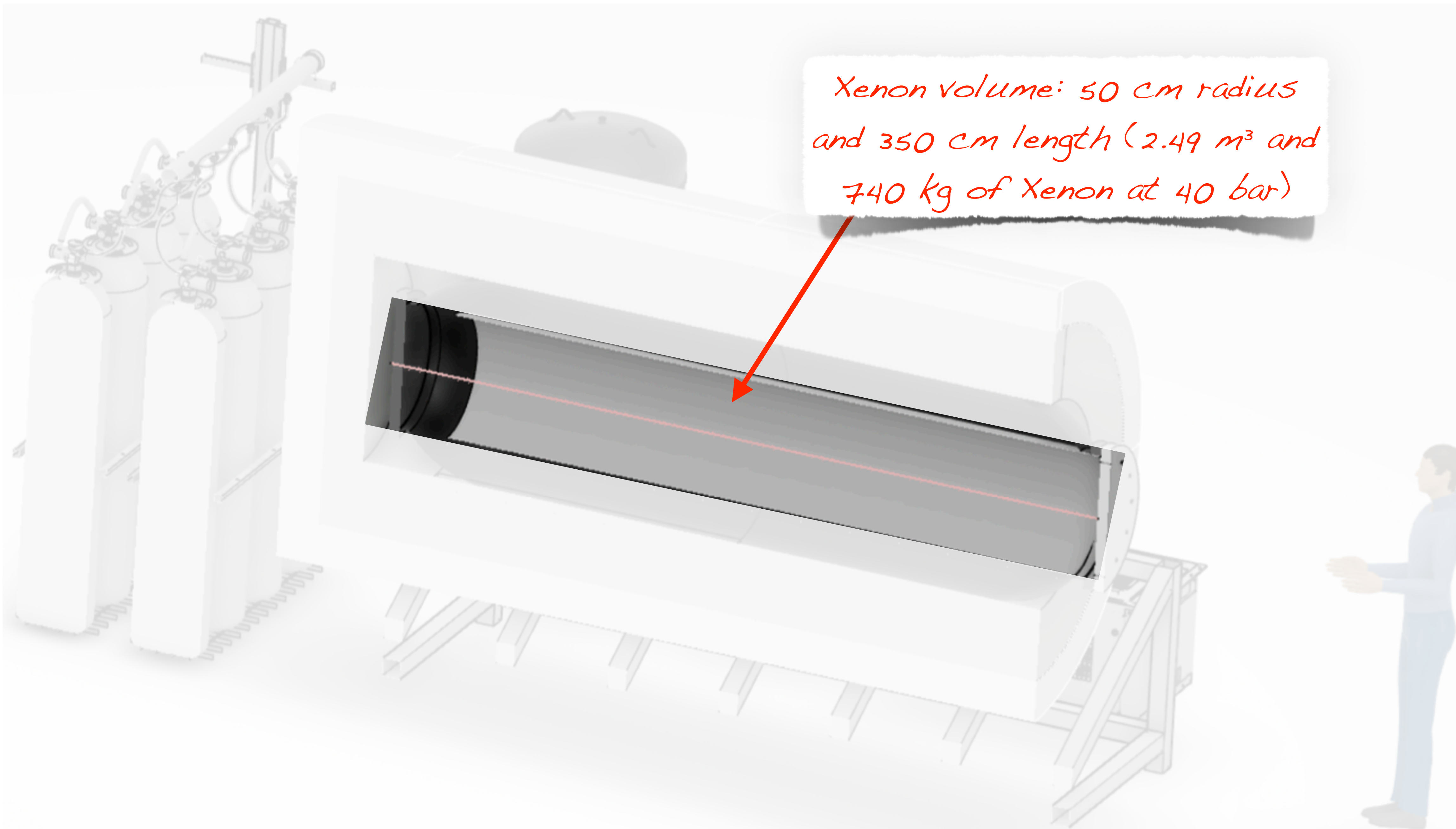

The detector

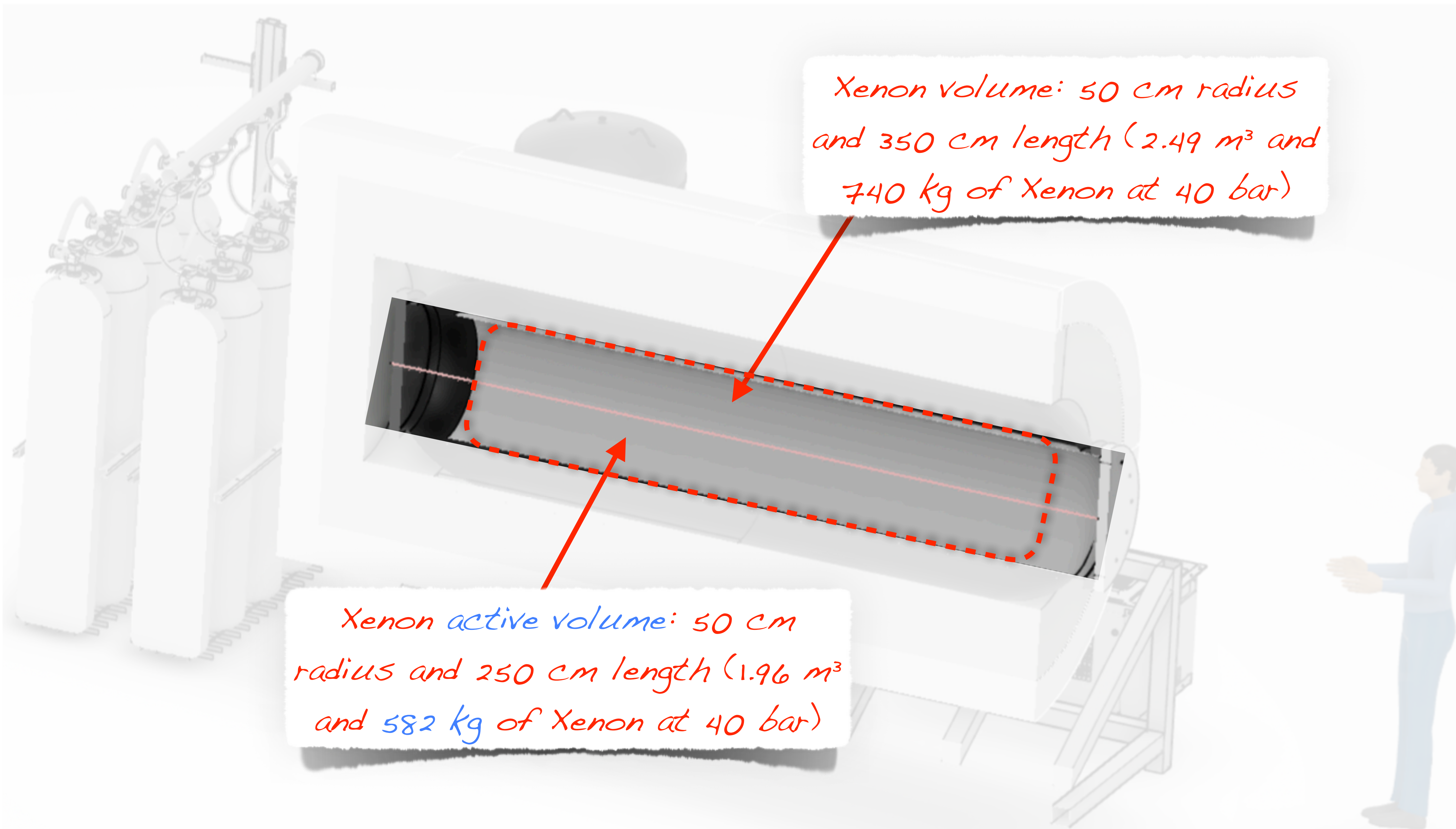

The detector

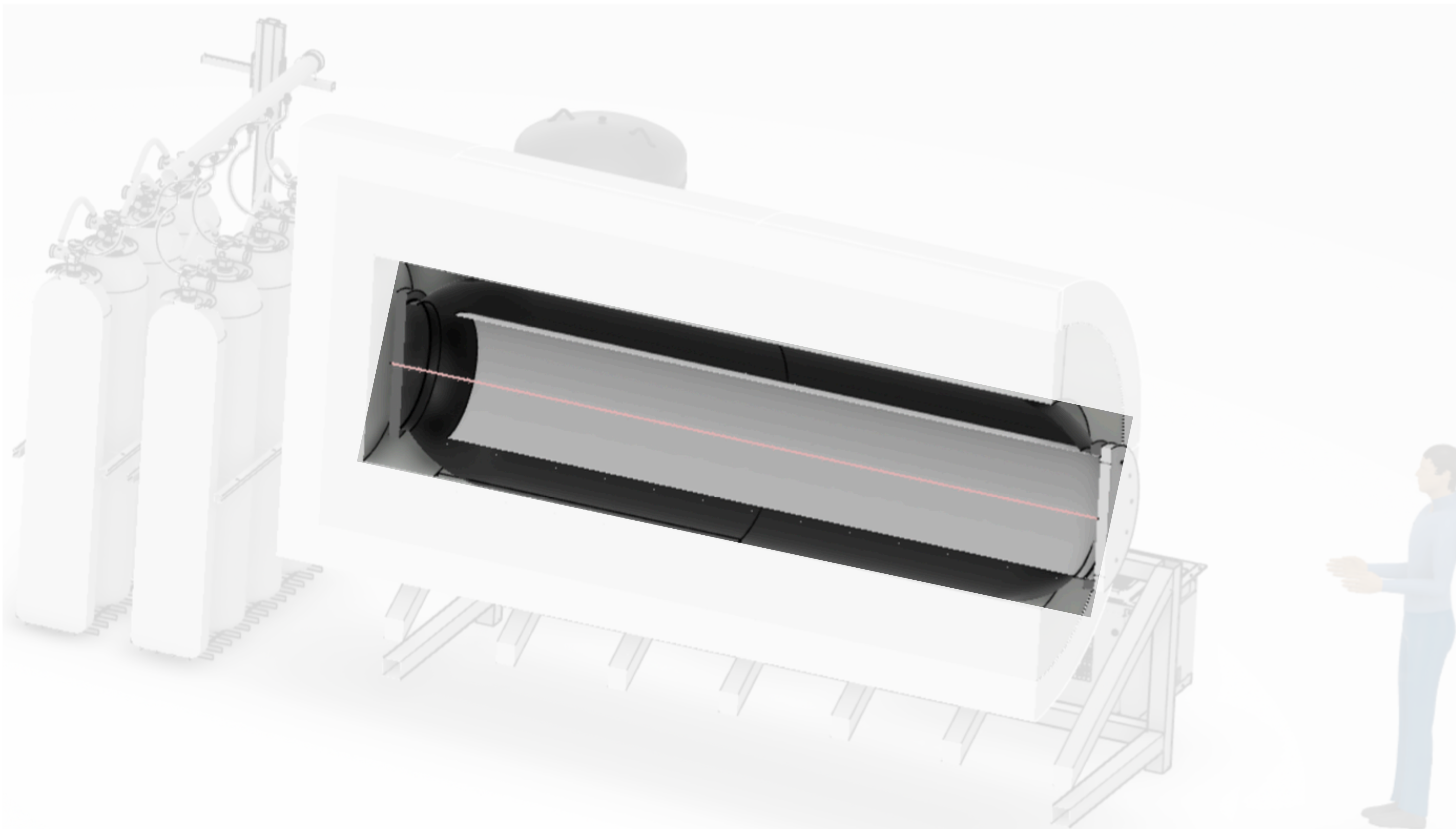

The detector

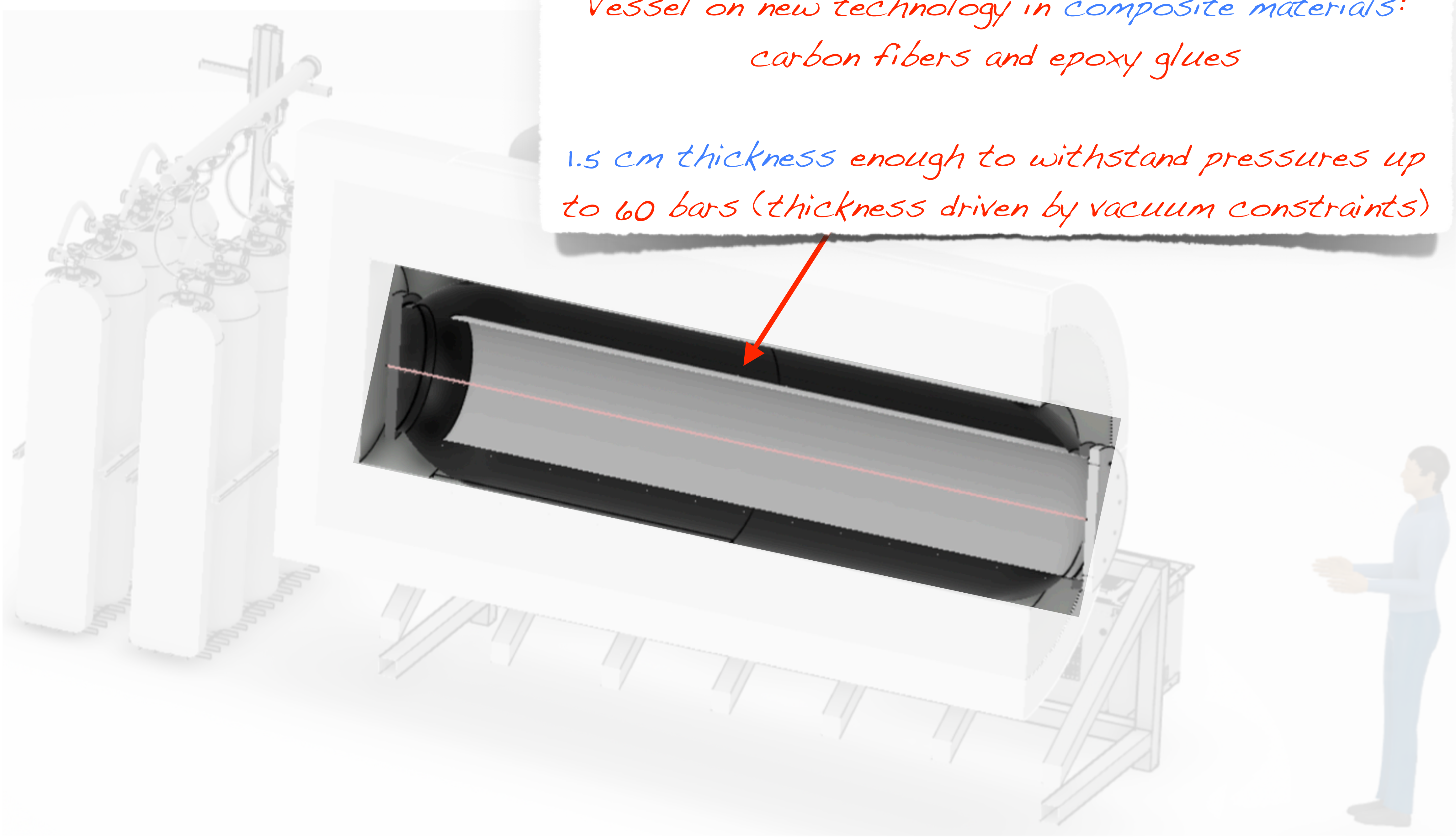

Vessel on new technology in composite materials: carbon fibers and epoxy glues

1.5 cm thickness enough to withstand pressures up to 60 bars (thickness driven by vacuum constraints)

The detector

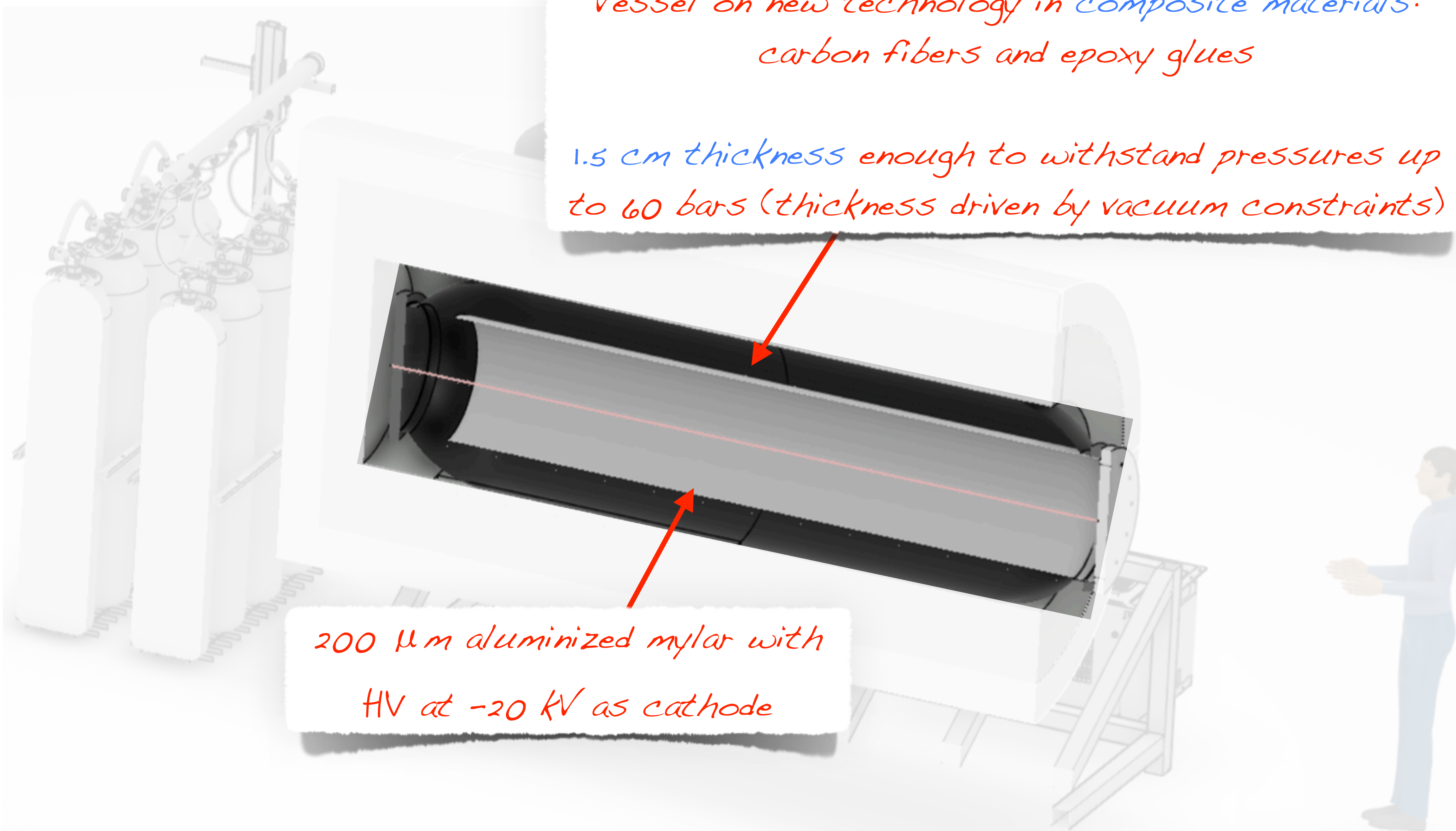

Vessel on new technology in composite materials: carbon fibers and epoxy glues

1.5 cm thickness enough to withstand pressures up to 60 bars (thickness driven by vacuum constraints)

200 μm aluminized mylar with HV at -20 kV as cathode

The detector

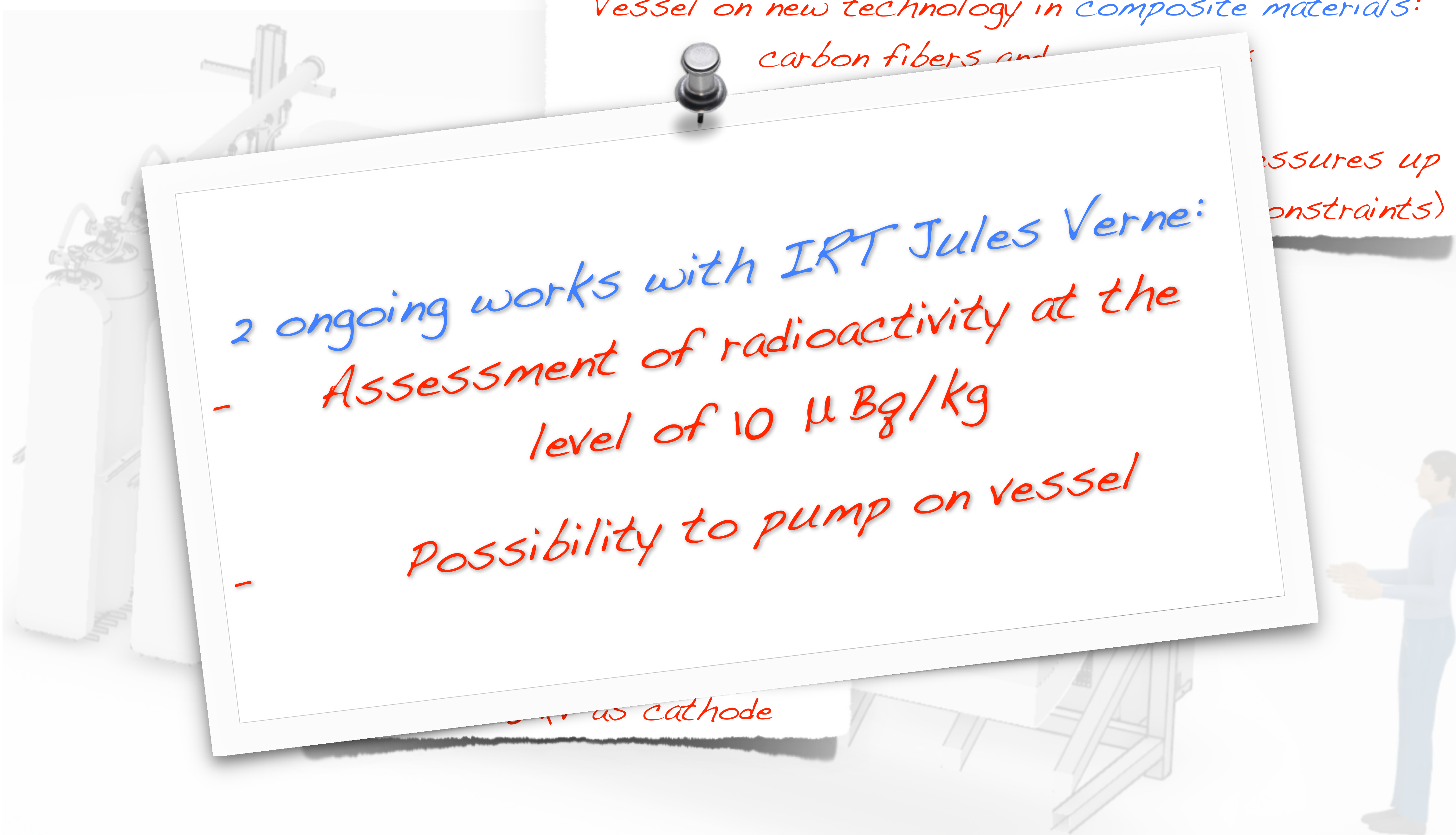

Vessel on new technology in composite materials:
carbon fibers and
...ssures up
...onstraints)
... as cathode

2 ongoing works with IRT Jules Verne:
- Assessment of radioactivity at the level of 10 μBq/kg
- Possibility to pump on vessel

The detector

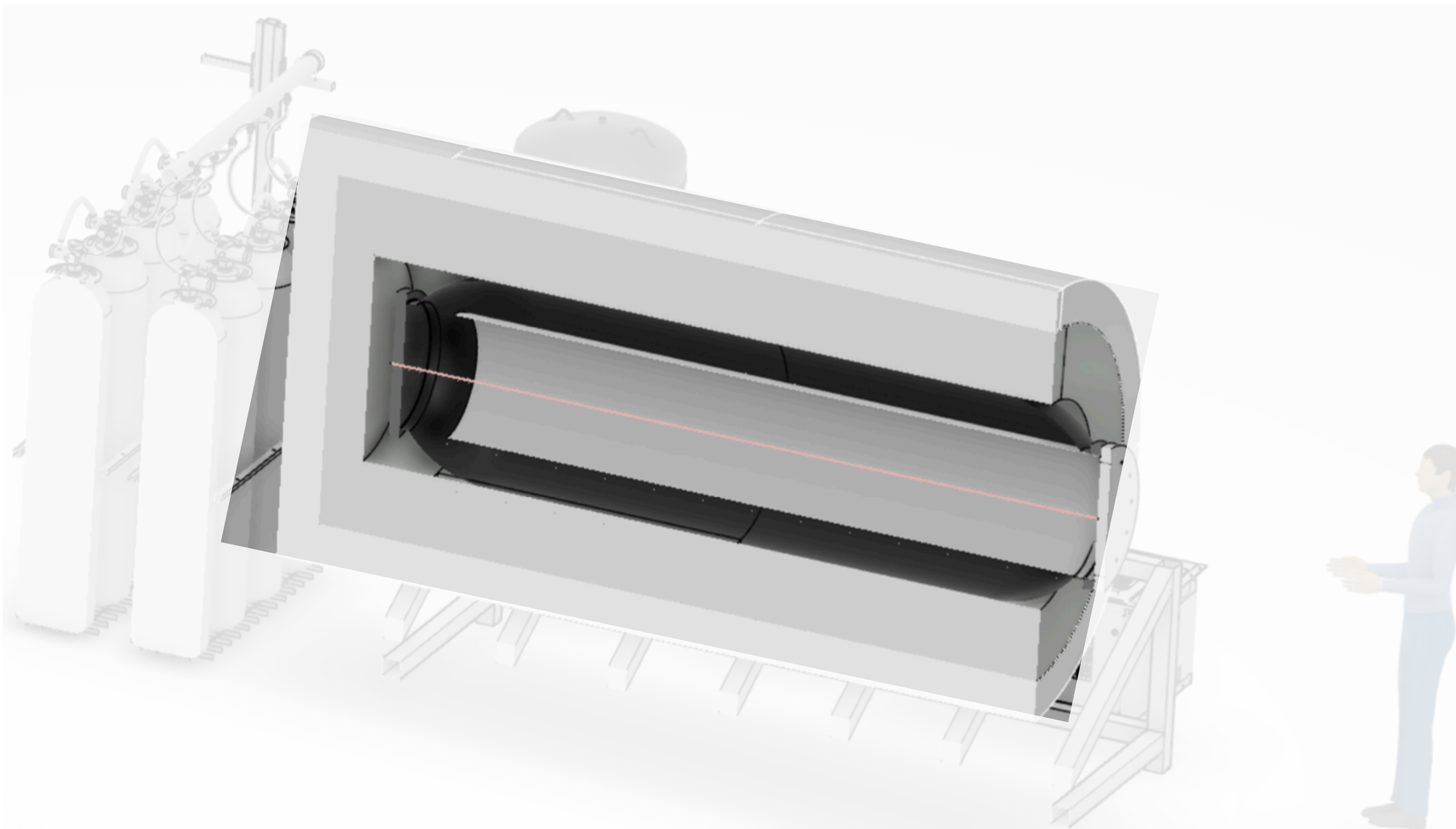

The detector

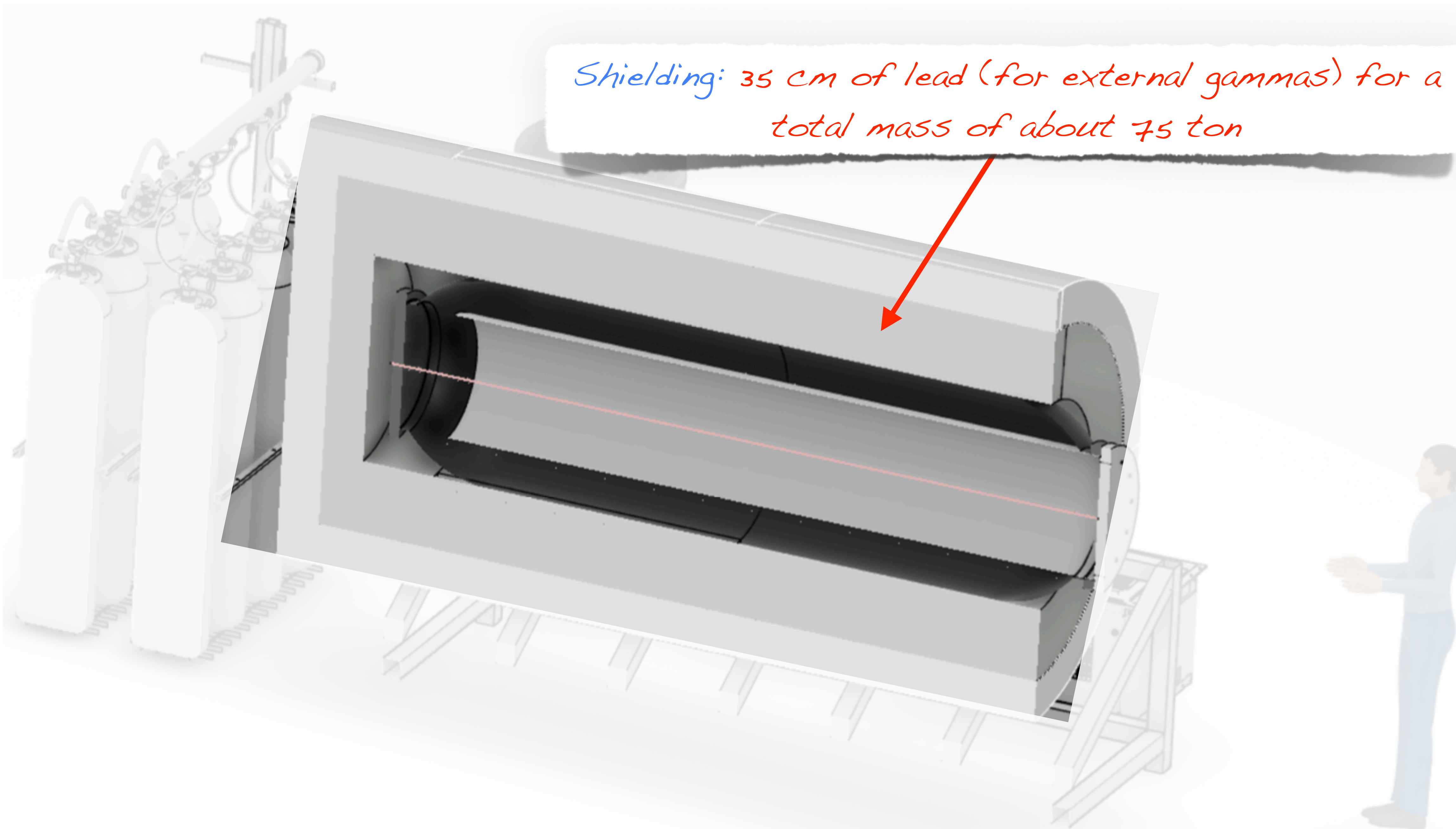

The detector

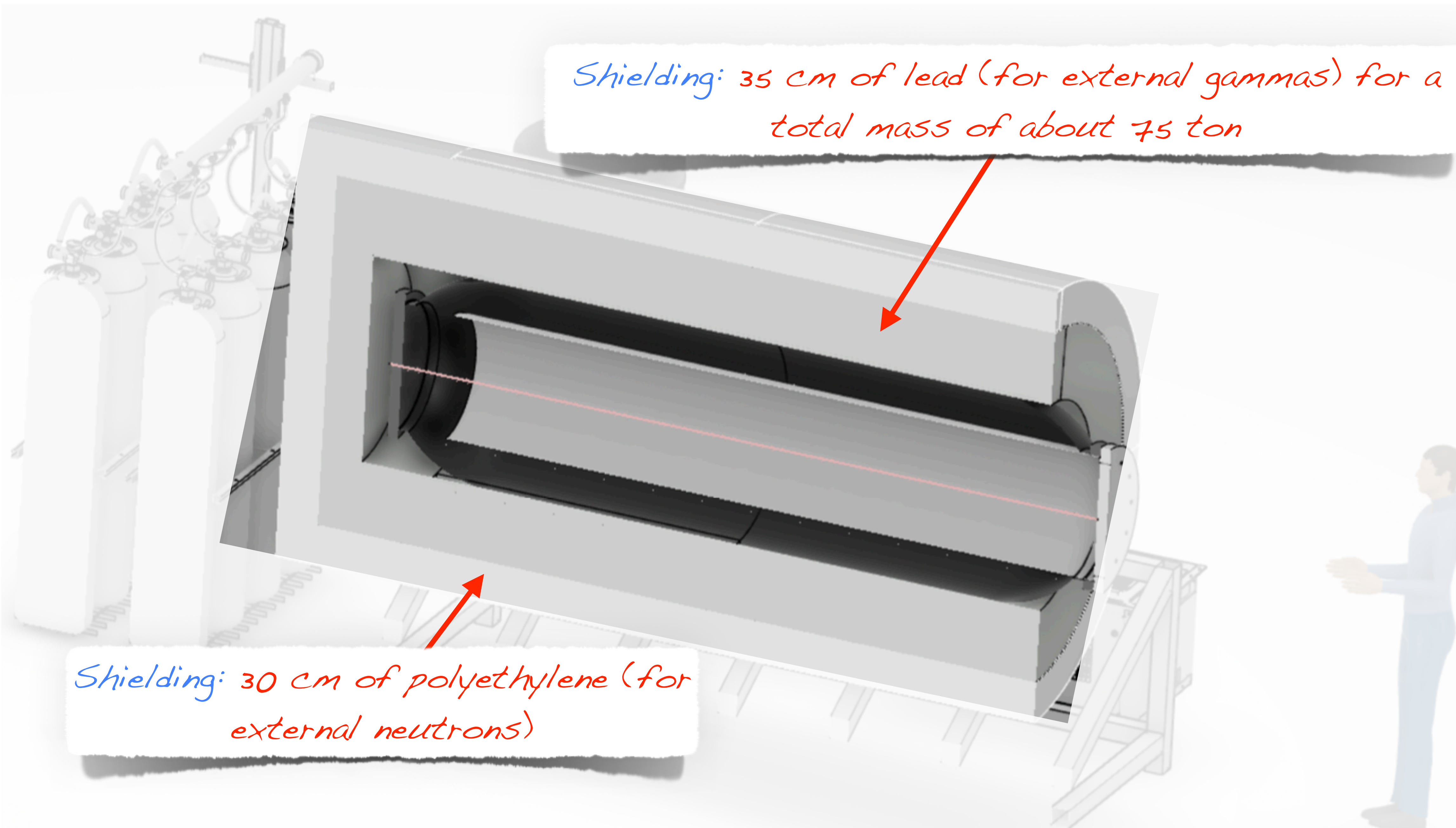

The detector

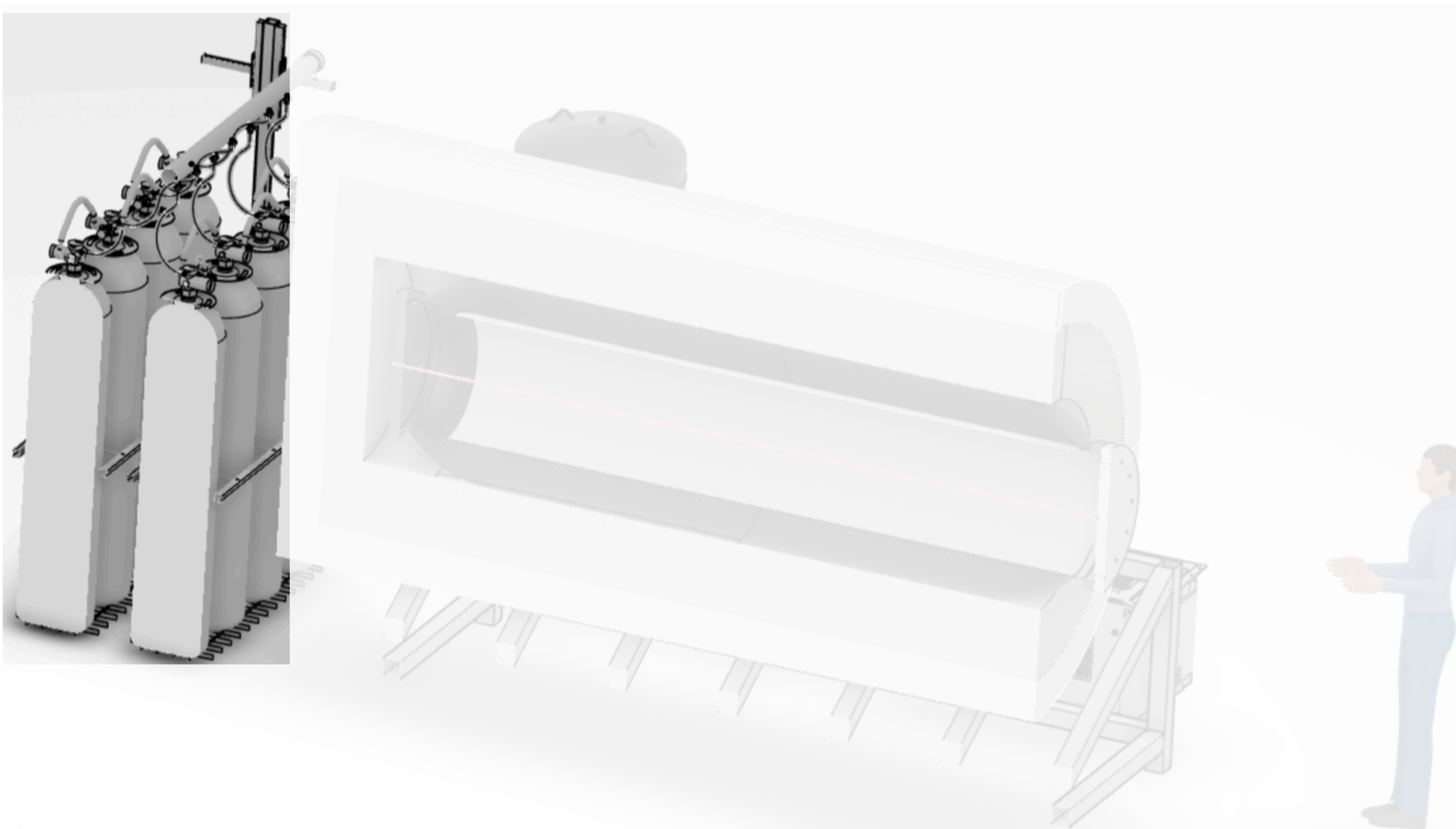

The detector

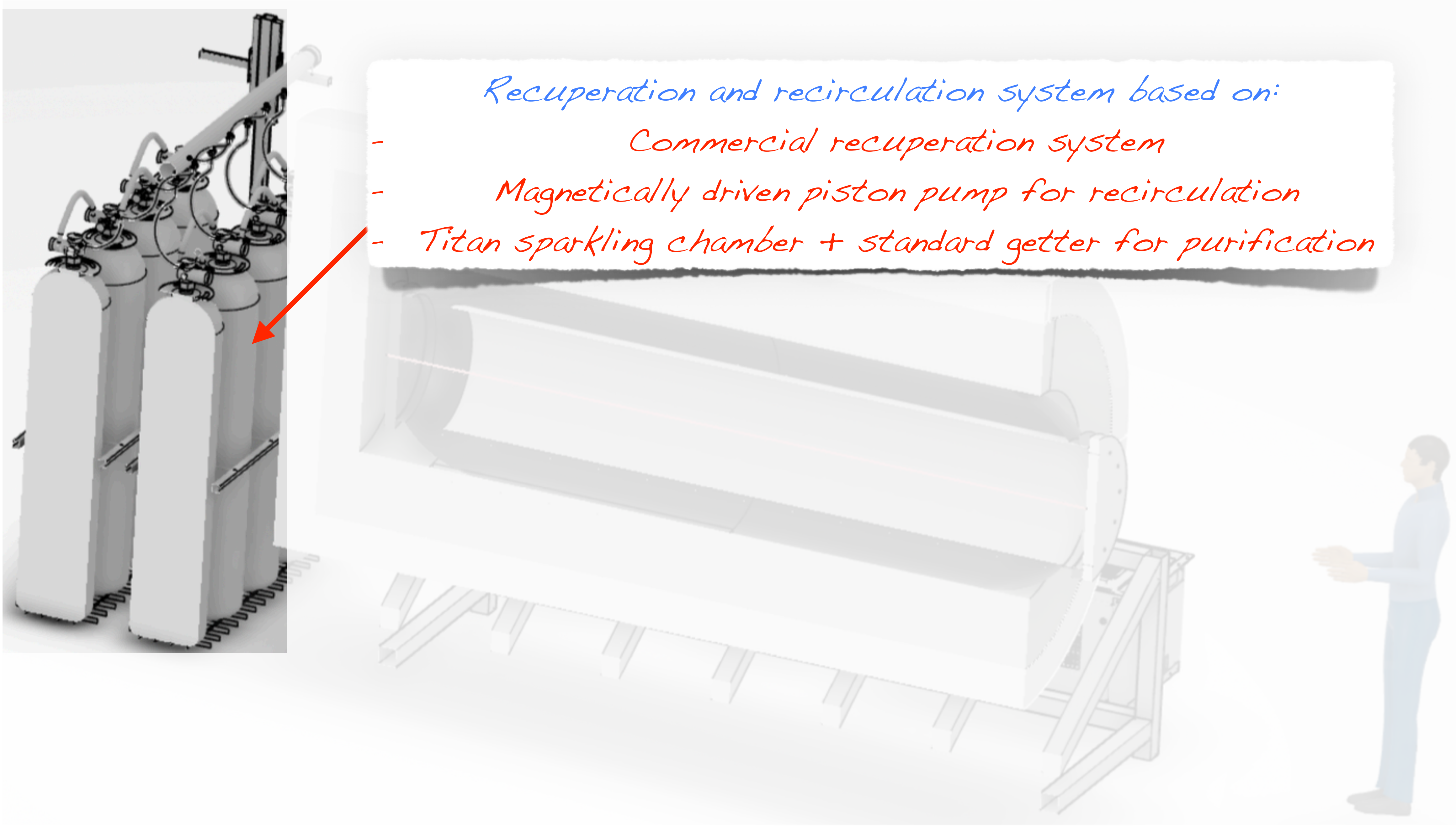

Recuperation and recirculation system based on:

- Commercial recuperation system
- Magnetically driven piston pump for recirculation
- Titan sparkling chamber + standard getter for purification

Sensitivity study

- We carried out a **complete Monte Carlo simulation** to evaluate the signal efficiency and background reduction.

Sensitivity study

- We carried out a **complete Monte Carlo simulation** to evaluate the signal efficiency and background reduction.

GEANT 4 simulation

Account for detector geometry

Simulate energy deposits for signal and backgrounds

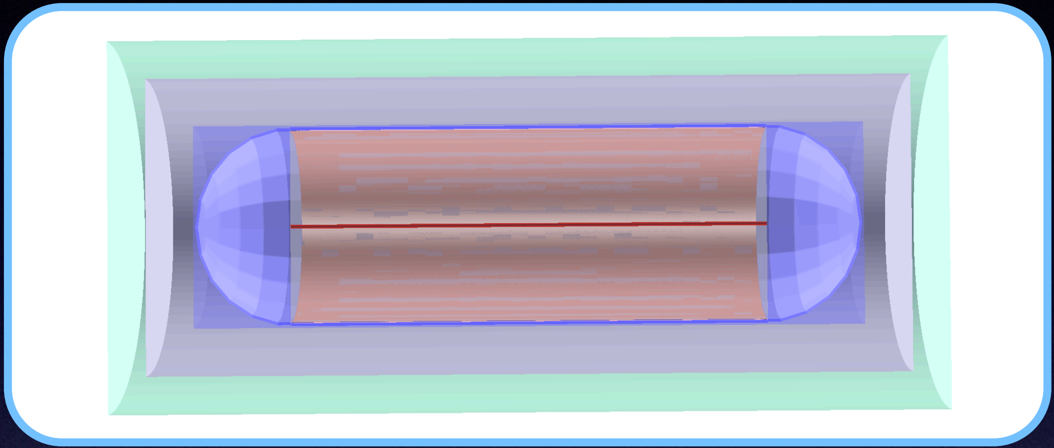

Sensitivity study

- We carried out a **complete Monte Carlo simulation** to evaluate the signal efficiency and background reduction.

Signal simulation

Based on the detector knowledge and GARFIELD the signals are constructed

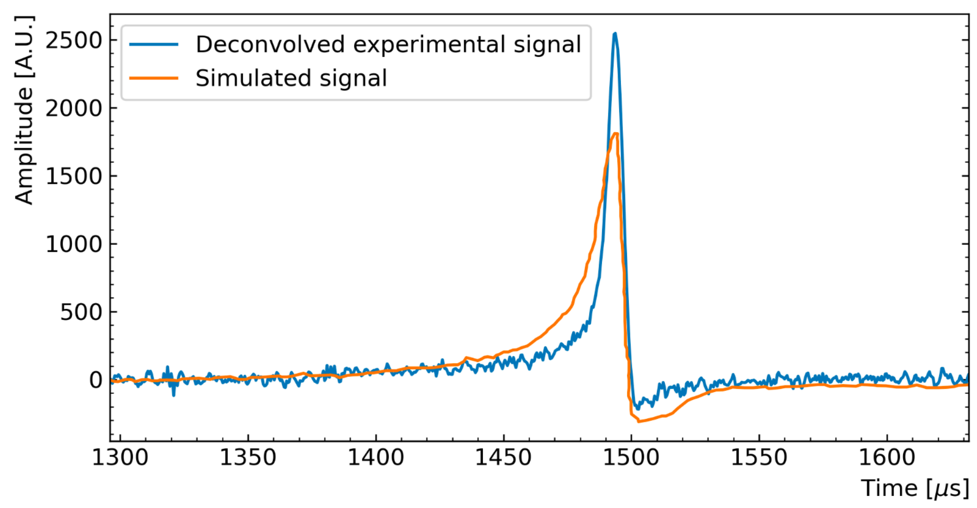

Sensitivity study

- We carried out a **complete Monte Carlo simulation** to evaluate the signal efficiency and background reduction.

Sensitivity study

- We carried out a **complete Monte Carlo simulation** to evaluate the signal efficiency and background reduction.

Signal reconstruction

The signal si analyzed to deconvolve it from the electronics and to reconstruct the observables used in the analysis

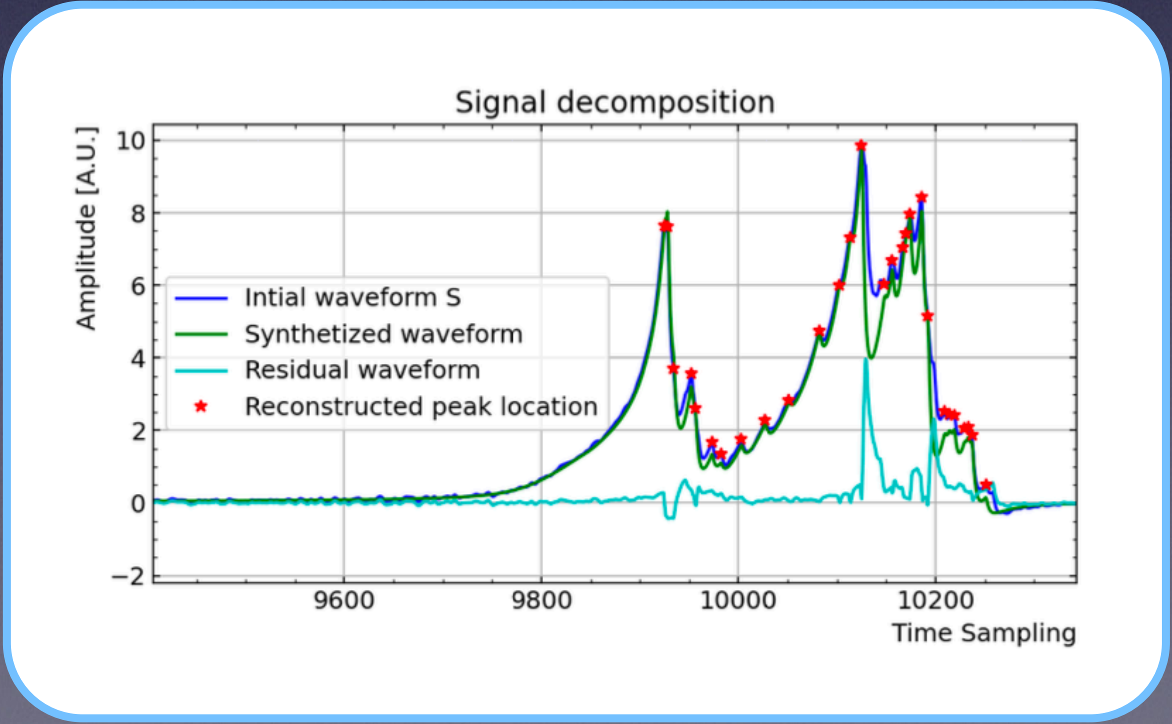

Sensitivity study

- We carried out a **complete Monte Carlo simulation** to evaluate the signal efficiency and background reduction.

Data analysis

The selection cuts are applied on the reconstructed variables to select the searched for signal signature

Sensitivity study

- We carried out a **complete Monte Carlo simulation** to evaluate the signal efficiency and background reduction.

ENERGY SMEARING!

Data analysis

The selection cuts are applied on the reconstructed variables to select the searched for signal signature

Energy resolution

NOTE: We assume that the energy resolution scales as a function of the energy as 1/sqrt(E).

Energy resolution at Xenon Qββ of 2.458 MeV

Energy resolution

NOTE: We assume that the energy resolution scales as a function of the energy as 1/sqrt(E).

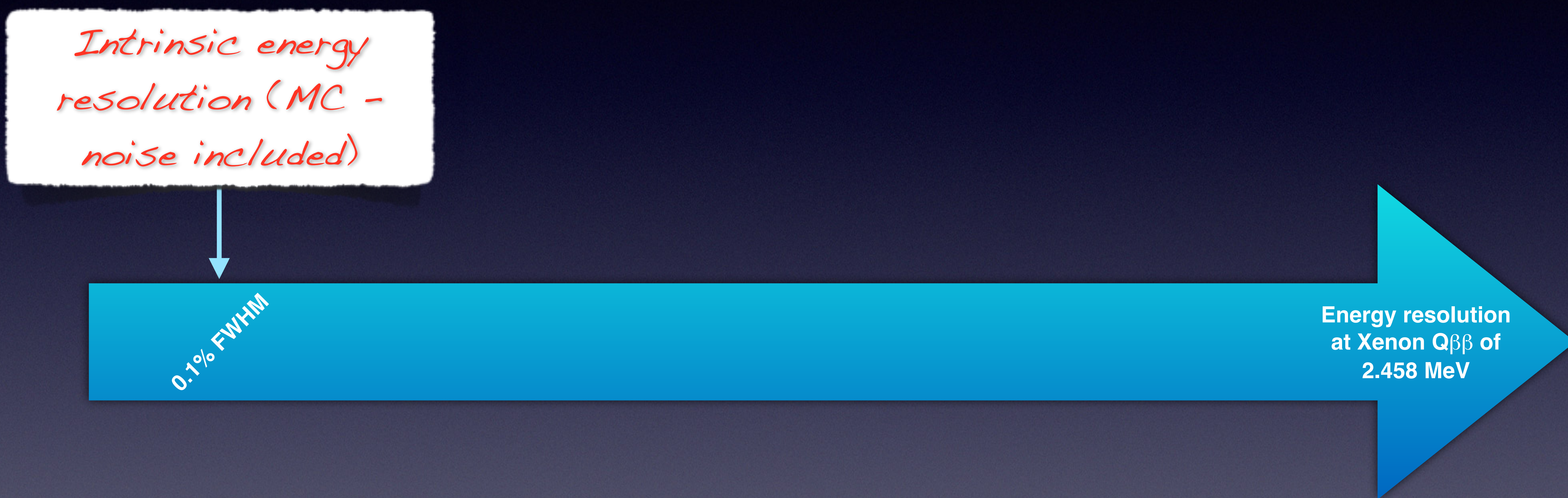

Energy resolution

NOTE: We assume that the energy resolution scales as a function of the energy as 1/sqrt(E).

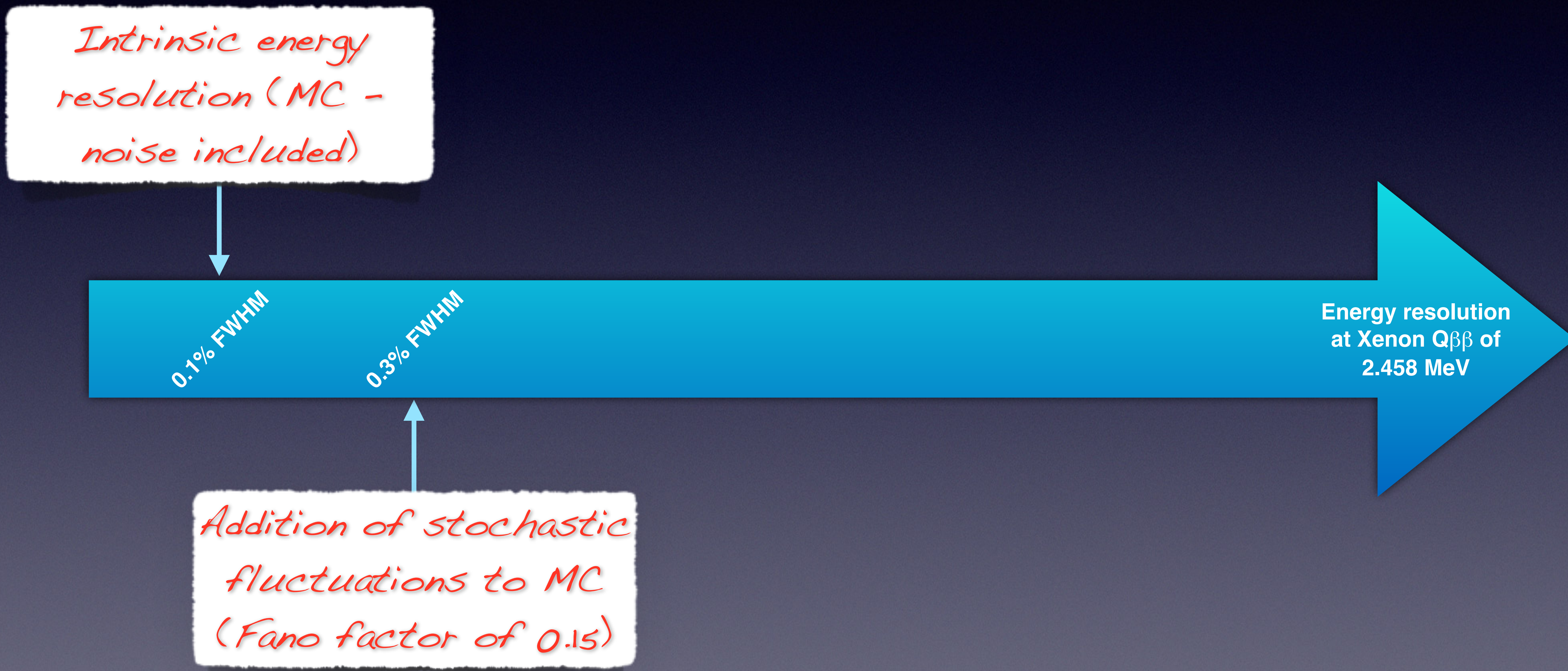

Energy resolution

NOTE: We assume that the energy resolution scales as a function of the energy as 1/sqrt(E).

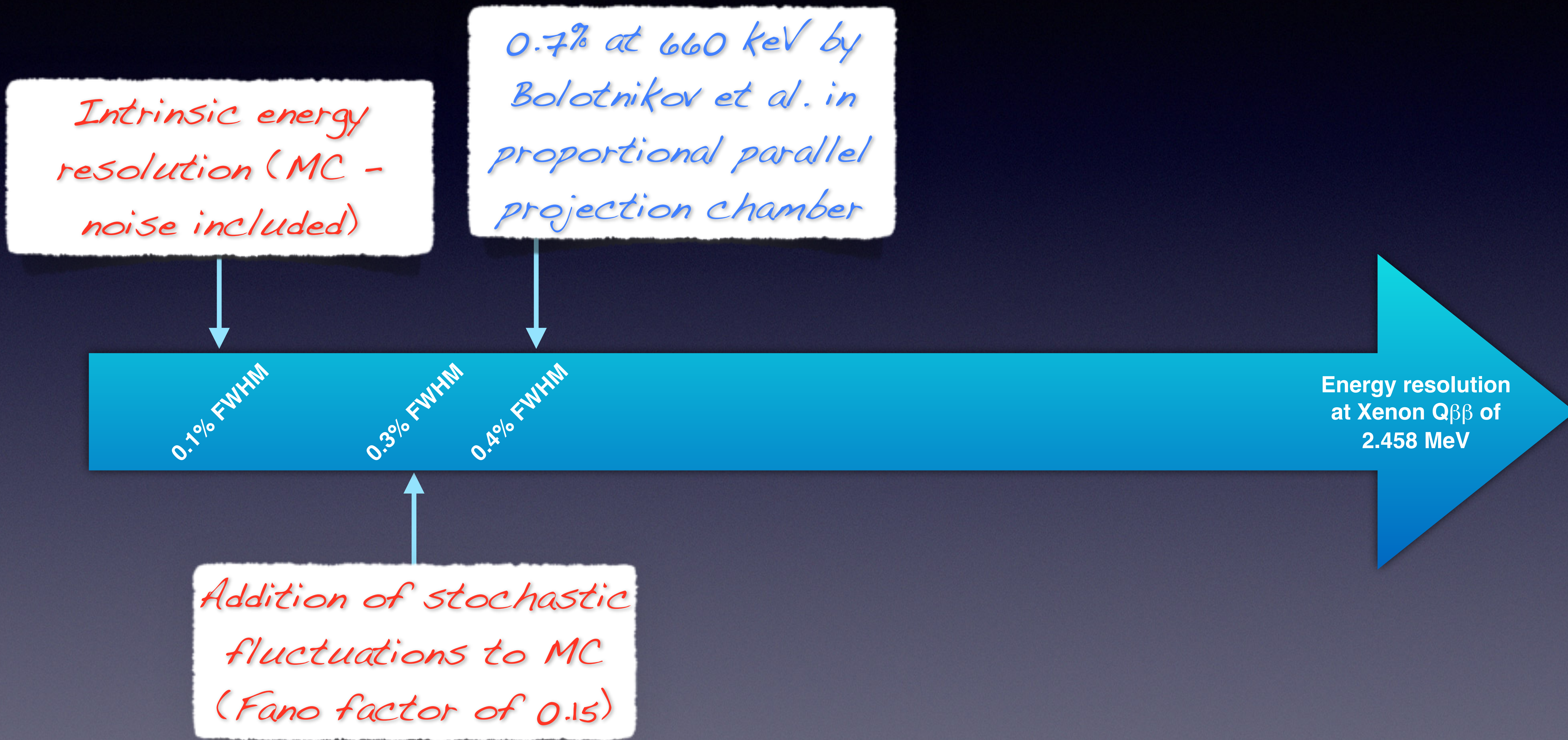

Energy resolution

NOTE: We assume that the energy resolution scales as a function of the energy as 1/sqrt(E).

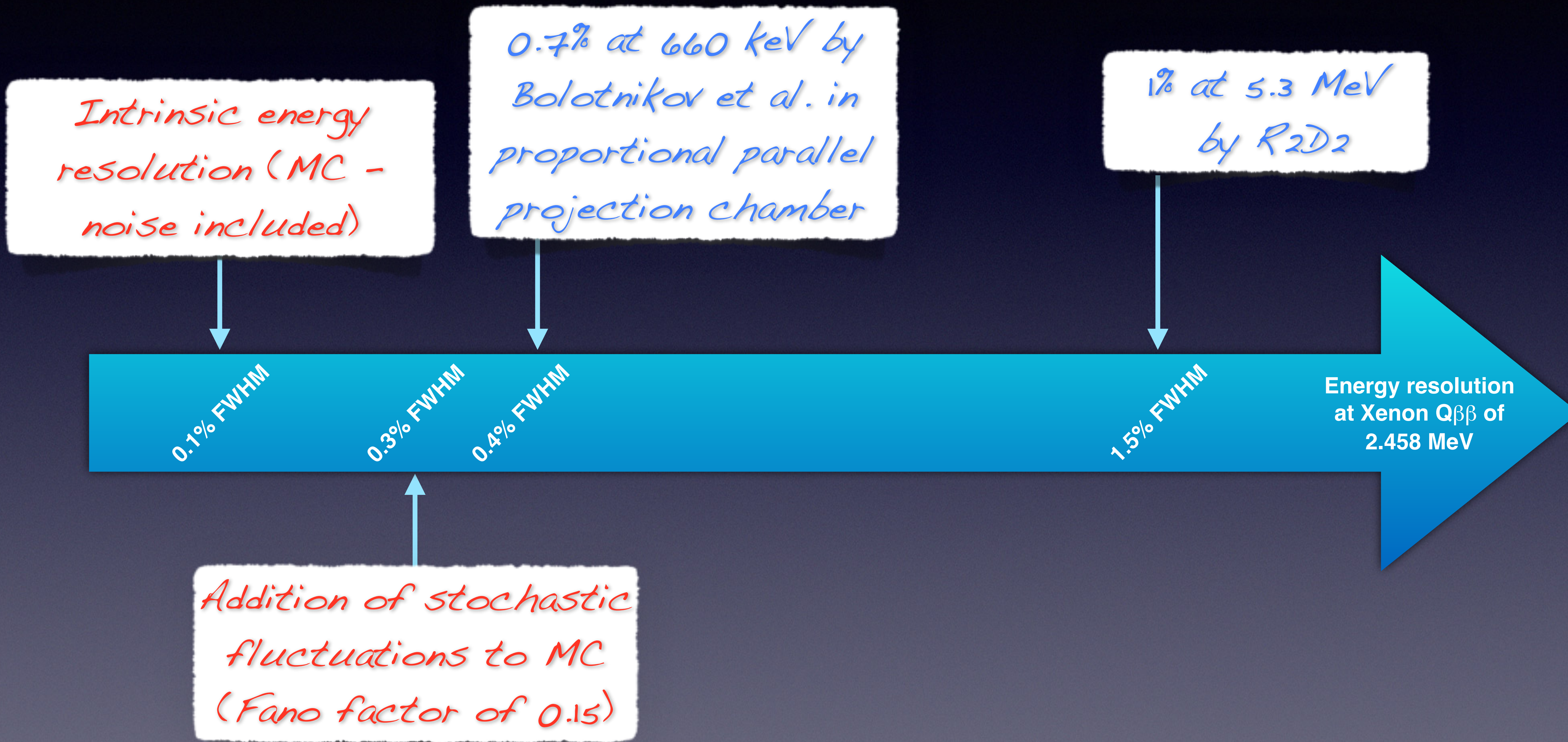

Energy resolution

NOTE: We assume that the energy resolution scales as a function of the energy as 1/sqrt(E).

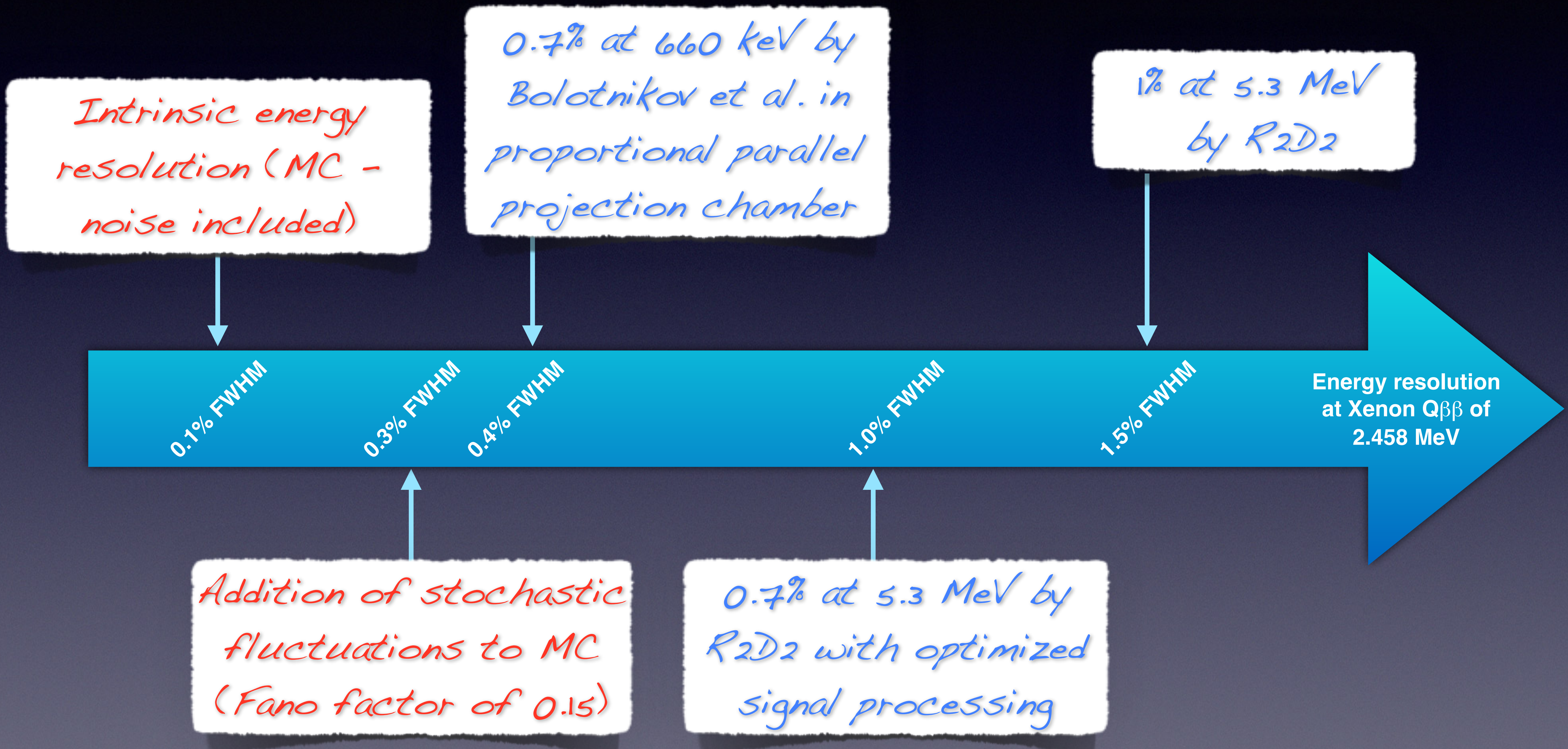

Energy resolution

NOTE: We assume that the energy resolution scales as a function of the energy as 1/sqrt(E).

R2D2 results are still dominated by noise and gas purity therfore 1% can be considered a conservative assumption

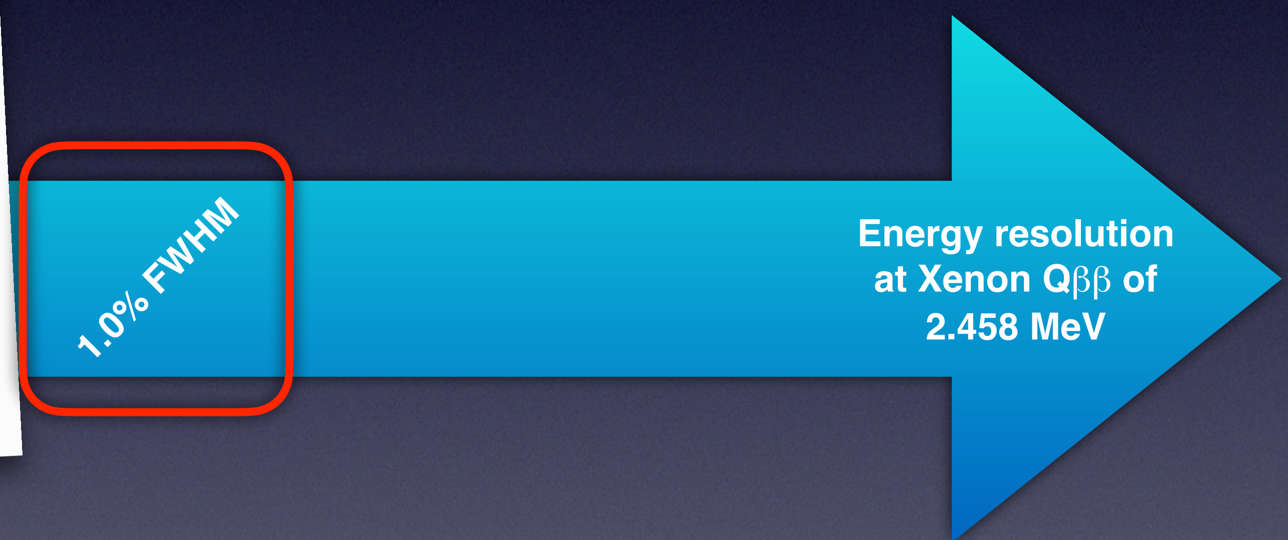

ROI and selections

- The first selection is to ask that the **events are in the ROI** (Region Of Interest) **after the Gaussian energy smearing** assumed of 1%FWHM at 2.458 MeV.

- The **optimal ROI choice** corresponds to an half width equal to the energy resolution [*JINST 13 (2018) 01, P01009*] i.e. we selected events in the range [2.433-2.483] MeV

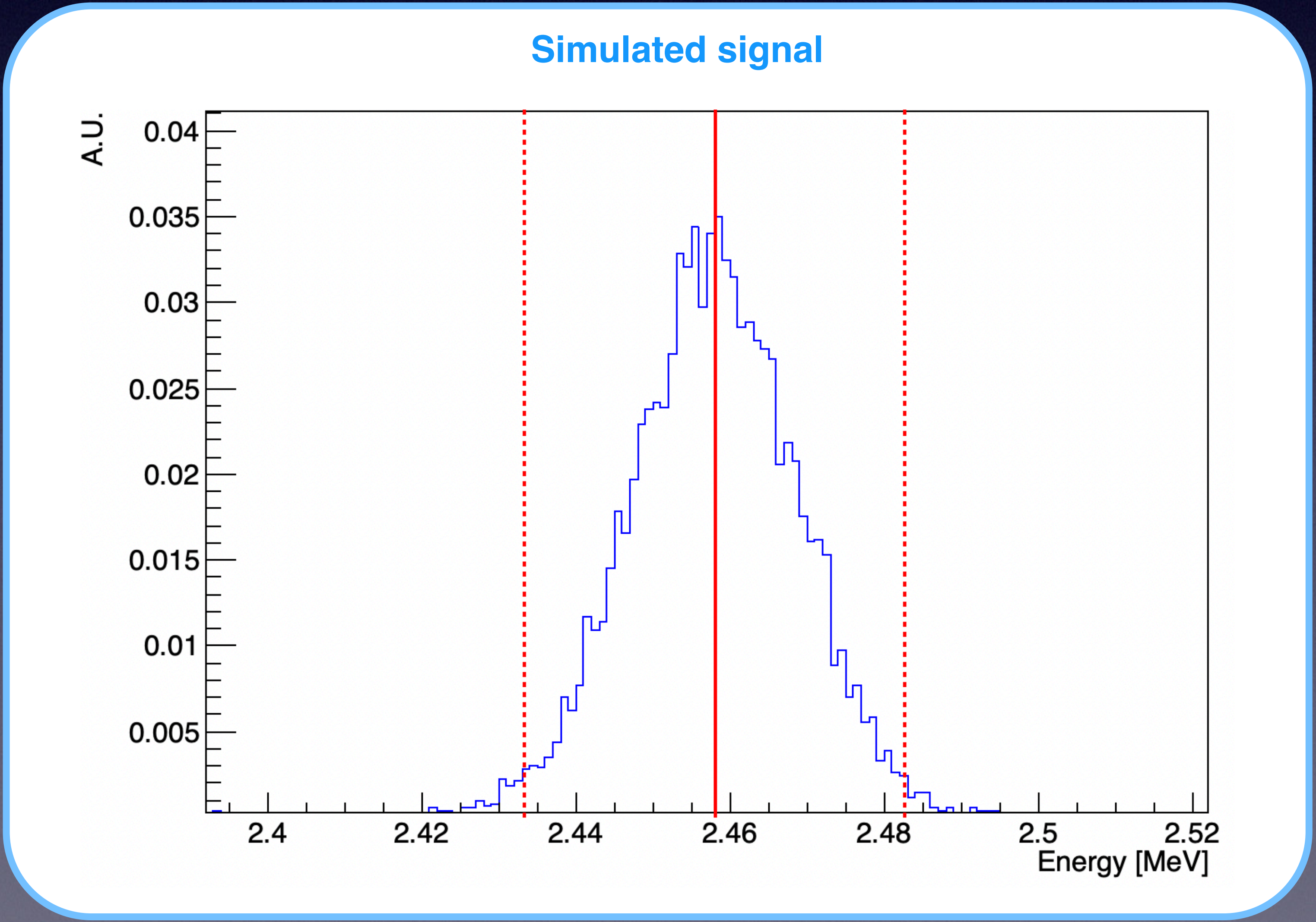

ROI and selections

- The first selection is to ask that the **events are in the ROI** (Region Of Interest) **after the Gaussian energy smearing** assumed of 1%FWHM at 2.458 MeV.

- The **optimal ROI choice** corresponds to an half width equal to the energy resolution [*JINST 13 (2018) 01, P01009*] i.e. we selected events in the range [2.433-2.483] MeV

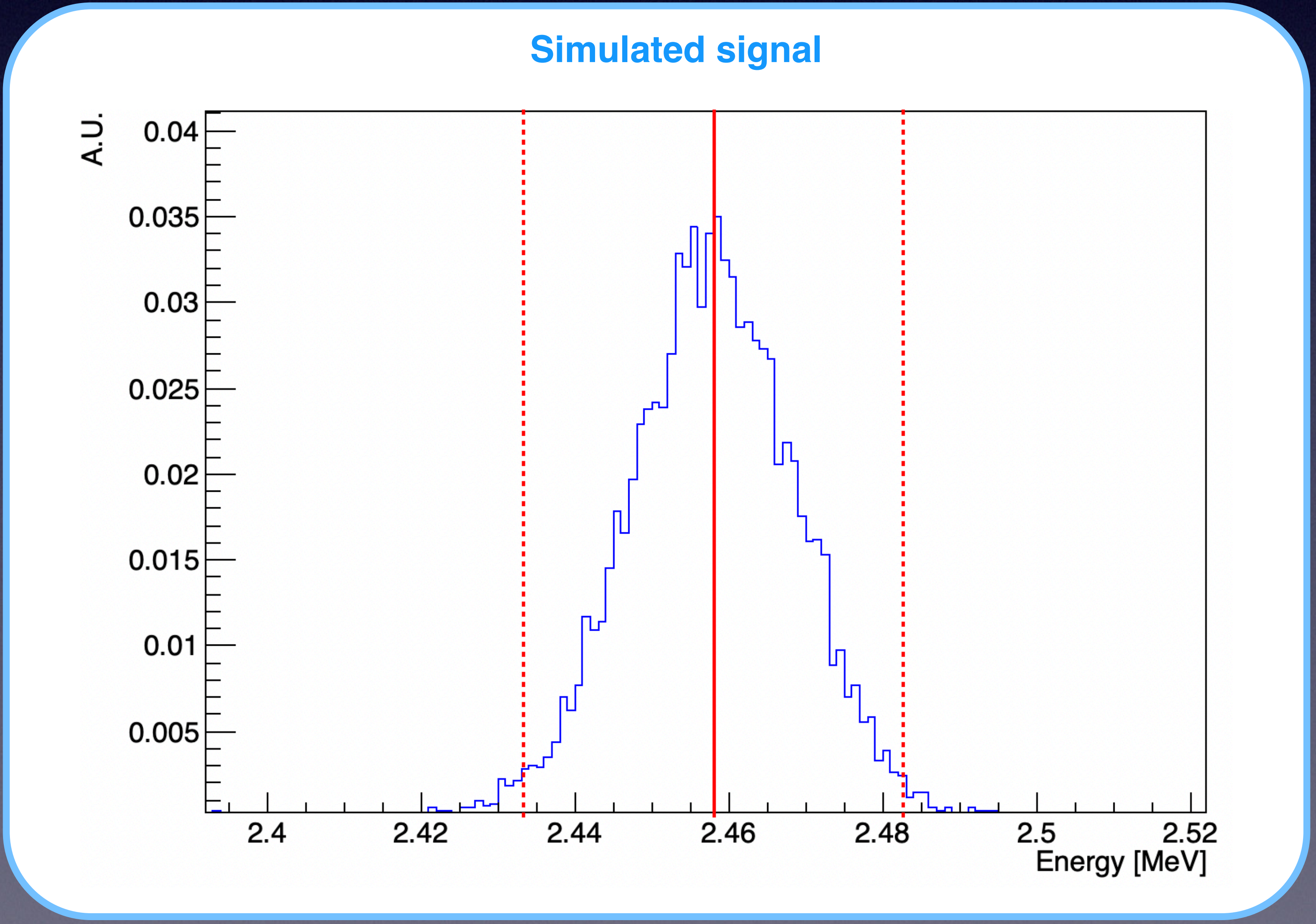

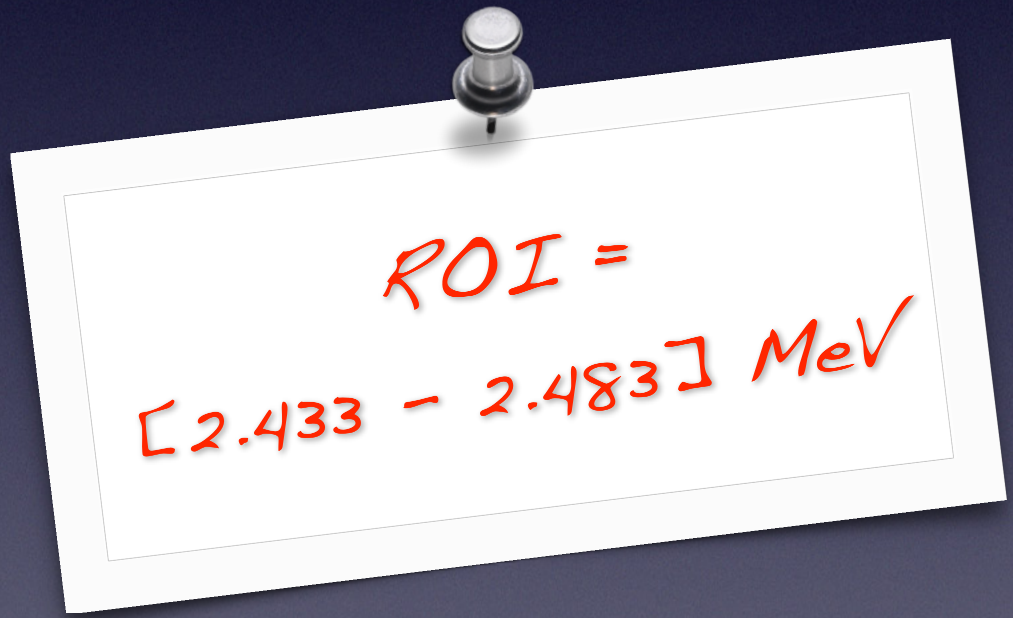

ROI and selections

- The first selection is to ask that the **events are in the ROI** (Region Of Interest) **after the Gaussian energy smearing** assumed of 1%FWHM at 2.458 MeV.

- The **optimal ROI choice** corresponds to an half width equal to the energy resolution [*JINST 13 (2018) 01, P01009*] i.e. we selected events in the range [2.433-2.483] MeV

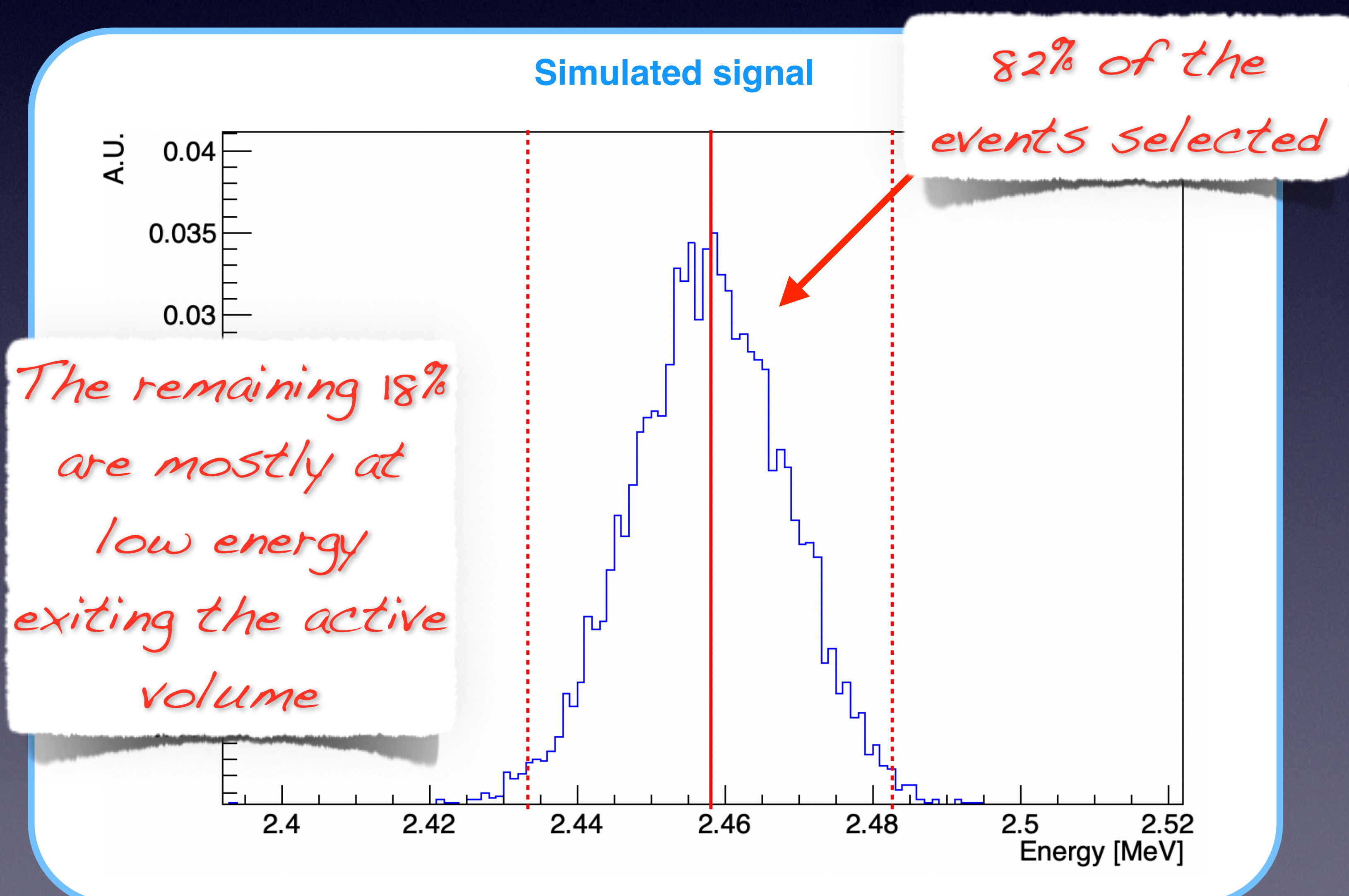

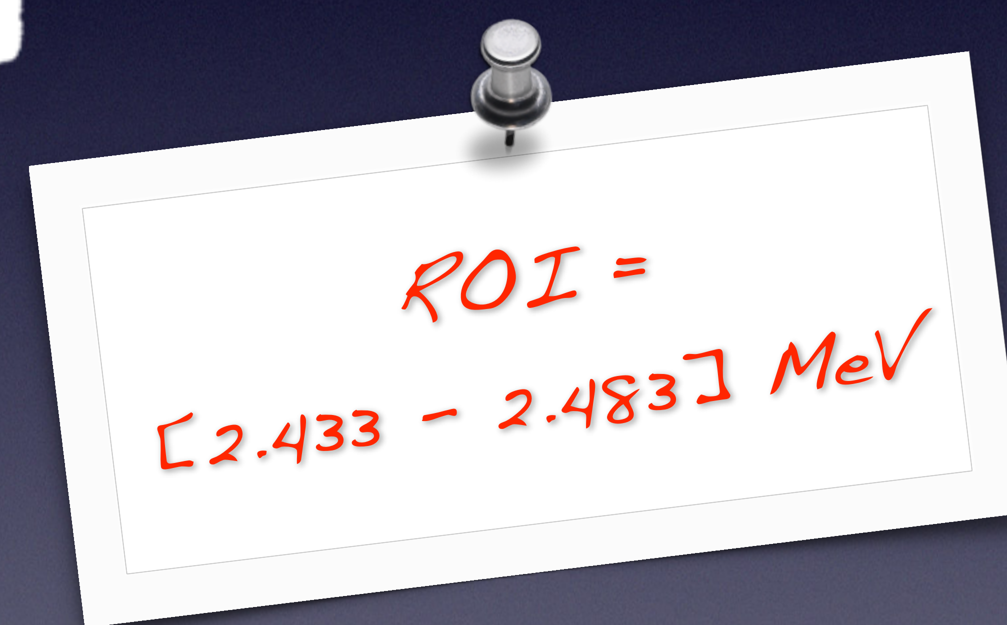

ROI and selections

- The events in the ROI are then selected based on **5 variables.**
- The **cuts** are chosen to reduce the background while **assuring a signal efficiency larger than 60%**.

ROI and selections

- The events in the ROI are then selected based on **5 variables.**
- The **cuts** are chosen to reduce the background while **assuring a signal efficiency larger than 60%**.

Np = Number of reconstructed peaks in the waveform

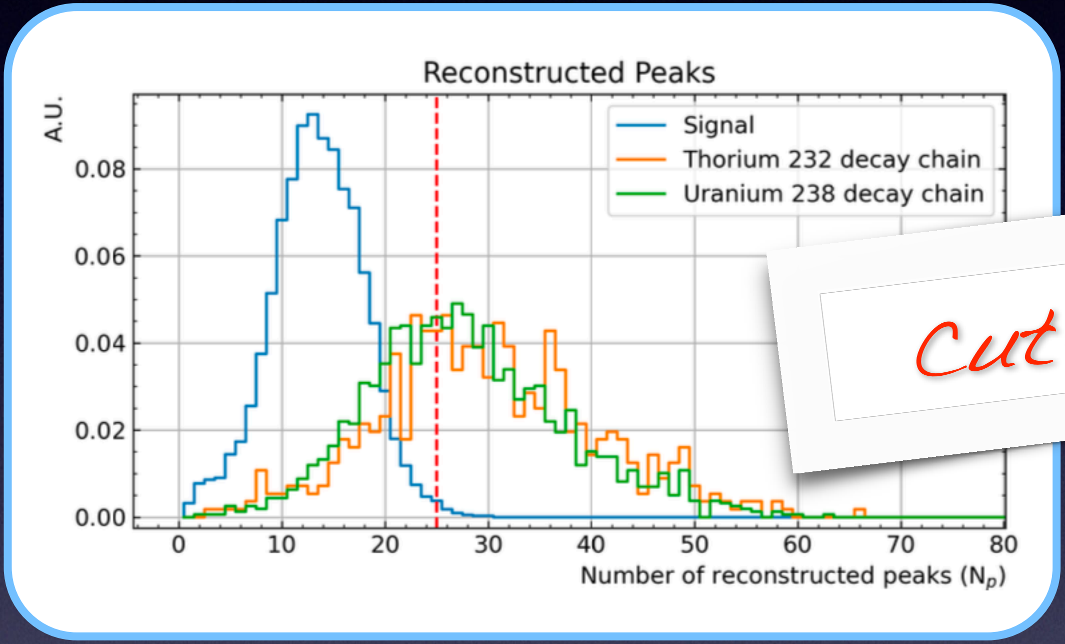

Cut: Np<25

ROI and selections

- The events in the ROI are then selected based on **5 variables.**
- The **cuts** are chosen to reduce the background while **assuring a signal efficiency larger than 60%**.

N_p = Number of reconstructed peaks in the waveform

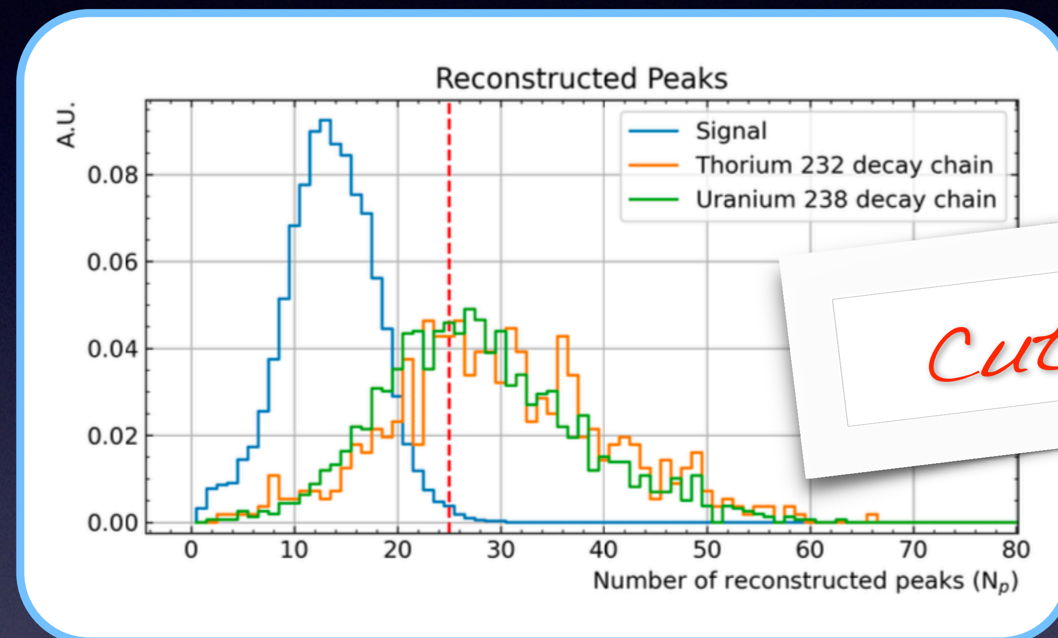

Cut: $N_p<25$

ΔR = Maximal radial distance between reconstructed peaks

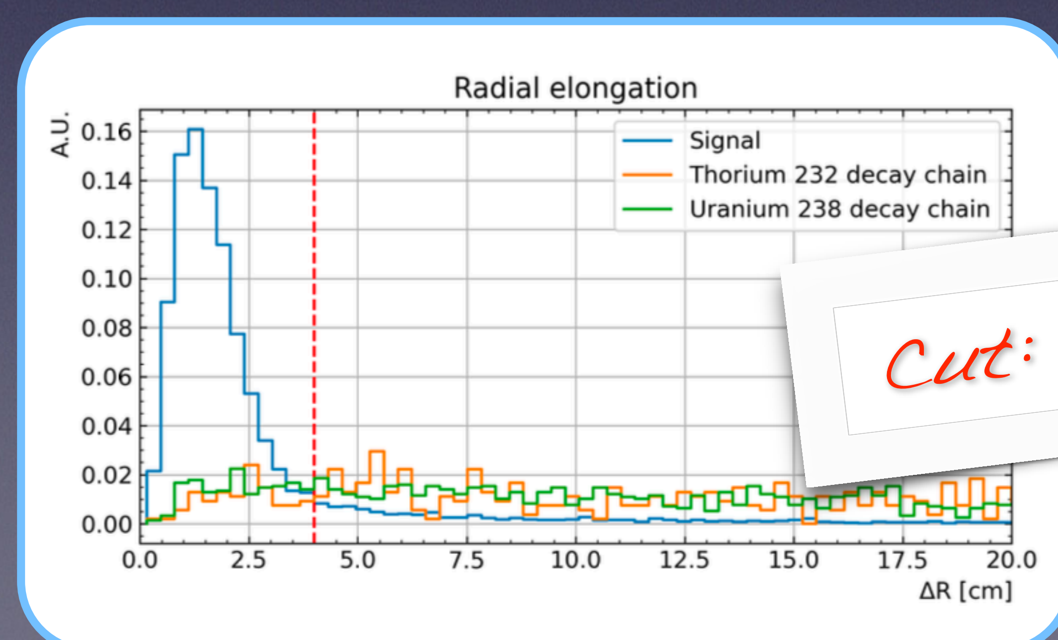

Cut: $\Delta R<4$ cm

ROI and selections

- The events in the ROI are then selected based on **5 variables.**
- The **cuts** are chosen to reduce the background while **assuring a signal efficiency larger than 60%**.

ROI and selections

- The events in the ROI are then selected based on **5 variables.**
- The **cuts** are chosen to reduce the background while **assuring a signal efficiency larger than 60%**.

ΔZ = Maximal longitudinal distance between reconstructed peaks

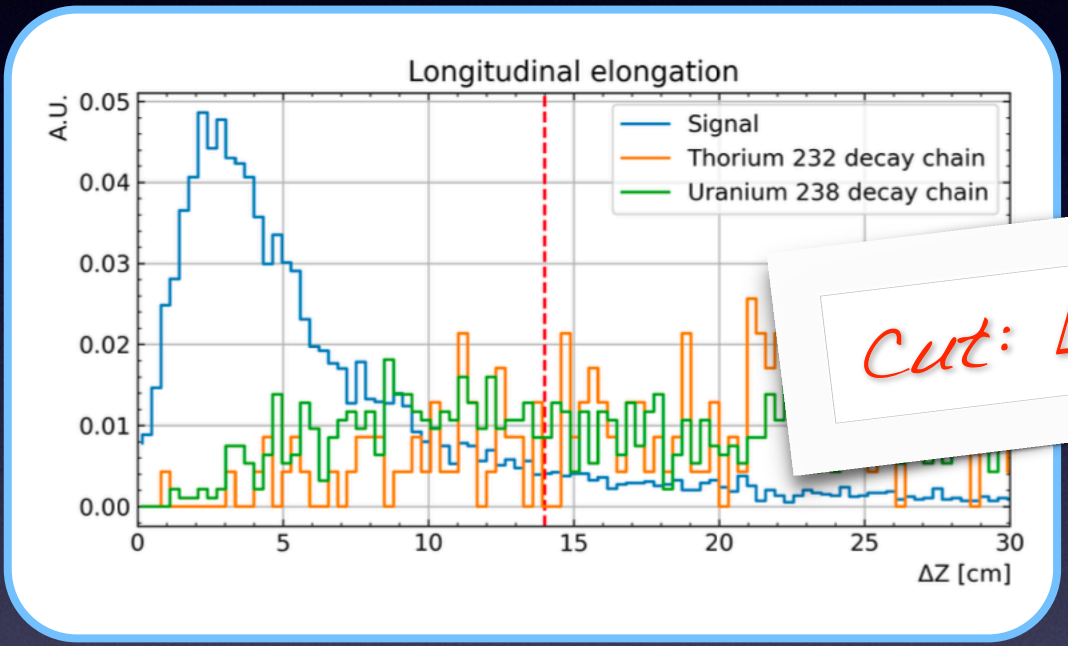

Cut: $\Delta Z < 14$ cm

ROI and selections

- The events in the ROI are then selected based on **5 variables.**
- The **cuts** are chosen to reduce the background while **assuring a signal efficiency larger than 60%**.

ΔZ = Maximal longitudinal distance between reconstructed peaks

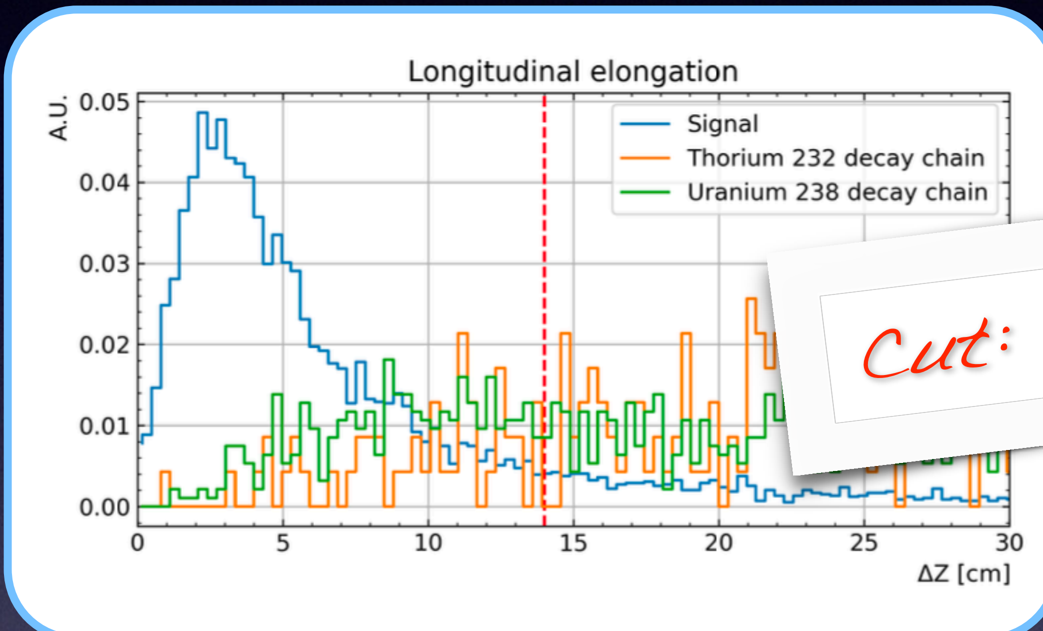

Cut: ΔZ<14 cm

ΔR x ΔZ= Maximal bidimensional distance between reconstructed peaks

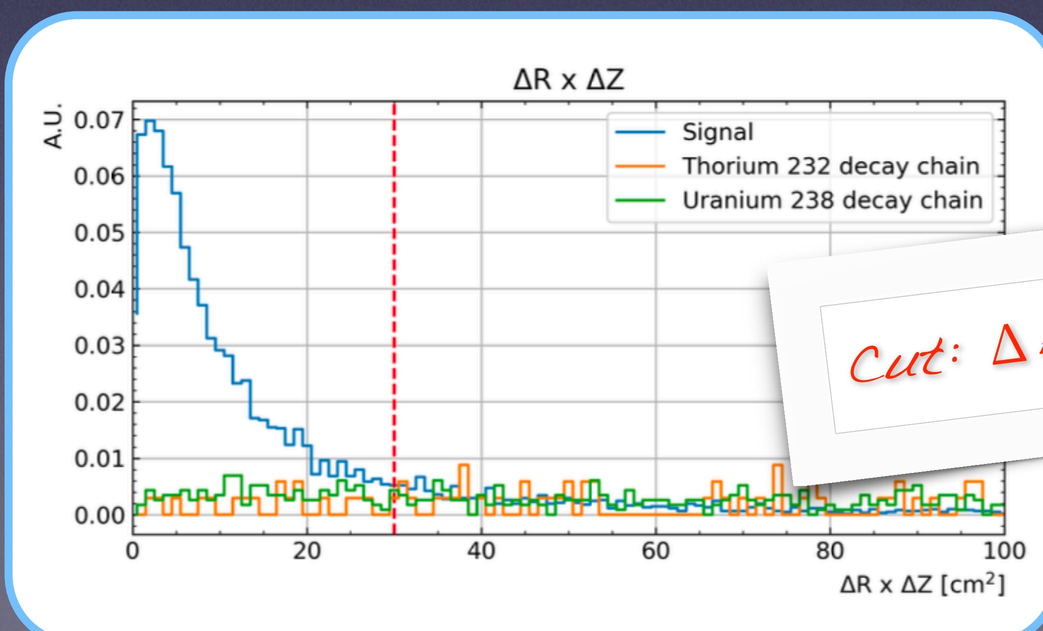

Cut: ΔR×ΔZ<30 cm²

ROI and selections

- The events in the ROI are then selected based on **5 variables.**
- The **cuts** are chosen to reduce the background while **assuring a signal efficiency larger than 60%**.

ROI and selections

- The events in the ROI are then selected based on **5 variables.**
- The **cuts** are chosen to reduce the background while **assuring a signal efficiency larger than 60%**.

MaxR = Largest radial position for reconstructed peaks

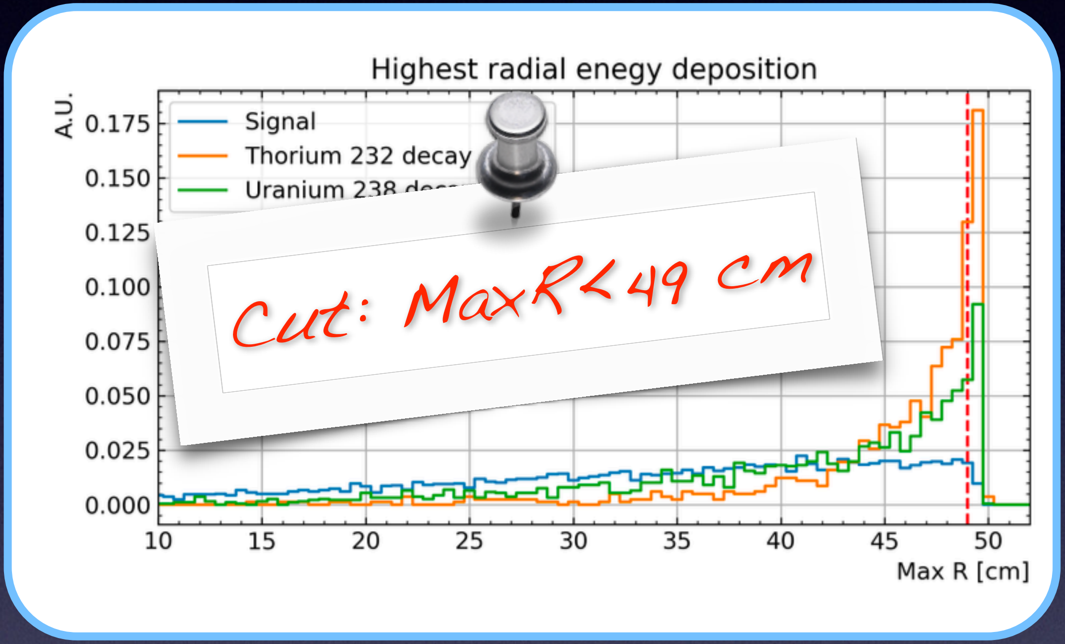

ROI and selections

- The events in the ROI are then selected based on **5 variables.**
- The **cuts** are chosen to reduce the background while **assuring a signal efficiency larger than 60%**.

MaxR = Largest radial position for reconstructed peaks

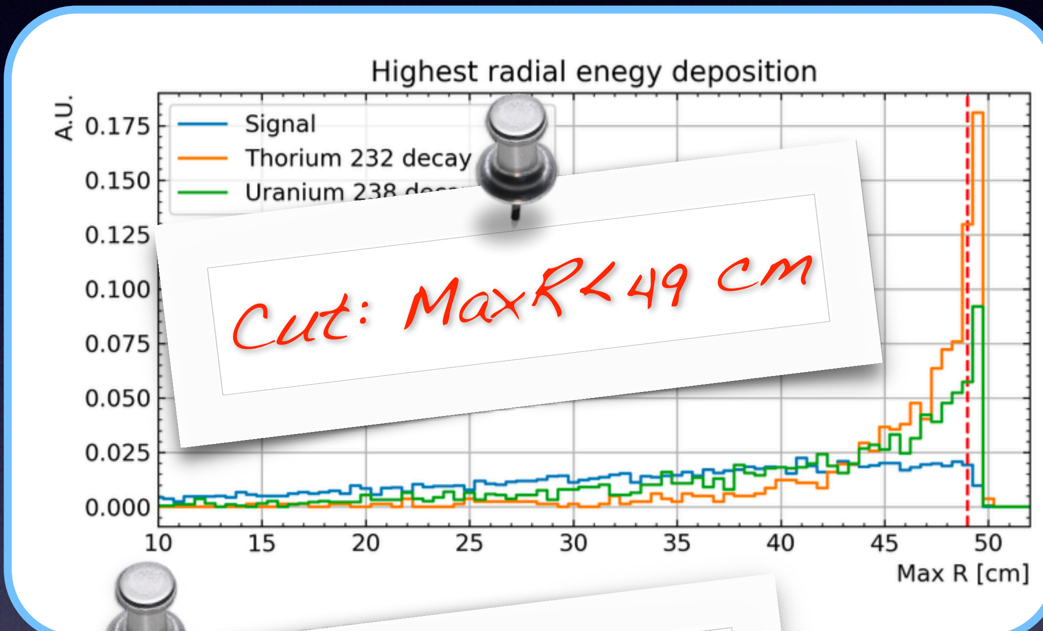

Cut: MaxR<49 cm

NOTE

MaxR rejects mostly α from the vessel whereas the other topological cuts rejects mostly multi-Compton from γ's.

Simulations

- $0\nu\beta\beta$ decay is not included in GEANT4, therefore two electrons are generated based on a pre-computed energy spectrum by J. Kotila and F. Iachello (*Phys. Rev. C 85, 034316 (2012)*).
- No angular correlation is included but this is a second order effect.
- Events are generated inside the xenon active volume.

Events in ROI	+ Topology cuts
82.2%	60.8%

Simulations

Signal

- $0\nu\beta\beta$ decay is not included in GEANT4, therefore two electrons are generated based on a pre-computed energy spectrum by J. Kotila and F. Iachello (*Phys. Rev. C 85, 034316 (2012)*).
- No angular correlation is included but this is a second order effect.
- Events are generated inside the xenon active volume.

Events in ROI	+ Topology cuts
82.2%	60.8%

Simulations

Signal

- $0\nu\beta\beta$ decay is not included in GEANT4, therefore two electrons are generated based on a pre-computed energy spectrum by J. Kotila and F. Iachello (*Phys. Rev. C 85, 034316 (2012)*).
- No angular correlation is included but this is a second order effect.
- Events are generated inside the xenon active volume.

Events in ROI	+ Topology cuts
82.2%	60.8%

Mostly due to events lost at the boundary

By construction when selecting the cuts

Simulations

- The high energy tail of the $\beta\beta2\nu$ spectrum could fall in the ROI.
- However, assuming a lifetime of 2.165 x 10^{21} years we expect **825000 decays in the active volume per year**.
- Considering the chosen ROI and an energy smearing at the level of 1%, **the fraction of events in the ROI is 9 x 10^{-10}** which corresponds to **0.001 events per year**.

Simulations

Background
$\beta\beta 2\nu$

- The high energy tail of the $\beta\beta 2\nu$ spectrum could fall in the ROI.
- However, assuming a lifetime of 2.165 x 10^{21} years we expect **825000 decays in the active volume per year**.
- Considering the chosen ROI and an energy smearing at the level of 1%, **the fraction of events in the ROI is 9 x 10^{-10}** which corresponds to **0.001 events per year**.

Simulations

Background
$\beta\beta 2\nu$

- The high energy tail of the $\beta\beta 2\nu$ spectrum could fall in the ROI.
- However, assuming a lifetime of 2.165 x 10^{21} years we expect **825000 decays in the active volume per year**.
- Considering the chosen ROI and an energy smearing at the level of 1%, **the fraction of events in the ROI is 9 x 10^{-10}** which corresponds to **0.001 events per year**.

Background totally negligible

Simulations

- The vessel radioactivity was assumed to be at the level of **10 μBq/kg**.
- **Decay chains** of ^{238}U and ^{232}Th, were **simulated uniformly within the carbon fibre layer** (total mass of about 330 Kg), with a large statistics corresponding to about 10 years of data taking.

Source	Events in ROI	+ Topology cuts
^{232}Th	80.5	0.5
^{238}U	25.8	0.7
Total	106.3	1.2

Simulations

Background from composite radioactivity

- The vessel radioactivity was assumed to be at the level of **10 μBq/kg**.
- **Decay chains** of ^{238}U and ^{232}Th, were **simulated uniformly within the carbon fibre layer** (total mass of about 330 Kg), with a large statistics corresponding to about 10 years of data taking.

Source	Events in ROI	+ Topology cuts
^{232}Th	80.5	0.5
^{238}U	25.8	0.7
Total	106.3	1.2

Simulations

Background from composite radioactivity

- The vessel radioactivity was assumed to be at the level of **10 μBq/kg**.
- **Decay chains** of ^{238}U and ^{232}Th, were **simulated uniformly within the carbon fibre layer** (total mass of about 330 Kg), with a large statistics corresponding to about 10 years of data taking.

Source	Events in ROI	+ Topology cuts
^{232}Th	80.5	0.5
^{238}U	25.8	0.7
Total	106.3	1.2

Events from Tl208 falling in ROI with no multi-Compton observed

Events from Bi214 falling in ROI with no multi-Compton observed

Simulations

- The same decay chains were studied for the anode.
- In real life we plan to use a 1 mm thick tube made of polymer materials coated with a resistive foil of few μm.
- The mass is extremely small at the level of 200 g and the background can be considered **negligible even considering an increase of a factor 100 in the activity** at the level of at the level of **1 mBq/kg**.

Simulations

Background from anode radioactivity

- The same decay chains were studied for the anode.
- In real life we plan to use a 1 mm thick tube made of polymer materials coated with a resistive foil of few μm.
- The mass is extremely small at the level of 200 g and the background can be considered **negligible even considering an increase of a factor 100 in the activity** at the level of at the level of **1 mBq/kg**.

Simulations

Background from anode radioactivity

- The same decay chains were studied for the anode.
- In real life we plan to use a 1 mm thick tube made of polymer materials coated with a resistive foil of few μm.
- The mass is extremely small at the level of 200 g and the background can be considered **negligible even considering an increase of a factor 100 in the activity** at the level of at the level of **1 mBq/kg**.

Background totally negligible

Simulations

- The lead shielding is also source of background.
- To bring such a background to anegligible level, assuming upper limits on the ^{238}U and ^{232}Th chain of 12 μBq/kg and 4 μBq/kg, respectively (*NIM A 591, 490 (2008)*) and additional layer is needed in the detector.
- The simulation shows that 5 cm of low-radioactivity commercial copper (e.g. 1 μBq/kg from Aurubis) or water passive veto could bring the background **below 0.1 events per year**.

Simulations

Background from lead shielding radioactivity

- The lead shielding is also source of background.
- To bring such a background to anegligible level, assuming upper limits on the ^{238}U and ^{232}Th chain of 12 μBq/kg and 4 μBq/kg, respectively (*NIM A 591, 490 (2008)*) and additional layer is needed in the detector.
- The simulation shows that 5 cm of low-radioactivity commercial copper (e.g. 1 μBq/kg from Aurubis) or water passive veto could bring the background **below 0.1 events per year**.

Simulations

Background from lead shielding radioactivity

- The lead shielding is also source of background.
- To bring such a background to anegligible level, assuming upper limits on the ^{238}U and ^{232}Th chain of 12 μBq/kg and 4 μBq/kg, respectively (*NIM A 591, 490 (2008)*) and additional layer is needed in the detector.
- The simulation shows that 5 cm of low-radioactivity commercial copper (e.g. 1 μBq/kg from Aurubis) or water passive veto could bring the background **below 0.1 events per year**.

Background could be reduced to 0.1 events per year although the practical option is still under discussion

Simulations

- External gamma background strongly depends on the environment. We assumed the rate and spectrum measured at LSM (*Nucl. Instrum. Meth. A 482, 832*).
- Gammas for a statistics of more than 10 years were generated in the GEANT4 on a sphere of 280 cm radius, homogeneously and isotropically.

Energy	Events in ROI	+ Topology cut
1-4 MeV	2.9	0.1
4-6 MeV	0.03	< 0.03
6-10 MeV	< 0.02	< 0.02
Total	2.9	0.1

Simulations

Background from external gammas

- External gamma background strongly depends on the environment. We assumed the rate and spectrum measured at LSM (*Nucl. Instrum. Meth. A 482, 832*).
- Gammas for a statistics of more than 10 years were generated in the GEANT4 on a sphere of 280 cm radius, homogeneously and isotropically.

Energy	Events in ROI	+ Topology cut
1-4 MeV	2.9	0.1
4-6 MeV	0.03	< 0.03
6-10 MeV	< 0.02	< 0.02
Total	2.9	0.1

Simulations

Background from external gammas

- External gamma background strongly depends on the environment. We assumed the rate and spectrum measured at LSM (*Nucl. Instrum. Meth. A 482, 832*).
- Gammas for a statistics of more than 10 years were generated in the GEANT4 on a sphere of 280 cm radius, homogeneously and isotropically.

Energy	Events in ROI	+ Topology cut
1-4 MeV	2.9	0.1
4-6 MeV	0.03	< 0.03
6-10 MeV	< 0.02	< 0.02
Total	2.9	0.1

External radioactivity → 1-4 MeV

Gammas related to the detector used for the measurement (difficult to extrapolate...) → 4-6 MeV

Gammas from radiative captures → 6-10 MeV

Simulations

Background from external gammas

- External gamma background strongly depends on the environment. We assumed the rate and spectrum measured at LSM (*Nucl. Instrum. Meth. A 482, 832*).
- Gammas for a statistics of more than 10 years were generated in the GEANT4 on a sphere of 280 cm radius, homogeneously and isotropically.

Energy	Events in ROI	+ Topology cut
1-4 MeV	2.9	0.1
4-6 MeV	0.03	< 0.03
6-10 MeV	< 0.02	< 0.02
Total	2.9	0.1

External radioactivity

Gammas related to the detector used for the measurement (difficult to extrapolate...)

Gammas from radiative captures

Background almost negligible (shielding can be adjusted)

Simulations

- Different neutrons sources were considered:

Simulations

Background from external neutrons

- Different neutrons sources were considered:

Simulations

Background from external neutrons

- Different neutrons sources were considered:
  - ➡ Neutrons captures on detector shielding and material → Production of high energy (6-10 MeV) gammas already accounted for

Simulations

Background from external neutrons

- Different neutrons sources were considered:
  - ➡ Neutrons produced by muons inside the detector

Tagged easily with the muon. Possible deadtime (negligible with few per m^2 per day)

Simulations

Background from external neutrons

- Different neutrons sources were considered:
  - ➡ Neutrons captures on xenon

Simulation on ^{136}Xe performed in GEANT4 (gammas with energy of few MeV)

Simulations

Background from external neutrons

- Different neutrons sources were considered:
  - ➡ Neutrons captures on xenon
  - ➡ Spallation neutrons

Simulation on ^{136}Xe performed in GEANT4 (gammas with energy of few MeV)

Neutrons simulated assuming 4800 m.w.e. depth (e.g. LSM)

Simulations

Background from external neutrons

- Different neutrons sources were considered:
  - ➡ Neutrons captures on xenon
  - ➡ Spallation neutrons

Simulation on ^{136}Xe performed in GEANT4 (gammas with energy of few MeV)

Neutrons simulated assuming 4800 m.w.e. depth (e.g. LSM)

Source	Events in ROI	+ Topology cut
Capture on ^{136}Xe	6.7	0.02
Spallation neutrons	3.7	0.02
Total	10.4	0.04

Background totally negligible

Simulations

- Radon is one of the ultimate sources of background in low-radioactivity experiments.
- Cryogenic distillation is an effective method for radon removal although quite demanding in terms of nitrogen. Alternative methods based on absorbers under study (*Progress of Theoretical and Experimental Physics 2024(2), 023C01 (2023)*).
- We assumed a radon activity level of **5 μBq/kg** (corresponding to1.5 mBq/m^3), a **conservative estimate** (0.3 μBq/kg for nEXO, 1 μBq/kg for XENONnT and 3.5 μBq/kgfor PandaX-4T).

Simulations

Background from Radon

- Radon is one of the ultimate sources of background in low-radioactivity experiments.
- Cryogenic distillation is an effective method for radon removal although quite demanding in terms of nitrogen. Alternative methods based on absorbers under study (*Progress of Theoretical and Experimental Physics 2024(2), 023C01 (2023)*).
- We assumed a radon activity level of **5 μBq/kg** (corresponding to1.5 mBq/m^3), a **conservative estimate** (0.3 μBq/kg for nEXO, 1 μBq/kg for XENONnT and 3.5 μBq/kgfor PandaX-4T).

Simulations

Background from Radon

- Radon is one of the ultimate sources of background in low-radioactivity experiments.
- Cryogenic distillation is an effective method for radon removal although quite demanding in terms of nitrogen. Alternative methods based on absorbers under study (*Progress of Theoretical and Experimental Physics 2024(2), 023C01 (2023)*).
- We assumed a radon activity level of **5 μBq/kg** (corresponding to1.5 mBq/m^3), a **conservative estimate** (0.3 μBq/kg for nEXO, 1 μBq/kg for XENONnT and 3.5 μBq/kgfor PandaX-4T).

Background at the level of 0.2 events per year

Simulations

- Cosmogenic nuclei produced by muons passing through the xenon volume could contribute to the background.
- A detailed simulation by the EXO-200 collaboration identified ^{137}Xe as the primary contributor to signals near the ^{136}Xe $Q_{\beta\beta}$.
- The production rate of ^{137}Xe depends on both the muon flux and their energy.
- We assumed the **muon rate expected at LSM** and we obtained 10 events per year. After the selection cuts the **expected number of events is below 2×10^{-3}**.

Simulations

Cosmogenic Background

- Cosmogenic nuclei produced by muons passing through the xenon volume could contribute to the background.
- A detailed simulation by the EXO-200 collaboration identified ^{137}Xe as the primary contributor to signals near the ^{136}Xe $Q_{\beta\beta}$.
- The production rate of ^{137}Xe depends on both the muon flux and their energy.
- We assumed the **muon rate expected at LSM** and we obtained 10 events per year. After the selection cuts the **expected number of events is below 2 x 10^{-3}**.

Simulations

Cosmogenic Background

- Cosmogenic nuclei produced by muons passing through the xenon volume could contribute to the background.
- A detailed simulation by the EXO-200 collaboration identified ^{137}Xe as the primary contributor to signals near the ^{136}Xe $Q_{\beta\beta}$.
- The production rate of ^{137}Xe depends on both the muon flux and their energy.
- We assumed the **muon rate expected at LSM** and we obtained 10 events per year. After the selection cuts the **expected number of events is below 2 x 10^{-3}**.

Negligible background

Background and pile-up

- The total **expected background is of 1.6 events per year**.
- The same sources were used to computed the possible pile-up assuming an event time window of 5 ms.
- The **expected rate is about 0.19 Hz, well below the acceptable limit** of 1 Hz.

Contribution	Events per year
$\beta\beta2\nu$	1.0×10^{-3}
Composite radioactivity	1.2
Anode radioactivity	1.0×10^{-3}
Lead radioactivity	0.1
External gammas	0.1
External neutrons	0.04
Radon	0.2
Cosmogenic background	1.6×10^{-3}
Total	1.6

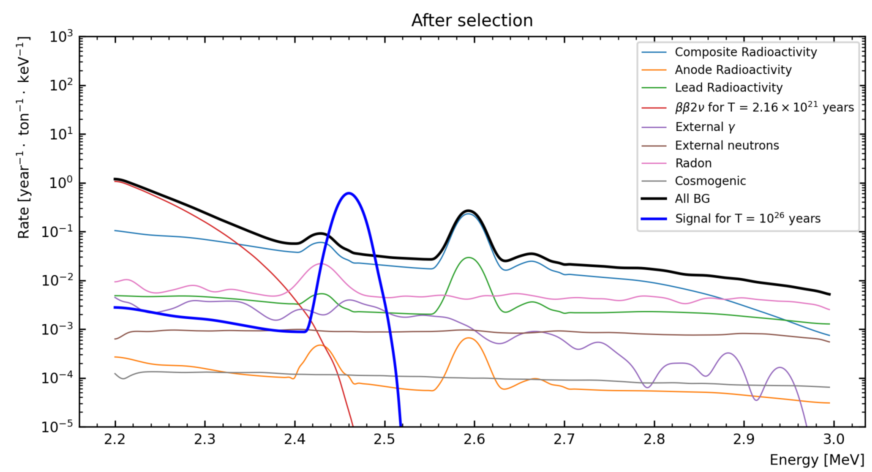

Contribution	Rate (Hz)
$\beta\beta2\nu$	0.03
Composite radioactivity	5.8×10^{-3}
Anode radioactivity	4.7×10^{-5}
Lead radioactivity	8.0×10^{-3}
External gammas	1.2×10^{-3}
External neutrons	5×10^{-4}
Radon	0.02
Cosmogenic background	0.015
^{40}K	0.12
Total	0.20

Background and pile-up

- The total **expected background is of 1.6 events per year**.
- The same sources were used to computed the possible pile-up assuming an event time window of 5 ms.
- The **expected rate is about 0.19 Hz, well below the acceptable limit** of 1 Hz.

Background summary

Contribution	Events per year
$\beta\beta2\nu$	1.0×10^{-3}
Composite radioactivity	1.2
Anode radioactivity	1.0×10^{-3}
Lead radioactivity	0.1
External gammas	0.1
External neutrons	0.04
Radon	0.2
Cosmogenic background	1.6×10^{-3}
Total	1.6

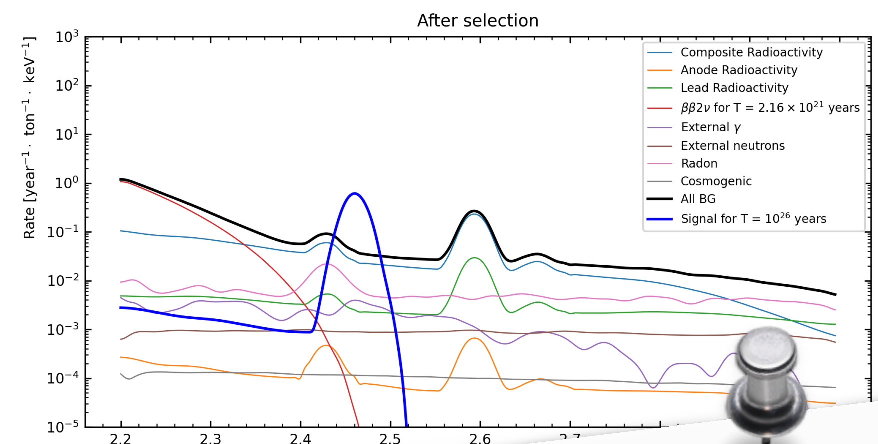

Dominated by the composite radioactivity

Event rate summary

Contribution	Rate (Hz)
$\beta\beta2\nu$	0.03
Composite radioactivity	5.8×10^{-3}
Anode radioactivity	4.7×10^{-5}
Lead radioactivity	8.0×10^{-3}
External gammas	1.2×10^{-3}
External neutrons	5×10^{-4}
Radon	0.02
Cosmogenic background	0.015
^{40}K	0.12
Total	0.20

NOTE that ^{40}K is not in the background since the maximal energy of 1.5 MeV below the ROI

Sensitivity

- The experimental sensitivity can be computed in terms of a limit of the half life.

$$T^{0\nu}_{1/2} > \ln(2)\varepsilon \frac{N_A m}{M}\frac{t}{S_{up}}$$

Signal efficiency of 60.8%

Xenon-136 active mass of 580 kg

Exposure in years

Signal upper limit

^{136}Xe molar mass of 0.136 Kg

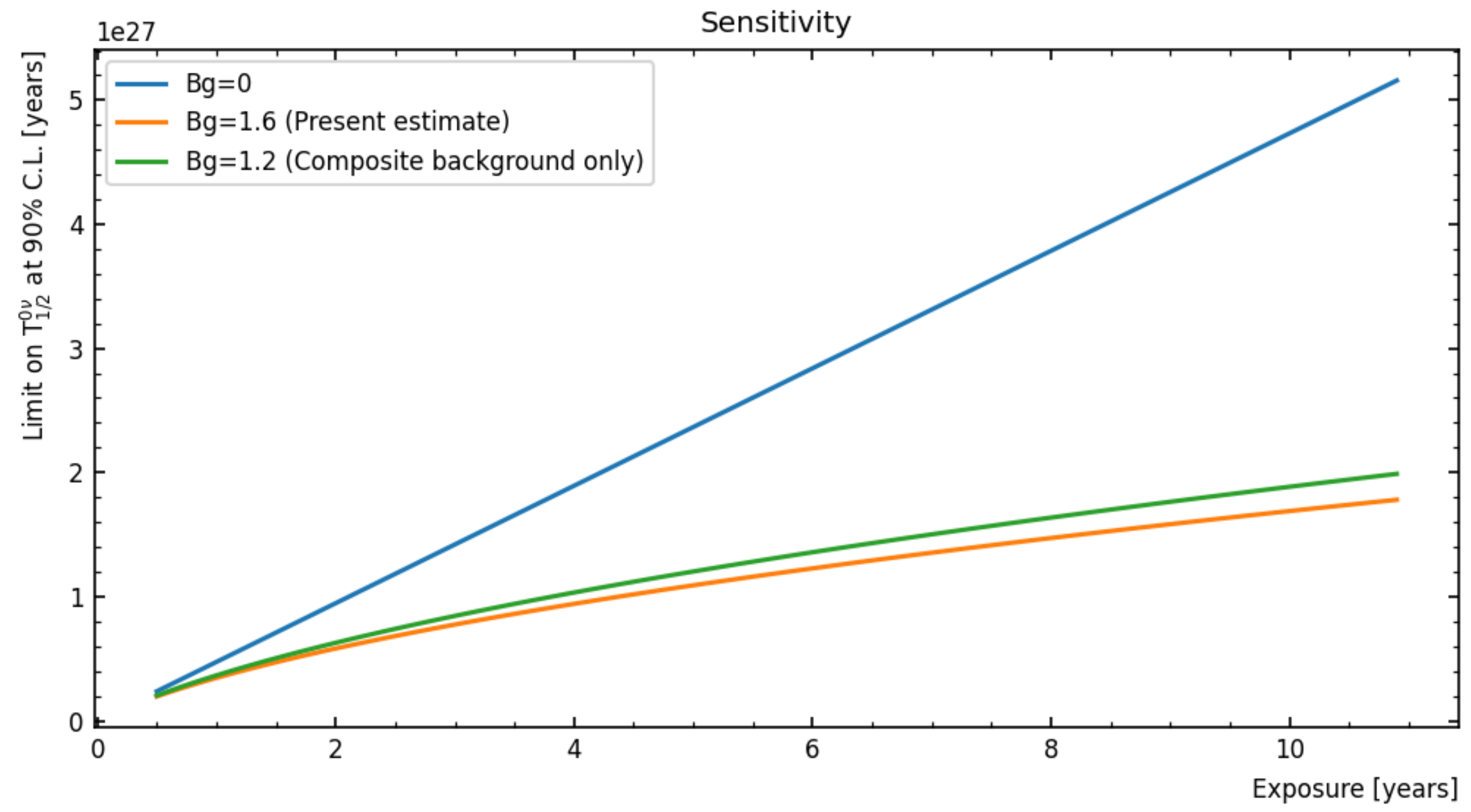

Sensitivity

- The experimental sensitivity can be computed in terms of a limit of the half life.

Signal efficiency of 60.8%

Xenon-136 active mass of 580 kg

$$T^{0\nu}_{1/2} > \ln(2)\varepsilon\frac{N_A m}{M}\frac{t}{S_{up}}$$

Exposure in years

Signal upper limit

^{136}Xe molar mass of 0.136 Kg

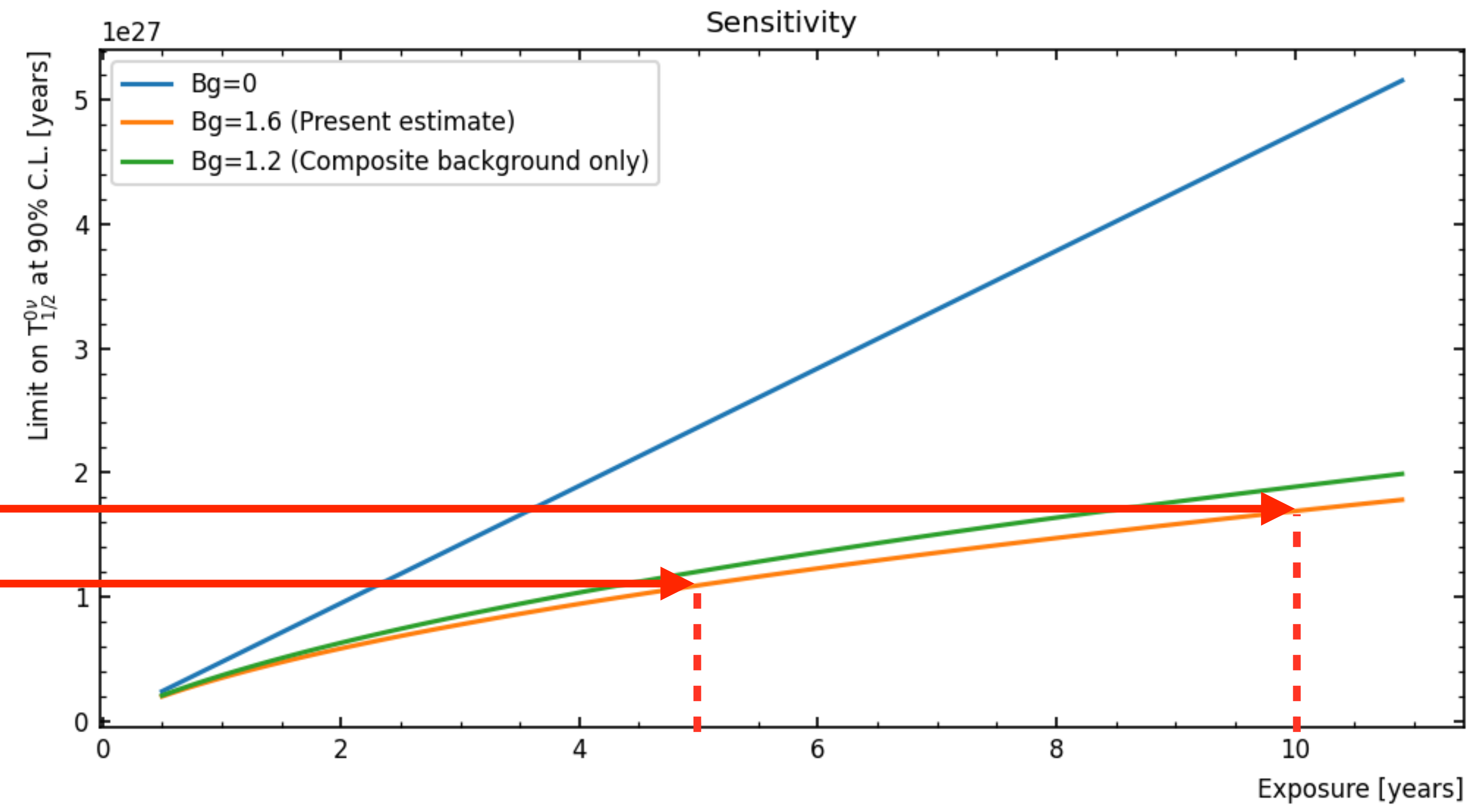

1.7×10^{27} years in 10 years

1.1×10^{27} years in 5 years

Sensitivity

- The lifetime is related to the effective Majorana mass <mββ>:

$$\frac{1}{T_{1/2}^{0\nu}} = G^{0\nu}|M^{0\nu}|^2 < m_{\beta\beta} >^2$$

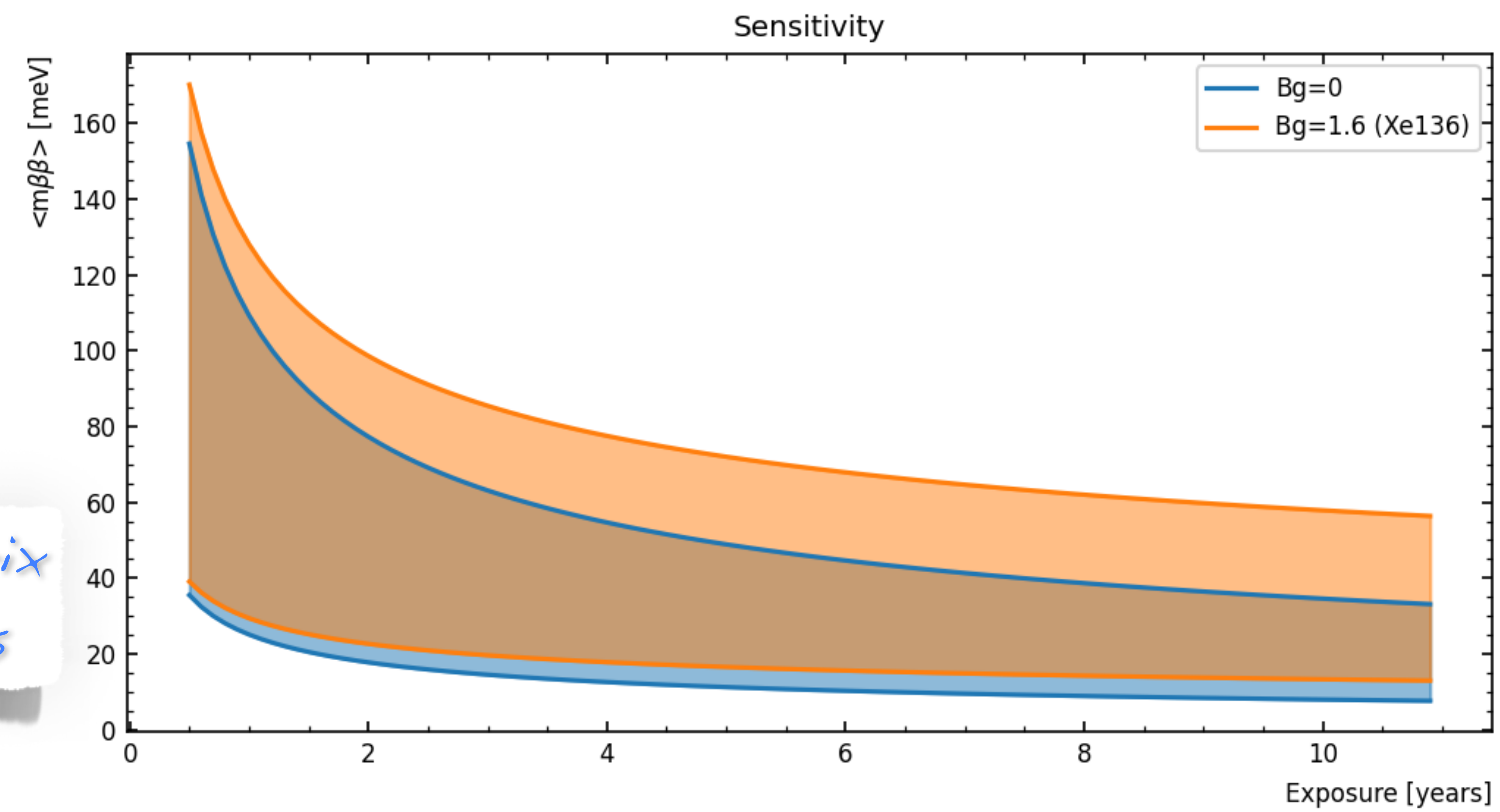

Band width due to matrix elements uncertainties

Sensitivity

- The lifetime is related to the effective Majorana mass <mββ>:

$$\frac{1}{T^{0\nu}_{1/2}} = G^{0\nu}|M^{0\nu}|^2 < m_{\beta\beta} >^2$$

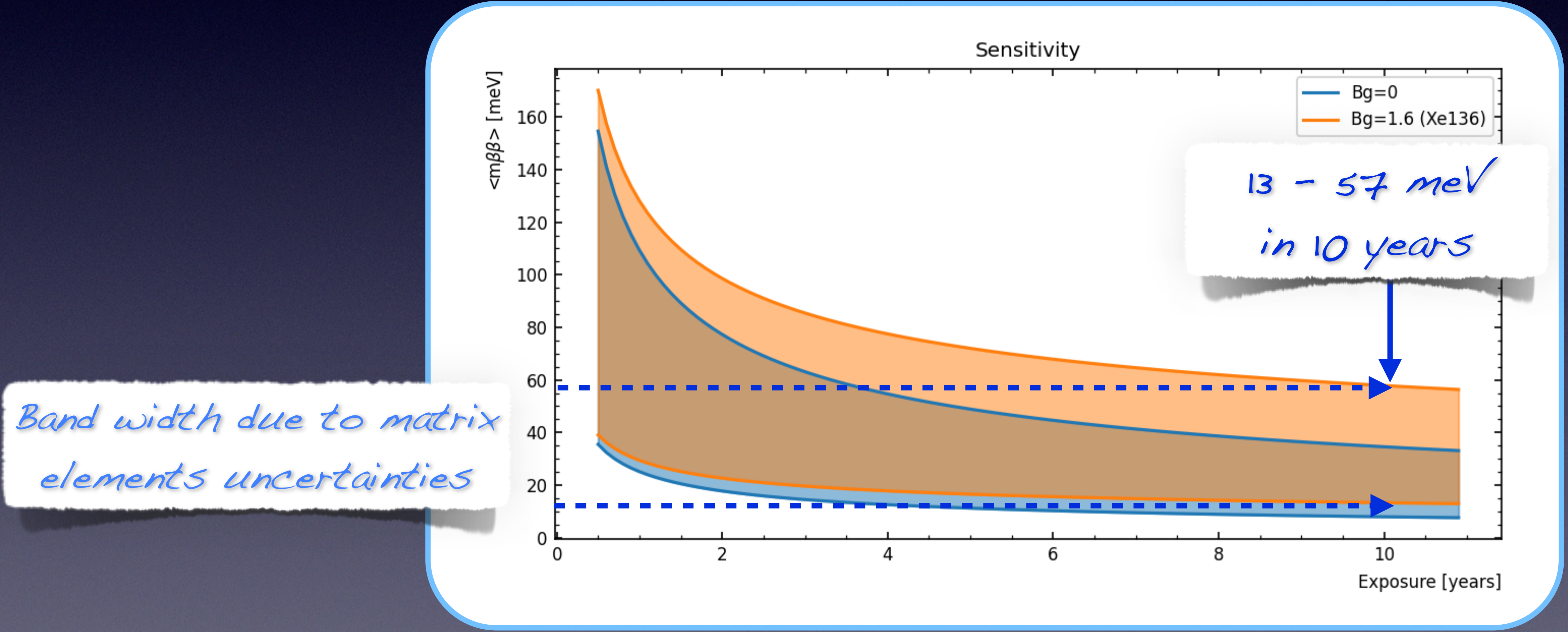

Sensitivity

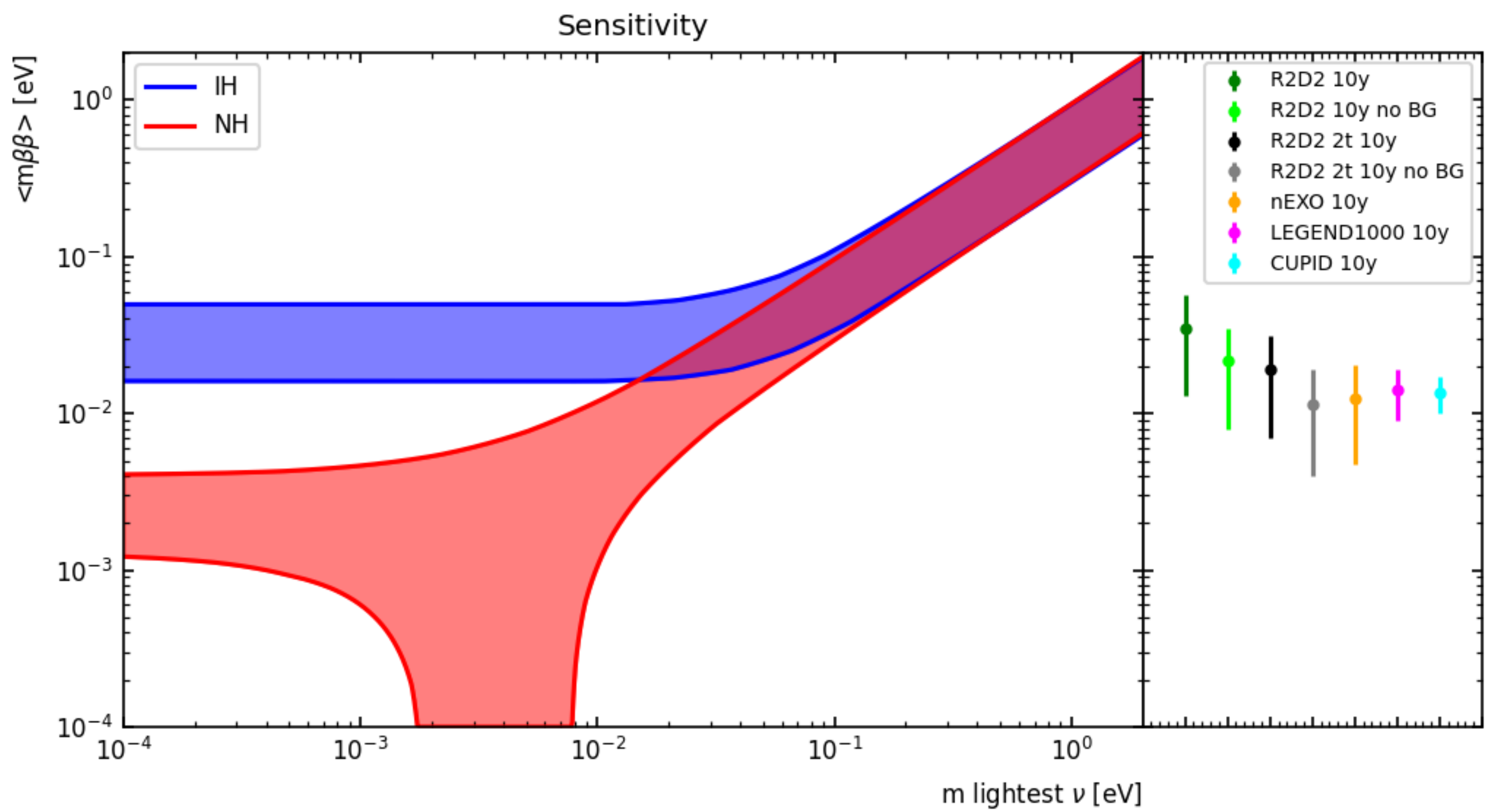

Sensitivity

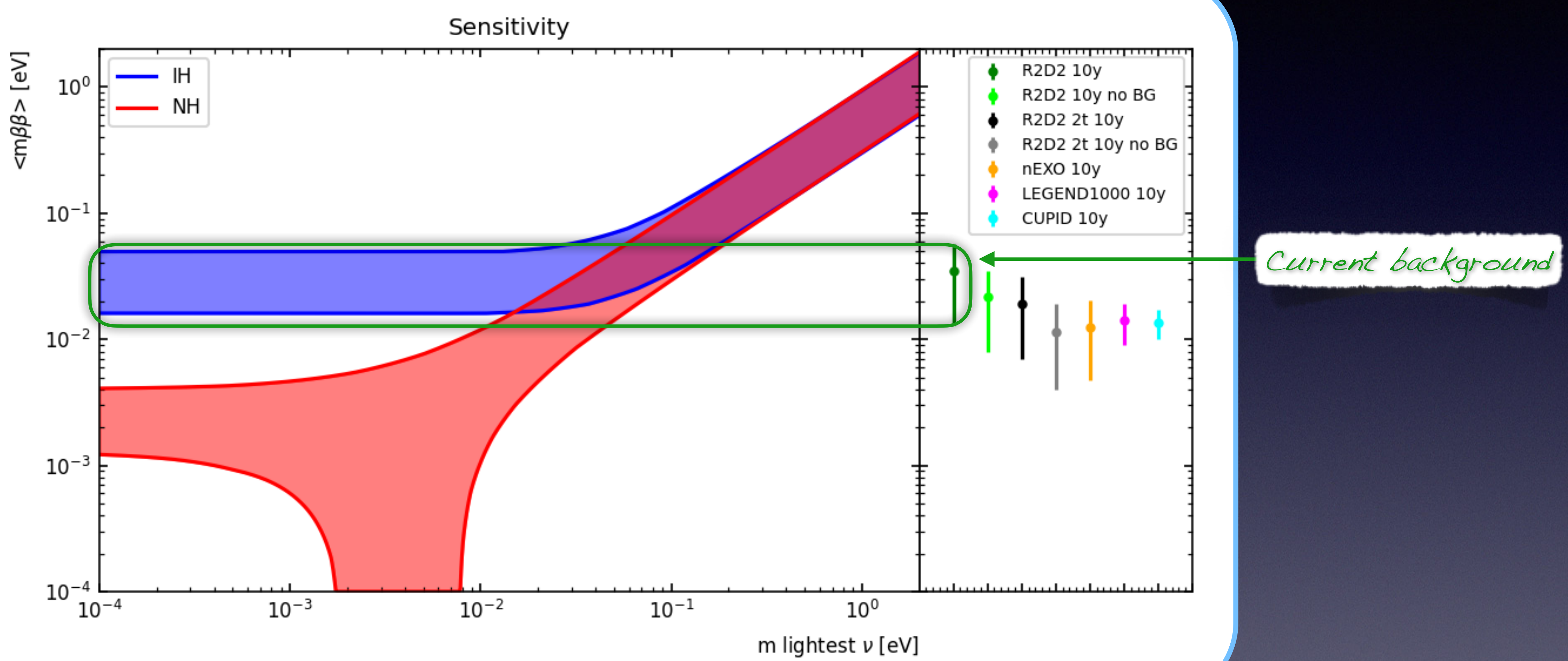

Sensitivity

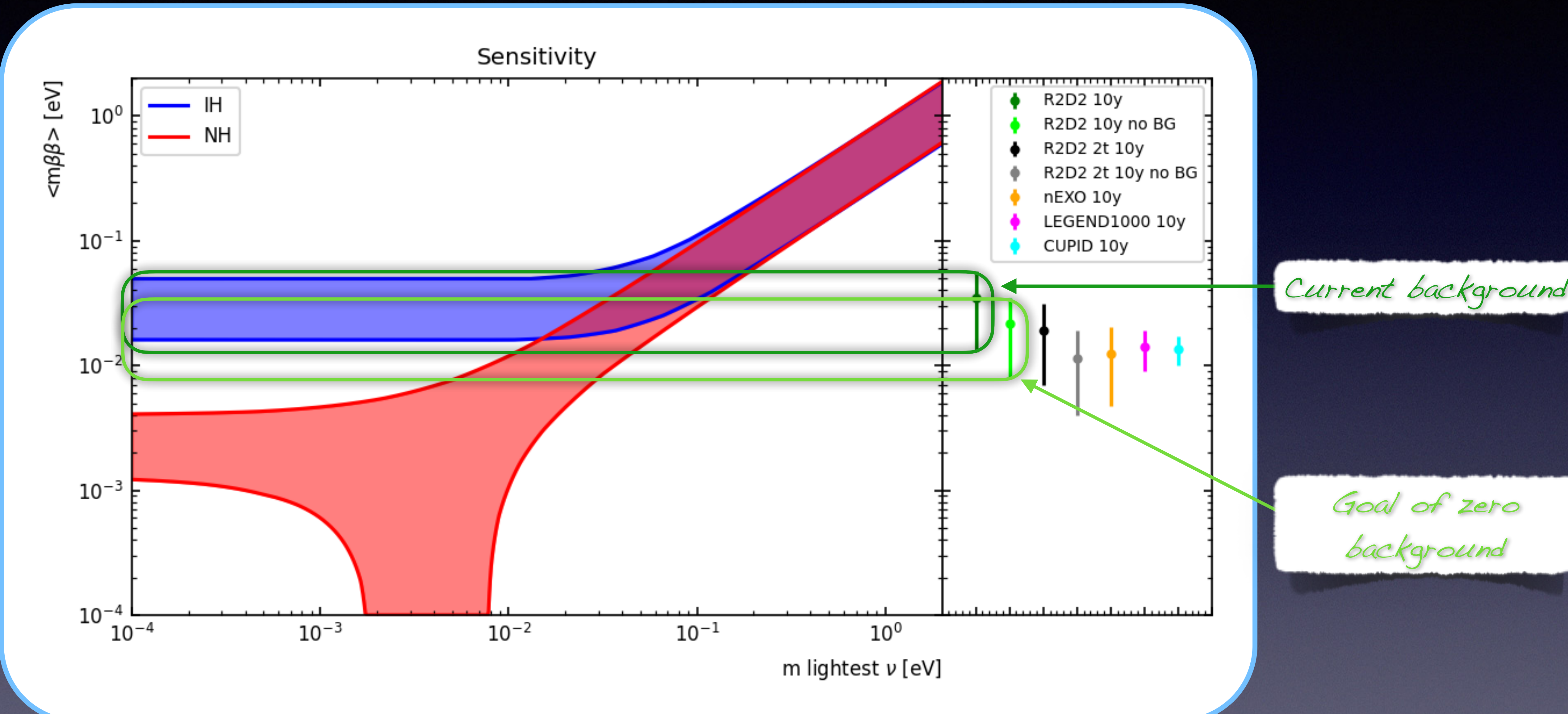

Sensitivity

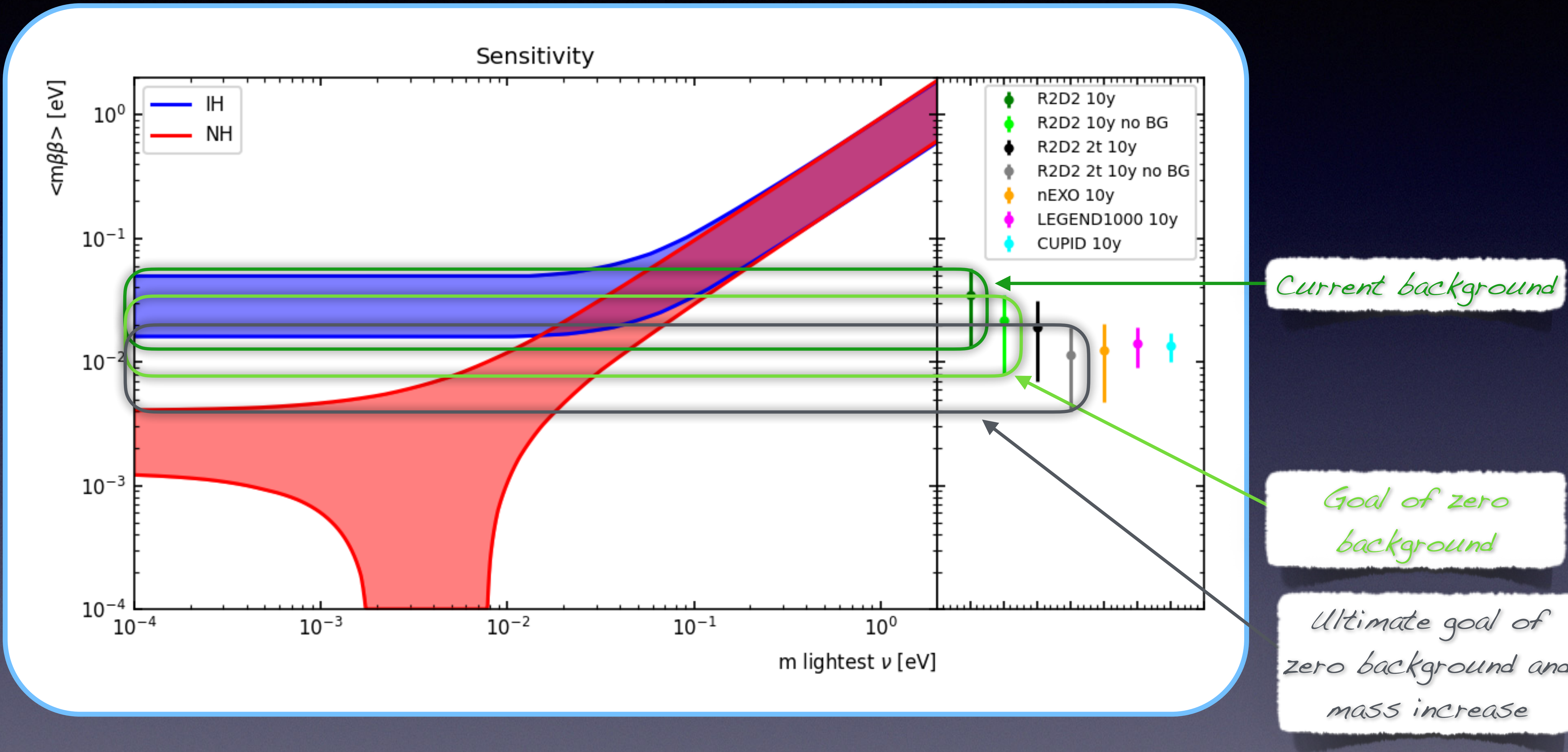

Sensitivity

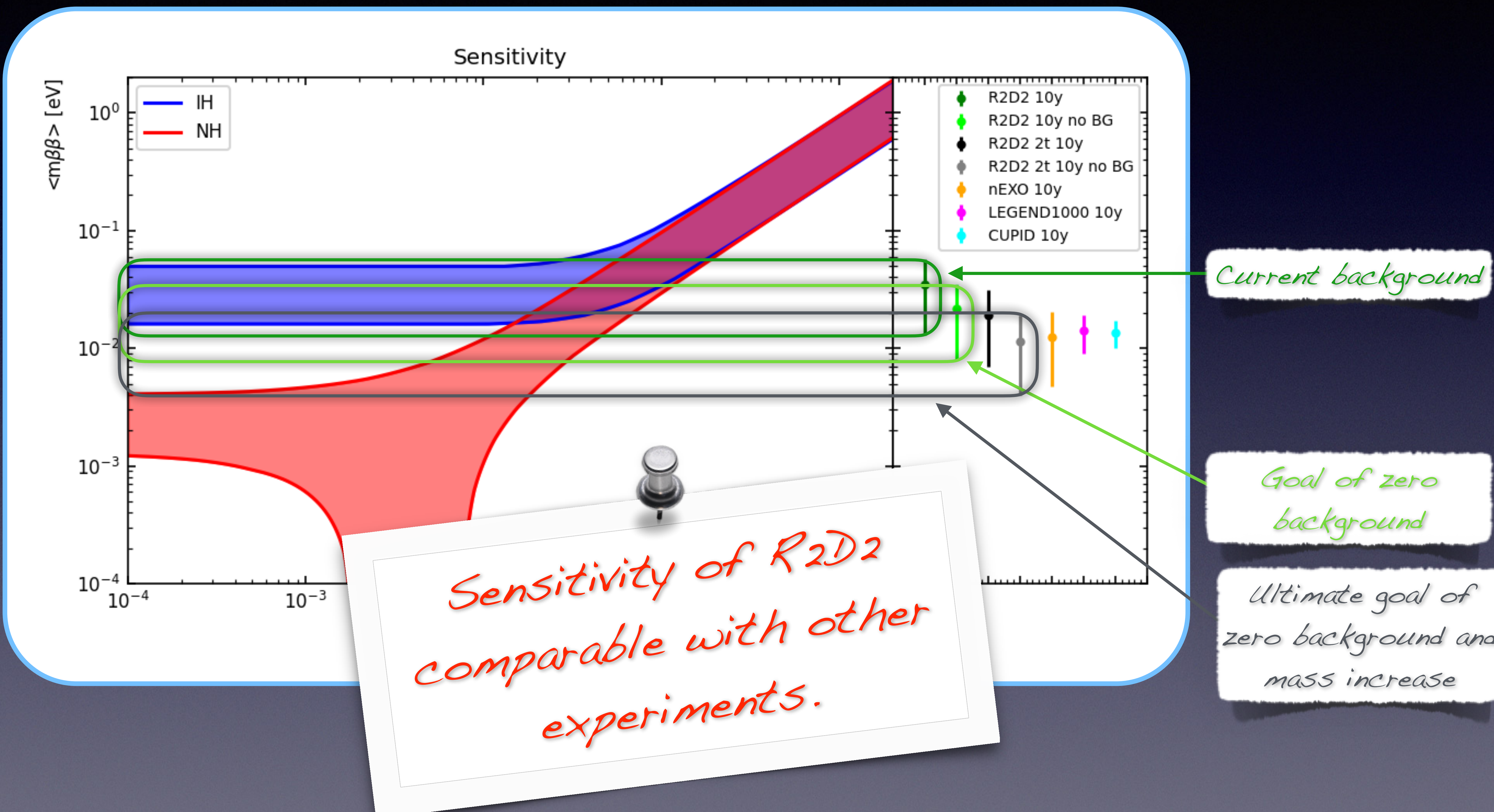

Conclusions

- The R2D2 R&D demonstated **the simple CTPC detector can be used for neutrinoless double beta decay search**.
- All **possible technical issues** (gas purification, recirculation etc.) **can be solved** based on the know-how developed by R2D2 and the existing one in the xenon community.
- The R&D to achieve a composite low radioactivity thin vessel is ongoing with industrial partners.
- The simplicity of the detector results on low electric consumption, no need of cryogenics, and a relatively low cost.

Conclusions

- The R2D2 R&D demonstated **the simple CTPC detector can be used for neutrinoless double beta decay search**.
- All **possible technical issues** (gas purification, recirculation etc.) **can be solved** based on the know-how developed by R2D2 and the existing one in the xenon community.
- The R&D to achieve a composite low radioactivity thin vessel is ongoing with industrial partners.
- The simplicity of the detector results on low electric consumption, no need of cryogenics, and a relatively low cost.

The full experiment is timely, and if the final goal of zero background is reached a ton scale detector could rule out the inverted mass hierarchy region in 10 years of data taking.

Conclusions

R. Bouet [1], J. Busto [2], A. Cadiou [3], P. Charpentier [1], D. Charrier [3], M. Chapellier [4], A. Dastgheibi-Fard [5], F. Druillole [1], P. Hellmuth [1], C. Jollet [1], J. Kaizer [8], I. Kontul [8], P. Le Ray [3], M. Gros [6], P. Lautridou [b,3], M. Macko [7], A. Meregaglia [a,1], F. Piquemal [1], P. Povinec [8], M. Roche [1]

[1]LP2I Bordeaux, Université de Bordeaux, CNRS/IN2P3, F-33175 Gradignan, France
[2]CPPM, Université d'Aix-Marseille, CNRS/IN2P3, F-13288 Marseille, France
[3]SUBATECH, IMT-Atlantique, Université de Nantes, CNRS-IN2P3, France
[4]IJCLab, CNRS/IN2P3, Paris, France
[5]LPSC-LSM, CNRS/IN2P3, Université Grenoble-Alpes, Modane, France
[6]IRFU, CEA, Université Paris-Saclay, F-91191 Gif-sur-Yvette, France
[7]IEAP, Czech Technical University in Prague, CZ-11000 Prague, Czech Republic
[8]Faculty of Mathematics, Physics and Informatics, Comenius University, Bratislava, Slovakia

Conclusions

Current Collaboration

R. Bouet [1], J. Busto [2], A. Cadiou [3], P. Charpentier [1], D. Charrier [3], M. Chapellier [4], A. Dastgheibi-Fard [5], F. Druillole [1], P. Hellmuth [1], C. Jollet [1], J. Kaizer [8], I. Kontul [8], P. Le Ray [3], M. Gros [6], P. Lautridou [b,3], M. Macko [7], A. Meregaglia [a,1], F. Piquemal [1], P. Povinec [8], M. Roche [1]

[1]LP2I Bordeaux, Université de Bordeaux, CNRS/IN2P3, F-33175 Gradignan, France
[2]CPPM, Université d'Aix-Marseille, CNRS/IN2P3, F-13288 Marseille, France
[3]SUBATECH, IMT-Atlantique, Université de Nantes, CNRS-IN2P3, France
[4]IJCLab, CNRS/IN2P3, Paris, France
[5]LPSC-LSM, CNRS/IN2P3, Université Grenoble-Alpes, Modane, France
[6]IRFU, CEA, Université Paris-Saclay, F-91191 Gif-sur-Yvette, France
[7]IEAP, Czech Technical University in Prague, CZ-11000 Prague, Czech Republic
[8]Faculty of Mathematics, Physics and Informatics, Comenius University, Bratislava, Slovakia

Conclusions

Current Collaboration

R. Bouet [1], J. Busto [2], A. Cadiou [3], P. Charpentier [1], D. Charrier [3], M. Chapellier [4], A. Dastgheibi-Fard [5], F. Druillole [1], P. Hellmuth [1], C. Jollet [1], J. Kaizer [8], I. Kontul [8], P. Le Ray [3], M. Gros [6], P. Lautridou [b,3], M. Macko [7], A. Meregaglia [a,1], F. Piquemal [1], P. Povinec [8], M. Roche [1]

[1]LP2I Bordeaux, Université de Bordeaux, CNRS/IN2P3, F-33175 Gradignan, France
[2]CPPM, Université d'Aix-Marseille, CNRS/IN2P3, F-13288 Marseille, France
[3]SUBATECH, IMT-Atlantique, Université de Nantes, CNRS-IN2P3, France
[4]IJCLab, CNRS/IN2P3, Paris, France
[5]LPSC-LSM, CNRS/IN2P3, Université Grenoble-Alpes, Modane, France
[6]IRFU, CEA, Université Paris-Saclay, F-91191 Gif-sur-Yvette, France
[7]IEAP, Czech Technical University in Prague, CZ-11000 Prague, Czech Republic
[8]Faculty of Mathematics, Physics and Informatics, Comenius University, Bratislava, Slovakia

A lot of work to be done and interested people are welcome to join the R2D2 effort